# Calculating Thermochemical Equilibrium for Multiphysics Simulations of Nuclear Materials

## Development of Yellowjacket Gibbs Energy Minimiser

by

**Parikshit Bajpai**

A thesis submitted to the
School of Graduate and Postdoctoral Studies
in partial fulfilment of the requirements for the degree of

**Doctor of Philosophy**
in
**Modelling and Computational Science**

School of Graduate and Postdoctoral Studies
University of Ontario Institute of Technology (Ontario Tech University)
Oshawa, Ontario, Canada
November 2022

## THESIS EXAMINATION INFORMATION

Submitted by: **Parikshit Bajpai**

**Doctor of Philosophy** in **Modelling and Computational Science**

Thesis title: **Calculating Thermochemical Equilibrium for Multiphysics Simulations of Nuclear Materials**

An oral defense of this thesis took place on 15-November-2022 in front of the following examination committee:

**Examining Committee:**

| | |
|---|---|
| Chair of Examining Committee | Dr. Gregory M. Lewis |
| Research Supervisor | Dr. Markus H.A. Piro |
| Examining Committee Member | Dr. Lennaert van Veen |
| Examining Committee Member | Dr. Hendrick W. de Haan |
| University Examiner | Dr. Kirk Atkinson |
| External Examiner | Dr. Maria Emelianenko, George Mason University |

The above committee determined that the thesis is acceptable in form and content and that a satisfactory knowledge of the field covered by the thesis was demonstrated by the candidate during and oral examination. A signed copy of the Certificate of Approval is available from the School of Graduate and Postdoctoral Studies.

# Abstract

Nuclear fuels and structural materials are highly complex systems that are remarkably challenging to understand and model. Material behaviours are influenced by multiple physical phenomena such as mechanics, chemistry, heat and mass transport, etc. Moreover, lower scale phenomena inform and drive the phenomena at larger scales. The strong interactions between multiple physics at different length and time scales creates a need for multi-scale, multi-physics modelling tools. In nuclear fuels and structural materials, the problem gets compounded by the fact that, in addition to an extreme environment, the composition of the system changes with time. For such complex systems, computational thermodynamics plays a valuable role in predicting many phenomena and is often necessary for understanding and informing others. For this reason, there has been an increasing interest in incorporating equilibrium thermodynamics calculations in multi-physics frameworks such as the Multiphysics Object Oriented Simulation Environment (MOOSE). To simulate corrosion in molten salt reactors, a new MOOSE-based tool named Yellowjacket has been developed and this work contributes to it.

The objective of this work is to develop a new equilibrium thermodynamic solver to provide thermodynamic material properties and boundary conditions for Yellowjacket and other MOOSE-based codes. While several thermodynamics codes already exist, the new software, called Yellowjacket–GEM, adds native equilibrium thermodynamic capability to MOOSE and aims to address several concerns such as computational performance, limitations on system size and models, and Software Quality Assurance (SQA).

Yellowjacket–GEM exploits the fundamental laws of thermodynamics to solve a non-linear, non-convex optimisation problem. Several thermodynamic models, including the Modified Quasichemical Model in Quadruplet Approximation (MQMQA) were implemented, and state-of-the-art numerical solvers in Portable, Extensible Toolkit for Scientific Computation (PETSc) were used to efficiently solve the optimisation problem. In doing so, the work contributes to the understanding of MQMQA which until recently wasn't well comprehended. Ensuring that the solver gives a true equilibrium solution also requires solving a global optimisation problem without severely compromising performance and reliability. Several global optimisation methods were compared through numerical experiments to objectively select the best approach for implementation. The C++ code follows MOOSE coding standards and SQA procedures and enables direct coupling of thermodynamic equilibrium calculations in multiphysics simulations performed using MOOSE.

**Keywords:** Computational Thermodynamics; Gibbs Energy Minimisation; Global Optimisation; Yellowjacket Gibbs Energy Minimiser; Mutiphysics Object Oriented Simulation Environment (MOOSE)

# Author's Declaration

I hereby declare that this thesis consists of original work of which I have authored. This is a true copy of the thesis, including any required final revisions, as accepted by my examiners.

I authorize the University of Ontario Institute of Technology (Ontario Tech University) to lend this thesis to other institutions or individuals for the purpose of scholarly research. I further authorize University of Ontario Institute of Technology (Ontario Tech University) to reproduce this thesis by photocopying or by other means, in total or in part, at the request of other institutions or individuals for the purpose of scholarly research. I understand that my thesis will be made electronically available to the public.

**Parikshit Bajpai**

# Statement of Contributions

Some of the work presented in this thesis was completed as part of coauthored works and the main body of this thesis reflects the contributions made as the primary author. Where the work as a secondary author has been presented, it has been significantly abridged to emphasise only the significant contribution of the author of this thesis and the same has been acknowledged in the text.

In section 4.3.2, the following two articles have been used with permission from the publisher:

1. P. Bajpai, M. Poschmann, M.H.A. Piro, *Derivations of useful partial molar excess Gibbs energy of mixing expressions of common thermodynamic models*, Journal of Phase Equilibria and Diffusion, 42 (2021) 333-347. The author of this thesis was solely responsible for performing the analysis and mathematical derivations and was co-responsible for the verification along with M. Poschmann. The author also wrote the majority of the manuscript.
2. M. Poschmann, P. Bajpai, B.W.N. Fitzpatrick, M.H.A. Piro, *Recent developments for molten salt systems in Thermochimica*, Calphad, 75 (2021) 102341. Thesis author's main contribution was the analysis of the MQMQA and derivation of expressions presented in section 2 of the article. Both these activities were performed in conjunction with the primary author of the paper. As such, only section 2 has been presented here and the other sections of the article which do not represent the author's contribution have been omitted.

In section 5.3.4, the article: P. Bajpai, M.H.A. Piro, *Corrigendum to 'The thermochemistry library Thermochimica'*, Computational Materials Science, 198 (2021) 110659, has been used with permission from the publisher. The author of this thesis carried out all the analysis and wrote the manuscript. M.H.A. Piro conceptualised and revised the manuscript.

The work described in chapter 6 was performed, in part, during a virtual internship at the Idaho National Laboratory (Idaho Falls, Idaho, United States). The work was performed under the supervision of Dr. D. Schwen and the thesis author was responsible for design and implementation of the software. Dr. D. Schwen reviewed the code and suggested minor code patches.

In section 6.4.4, the article M.H.A. Piro, M. Poschmann, P. Bajpai, *On the interpretation of chemical potentials computed from equilibrium thermodynamic codes: Applications to molten salts*, Journal of Nuclear Materials, 526 (2019) 151756 was used with permission from the publisher. Thesis author contributed to the discussion which evolved into the letter and co-authored the example section of the manuscript.

In section 7.5, results from a coupled simulation are presented. This work was performed in collaboration with C. Bhave of the University of Florida. The author of this thesis was responsible for the development of the thermodynamic equilibrium solver and for all the thermodynamic calculations performed as part of the simulation. C. Bhave performed the phase-field part of the simulation.

# Acknowledgements

I am deeply grateful to my supervisor Prof. Markus Piro for not only giving me the opportunity to work this research but also for his constant guidance and encouragement. His contribution to this work and to my development as a researcher has been invaluable and his advice and enthusiasm has made this work extremely rewarding and delightful. I can't appreciate enough the support of Dr. Daniel Schwen who mentored me as an intern at the Idaho National Laboratory and from whom I have learnt innumerable things about MOOSE but more importantly on how to design and write good code.

This work has benefited from the numerous discussions with our collaborators, Chaitanya Bhave and Prof. Michael Tonks from the University of Florida. These discussions provided a great insight into the objectives and were always useful in deciding the direction we want to pursue with the development of the code and its coupling with the phase field code developed by Chaitanya. Along the same lines, I must also thank Dr. Ben Spencer, Prof. Ted Besmann, Dr. Jake McMurray and Dr. David Andersson, as the leaders of the NEAMS Chemistry and Corrosion technical area facilitated and guided this work. I would like to thank Dr. Rich Martineau who initiated this work and Dr. David Andrs who supported the initial development of the code.

I wish to thank Prof. Lennaert van Veen and Prof. Hendrick de Haan who have provided constant help as members of the supervisory committee and also to the members of the examining committee Prof. Kirk Atkinson and Prof. Greg Lewis for taking time out of their very busy schedules to review this work. In particular, I would like to thank Prof. Maria Emelianenko (George Mason University) for very kindly agreeing to be the external examiner and for providing her valuable feedback on this work.

This work is an outcome of several years of research with numerous collaborations and inputs from many individuals and to acknowledge everyone would certainly be impossible. With that being said, I would like to start with Dr. Max Poschmann with whom I've worked throughout this research and who probably understands and shares a lot of my frustrations with figuring out models and finding bugs. Max was always available to discuss models, methods, code and a lot more. To all the members of the Computational Methods Development Team at INL who were always the most helpful and brilliant people to work with, I can't describe how much I've learnt from you all. To my colleagues and friends in both Nuclear Fuels and Material group and Collaborative Laboratory for Applied and Industrial Mathematics, I appreciate all our conversations about work and more, the lunches and coffee-breaks, staying well past midnights to work on assignments but most importantly for adding fun to work. Though I cannot name everyone here, I must mention Ernesto Geiger, Ksenia Lipkina, and Marcos Machado who started out as colleagues but are the greatest friends one can make.

Lastly, but most importantly, I would like to thank my family without whom I would never be here. In particular, my mother, Vibha, my father, Vinod, and my sister, Sonakshi, who have all supported me, motivated me and inspired me.

# Contents

# List of Figures

# List of Tables

# List of Algorithms

# Acronyms

**API** Application Programming Interface

**APSO** Adaptive Particle Swarm Optimisation

**APSO-VI** APSO based on Velocity Information

**BB** Branch & Bound

**BCC** Body Centered Cubic

**BWRs** Boiling Water Reactors

**CALPHAD** CALculation of PHAse Diagram

**CANDU** CANada Deuterium Uranium

**CEF** Compound Energy Formalism

**CI** Continuous Integration

**CIVET** Continuous Integration, Verification, Enhancement and Testing tool

**DFT** Density Functional Theory

**FBBT** Faster-Feasibility Bounds Tightening

**FCC** Face Centered Cubic

**FNN** First Nearest Neighbour

**GEM** Gibbs Energy Minimisation

**HCP** Hexagonal Close Packed

**HWRs** Heavy Water Reactors

**LWRs** Light Water Reactors

**MINLP** Mixed Integer Non-Linear Programming

**MOOSE** Multiphysics Object Oriented Simulation Environment

**MOX** Mixed OXide fuel

**MQM** Modified Quasichemical Model

**MQMQA** Modified Quasichemcial Model in Quadruplet Approximation

**MSRs** Molten Salt Reactors

**MSTDB-TC** Molten Salt Thermodynamic Database–Thermochemical

**NEAMS** Nuclear Energy Advanced Modelling and Simulation

**NLP** Non-Linear Programming

**NQA** Nuclear Quality Assurance

**OBBT** Optimality-Based Bounds Tightening

**PCI** Pellet Cladding interaction

**PETSc** Portable Extensible Toolkit for Scientific Computation

**PGE** Partitioning of Gibbs Energy

**PSO** Particle Swarm Optimisation

**PWRs** Pressurised Water Reactors

**RTA** Random Tunnelling Algorithm

**sBB** Spatial Branch & Bound

**SFRs** Sodium-cooled Fast Reactors

**SNN** Second Nearest Neighbour

**SQA** Software Quality Assurance

**SRO** Short-Range Ordering

**TAF-ID** Thermodynamics of Advanced Fuels–International Database

**TRUST** Terminal Repeller and Unconstrained Subenergy Tunnelling

*Thermodynamics is a funny subject. The first time you go through it, you don't understand it at all. The second time you go through it, you think you understand it, except for one or two small points. The third time you go through it, you know you don't understand it, but by that time you are so used to it, it doesn't bother you any more.*

Arnold Sommerfeld

# 1

# Introduction

*Nuclear energy is at the core of world's sustainable development efforts and poised to take on an even bigger role as the world collectively moves to decarbonise many sectors of the economy. Despite its potential, several challenges remain and are related to sustainability, reliability, economic competitiveness, safety, risk of proliferation and anticipated future needs beyond electricity [1]. Several advanced reactors, like Molten Salt Reactors (MSRs), are being developed to overcome these challenges but such reactors pose unique challenges in terms of engineering design, modelling and construction of these reactors. The design issues are themselves quite complicated and span a wide array of knowledge domains such reactor physics, chemistry, materials science, fluid flow and heat transfer, etc. To address these challenges, modelling and simulation and high-performance computing resources are being heavily leveraged. This is driving the development of advanced simulation tools such as those being developed under the Nuclear Energy Advanced Modelling and Simulation (NEAMS) program.*

*This work aims to support and augment the material modelling capabilities developed under NEAMS by adding capabilities which, until now, had been missing from the NEAMS code suite. This chapter aims to give the context to the work by describing the challenges faced in nuclear material design, the effect of thermochemistry and how modelling and simulation is key to tackling the challenges. This is followed by a description of the Multiphysics Object Oriented Simulation Environment (MOOSE) framework which this work contributes to through the development of a new code called Yellowjacket–GEM which has also been introduced. The developed code is applicable to all reactor technologies but the main thrust*

*was MSRs so the discussion will be in that context.*

## 1.1. Material Challenges in Nuclear Systems

Design and discovery of materials most suited for a specific application is an intrinsic part of development of new technology as many engineering designs can only be as good as the materials available during design and innovation. In conventional materials, the mechanical, thermophysical and chemical properties are often of main interest but nuclear materials must overcome significant challenges to provide the desired levels of reliability and safety commensurate to strict quality assurance requirements. Nuclear reactors present extreme environments for components irrespective of the reactor technology and not only do materials need to meet the physical and chemical performance requirements, but must also demonstrate desirable nuclear physics characteristics. The core in particular presents an exceptionally harsh environment of high temperature, high pressure in many cases, high stresses, intense radiation and a chemically aggressive environment and the properties desirable from a nuclear perspective, such as high power density, exert high operational burdens on fuels and structural materials [2]. As advanced reactor designs gain increasing traction, the material challenges are only going to get worse. Advanced reactors, such as MSRs, operate not only at higher temperature and irradiation flux but also with coolants that present more challenging corrosion problems than the current lot of Light Water Reactors (LWRs) and Heavy Water Reactors (HWRs) [3]. Moreover, Generation IV reactors are expected to have a longer operating time of at least sixty years.

Thermochemistry and principles of computational thermodynamics play a key role in nuclear material modelling. Since nuclear materials are continuously evolving due to transmutations, fission product generation and decay, so do their material properties. The laws of thermodynamics govern many phenomena in nuclear materials and are important for applications such as understanding phase equilibria, which affects nucleation and dissolution of phases, oxidation potential of cladding, thermochemical properties of fuels and many others. As such, thermodynamic principles are sufficient for predicting many phenomena and are, at a minimum, imperative to understanding more complex and dynamic physics. Some of the key applications of thermodynamics that make it indispensable to MSRs design and development process include but are not limited to:

1. Optimising fuel salt composition and prediction of thermal stability of fuel and structural materials materials.
2. Understanding fission product chemistry and their effect on material properties.
3. Predicting chemical interactions between fuel and structural materials.

4. Predicting impact of impurities on molten salt corrosion in MSRs.
5. Source term analyses and predicting phases that form between reactor materials under severe accident scenarios.

While the concepts of thermodynamics can be embodied in both non-equilibrium and equilibrium descriptions, it is often thermodynamic equilibrium that is leveraged in applications. Even when the materials are, in many cases, in non-equilibrium conditions, an understanding of the phases that shall form under equilibrium conditions provides valuable knowledge as it gives the direction of evolution of the system. In fact, in nuclear materials, the high temperature conditions lead to a rapid approach to equilibrium and under suitable conditions, make equilibrium thermodynamics a suitable approximation.

## 1.2. Modelling and Simulation

The traditional approach to studying materials was almost entirely experimental but recent developments in modelling and high performance computing have resulted in a much stronger collaboration and integration among theory, experiments and computational science [4]. Multiscale, multiphysics models and simulations enable investigations over a wide range of length and time scales which would otherwise be unfeasible using only experiments. Thus, computational models help augment and guide experimental campaigns and support economical discovery and design of materials within reasonable lead times.

Complex interactions between the different physical phenomena occurring in the materials are often very tightly coupled and many important aspects are inherently multidimensional as well [5]. As an example, one can consider MSRs where, as shown in Figure 1.1, multiple physics are required for understanding the behaviour and for predicting phenomena such as mass accountancy. Another aspect to consider is that of the different time and length-scales involved with length-scales ranging from inter-atomic spacing to meters, and time-scales ranging from microseconds to years. For example, radiation defects start within picoseconds at the atomistic scales and propagate to larger length-scales over time-scales which are several magnitudes longer.

Evidently, modelling and simulation of nuclear materials requires a multiscale, multiphysics approach. However, such simulations have been decently challenging until recently and with significant limitations on the amount of computational resources available even a couple of decades ago, a majority of modelling and simulation efforts adopted an operator-splitting approach based on Picard iterations. Such simulations usually focused on only the engineering scale behaviour and usually relied on continuum or bulk description of the phenomena. In doing

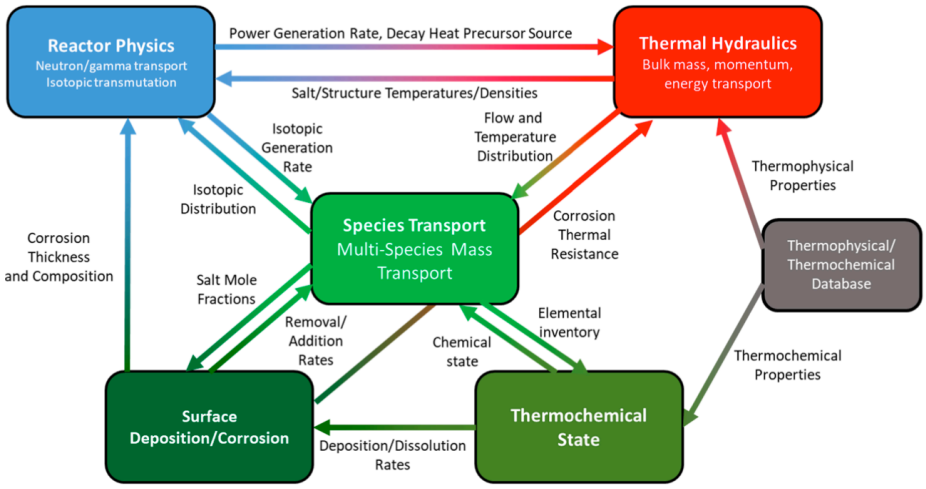


Figure 1.1: Multiphysics phenomena in Molten Salt Reactors (MSRs) [6].

so, experimental observations and operational experience were relied on for the validity of results and often very conservative safety margins were added to design parameters. As an example, nuclear fuel behaviour has been modelled as a solid mechanics problem coupled with conductive heat transfer and fission gas release wherein the material properties are often either assumed to be constant or described using simplified models based on empirical correlations. Though these methods were suitable for previous and current generation of nuclear reactors, addressing the materials challenges for advanced reactors is usually beyond their capability. In fact, there has been an increasing impetus on leveraging lower scale information to inform models on larger scales and solving the governing equations as a system rather than as individual problems. Since such an approach is rooted in fundamental principles, the transfer of information between scales, through characteristic parameters such as density, energy, temperature, etc., results in a much more accurate description of material behaviour [4]. The numerous modelling and simulation tools available at different length and time scales are shown in Figure 1.2.

### 1.2.1. Computational Thermodynamics

The modelling and simulation tool that is of particular relevance to this work is computational thermodynamics. Phase and chemical behaviour of nuclear materials is governed by the thermochemical equilibrium state. Computational thermodynamics is an essential tool for calculating both phase equilibria and thermodynamic properties of the system. It is rooted in the *CALculation of PHAse Diagram (CALPHAD)* approach shown in Figure 1.3. CALPHAD combines experimental and theoretical information and tunes parametric models to describe thermodynamic properties of materials like Gibbs energy, enthalpy, heat capacity, etc. [7].

Capturing thermodynamic equilibria in multiphysics codes has traditionally relied on empir-

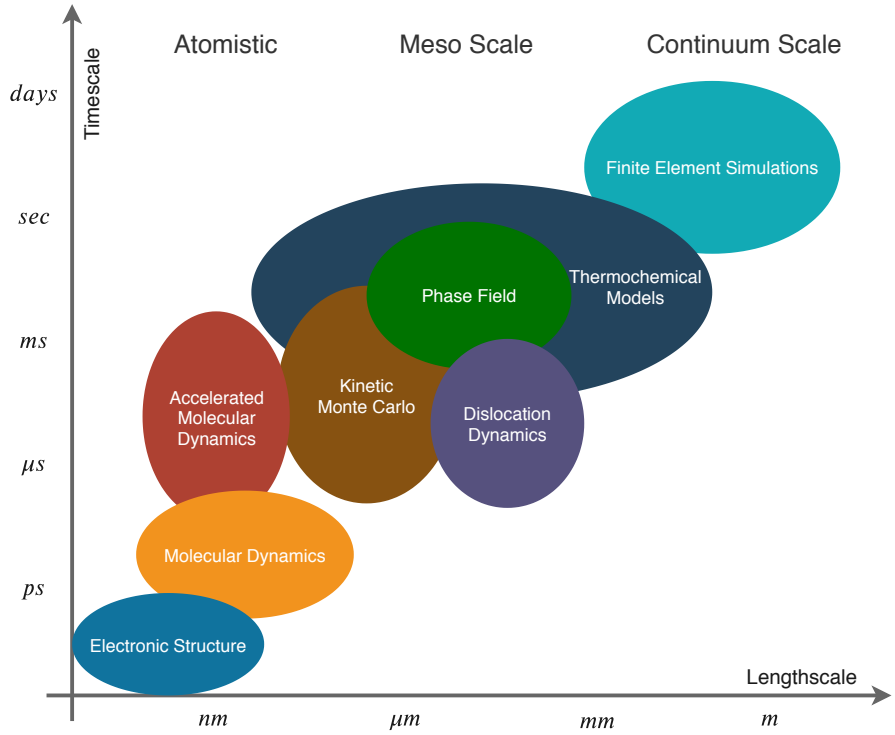


Figure 1.2: Multiscale theoretical and computational methods used for materials model development and computer simulation [4].

ical correlations and the interest in direct coupling of thermodynamic equilibrium codes with multiphysics models is only a recent trend. While the empirical correlations do not convey the high fidelity of full thermodynamic analysis, performing thermodynamic equilibrium analysis within multiphysics codes is normally a very complex process and can significantly impede the computational performance of such codes. However, the recent developments in high performance computing have facilitated the use of equilibrium thermodynamics in multiphysics simulations and it is enabling the study of many phenomena which until now were not well understood.

The inputs and outputs of thermodynamic equilibrium calculations are shown in Figure 1.4. While, other physical conditions are possible, e.g. isochoric processes, the discussion here is restricted to isothermal, isobaric conditions. The Gibbs energy functions are available in many databases, such as Molten Salt Thermodynamic Database–Thermochemical (MSTDB-TC) and Thermodynamics of Advanced Fuels–International Database (TAF-ID), which are developed experimentally using the CALPHAD method described above and atomistic calculations are often used to inform and fill in the knowledge gaps where experiments might not be possible. The results from equilibrium calculations include the stable phases, speciation of the phases, and thermodynamic properties like Gibbs energy, chemical potentials, heat capacities, etc.

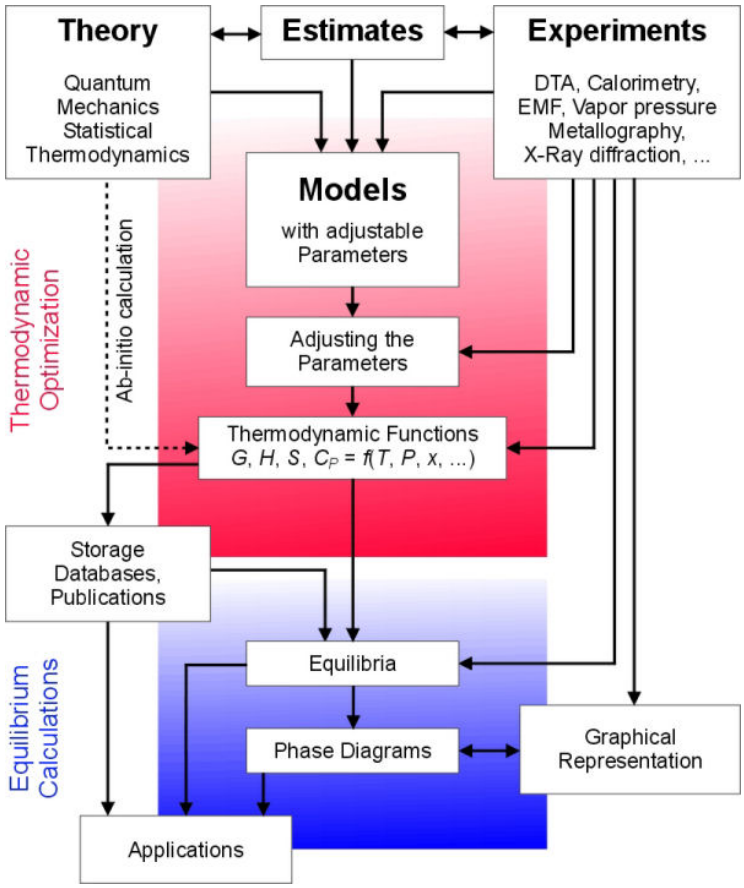


Figure 1.3: Principle of CALPHAD method by Zinkevich [8].

### 1.2.2. Multiphysics Object Oriented Simulation Environment

The Multiphysics Object Oriented Simulation Environment (MOOSE) is a simulation framework that has been developed with the aim of harnessing modern massively parallel computing resources to perform complex multiphysics simulations. The goal of MOOSE is to provide simplified interfaces for user facing tasks such as specification of partial differential equations, boundary conditions, material properties and all aspects of a simulation while handling complex background tasks such as parallel, adaptive, nonlinear, finite element solve internally [9]. Originally created at the Idaho National Laboratory in the United States, MOOSE is open-source framework which leverages state-of-the-art libMesh code [10] for finite elements and the Portable Extensible Toolkit for Scientific Computation (PETSc) [11, 12] for leading-edge numerical methods/solvers. MOOSE has been used to build multiple community-developed physics "modules" [13–17] and several application libraries which are used by governments, industry and academia.

For nuclear reactor modelling, apart from the MOOSE modules, several export-controlled

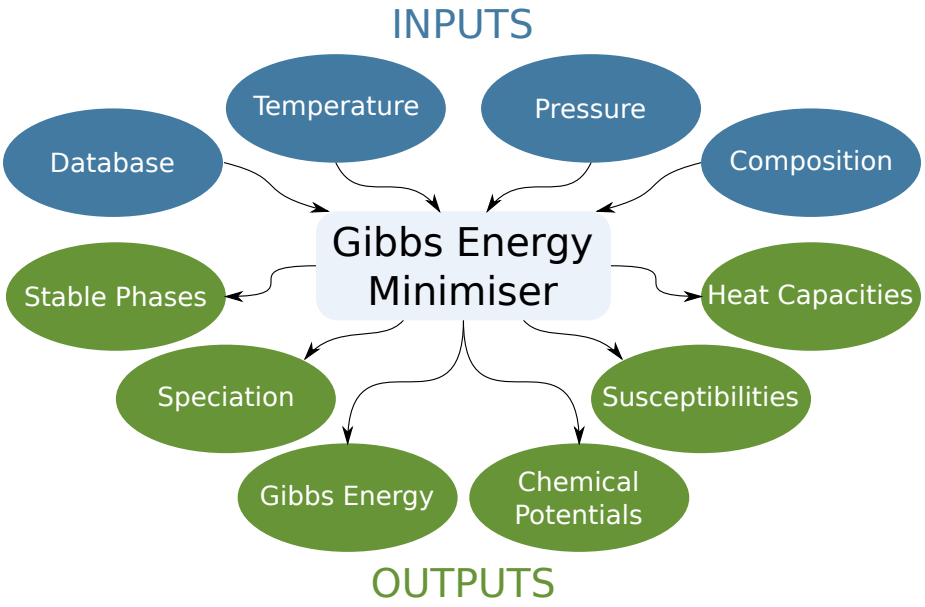


Figure 1.4: Input and output parameters of thermodynamic equilibrium calculations.

applications have been developed. These include RELAP-7 [18] for system level thermal hydraulics, Rattlesnake [19] for neutronics, etc. For nuclear material simulations, the MOOSE framework consists of two main applications the macroscale fuel performance code BISON [5] and the mesoscale phase field code Marmot [20].

Simulation of nuclear reactor fuel performance involves complex thermomechanical processes between fuel pellets, made of fissile material, and the protective cladding barrier that surrounds the pellets. BISON is an engineering scale code developed to predict the nuclear fuel performance under normal, off-normal, and accident conditions. By using highly efficient computational methods, it enables three dimensional, fully coupled multiphysics simulations on high fidelity geometric representations of fuel pins/pellets. BISON has been designed to be highly scalable and does not require the use of operator splitting, staggered or predictor-corrector approaches [5].

Due to its simple concept and large range of applicability, the phase field approach is a popular and powerful tool to model microstructure and has been applied in problems such as grain boundary migrations, martinistic transformation, two-phase flow, etc. The phase field approach treats all material interfaces as diffuse by representing structural features with continuous variables which smoothly transition from one value to another. Thus, phase field method not only eliminates the need to explicitly discretise boundaries and interfaces, it also enables describing microstructure through a system of partial differential equations. The Marmot phase field application has been developed to enable simulations of the microstructure evolution of nuclear fuels and materials under irradiation. By exploiting the object-oriented architecture

of MOOSE, Marmot allows easy coupling of phase field with additional physics such as solid mechanics or heat conduction, to effectively predict the microstructural evolution at mesoscale. This allows prediction of evolution of material properties of nuclear materials under irradiation and can be used to inform engineering scale simulations and reduce the dependence of such simulations on empirical correlations. As a result, the multiscale framework can achieve true predictability even in compositional and operational regimes where little or no experimental data exists [20].

Despite the wide ranging capability of MOOSE, there has been a lack of dedicated tools for modelling molten salt corrosion and to bridge this gap, a suite of tools have been developed under the NEAMS program of the United States Department of Energy. Corrosion is an electrochemical process composed of oxidation and reduction reactions, which are defined by the thermodynamics and kinetics of the system. While thermodynamics controls whether or not a material may corrode, kinetics influences how quickly the material will corrode. This corrosion behaviour is also significantly affected by the material microstructure and predicting corrosion therefore requires a multiphysics approach that can couple quantitative electrochemistry models of corrosion and chemical reactions with thermochemical equilibrium computations. Effectively, predicting corrosion and related phenomena like leaching and deposition requires a multiscale, multiphysics approach [21]. The corrosion suite, shown in Figure 1.5, aims to couple atomistic and mesoscale modelling to thermochemical equilibrium calculations to create a unique corrosion modelling capability on the microstructural scale and use it to inform engineering scale codes aimed at solving species transport problem. At the core of the corrosion suite is the MOOSE-based application Yellowjacket that couples quantitative models of corrosion with thermodynamic equilibrium and chemical kinetics models to predict the rate of material loss, corrosion product production and precipitate production in advanced nuclear reactors.

The software developed as part of this work adds native equilibrium thermodynamic capability to MOOSE and its applications and is described in the following section.

### 1.2.3. Yellowjacket

Many emerging nuclear technologies, such as MSRs, use high temperature fluids like molten fluoride/chloride salts, which can lead to the corrosion of salt-facing structural materials. Not only does corrosion impact the performance of structural materials with the possibility of compromising their integrity but it can also lead to other problems just as blocking of salt flow loops due to leaching from hot sections of the loop and deposition in the colder sections. In molten fluoride salts, the protective oxide layer on alloys typically relied upon for high-temperature corrosion resistance dissolves, thereby exposing the fresh alloy surface to the molten salt. In molten

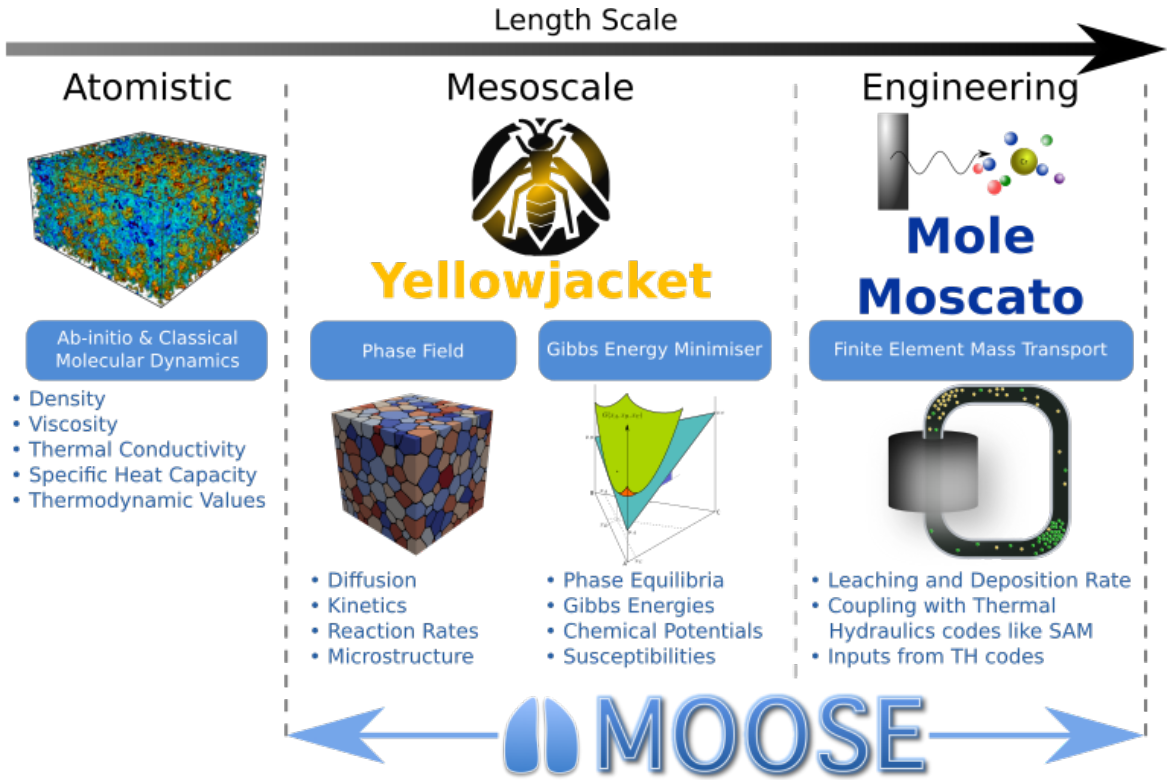


Figure 1.5: Yellowjacket corrosion suite. After McMurray et al. [22].

chloride salts, passivity has been observed; however, the oxide layer is prone to attack and may not provide the necessary corrosion protection [23]. The corrosion process is accelerated by the impurities present in the salt and enhanced further by the presence of dissimilar metals due to activity-driven corrosion. It has been observed the corrosion in molten salt is a microstructural phenomena with preferential leaching at grain boundaries as compared to bulk of the grain but there are significant gaps in the scientific understanding of the governing mechanisms such as the impact of impurities and irradiation [24–29]. Yellowjacket relies on the phase field method for structural evolution and couples it with electrochemical descriptions, fracture models and thermochemical equilibrium solver to create a holistic environment for corrosion modelling and simulation [30].

As shown in Figure 1.6, Yellowjacket phase field model requires several thermodynamic properties like Gibbs energies, chemical potentials and driving forces for the various phases which can be present in the system. This requires knowing the molar amounts of the different phases which would be present under given temperature, pressure and composition. However, at the interfaces, more than one phase can co-exist and the phase field models face a challenge in estimating the assemblage and thermodynamic properties. In such cases, a thermodynamic equilibrium solver can provide the required information to the phase field module. This is

the prime driving force behind the development of Yellowjacket–GEM. One may argue that the system will not be at equilibrium and that kinetics of the system will drive the corrosion behaviour and therefore might question the appropriateness of thermochemical equilibrium calculations. While the system is not really at equilibrium, it can be safely assumed that in the limiting case the system will be at equilibrium at any point in space and time.

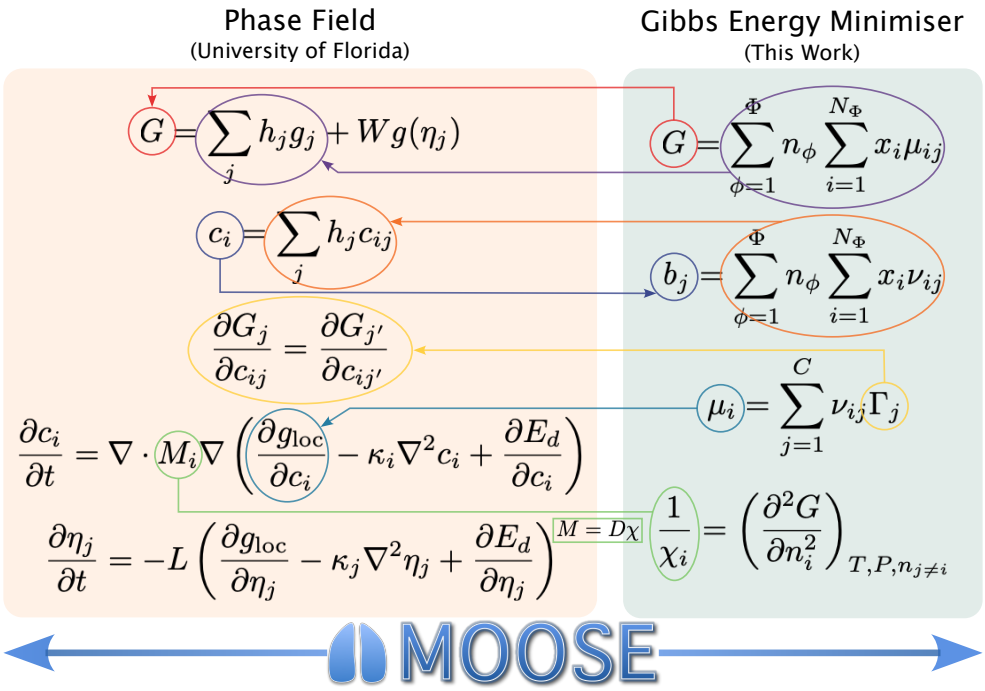


Figure 1.6: Information exchange between the phase field and equilibrium thermodynamics modules of Yellowjacket.

Yellowjacket is a multi-institutional collaborative effort between the Idaho National Laboratory, University of Florida, and Ontario Tech University. In Yellowjacket, the phase field module was implemented at the University of Florida, computational thermodynamics development was performed as part of this PhD thesis at Ontario Tech University and MOOSE-integration was primarily done at Idaho National Laboratory. The main motivation behind this work was to enable direct coupling of thermodynamic equilibrium calculations in MOOSE-based multiphysics simulation and a new Gibbs energy minimiser called Yellowjacket–GEM and the objectives, tasks and main outcomes are described in the next chapter.

The rest of this thesis is organised as follows: the motivation, objectives and tasks are summarised in Statement of Work. A comprehensive literature review of the current computational thermodynamics methods and codes, and global optimisation tools for phase equilibria is provided in Literature Review. Then, the basic thermodynamics principles that form the basis of this work are described in Thermodynamic Basis and conditions of phase equilibrium and

the methods for computing them are described in Equilibrium Thermodynamics. The implementation of algorithms in Yellowjacket–GEM is discussed in Computational Implementation. To highlight the capability and potential impact of the developed tool, several applications of Yellowjacket–GEM are shown in Demonstration Problems, which is followed by the Conclusions and Recommendations.

# 2

# Statement of Work

## 2.1. Problem Statement

Thermodynamic equilibrium calculations are key to providing material properties and boundary conditions in multiphysics simulations. For advanced reactors such as MSRs, there's a need to replace empirical material properties with calculations rooted in fundamental laws of thermodynamics. Despite the growing interest in direct coupling of thermodynamic equilibrium, the MOOSE framework lacks a tool for such calculations.

While several equilibrium thermodynamics codes already exist, the rationale behind developing a new equilibrium thermodynamics code lies in the numerous limitations of these pre-existing tools. All but a handful of these codes are standalone codes aimed at single calculations, phase diagram generation and database development. Moreover, these codes usually support only a small number of system components. Among the codes that do exist with the capability of handling large systems and are aimed at multiphysics simulations, there are still several drawbacks and they do not meet many requirements of the MOOSE framework. These drawbacks include unavailability of readily available Application Programming Interface (API) for coupling to MOOSE apps and lack of Software Quality Assurance (SQA) standards. Thus, a new equilibrium thermodynamics solver needed to be developed.

## 2.2. Objective Statement

The overarching objective of this work was to incorporate native computational thermodynamics capabilities into the multiphysics framework MOOSE through the development of a new

state-of-the-art equilibrium thermodynamic solver called Yellowjacket–GEM. The software consolidates and integrates years of advancements and research in computational thermodynamics and leverages state-of-the-art nonlinear equation solvers and optimisation algorithms to enable on-the-fly thermodynamic property calculation in multiphysics simulations.

## 2.3. Challenges

There are several challenges that had to be addressed in order to achieve the aforementioned objective.

1. Several thermodynamic models are used for representing the Gibbs energies of phases. Many models, in particular the Modified Quasichemical Model (MQM), are not well understood and the details required for implementing them in a solver are not readily available.

2. Thermodynamic calculations are inherently very expensive and the computational cost increases very rapidly with the number of system components. In fact, the cost scales cubically ($O(C^3)$) with the number of system components $C$ and the choice of algorithms can significantly impact the calculation time. This can be prohibitive in multiphysics simulations.

3. Equilibrium calculations require solving a non-convex global optimisation problem. The algorithms used in literature are either primitive or limited to relatively very simple problems. This can affect both performance and reliability of the solver which is critical considering the intended application.

## 2.4. Tasks

The work was split into a series of tasks aimed at navigating the challenges to achieve the objective. These tasks also highlight the main contributions of this work:

- Analyse several thermodynamic models used to describe nuclear materials and derive the chemical potential expressions required for implementing the models in the code. See Thermodynamic Basis.

- Critically survey the numerous algorithms used for thermodynamic equilibrium calculations and identify the solution approach to be adopted. Identify key software design choices and optimise the algorithms for implementation in Yellowjacket–GEM. See Equilibrium Thermodynamics and Computational Implementation.

- Develop the new equilibrium solver in C++ following MOOSE coding conventions. The code must meet the rigorous source code control, continuous integration and verification requirements of MOOSE. Though Yellowjacket–GEM is not NQA-1 certified, it must try to achieve same quality standards as MOOSE is NQA-1 certified. See Computational Implementation.

- Quantitatively compare various global optimisation algorithms available in literature, and, based on performance and reliability, select and implement the algorithm in Yellowjacket–GEM. See Computational Implementation.

- Demonstrate the capabilities of the developed thermodynamic solver through potential applications and benchmark against results available in literature and through other codes. See Demonstration Problems.

- An internship at Idaho National Laboratory from June 2021 to September 2022, working on MOOSE integration of Yellowjacket–GEM. Owing to COVID-19 induced travel restrictions, this internship was virtual.

## 2.5. Deliverables

The outcomes of this research were documented in several ways including publications in peer-reviewed journals, conference presentations and annual progress reports submitted to the Idaho National Laboratory (INL). The main deliverables of this work were as follows:

1. Code base for Yellowjacket–GEM delivered to INL via export controlled repository on Nuclear Science User Facility (NSUF) High Performance Computing (HPC)'s GitLab instance. Since Yellowjacket is export controlled, the code cannot be provided here.

2. Four annual progress reports submitted to INL in September 2019, September 2020, August 2021 and September 2022.

3. Six publications in peer-reviewed journals and seven conference presentations and posters. See List of Publications.

# 3

# Literature Review

*Robust and fast methods for computing chemical equilibrium in complex systems are widely used in materials and chemical industries. While industrial applications essentially require calculation tools capable of discriminating between stable and unstable phases and converging to nontrivial solutions, numerical equilibrium calculations have historically focused on representing dominant chemical reactions using the Law of Mass Action. It was only during and after World War II that numerical approaches amenable to computer programming were developed. Since then, there has been significant growth in the number of methods and softwares for solving the equilibrium thermodynamics problem. The intent of this chapter is to review the current state-of-the-art and identify not only the gaps that must be filled but also to recognise the promising avenues that can be leveraged in this work. The chapter starts by reviewing the numerical methods and codes that have been used for computing thermodynamic equilibrium in the past and follows it with a survey of global optimisation methods used in the field. Lastly, some efforts at coupling thermodynamic equilibrium to other codes has been examined.*

## **3.1.** Numerical Methods for Thermodynamic Equilibrium

Up until the 1940s, chemical equilibria computations were based on two different methods. The first relied heavily on the assumption that only a few molecular species would be present in the final equilibrium and the law of mass action could be applied to these systems and the resulting system of non-linear equations was solvable using the relatively unsophisticated techniques of the time. The second method relied on a tedious trial-and-error approach with the

user's intuition playing a significant role [31]. It was only during the Second World War that, fuelled by the development of rockets, research towards developing computational methods for chemical equilibrium gained momentum. This research was mainly driven by the fact that an accurate knowledge of chemical equilibrium of the propellants was a requirement for the design of rockets. However, all the methods developed at the time were based on the law of mass action and the procedure was not scalable to very large systems where it would be difficult to account for all the possible reactions.

The first major breakthrough in computerising chemical equilibrium calculations was made after the Second World war. In 1946, Brinkley came up with a generalised scheme to approach equilibrium computation by giving an analytical criterion for the number of independent components in a multi-component system [31]. However, the most significant breakthrough in the calculation of thermodynamic equilibria was made at the RAND Corporation by White, Johnson and Dantzig [32]. Since then a few other methods have been proposed but none has found as much success as the method proposed by White et al. In fact, even the method proposed by White et al. has only undergone a few minor changes and more recent algorithm developments have focused on other complimentary routines, such as initialisation, describes later. This section reviews the major methods that have been proposed to compute thermodynamic equilibria.

### 3.1.1. Equilibrium constants

The earliest computational method for finding thermodynamic equilibrium relied on the equilibrium constants of individual reactions and were primarily applied to gas phase equilibria. The equilibrium constant, $K$, is defined as follows:

$$K = \frac{\prod^{N_p} x_{i,p}^{\nu_i}}{\prod^{N_r} x_{i,r}^{\nu_i}}, \tag{3.1}$$

where $x_{i,p}$ and $x_{i,r}$ denote the mole fractions of species $i$ in product and reactants respectively, $\nu_i$ denotes the stoichiometric coefficient of $i$, and, $N_p$ and $N_r$ denote the number of product and reactants, respectively.

While equation (3.1) is easily applicable to single reactions, calculating the concentration of species in multiple simultaneous reactions each with a unique equilibrium constant is quite laborious. The first computational procedure for the calculation of the composition at chemical equilibrium of systems of many constituents was proposed by Brinkley [33] and is known as *Brinkley's method*. Subsequently, a number of modifications were made to this method resulting

in a number of other variant methods, such as the *Brinkley-Krieger-White method* [34], the *NASA method* [35], etc. The Brinkley-Krieger-White method, also known as the *Brinkley-Newton-Raphson* method, is perhaps the most popular and, as is evident from the name, used the Newton-Raphson method to solve the system of non-linear equations [31]. The NASA method [35] shares the same fundamentals as Brinkley's method.

Although Brinkley's method serves well for small systems suitable for hand calculations, it relies heavily on user intuition and prior knowledge of the reactions taking place. Furthermore, it neglects the effects of non-ideality and its derivatives due to mathematical difficulties [35]. Eventually, owing to generalities and numerical superiority of the Gibbs Energy Minimisation (GEM) method, the Brinkley method fell out of favour among the scientific community.

### 3.1.2. Computing thermodynamic equilibria

The numerical technique of minimising the Gibbs energy of the system was originally proposed by White, Johnson and Dantzig [32] and is based on the method of steepest descent of second order and was therefore referred to as the *Second Order Steepest Descent Method*. This methodology, now commonly described as *GEM*, has also been called as the *RAND method* owing to the employer of the developers of the method.

GEM is based on identifying a unique combination of species and phases that yield a minimum in the integral Gibbs of a closed isothermal isobaric system from amongst the many possible candidates. The selection of candidates is based on the first and second laws of thermodynamic and is subject to the conditions of thermochemical equilibrium – satisfaction of the Gibbs phase rule, conservation of mass. Numerically, this amounts to systematically adjusting the Lagrangian multipliers – some which represent the chemical potential of the system components – to change the estimated amount of each species, making the Gibbs energy of the system progressively more negative.

While the initial popularity of the GEM method was fuelled by its generality, reduced dependence on user intuition and convenience of programmability [35], several other advantages have become more apparent as time progressed. Boynton advanced the method to include stoichiometric phases coexisting with solution phases [36] and Eriksson [37] demonstrated the use of the method for non-ideal solutions and showed that when dealing with multiple solution phases, the numerics do not get significantly complicated. In fact, the number of simultaneous linear equations to be solved is equal to the number of system components and the number of phases estimated to be stable at equilibrium [31, 36–38].

Over a period of time, a number of other techniques have been proposed for the thermochemical equilibrium problem. Most of them, however, have relied on the original GEM

method [32] as the fundamental approach with minor modifications to adapt to the nature of specific problem at hand. These modifications include accounting for charged species [39], accounting for non-traditional effects such as surface tension [40], magnetic ordering [41] and Donnan effect [42]. Some of the more significant variations, such as the *First Order Steepest Descent Method* proposed by Storey and van Zeggeren [43], demonstrated poorer performance and lacked the ability to distinguish between local minima and maxima [31, 43]. Another variation relies on removing the mass balance constraint resulting in an unconstrained optimisation problem. This method, proposed by Lantagne et al. and based on a penalty function using the Broyden-Fletcher-Goldfarb-Shanno (BFGS), technique simultaneously minimises two objective functions - Gibbs energy of the system and the residual of the mass constraint vector [44, 45]. The method must also satisfy the linear inequality constraints related to mole numbers being non-negative. While the approach offers the advantage of solving fewer linear equations, the dual optimisation method is less numerically stable compared to single optimisation methods [45].

An impediment in numerically solving thermodynamic equilibria is the requirement of an initial estimate for the optimisation. Eriksson and Thompson [46] proposed a method called *Levelling*, which is capable of closely estimating the dominant species and their quantities in the phase assemblage. The process requires a relatively small number of iterations and the number of iterations to reach convergence does not rapidly increase with the number of species in the system. These characteristics of levelling are well suited to large systems, such as nuclear materials. Another problem that arises when using GEM method is the negative mole fraction arising due to the evaluation of logarithmic term while computing the chemical potentials. White et al. proposed using a numerical dampening technique to avoid erroneous results. Finally, ensuring that the Gibbs energy of the system is at global minimum and not at one of the many local equilibria is a significant challenge that must be handled properly to ensure correct results. Despite the challenges, GEM has been shown to be the best available method for computing thermodynamic equilibrium and is the de-facto default solver in almost all the thermodynamic equilibrium codes. Piro and Simunovic [47] proposed an enhancement to levelling, which they called *Post-Levelling*, to further improve on the initial estimate. In addition to the reference Gibbs energy terms, post-levelling accounts for the ideal mixing terms as well but unlike the non-linear solver, it doesn't take into account non-linear mixing. Though the method showed decent performance gains, it was often sensitive to the thermodynamic system in consideration.

Another problem that can significantly compromise the performance of thermodynamic equilibrium codes is the need to change the phase assemblage when a phase which may yield

a lower Gibbs energy is identified. One must make several decisions when doing this - can a phase be directly added without violating conditions of equilibrium? If not, does a phase need to be removed and which phase will result in the quickest convergence. There has been no discussion of algorithms for handling phase change except for Piro and Simunovic [47] who proposed a strategy for managing these choices. Together, many of these algorithms can have significant impact on the performance of thermodynamic equilibrium solvers and even the simplest strategies can sometimes lead to significant performance gains.

### 3.1.3. Partitioning of Gibbs energy (PGE)

The developer of Gibbs energy minimisation, W.B. White, proposed another numerical technique named *Partitioning of Free Energy* [48], which is substantially different from the GEM method. In this method, the mass equations are differentiated with respect to Lagrange multipliers and though a number of numerical advantages were shown, the method was only applicable to homogeneous systems comprised of ideal gas and could not be used for heterogeneous systems involving pure stoichiometric phases and/or multiple solution phases [31, 48]. The significant disadvantages of this method compared to GEM led to it being mostly dismissed by the thermodynamic community until Piro [49] reconsidered a modified form of the method by incorporating principles of the levelling method and employed it in an earlier version of the thermochemistry library Thermochimica [50]. Piro called the modified method Partitioning of Gibbs Energy (PGE)

Piro's approach [50] constrains Gibbs' phase rule while iterating to satisfy the mass balance constraint. The method constrains the chemical potential of all species and phases in terms of the chemical potentials of the system components, thus formally relating the mass balance equations to the chemical potentials of the system components. The objective of the method is to partition the Gibbs energy of the system among the elements to minimise the residuals of the mass balances. Thus, in this method, the solver attempts to find the roots of the mass balance residual vector while the Gibbs criteria is inherently verified and need not be verified at every iteration thus simplifying the numerical approach. This approach can then be used for heterogeneous systems, which may include stoichiometric phases, ideal solution phases and even non-ideal solution phases.

Numerically, GEM is an optimisation procedure while PGE solves for the roots of a simultaneous system of linear equations [31]. As a result, the chemical potential terms for the solution phase are included in the GEM method but absent from the functional vectors in PGE. Additionally, the approaches differ in the computation of a new set of mole numbers, which must be positive. Computation of non-negative logarithmic terms can result in non-real numbers in

GEM causing numerical difficulties and necessitating the use of numerical dampening which in turn reduces the rate of convergence. However, in PGE, additional dampening is not required since the mole fractions, being defined as exponentials of real numbers, will always be positive.

A disadvantage of the PGE method is that it requires moles fractions to be explicitly expressed as functions of chemical potentials of the species. As shown before, chemical potentials of the species can be uniquely expressed as a functions of mole fraction but not the other way around. Thus for non-ideal species, the PGE method fails in the absence of explicit functions of mole fractions in terms of chemical potentials. Despite all its numerical advantages, the PGE method proved to be less robust than the GEM approach and was eventually replaced by GEM in Thermochimica [51]. Though promising, the method has only been used in a limited number of other applications, a couple of them being by Riel et al. [52] and by Kruskopf [53].

### 3.1.4. Other methods

Several other numerical methods have been proposed for computing thermodynamic equilibria but none has received success like GEM. The most notable of these is the approach by Srinivas and Rangaiah which uses the *Random Tunnelling Algorithm (RTA)* based on the concept of *Terminal Repeller and Unconstrained Subenergy Tunnelling (TRUST)* algorithm [54]. The TRUST algorithm is akin to the steepest descent method but differs in that the minimisation is performed in two stages - a local minimisation followed by global minimisation through tunnelling [45]. However, the method is limited by the system size and shows satisfactory performance for relatively small systems of up to 10 variable [45].

Another method that was proposed by the developers of the GEM method is based on linear programming. George B. Dantzig applied the *Simplex* method to thermodynamic equilibrium problem at constant temperature and pressure [55, 56]. In the simplex method, a linear approximation of Gibbs energy of the system is minimised instead of the non-linear system. The linearised model is obtained by representing the logarithmic function in the chemical potential term by the following:

$$\beta_i = \alpha_i \ln \alpha_i \tag{3.2}$$

which is represented as a piecewise linear approximation as shown in fig. 3.1. Though the Simplex method has been successful in many optimisation problems [57], the linearisation of $\beta$ generates a relatively large number of additional unknowns and the computational expense becomes quite large. Furthermore, the method is unable to determine the composition of dilute species [31]. As a result, the simplex method has not received widespread usage in thermodynamic equilibrium calculations.

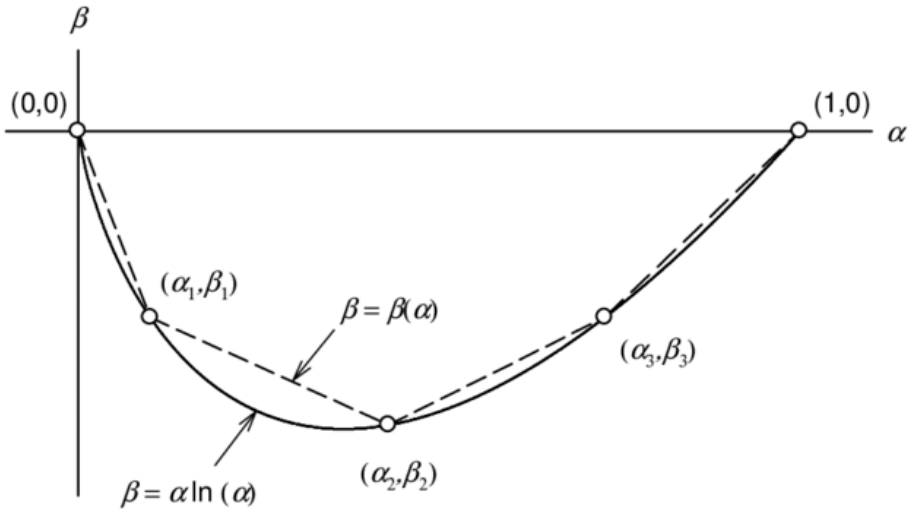


Figure 3.1: Approximation of the function $\beta$ in Simplex method. Reproduced by Piro [49] from Dantzig et al. [55]

### 3.1.5. Gibbs energy minimisers (GEM)

Over the years, a number of codes have been developed to compute thermodynamic equilibria in complex systems and many of these codes are summarised in Table 3.1. The most noticeable of these codes include SOLGAS [58] and its successor SOLGASMIX [37], which are well known for their versatility, computational efficiency and the widespread availability of source code. Moreover, SOLGAS has been used as the solver in codes like HSC [59], ChemSage [41] and FACT [60]. FACT combined the thermodynamic equilibrium solver with a comprehensive thermodynamic database and, by implementing the levelling method, eliminated the need for the user to manually input initial estimates. This made FACT a popular choice in the thermodynamics community. FACT merged with ChemSage to create a new standalone software called FactSage [61], which is the current version of the SOLGAS family. Another app in the family, called ChemApp [62, 63], is a software library that can be called from external codes and has similar capabilities as FactSage.

Another family of popular thermodynamic equilibria tools is ThermoCalc [64] and is widely used in thermodynamic model development, thermodynamic equilibrium calculations, and phase diagram construction. It has been developed for complex heterogeneous interaction systems with strongly non-ideal solution phases and can be applied to any thermodynamic system in the fields of chemistry, metallurgy, material science, alloy development, geochemistry, semiconductors etc. depending on the kind of database it is connected to. A unique advantage of ThermoCalc compared to other thermodynamic codes is that it allows explicit conditions on individual phase compositions or configuration whereas most software can handle conditions on

the overall composition only. For example, activities and chemical potentials of the components, volumes, enthalpies, entropies etc can also be set as conditions. OpenCalphad [65] is an open-source code led by Bo Sundmann, one of the original developers of ThermoCalc, and it aims to provide facilities for multicomponent equilibrium calculations using the Compound Energy Formalism (CEF) and other models both for interactive calculations and in application software. It has been designed to allow interested scientists to develop thermodynamic models and assess model parameters for thermodynamic databases to describe experimental data as well as theoretical results from Density Functional Theory (DFT) calculations to calculate phase equilibria and phase diagrams. Another notable code developed with the goal of enabling uncertainty quantification is PyCalphad developed by Otis et al. [66].

Amongst the many thermodynamic equilibrium codes available in the open literature, one of the common limitations pertains to the relatively small number of standalone calculations that these codes are designed to perform. While suitable for problem specific calculations, where a few failures in convergence would have no significant bearing on the performance, these codes cannot be integrated into multiphysics softwares. In addition, since the mathematical difficulty in achieving convergence increases with the number of phases that can coexist in the system, most of these softwares limit the maximum number of phases and system components that can be simultaneously considered. While this has no bearing on applications such as combustion, the limited number of phases that can be solved creates a severe impediment for nuclear applications.

In the nuclear materials community, three code families have garnered particular attention - GEMINI [67], ThermoCalc [64] and FactSage [61]. Due to their established reputation in the nuclear community, these codes have traditionally been applied in development of several thermodynamic treatments for nuclear fuels and materials. In fact, these three codes offer a number of advantages over the other codes reviewed here, including the capability of handling a very large number of system components, phases and species, and the ability to use a wide range of sophisticated thermodynamic models.

Table 3.1 summarises the current thermodynamic equilibrium codes which are available in open literature. The table classifies codes based on the choice of algorithms and the class of thermodynamic models that they support. While not explicitly written out in the table, most of the codes are only designed for handling small systems and aimed at creating phase diagrams. Of more interest to this work is the Modified Quasichemcial Model in Quadruplet Approximation (MQMQA) model since it is the model most commonly used to describe molten salts. In fact, apart from commercial code FactSage in which the model was initially implemented, most codes did not support MQMQA until very recently. Recently, however, and in conjunction with the

work done in this thesis, this model has been implemented in Thermochimica [68]. Lastly, only very recently, the model has been implemented in PyCalphad [69]. Even beyond MQMQA, most papers in the open literature don't give sufficient details about models for one to easily adopt them into their own programming.

Table 3.1: A review of the major thermodynamic equilibrium codes.

| Code / Author | Method | Models | | | |
|---|---|---|---|---|---|
| | | Stoich. | Ideal | Non-ideal | Ionic |
| ANGE (SAGE) [70] | GEM | Yes | Yes | Yes | Yes |
| CALMIX [71] | GEM | Yes | Yes | Yes | No |
| Cantera [72] | GEM | No | Yes | Yes | No |
| Castier et al. [73] | GEM | No | Yes | No | No |
| CatCalc [74] | GEM | Yes | Yes | Yes | No |
| CEA [75] | GEM | Yes | Yes | No | No |
| ChemApp [62] | GEM | Yes | Yes | Yes | Yes |
| ChemSage [41] | GEM | Yes | Yes | Yes | Yes |
| ChemSheet [76] | GEM | Yes | Yes | Yes | Yes |
| COEXIST [77] | Levelling | Yes | No | No | No |
| Dantzig et al. [56] | Simplex | No | Yes | No | No |
| Ebel et al. [78] | BNR | Yes | Yes | No | No |
| ESP [79] | LMA | No | Yes | No | No |
| FACT [60] | GEM | Yes | Yes | Yes | Yes |
| FactSage [80] | GEM | Yes | Yes | Yes | Yes |
| GEMINI 1 [67] | GEM | Yes | Yes | No | No |
| GEMINI 2 [67] | GEM | Yes | Yes | Yes | Yes |
| GEM-Selektor [81] | GEM | Yes | Yes | No | Yes |
| GEMIPM2K [81] | GEM | Yes | Yes | No | Yes |
| Gibbs [82] | C-Hull | | Yes | Yes | |
| GLOPEQ [83] | GEM* | No | Yes | No | No |
| HALTA [84] | LMA | No | Yes | No | No |
| HALTAFALL [85] | LMA | Yes | Yes | No | No |
| Han et al. [86] | LMA* | No | Yes | No | No |
| HSC [59] | GEM | Yes | Yes | Yes | Yes |
| Koukkari et al. [40] | Const. GEM | Yes | Yes | Yes | Yes |
| Kruskopf [53] | PGE | Yes | Yes | Yes | Yes |
| Lantagne et al. [44] | GEM | No | Yes | Yes | No |
| Lee et al. [87] | GEM | No | Yes | Yes | No |
| Lukas et al. [88] | GEM | Yes | Yes | Yes | No |
| MAGEMin [52] | PGE | | Yes | Yes | |
| MatCalc [89] | GEM | | Yes | Yes | |
| MTDATA [90] | GEM | No | Yes | Yes | No |
| NUTS [91] | GEM | Yes | Yes | Yes | Yes |
| OpenCalphad [65] | GEM | Yes | Yes | Yes | Yes |
| PANDAT [92] | GEM | Yes | Yes | Yes | Yes |
| Pereira et al. [93] | HEM | No | Yes | No | No |
| PyCalphad [66] | Lower C-Hull | Yes | Yes | Yes | No |

Table 3.1: A review of the major thermodynamic equilibrium codes (contd).

| Code / Author | Method | Models | | | |
|---|---|---|---|---|---|
| | | Stoich. | Ideal | Non-ideal | Ionic |
| Rossi et al. [94] | GEM | Yes | Yes | No | No |
| Schnedler [95] | GEM | Yes | Yes | No | No |
| Smith and Missen [96] | GEM | No | Yes | No | No |
| SOLGAS [58] | GEM | No | Yes | No | No |
| SOLGASMIX [37] | GEM | Yes | Yes | Yes | No |
| SOLGASMIX-PV [97] | GEM | Yes | Yes | Yes | No |
| SOLGASWATER [39] | GEM | Yes | Yes | Yes | Yes |
| Song et al. [98] | GEM* | Yes | Yes | No | No |
| Srinivas et al. [54] | GEM-RTA | No | Yes | No | No |
| STANJAN / EQUIL [99] | PGE | No | Yes | No | No |
| Storey et al. [43] | GEM | Yes | Yes | No | No |
| THERIAK [100] | GEM | No | Yes | Yes | No |
| ThermoCalc [64] | GEM | Yes | Yes | Yes | Yes |
| Thermochimica [50] | GEM | Yes | Yes | Yes | Yes |
| ThermoSolver [49] | PGE | Yes | Yes | Yes | Yes |
| VICTORIA [101] | LMA | Yes | Yes | No | No |
| White et al. [32] | GEM | No | Yes | No | No |
| NASA [35] | NASA | No | Yes | No | No |

## 3.2. Global Optimisation

Calculation of thermodynamic equilibrium is a challenging problem since the objective functions are multivariable and can often be non-convex and highly non-linear. Furthermore, additional complexities arise near the phase boundaries, in the vicinity of critical points, etc. [102, 103]. Over the years, a number of different methods have been proposed to find the global minimum for non-convex problems in the applied mathematics community. These methods can be classified into stochastic and deterministic methods. However, even with a large number of different methods available in the literature, finding a method that can be applied to all types of problems has proven impractical. The success of every method is problem-specific and most of the methods reported in the literature have focussed on either relatively small systems, such as liquid-vapour equilibria, or perform relatively small number of calculations.

### 3.2.1. Deterministic methods

Deterministic optimisation methods exploit the analytical properties of the problem to generate a deterministic sequence of points converging to a global optimum [104]. While these methods can provide a guaranteed global optimum, they require certain properties of objective function

and constraints such a continuity and convexity. These methods include the *Branch & Bound (BB)* algorithm, *Homotopy Continuation Methods* and *Interval Analysis* [105].

The branch and bound algorithm is a class of adaptive partitioning strategies that iteratively apply partitioning, sampling and subsequent upper and lower bounding procedures to solve global optimisation problems [105]. These methods typically rely on some a priori knowledge of the form of the objective function to develop convex terms of the optimisation problem. However, they are often computationally expensive and slow [102, 106] because the method recursively splits the search space into smaller subspaces and performs function evaluations within each subspace. The homotopy continuation method provides a smooth transition between an approximate solution (often linear) and the true solutions of a non-linear system of equations by gradually introducing the non-linearities through a scalar homotopy parameter [107, 108]. As a result, the method is capable of finding all roots of a set of non-linear equations. While the method guarantees global convergence to a single solution, it does not guarantee global convergence to multiple solutions. Moreover, the method has been successfully demonstrated only for simple polynomials [109]. For the case of thermodynamic equilibrium calculations, Piro and Simunovic [110] have shown that the branch and bound algorithm has proven to be the most promising of all deterministic methods

### 3.2.2. Stochastic methods

By employing probabilistic elements and using random sequences in the search for the global optimum, stochastic methods provide a high probabilistic convergence to global minimum with little or no assumption on the characteristics of the optimisation problem [111]. These methods employ heuristics for exploring (diversification) and exploiting (intensification) the search space, and learning strategies are used to find near-optimal solutions at a rapid speed [112]. This class of optimisation methods include *Random Search*, *Tabu Search*, *RTA*, *Particle Swarm Optimisation (PSO)*, *TRUST*, etc.

The pure random search algorithm by Brooks [113] is based on generating a sequence of uniformly distributed points in the search space, while keeping a track of the best point that was already found. The method offers a probabilistic asymptotic guarantee that a global minimum will be found with probability equal to one when the sample size grows to infinity. Luus and Jaakola have proposed an *Adaptive Random Search* algorithm which uses random points and systematic region reduction for locating the global optimum [114].

The Tabu search algorithm proposed by Glover and Laguna [115] is aimed at enhancing the searching capability of the solution space economically and effectively by discarding the points in the solution space, which have been previously evaluated and found to be not feasible. The

method has been successfully applied to a wide range of optimisation problems but applications to thermodynamic equilibrium computations have been limited [116, 117]. One of the other notable algorithms is the random tunnelling algorithm which is a derivative of the TRUST algorithm. The TRUST algorithm [118] combines the novel concepts of subenergy tunneling, and non-Lipschitzian terminal repellers. In subenergy tunnelling, non-linear transformation is applied to the objective function resulting in the values of the function that are greater than the value at the current local minimum to be set equal to the current minimum. This flattens the search space and the process gets trapped at the current position because the successive gradients remain within the stopping criterion. At this point, the terminal repeller gets activated to allow an escape from the current solution to a point where the function begins another descent. The random tunnelling algorithm. on the other hand, consists of a combination of a local and global phase. In the global phase, the system is randomly perturbed from the last local minimum and a system of differential equations is solved from the perturbed point to explore new regions of attraction. The local phase employs a fast convergent Quasi-Newton minimisation technique to find an improved point in the new region. Amongst the stochastic global optimisation algorithms, Piro and Simunovic [110] have shown that the particle swarm algorithm has proven to be the most promising of all stochastic methods.

The diversification and intensification plays a key role in ensuring a compromise between reliability and computational efficiency of stochastic algorithms and while the stochastic algorithms can often locate the global minimum in modest computational times compared to deterministic methods, they do not guarantee global optimality [109, 112].

### 3.2.3. Global optimisation review

A few of the studies on global optimisation in thermodynamic equilibrium calculation have been summarised in table 3.2. While most of the global optimisation methods applied to phase equilibrium have been studied with reference to liquid-liquid or vapour-liquid equilibrium, a few of the remarkable ones can be applied to more general phase equilibrium problems. Chaikunchuensakun et al. [119] applied a hybrid algorithm based on non-linear parametric optimisation routines which solves the Kuhn-Tucker conditions by minimising a quadratic subproblem with linearised equality and inequality constraints. While the method can equilibrium solutions, a global solution cannot be guaranteed [109]. Another notable study is by Nichita et al. [106] who tested the tunnelling method for multi-phase equilibrium calculation by direct minimisation of Gibbs energy of the components. Rossi et al. [94] applied a convex analysis method to chemical and phase equilibrium of closed multi-component reactive system. Though the method is highly efficient and reliable, it is only applicable to convex functions. A duality

based approach proposed by Pereira et al. [93] can guarantee the global optimum but requires a differentiable objective function [109].

Amongst the stochastic methods, the most notable works are from Teh and Rangaiah [117] who show that the tabu search is more efficient that the genetic algorithm but requires further improvement for 100% reliability. However, the system size considered by them is relatively small. Srinivas and Rangaiah [54] used the RTA which can evaluate the global minimum for most of the examples tested but suffers from low reliability and is feasible only for small systems.

In conclusion, the available literature suggests that both deterministic and stochastic methods face difficulties for highly non-ideal mixtures and are prone to convergence problems. Moreover, many of the studies assume the number of phases that would be stable to be known *a priori* which is not true and limits capability. As a result, several calculations must be performed using different combination of phases to arrive at the true global minimum. The global optimisation problem applied to computational thermodynamics warrants a more effective and rigorous study of both deterministic and stochastic methods applied to a variety of case studies with varying levels of complexity. An effort in this direction was made by Piro and Simunovic [110] and they found the PSO and BB algorithms to be the most promising stochastic and deterministic methods, respectively.

## 3.3. Multiphysics Integration of Computational Thermodynamics

Interest in incorporating thermodynamic equilibrium calculations in multiphysics simulations has been relatively recent. Even though the importance of thermodynamic variables in various physical simulations has been long recognised, the limitations on computational resources along with the high cost of equilibrium calculations made thermodynamically informed coupled simulations infeasible for most simulations beyond those aimed at purely demonstrating capability. However, over the last few years, the efforts towards coupling thermochemistry have been ever-increasing. Some of such coupling efforts, primarily the ones focused on nuclear applications are reviewed here.

Most of the applications of coupling computational thermochemistry have been in nuclear fuel codes with some applications in microstructural evolution using phase field method and even lesser applications in safety analyses. A couple of works that have coupled computational thermodynamics with the commercial software package COMSOL include those of Higgs et al. [135] and Welland et al. [136]. Piro integrated the thermochemistry solver Thermochimica into the Advanced Multi-Physics AMP code developed by Oak Ridge National Laboratory [49]. This allowed the investigation of an irradiated fuel pellet by using isotopic evolution of irradiated nuclear fuel which was calculated through the software package ORIGEN.

Table 3.2: A review of the global optimisation methods applied to thermodynamic equilibrium calculations.

| Method | Class | Problem Formulation |
|---|---|---|
| Sampling [120, 121] | Deterministic | Gibbs energy |
| Branch and Bound [122] | Deterministic | Potential energy |
| Branch and Bound [110] | Deterministic | Gibbs energy |
| Convex optimisation [94] | Deterministic | Gibbs energy |
| Differential evolution and tabu search [116] | Stochastic | Gibbs energy |
| Differential evolution with tabu list [123] | Stochastic | Gibbs energy |
| Duality based optimisation [93] | Deterministic | Helmholtz energy |
| Enhanced simulated annealing [124] | Stochastic | Gibbs energy |
| Enhanced tabu search [117] | Stochastic | Gibbs energy |
| Genetic algorithm and simulated annealing [125] | Stochastic | Gibbs energy |
| Genetic algorithm and differential evolution with tabu list [126] | Stochastic | Gibbs energy with reaction |
| Hybrid artificial immune system [127] | Stochastic | Gibbs energy with reaction |
| Hybrid genetic algorithm with interior point method [128] | Stochastic | Gibbs energy |
| Interval analysis [129] | Deterministic | Gibbs energy surface |
| Nonlinear parametric optimisation [119] | Deterministic | Gibbs energy |
| Particle swarm optimisation [110, 130, 131] | Stochastic | Gibbs energy |
| Random tunnelling algorithm [54] | Stochastic | Gibbs energy |
| Simulated annealing [132] | Stochastic | Gibbs energy |
| Successive quadratic programming [133] | Deterministic | Gibbs energy |
| Tunnelling method [106, 134] | Deterministic | Gibbs energy |

The software integration of Thermochimica with BISON was performed by Simunovic et al. [137]. Use of Thermochimica was demonstrated by modelling oxygen transport in irradiated $UO_2$ oxide fuel, such as calculation of oxygen to metal ratio in the fluorite phase, oxygen partial pressure, oxygen chemical potential and oxygen transport. Experimental measurements from the open literature were used to validate the implemented models and illustrate functionality of the developed thermodynamics module. The calculations were based on chemical element inventory provided by neutronics, isotopic depletion, transmutation and decay calculations using the ORIGEN-S software[138]. To overcome some of the computational cost increase observed by Simunovic et al., Poschmann et al. used a reinitialisation strategy whereby the Thermochimica results were saved at each node at each time step and used to initialise the calculations at the next time step [139]. Poschmann et al. [140] extended the model by Simunovic et al. to simulate the U and Zr interdiffusion in U−Pu−Zr metallic fuel. A similar effort by Hirschhorn et al. used BISON as well but with pre-computed thermodynamic values obtained from PyCalphad

[141].

In France, 3D coupled multiphysics simulations of power ramps in Pressurised Water Reactors (PWRs) were performed by Baurens et al. [70] and Konarski et al. [142]. The fuel performance code ALCYONE, which is part of the computing environment PLEIADES, was coupled with the thermodynamics code ANGE to provide a description of irradiated fuel thermochemistry with oxygen transport taking into account thermodiffusion. Konarski et al. also performed Pellet Cladding interaction (PCI) failure analyses [143], by coupling thermochemistry and thermo-mechanics to investigate both chemical and mechanical factors simultaneously. 3D thermochemical-mechanical simulations of PWR power ramps on Cr-doped $UO_2$ with the fuel performance code ALCYONE including oxygen transport were performed to study the impact of oxygen redistribution on irradiated fuel thermochemistry and on chemically reactive fission gas release. OpenCalphad has been coupled with ALCYONE for several applications such as those by Michel et al. [144] and Introïni et al. Introïni et al. proposed multiple coupling strategies to improve the computational performance of the OpenCalphad - ALCYONE coupling and through a set of numerical experiments, demonstrated the performance gain compared to ANGE - ALCYONE coupling. Another code in the PLEIADES environment is GERMINAL which is specifically aimed at Sodium-cooled Fast Reactors (SFRs) and was coupled to OpenCalphad by Samuelsson et al. [145] to model Joint Oxyde-Gaine (JOG) [146].

Use of thermodynamic equilibrium data finds a lot of value in phase field calculations where quantities like Gibbs energy, chemical potentials are all required as inputs. Among the first applications of such coupling were those in the field of metallurgy like those by Grafe et al. [147] and Chen et al. [148] Several other models have been developed with some examples being of those by Zhang et al. [149] who directly incorporated CALPHAD into the phase-field formalism and validated the coupling technique for $Fe-C$ and $Ni-Al$ alloys and by Schwen et al. [150] who used PyCalphad for thermodynamic data in MOOSE-based phase field application Marmot. Schwen et al. have also developed a multiphase field model for better integration of thermodynamic phases with multiple sublattices in the phase field model implemented in MOOSE [151]. Other similar works include those of Böttger et al. [152], Chatterjee and Moelens [153], Zuo et al. [154] and Coutinho et al. [155].

Among other applications, Poschmann et al. [156] coupled Thermochimica to dynamic systems modelling software TRANSFORM for dynamic mass accountancy in liquid-fuelled MSRs and Fitzpatrick et al. [157] coupled Thermochimica with thermal-hydraulics code COBRA-TF and isotopic evolution code ORIGEN to demonstrate fission product transportation by coolant flow in molten salt reactors. Thermochimica has recently been coupled with MELCOR for severe accident modelling in Boiling Water Reactors (BWRs) [158].

Thus, thermodynamic equilibrium calculations have found applications in modelling and simulation of several physical phenomena. Full integration of a thermodynamic equilibrium code in MOOSE would make such coupled calculations easy and allow high fidelity multiphysics simulations allowing much more realistic simulations of various problems. In doing so, however, one must be considerate of the increase in computational cost and should carefully do a cost-benefit analysis before proceeding with such high-fidelity but costly simulations.

## 3.4. Summary

Computing thermodynamic equilibrium is a challenging problem and over the years a large number of software codes have been developed to tackle it. Most of these codes can be classified into three broad categories based on the numerical methods and the most popular numerical method has undoubtedly been White's method based on Lagrange multipliers which is now often described as the Gibbs Energy Minimisation method. Despite numerous codes existing in literature, there are several limitations that must be addressed as part of this work. Firstly, a majority of the codes are designed for small systems and mostly aimed at phase diagram construction. Secondly, until very recently only FactSage supported MQMQA and even now only Thermochimica and PyCalphad have added support for it. Thirdly, most of the codes have been designed as standalone applications instead of for coupling to other codes. Lastly, the state of global optimisation algorithms used in thermodynamic equilibrium is relatively simplistic. Most codes designed for general applications use simple sampling methods and the few codes which use better global optimisation algorithms are designed for very simple problems such as liquid vapour equilibrium. Furthermore, there's almost no systemic study of optimisation algorithms and their performance when applied to equilibrium problems of reasonable complexity. For any general thermodynamic equilibrium solver developed for multiphysics simulations, such as the one in this work, several of these limitations must be addressed.

# 4

# Thermodynamic Basis

*Die Energie der Welt ist konstant.*
*Die Entropie der Welt strebt einem Maximum zu.*

Rudolf Clausius

*The laws that govern all material systems can be expressed in the two seemingly simple statements of Rudolf Clausius mentioned above which translate to* "The energy of the universe is constant. The entropy of the universe tends to a maximum.". *Yet thermodynamics has drawn the attention of many great scientists including Maxwell, Boltzmann, Planck and Mach. A number of definitions and laws of thermodynamics form the basis of equilibrium thermodynamics and the Gibbs energy models and equations play a key role in the structure of the equilibrium solver. This chapter discusses these fundamental laws of thermodynamics and defines the key thermodynamic properties of the system. This is followed by a description of the Gibbs energy models and chemical potential which are the main thermodynamic properties used in this work. Finally, the derivations of chemical potentials for the thermodynamic models used in this work are shown via the articles which were first published as part of this work.*

## **4.1.** Fundamental Laws of Thermodynamics

The statements of Rudolf Clausius are now known as the *First and Second Laws of Thermodynamics*. Before looking at these laws, the basic definitions used in subsequent sections are

reviewed for clarity. A *thermodynamic system* is a portion of the universe with a perimeter defined by real or imaginary boundaries and usually consists of many chemical components whose thermodynamic behaviour can be analysed. For example, the volume element shown in Figure 4.1 can be treated as a thermodynamic system. A system that may exchange matter with its system boundary is called *open* while a system that can only exchange energy and not matter is called *closed*. The term *isolated* is used for a system that is cut off from the surroundings and can neither exchange matter nor energy. In material thermodynamics, the system is often treated as closed, notable exceptions being chemical reactors where reactants and products continuously flow in and out of the system.

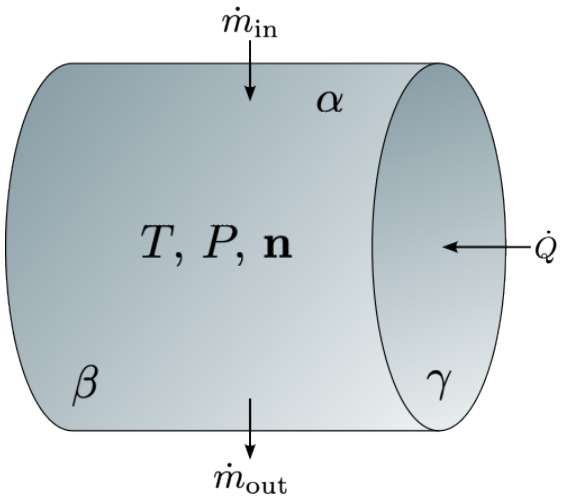


Figure 4.1: Volume element of a general thermodynamic system with mass flow of chemical components $\dot{m}$ and heat flux $\dot{Q}$. The Greek letters indicate presence of separate phases.

A thermodynamic system can be described macroscopically using *state variables*, which are represented by measurable macroscopic quantities such as temperature, pressure, volume, amounts of different substances, etc. *Intensive variables* (e.g. temperature and pressure) are independent of the amount of matter in the system while *extensive variables* (e.g. volume and total internal energy) are dependent on the mass of the system. With a change in the internal variables, the system undergoes a change in state. If a system can be restored to the original condition without any change in the state of the surroundings, the process through which the state of the system was changes is described as a *reversible process*. However, all real processes are *irreversible processes*, that is, the system cannot be recycled.

Thermodynamics concerns the condition of a system as it interacts with its surroundings and is based on two physical laws: the first and second laws of thermodynamics. The first law of thermodynamics describes those interactions, which can involve exchanges of any combinations of heat, work, and mass, while the second law of thermodynamics governs the evolution of

conditions inside the system. Together, the two laws integrate the external and internal parts of the system.

### 4.1.1. First law of thermodynamics

The first statement of Clausius and what is now known as the first law of thermodynamics expresses the conservation of energy[1] and is formulated as follows:

> Energy cannot be created or destroyed, and the energy increase of a system ($dU$) equals the sum of the heat absorbed from the surroundings ($dQ$) and the work ($dW$) done by the surroundings on the system.

Mathematically, for an open system, the first law can be expressed as:

$$dU = dQ + dW + \sum H_i dN_i, \tag{4.1}$$

where $dN_i$ denotes the amount of component $i$ exchanged with the surroundings and $H_i$ is the unit energy of component $i$ in the surroundings, and the summation is for all the independent components in the system. Since the systems of interest in thermodynamics of materials are closed, there is no exchange of matter between the system and the surroundings and the first law of thermodynamics takes the following form:

$$dU = dQ + dW, \tag{4.2}$$

where both $dQ$ and $dW$ depend on the thermodynamic process and hence do not qualify as state functions.

### 4.1.2. Second law of thermodynamics

In 1850, Clausius formulated a criterion for the direction of spontaneous processes and called it *entropy*. His second statement translates to entropy of the universe tends to maximum and is now known as the second law of thermodynamics. Formally, the second law states that:

> For an internal process to take place spontaneously, or irreversibly, the change in entropy of the system ($dS$) must be positive.

[1] Considering Einstein's mass-energy equivalency, the classical first law can be modified to state that mass and energy together are constant. However, since we are considering chemical equilibrium and not dealing with nuclear reactions, the classical form of first law applies.

In mathematical form, the second law can be formulated as:

$$dS = dS_{\text{sys}} + dS_{\text{surr}} \geq 0, \tag{4.3}$$

where the $S_{\text{sys}}$ and $S_{\text{surr}}$ represents the entropy of the system and surroundings respectively. In the course of a reversible, isothermal process, the entropy change of the system $dS_{\text{sys}}$ can be defined as the heat exchange divided by temperature:

$$dS_{\text{sys}} = \frac{dQ}{T}. \tag{4.4}$$

### 4.1.3. Third law of thermodynamics

The third law of thermodynamics allows expressing the absolute value of the entropy in contrast to the internal energy by assigning an entropy equal to zero at $0\,\text{K}$ for any pure compound in stable and perfectly crystalline state.

## 4.2. Enthalpy, and Helmholtz and Gibbs Energies

Three important state functions of great practical importance in thermodynamics are the *enthalpy* $H$, *Helmholtz energy* $F$, and *Gibbs energy* $G$. Enthalpy changes are of importance in calorimetry experiments as they can be directly measured while Helmholtz and Gibbs energies are used in defining chemical equilibrium conditions.

The enthalpy of a thermodynamic system is an extensive property defined as:

$$H = U + PV, \tag{4.5}$$

where $U$ denotes the internal energy, $P$ denotes the hydrostatic pressure the system is at and $V$ represents the volume of the system.

The Helmholtz energy of a thermodynamic system is defined as:

$$F = U - TS, \tag{4.6}$$

where $T$ denotes the absolute temperature of the system and $S$ represents the entropy of the system.

The Gibbs energy of a thermodynamic system is defined as:

$$G = H - TS. \tag{4.7}$$

The equilibrium criterion can be derived in terms of Helmholtz and Gibbs energies. According to the second law of thermodynamics, a spontaneous irreversible process must be accompanied by an overall positive change of entropy, i.e.:

$$dS_{\text{sys}} + dS_{\text{surr}} > 0. \tag{4.8}$$

For a closed system in thermal and mechanical equilibrium but not in chemical equilibrium which acquires an infinitesimal quantity of heat from the surroundings:

$$dS_{\text{surr}} = -\frac{dQ_{\text{sys}}}{T}, \tag{4.9}$$

where it is assumed that the mass of the surroundings is large enough so that addition/removal of the heat does not cause a perceptible change in temperature. Thus,

$$dQ_{\text{sys}} - TdS_{\text{sys}} < 0. \tag{4.10}$$

Assuming that the heat exchange causes an infinitesimal change in the internal energy of the system by an amount $dU_{\text{sys}}$, according to the first law of thermodynamics,

$$dU_{\text{sys}} = dQ_{\text{sys}} + dW_{\text{sys}}. \tag{4.11}$$

For a closed, isobaric system the work is purely due to the change in the volume of the system and the following relationship is obtained:

$$dU_{\text{sys}} + PdV_{\text{sys}} - TdS_{\text{sys}} < 0. \tag{4.12}$$

If both the temperature and volume were held constant, the above inequality becomes:

$$d\left(U_{\text{sys}} - TS_{\text{sys}}\right)_{T,V} < 0. \tag{4.13}$$

Since the terms within the parentheses denote the Helmholtz energy, one obtains the criterion for spontaneous change of isothermal, isochoric system, which is expressed as:

$$dF_{\text{sys}} < 0. \tag{4.14}$$

Similarly, if the temperature and pressure were held constant, the inequality becomes:

$$d(U_{\text{sys}} + PV_{\text{sys}} - TS_{\text{sys}})_{T,P} < 0. \tag{4.15}$$

The terms inside the parentheses denote the Gibbs energy and subsequently yield the criterion for spontaneous change of an isothermal, isobaric system:

$$dG_{\text{sys}} < 0. \tag{4.16}$$

Thus, for the equilibrium of a closed system at constant temperature and volume, it is necessary and sufficient that the Helmholtz energy of the system is at minimum and equivalently, the Gibbs energy of the system must be at minimum for equilibrium in systems at constant temperature and pressure. In equilibrium thermodynamics, Gibbs energy is often preferred over Helmholtz energy since controlling pressure is easier than controlling volume during experiments. It must be emphasised that thermodynamic properties are fundamentally concerned with relative changes, a property that is often exploited in computations.

## 4.3. Gibbs Energy and Chemical Potential

Of particular interest in description of thermodynamic equilibrium are the quantities named *potentials*. A system is in thermodynamic equilibrium when it is simultaneously in thermal, mechanical, electrical and chemical equilibrium. This also refers to the state where there are no unbalanced potentials within the system. J.W. Gibbs used the term *thermodynamic potential* to represent all the relevant system potentials to characterise the conditions of thermodynamic equilibrium [159]. Thermodynamic equilibrium calculations are based on the principle that the potential for each component must be uniform throughout the system at thermodynamic equilibrium. This section and the following describe the relation between Gibbs energy and chemical potentials and their use in computing thermodynamic equilibrium.

The molar Gibbs energy, $g_i$ [J mol$^{-1}$], of a pure species $i$ is defined as [160]:

$$g_i = \Delta h_i - Ts_i, \tag{4.17}$$

where $\Delta h_i$ [J mol$^{-1}$] and $s_i$ [J mol$^{-1}$ K$^{-1}$] represent the molar enthalpy and absolute entropy of species $i$ in phase $\phi$ respectively. Many thermodynamic quantities, including Gibbs energy,

are relative in nature and equation (4.17) can be expanded as:

$$g_i = \left(\Delta h_i^\circ + \int_{T_0}^{T} c_{p,i} dT\right) - T\left(s_i^\circ + \int_{T_0}^{T} \frac{c_{p,i}}{T} dT\right) + \int_{P_0}^{P} V_i dP, \tag{4.18}$$

where $\Delta h_{i^\circ}$ [J mol$^{-1}$] and $s_i^\circ$ [J mol$^{-1}$ K$^{-1}$] are the standard enthalpy of formation and entropy respectively at standard temperature ($T_0 = 298.15$ K) and pressure ($P_0 = 1$ atm). The superscript / subscript $\circ$ represents a quantity at standard temperature and pressure, a notation that is used hereafter. $c_{p,i}$ [J mol$^{-1}$ K$^{-1}$] denotes the molar heat capacity at constant pressure, $P$ [atm] is the absolute pressure and $V_i$ [m$^3$ mol$^{-1}$] denotes the molar volume. For an ideal gas, from the gas law, the last term in equation (4.18) can be written as $RT \ln(P/P_0)$, where $R = 8.314462$ [J mol$^{-1}$ K$^{-1}$] is the ideal gas constant. For a pure ideal gas species $i$, the standard Gibbs energy is:

$$G_i = \left(\Delta H_i^\circ + \int_{T_0}^{T} C_{p,i} dT\right) - T\left(S_i^\circ + \int_{T_0}^{T} \frac{C_{p,i}}{T} dT - R \ln\left(\frac{P}{P_0}\right)\right). \tag{4.19}$$

The fact that Gibbs energies are relative quantities and can be numerically adjusted as long as the elemental differences are preserved is of practical importance and is often used in thermodynamic equilibrium calculation. Chemical potential of species $i$ in phase $\lambda$, $\mu_{i(\lambda)}$ [J mol$^{-1}$], is a measure of the change of the Gibbs energy of the system by the introduction of species $i$ and incorporates the reference Gibbs energy of pure species, $g_i^\circ$, and the entropic contribution due to mixing as a function of its mole fraction. Mathematically, the chemical potential of a species $i$ is defined as [160]:

$$\mu_i = \left(\frac{\partial G_{\text{sys}}}{\partial n_i}\right)_{T,P,n_{j\neq i}}. \tag{4.20}$$

For the species of a phase with only ideal mixing, the chemical potential is generally given as:

$$\tilde{\mu}_i = \tilde{g}_i^\circ + \ln x_i. \tag{4.21}$$

where $\tilde{\mu}_i$ represents the dimensionless form of the chemical potential of species $i$ and is given as $\tilde{\mu}_i = \mu_i / RT$[2]. For non-ideal solution phases, the chemical potential also includes the partial

[2]The dimensionless form $\tilde{\mu}_i$ has been used here as it reduces the number of floating point operations at each iteration and is the preferred form in computational implementations.

molar excess Gibbs energy of mixing, $g_i^{ex}$ [J mol$^{-1}$], to account for non-ideal mixing as follows:

$$\tilde{\mu}_i = \tilde{\mu}_i^{\circ} + \ln x_i + \tilde{\mu}_i^{ex}. \tag{4.22}$$

While the chemical potential of stoichiometric phases does not include a composition dependent term, the partial molar excess Gibbs energies of mixing for non-ideal solution models depend on the mixing model employed. Some of these models include the MQMQA [161–165], the CEF [166], etc. and are introduced in section 4.3.1.

The integral Gibbs energy of a multicomponent, multiphase system is represented as:

$$G_{\text{sys}} = RT \left( \sum_{\phi=1}^{\Phi} n_\phi \sum_{i=1}^{N_\phi} x_i \tilde{\mu}_i \right), \tag{4.23}$$

where $n_\phi$ denotes the number of species in phase $\phi$ of which there can be a maximum of $\Phi$ and $x_i$ represents the mole fraction of species $i$. For convenience, the Gibbs energy is often split into separate contributions from solution and stoichiometric phases as follows:

$$G_{\text{sys}} = RT \left( \sum_{\lambda=1}^{\Lambda} n_\lambda \sum_{i=1}^{N_\lambda} x_i \tilde{\mu}_i + \sum_{\omega=1}^{\Omega} n_\omega \tilde{\mu}_\omega \right), \tag{4.24}$$

$N_\lambda$ denotes the number of species in the solution phase $\lambda$ and $x_i$ represents the mole fraction of species $i$ in solution phase $\lambda$. $\Lambda$ and $\Omega$ represent the number of stable solution phases and stoichiometric phases, respectively, and the number of moles of the solution phase $\lambda$ and stoichiometric phase $\omega$ are denoted by $n_\lambda$ and $n_\omega$ [mol], respectively. Finally, $\tilde{\mu}_i$ and $\tilde{\mu}_\omega$ represent the dimensionless chemical potential of species $i$ in solution phase $\lambda$ and stoichiometric phase $\omega$ respectively.

The Gibbs energy of the system can also be expressed in terms of the element potentials, $\Gamma_j$ [J mol$^{-1}$], and the number of moles, $b_j$ [J], of the system components. Mathematically, this can be expressed as:

$$G_{\text{sys}} = \sum_{j=1}^{C} \Gamma_j b_j, \tag{4.25}$$

The mixing models used in materials modelling are briefly described in the following section.

### 4.3.1. Excess mixing models for Gibbs energy

A number of different models for excess mixing component of Gibbs energy have been proposed in literature. The different models are suitable for different materials, for example the Compound

Energy Formalism (CEF) is often used for $UO_2$ fuels while the Modified Quasichemcial Model in Quadruplet Approximation (MQMQA) is the state of the art model used to describe molten salts, which are of prime interest in the development of MSRs. However, only the relevant equations for some of the most commonly used models are shown here.

1. **Substitutional solution models**
   The regular solution model is a quantitative explanation of non-ideal behaviour. The model assumes that the entropy of mixing is the same as ideal mixing but that the enthalpy of mixing is not zero. A number of different regular solution models have been proposed, the most commonly used ones being based on Kohler-Toop and Redlich-Kister-Muggiano interpolation schemes [7].

   - **Kohler-Toop Interpolation**

$$g_\lambda^{ex} = \sum_{z=1}^{Z} \phi_z (x_1^{d_1} x_2^{d_2} x_3^{d_3}). \tag{4.26}$$

   - **Redlich-Kister-Muggiano Interpolation**

$$g_\lambda^{ex} = \sum_{z=1}^{Z} x_j x_k \sum_{\nu=0} {}^{\nu}L_j. \tag{4.27}$$

2. **Compound Energy Formalism (CEF)**
   CEF is a multi-sublattice model proposed by Hillert [166] for an adequate description of the properties of solution phases with sublattices. The molar Gibbs energy, $g_\lambda$, of solution phase $\lambda$ based on the CEF model is generally given as:

$$g_\lambda = \sum_{i=1}^{N_\lambda} g_i^\circ \prod_{s=1}^{N_s} y_{i(s)} + RT \left( \sum_{s=1}^{N_s} \nu_s \sum_{c=1}^{N_c} y_{c(s)} \ln(y_{c(s)}) \right) + g_\lambda^{ex}, \tag{4.28}$$

   where $g_i^\circ$ is the standard molar Gibbs energy of the pure component $i$, $y_{i(s)}$ represents the site fraction on sublattice $s$ corresponding to component $i$, $N_\lambda$ and $N_s$ denote the number of components and number of sublattices in solution phase $\lambda$, respectively. The stoichiometry coefficient for sublattice $s$ is represented by $\nu_s$, the number of constituents on sublattice $s$ is $N_c$ and the site fraction of constituent $c$ on sublattice $s$ is $y_{c(s)}$. It is to be understood that $y_{i(s)}$ refers to the site fraction of constituent $c$ associated with component $i$ on sublattice $s$ and is thus related to $y_{c(s)}$. Finally, the molar excess Gibbs

energy of mixing of solution phase $\lambda$ is $g_\lambda^{\text{ex}}$ and is given as:

$$g_\lambda^{\text{ex}} = \sum_{p=1}^{N_p} \left( \prod_{m=1} y_{m(s)} \right) \sum_{z=0}^{N_z} {}^{z}L_{j,k}(y_j - y_k)^z, \tag{4.29}$$

where $N_p$ denotes the number of excess mixing parameters (note: $N_p \geq N_s$), $y_m$ is the site fraction of constituent $m$ corresponding to mixing parameter $p$, $N_z$ is the number of terms corresponding to parameter $p$, and ${}^{z}L_{j,k}$ is the $z$th order mixing parameter. A detailed description of CEF can be found in the paper by Hillert [166].

3. **Modified Quasichemical Model (MQM)**
   The MQM in the quadruplet approximation is the most generalised thermodynamic model for treating Short-Range Ordering (SRO). MQM is fundamentally different than other thermodynamic models in that the focus is not on the mixing of chemical species or constituents on a lattice, but rather the mixing of species as quadruplets to capture SRO of both First Nearest Neighbour (FNN) and Second Nearest Neighbour (SNN) in liquid or solid solutions. The details of evolution of MQM from pair approximation for species mixing on only one sublattice to the current quadruplet approximation are provided by Pelton et al. [161–164].

   For a solution with two sublattices, which is occupied only by a single species on the second sublattice, the SNN pair exchange can be written as:

$$(A-[X]-A) + (B-[X]-B) = 2(A-[X]-B); \Delta g_{AB/X}, \tag{4.30}$$

where $\Delta g_{AB/X}$ is the non-configurational Gibbs energy for the formation of 2 mol of $(A-[X]-B)$ pairs. Similarly, when there is a single species on the first sublattice, the formation of SNN pairs is captured via:

$$(X-[A]-X) + (Y-[A]-Y) = 2(X-[A]-Y); \Delta g_{A/XY} \tag{4.31}$$

where $\Delta g_{A/XY}$ is the non-configurational Gibbs energy for the formation of 2 mol of $(X-[A]-Y)$ pairs. Among the FNN pairs, the following exchange reaction is considered:

$$(A-X) + (B-Y) = (A-Y) + (B-X); \Delta g_{A/XY}^{\text{exchange}} \tag{4.32}$$

where $\Delta g_{A/XY}^{\text{exchange}}$ is the non-configurational Gibbs energy. Let $n_i$ $(i = A, B, ..., X, Y...)$ represent the number of moles of species $i$, $n_{i/j}$ be the number of moles of FNN $((i-j))$

pairs, and $n_{ij/kl}$ be the number of moles of the quadruplets. The relationship between the foregoing terms is [164]

$$Z_A n_A = 2n_{A_2/X_2} + 2n_{A_2/Y_2} + 2n_{A_2/XY} + n_{AB/X_2} + n_{AB/Y_2} + n_{AB/XY} + \cdots, \tag{4.33}$$

$$Z_X n_X = 2n_{A_2/X_2} + 2n_{B_2/X_2} + 2n_{AB/X_2} + n_{A_2/XY} + n_{B_2/XY} + n_{AB/XY} + \cdots, \tag{4.34}$$

where $Z_A$ and $Z_B$ are the coordination numbers for A and B, respectively. A generic statement for a multi-component system is:

$$Z_i n_i = 2n_{ii} + \sum_{j \neq i} n_{ij}. \tag{4.35}$$

The mole fractions then follow:

$$x_i = \frac{n_i}{\sum n_j}, \tag{4.36}$$

$$x_k = \frac{n_k}{\sum n_l}, \tag{4.37}$$

where the indices $i$ and $j$ refer to the species on first sublattice while the indices $k$ and $l$ refer to the species on second sublattice. The FNN pair fractions and quadruplet fractions are defined as:

$$x_{i/k} = \frac{n_{i/k}}{\sum_j \sum_l n_{j/l}}, \tag{4.38}$$

$$x_{ij/kl} = \frac{n_{ij/kl}}{\sum n_{ij/kl}}. \tag{4.39}$$

Another useful term is the coordination equivalent fraction, which is

$$y_i = \frac{Z_i n_i}{\sum Z_j n_j}, \tag{4.40}$$

$$y_k = \frac{Z_k n_k}{\sum Z_l n_l}. \tag{4.41}$$

Omitting detailed description of the derivation of the model, the simplest form of MQM for binary solutions can be written as:

$$G_\lambda = (n_A g_A^\circ + n_B g_B^\circ) - T\Delta S^{\text{config}} + \frac{n_{AB}\Delta g_{AB}}{2} \tag{4.42}$$

where $g_i^\circ$ is the reference molar Gibbs energy of pure $i$ (computed from a database), $T$ is the absolute temperature, and $\Delta S^{\text{config}}$ is the configurational entropy, given by:

$$\begin{aligned}\Delta S^{\text{config}} = -R\,(&n_A \ln(x_A) + n_B \ln(x_B) \\ &+ n_{AA}\ln(x_{AA}/y_A^2) + n_{BB}\ln(x_{BB}/y_B^2) + n_{AB}\ln(x_{AB}/(2y_A y_B)))\end{aligned} \tag{4.43}$$

MQMQA is of particular interest in this work because it is the preferred model for thermodynamic modelling of molten salts. However, from the computational perspective, many a times, the MQM phases pose a unique challenge in that the Hessian matrix resulting from the GEM process can be rank-deficient. Therefore, any attempt to solve the corresponding system of linear equations will fail. Note that in practice it is possible that the system of equations can be solved with a sufficient numerical error associated with machine precision, which will yield some mathematically meaningless results. In this case, one must rely heavily on the quality and robustness of the linear equation solver employed [167]. A more detailed description of MQMQA is given in the article by Poschmann et al. [68] and is attached in the next subsection.

### 4.3.2. Chemical potential expressions for excess mixing models

Pertinent to the development of a Gibbs energy minimiser are the chemical potential expressions for the different species in phases represented by each of the excess mixing models. However, the derivations of these expressions are not trivial and the open-literature usually does not have these expressions in enough details to be directly implemented into a thermodynamics code. These expressions were derived as part of this work and have been published by Bajpai et al. [168] and Poschmann et al. [68]. The following articles show the chemical potential expressions for the substitutional solution models and the CEF in the article titled *Derivations of useful partial molar excess Gibbs energy of mixing expressions of common thermodynamic models* and the expressions for the MQMQA in section 2 of the article titled *Recent developments for molten salt systems in Thermochimica*.

The author of this thesis was the main author of [168] and performed the derivations of the expressions presented therein. The author was also responsible for the verification of the presented expressions in collaboration with the other authors. In [68], the author's main

contribution was the analysis of the MQMQA and derivation of expressions presented in section 2 of the article. Both these activities were performed in conjunction with the primary author of the paper. As such, only section 2 has been presented here and the other sections of the article which do not represent the author's contribution have been omitted.

J. Phase Equilib. Diffus. (2021) 42:333–347
https://doi.org/10.1007/s11669-021-00886-w

# Derivations of Partial Molar Excess Gibbs Energy of Mixing Expressions for Common Thermodynamic Models

**Parikshit Bajpai**[1] · **Max Poschmann**[2] · **Markus H. A. Piro**[1,2]

Submitted: 16 February 2021 / in revised form: 15 April 2021 / Accepted: 27 April 2021 / Published online: 16 May 2021


**Abstract** Modern computational thermodynamics methods rely on the use of numerical models that represent chemical systems. Typically, these models are formulated in terms of the Gibbs energy, which must be minimised to find the conditions of thermodynamic equilibrium. Numerous thermodynamic models have been developed to capture the behaviour of regular solid and liquid solutions, ionic ceramics, multi-sublattice metallic alloys, short and long range ordering, and much more. Some classes of commonly used thermodynamic models include substitutional solutions and compound energy formalism. The mathematical formulation of the Gibbs energy of a solution phase represented by any of the aforementioned models takes on a unique form, which requires special consideration for obtaining the partial derivatives in the Hessian matrix of a Gibbs energy minimiser. This paper provides derivations of the partial molar excess Gibbs energy of mixing of some common classes of thermodynamic models for use in a Gibbs energy minimiser.

**Keywords** CALPHAD · compound energy formalism · Gibbs energy minimisation · regular solution model

## 1 Introduction

Thermodynamic calculations play a fundamental role in solving a variety of complicated technical problems. In particular, the CALPHAD method[1] enables the computer calculation of phase diagrams and for calculating the properties of multicomponent, multiphase systems. Thermodynamic quantities such as Gibbs energies, heat capacities, enthalpies, chemical potentials and driving forces can be calculated using CALPHAD techniques.

Computations of thermodynamic equilibrium often exploit the Gibbs Energy Minimisation (GEM) method, which predicts a unique combination of phases and species that yield a minimum in the integral Gibbs energy of a closed isothermal, isobaric system. The objective is often achieved using the method of Lagrange multipliers that simultaneously minimises the integral Gibbs energy and the residuals of mass balance equations. In matrix form, this results in a system of linearised equations as shown by White et al.[2] For finding the undetermined Lagrange multipliers, the expressions for the Gibbs energy of different phases and the chemical potentials of the species in those phases are required to establish the constraint vector associated with the system of equations and also for computing the molar quantities of these species when using an iterative solver. The requirement for explicit expressions of the non-ideal contribution to chemical potential, i.e. partial molar excess Gibbs energy of mixing, in GEM software is the motivation behind this paper. While the derivations of these equations and the fundamental method

**Supplementary Information** The online version contains supplementary material available at https://doi.org/10.1007/s11669-021-00886-w.

✉ Parikshit Bajpai
parikshit.bajpai@ontariotechu.net

Max Poschmann
max.poschmann@ontariotechu.ca

Markus H. A. Piro
markus.piro@ontariotechu.ca

[1] Faculty of Science, Ontario Tech University, Oshawa, ON, Canada

[2] Faculty of Energy Systems and Nuclear Science, Ontario Tech University, Oshawa, ON, Canada

adopted were initially motivated by the development of Thermochimica,[3] the equations can be implemented in other software that are based on the GEM methodology,[2] including the development of thermochemistry solver for the mesoscale corrosion modelling code Yellowjacket.[4]

In the context of this paper, a *system* is defined as a closed isothermal-isobaric volume with a fixed composition. The system composition is represented by the *system components*, which may be equivalent to the chemical elements, a combination thereof, or an electron corresponding to ionic charge. A *species* is defined as any atom, molecule, ion or vacancy and a *constituent* refers to a certain species on a certain sublattice. In the context of a multi-sublattice phase, a fixed combination of constituents is referred to as a *compound end member*. The selection of the independent variable, for which reference Gibbs energies are defined and solved in the Hessian matrix, varies depending on the type of solution model. For example, a 'species' is used in an ideal gas or substitutional solution while a 'compound end member' is used in the Compound Energy Formalism (CEF). The derivation of chemical potentials will therefore be made with respect to the foregoing independent variables.

In a multicomponent, multiphase system, the integral Gibbs energy is given by the following expression:

$$G = \sum_{\lambda=1}^{\Lambda} n_\lambda g_\lambda + \sum_{\omega=1}^{\Omega} n_\omega g_\omega, \qquad \text{(Eq 1)}$$

where $g_\lambda$ and $g_\omega$ represent the molar Gibbs energies (i.e., the Gibbs energy per mole of the phase) of solution phase $\lambda$ and stoichiometric phase $\omega$, respectively. Quantities $n_\lambda$ and $n_\omega$ represent the mole number of solution phase $\lambda$ and stoichiometric phase $\omega$. $\Lambda$ and $\Omega$ denote the number of stable solution and stoichiometric phases, respectively.

Calculation of thermodynamic equilibrium requires a multicomponent database, which provides a consistent description of the thermodynamic functions for all the possible phases in the system. These databases are derived from experimental measurements, sometimes combined with first-principles calculations, to include Gibbs energy expressions as functions of temperature, pressure, and composition. It must be mentioned that since the composition of stoichiometric phases is invariant, their thermodynamic parameters are by definition independent of composition. The solution phase functions, however, do depend on the composition, and a number of models and parameters have been proposed to model different phases. These models include ideal solution models, models for a single sublattice and models for multiple sublattices. Despite the large number of models available to represent the Gibbs energy of a particular phase, the general representative expression is as follows:

$$G_\lambda = G_\lambda^\circ + G_\lambda^{\mathrm{id}} + G_\lambda^{\mathrm{ex}} + G_\lambda^{\mathrm{phys}}, \qquad \text{(Eq 2)}$$

where the Gibbs energy of phase $\lambda$ , $G_\lambda$, is a sum of the reference Gibbs energy, $G_\lambda^\circ$, the ideal mixing term of Gibbs energy, $G_\lambda^{\mathrm{id}} = -TS_\lambda^{id}$, which assumes random mixing of constituents with $S_\lambda^{id}$ denoting the entropy of mixing, and a term to account for excess mixing energy, $G_\lambda^{\mathrm{ex}}$. The term $G_\lambda^{\mathrm{phys}}$ captures the various physical phenomena that contribute to the Gibbs energy of the phase. The most important amongst these is the magnetic contribution to the Gibbs energy that results from the unpaired electron spins in atoms of magnetic substances. This paper focuses on the excess Gibbs energy of mixing and its contribution to the chemical potentials of the species in the system. Magnetic and other physical contributions to excess mixing energies will not be discussed here.

The chemical potential of species $i$ of phase $\lambda$ is the partial derivative of the integral Gibbs energy of the system with respect to the number of moles of that species at constant temperature, $T$, and pressure, $P$. Mathematically, this is represented as:

$$\mu_{i(\lambda)} = \left(\frac{\partial G_\lambda}{\partial n_{i(\lambda)}}\right)_{T,P,n_{j\neq i}}, \qquad \text{(Eq 3)}$$

where $n_i$ represents the number of moles of species $i$. One can obtain an expanded expression for chemical potential by substituting Eq 1 and 2 into Eq 3 above, which gives the following:

$$\mu_{i(\lambda)} = \underbrace{\left(\frac{\partial G_\lambda^\circ}{\partial n_i}\right)_{T,P,n_{j\neq i}}}_{\mu_{i(\lambda)}^\circ} + \underbrace{\left(\frac{\partial G_\lambda^{\mathrm{id}}}{\partial n_i}\right)_{T,P,n_{j\neq i}}}_{\mu_{i(\lambda)}^{\mathrm{id}}} + \underbrace{\left(\frac{\partial G_\lambda^{\mathrm{ex}}}{\partial n_i}\right)_{T,P,n_{j\neq i}}}_{\mu_{i(\lambda)}^{\mathrm{ex}}}, \qquad \text{(Eq 4)}$$

where the contributions to the integral Gibbs energy are obtained as the product of number of moles of a phase and the respective molar Gibbs energy contribution (i.e., $G_\lambda^\circ = n_\lambda g_\lambda^\circ$, $G_\lambda^{\mathrm{id}} = n_\lambda g_\lambda^{\mathrm{id}}$ and $G_\lambda^{\mathrm{ex}} = n_\lambda g_\lambda^{\mathrm{ex}}$), with $g_\lambda^\circ$, $g_\lambda^{\mathrm{id}}$ and $g_\lambda^{\mathrm{ex}}$ denoting the molar reference Gibbs energy, the molar ideal Gibbs energy of mixing and the molar excess Gibbs energy of mixing, respectively. The partial derivative terms are referred to as the partial reference molar Gibbs energy, partial molar ideal Gibbs energy of mixing and partial molar excess Gibbs energy of mixing and are denoted by $\mu_{i(\lambda)}^\circ$, $\mu_{i(\lambda)}^{\mathrm{id}}$, and $\mu_{i(\lambda)}^{\mathrm{ex}}$ respectively.

The expressions for molar Gibbs energy terms depend on the solution model used to describe the phase. This paper presents the derivation of the partial excess molar Gibbs energy terms for some commonly employed solution models and the partial molar reference Gibbs energy and partial molar ideal Gibbs energy terms are briefly presented

for completeness. While there are multiple papers in the open literature that describe these models, none give a full derivation of the partial molar excess Gibbs energy of mixing. Section 2 provides background to substitutional solution theory and presents the various parameters used in those models. Sections 3 and 4 provide the derivation of the partial molar excess excess Gibbs energy of mixing terms for the two most common substitutional models, i.e. the simple polynomial model with Kohler–Toop interpolation and the Redlich–Kister polynomial model with Muggiano interpolation. Section 5 describes the multi-sublattice CEF and the derivation of chemical potential for the compound end members of the model is presented. Furthermore, the methodology adopted for deriving the expressions is applicable to other thermodynamic models as well. The remainder of the paper will focus on calculations within a single solution phase, and therefore going forward the phase identifier $\lambda$ will be omitted to simplify the notation.

## 2 Substitutional Solution Theory

Several solids and liquids conform to substitutional solution behaviour, which is based on the assumption that the constituents mix randomly on a single lattice.[5] The reference Gibbs energy of solution phase $\lambda$ represents the Gibbs energy of an unreacted mixture of the different species and is given as follows:

$$G_{\lambda}^{\circ} = n_{\lambda} \sum_{i} x_{i(\lambda)} g_{i(\lambda)}^{\circ} \quad \text{(Eq 5)}$$

where $x_{i(\lambda)}$ denotes the mole fraction of species $i$ of phase $\lambda$ and is related to the molar amount of species $i$, $n_{i(\lambda)}$ per mole of phase $\lambda$, $n_{\lambda}$ (i.e., $x_{i(\lambda)} = {}^{n_{i(\lambda)}}/_{n_{\lambda}}$). Since the reference molar Gibbs energy of the independent species, denoted by $g_{i(\lambda)}^{\circ}$, depends only on the temperature and pressure of the system, the molar reference Gibbs energy of the phase is given as:

$$\mu_{i(\lambda)}^{\circ} = g_{i(\lambda)}^{\circ}. \quad \text{(Eq 6)}$$

The term $g_{i(\lambda)}^{\circ}$ is obtained from a thermodynamic database.

The second term of Eq 4 relates to the ideal Gibbs energy of mixing, which is written as:

$$G_{\lambda}^{\text{id}} = n_{\lambda} RT \sum_{i} x_{i(\lambda)} \ln x_{i(\lambda)} \quad \text{(Eq 7)}$$

where $R$ is the ideal gas constant. This results in the following expressions for the partial molar ideal Gibbs energy of mixing:

$$\mu_{i(\lambda)}^{\text{id}} = RT \ln x_{i(\lambda)}. \quad \text{(Eq 8)}$$

Substitutional solution models represent the excess Gibbs energy of mixing through a polynomial function, which helps in extrapolating the properties of higher order systems from lower order systems. In general, for a multi-component system, the excess molar Gibbs energy of mixing results from binary, ternary and quaternary interactions, which can be described separately as follows:

$$g^{\text{ex}} = g_{\text{bin}}^{\text{ex}} + g_{\text{ter}}^{\text{ex}} + g_{\text{qua}}^{\text{ex}}, \quad \text{(Eq 9)}$$

where the right subscripts bin, ter and qua denote the species interacting in the binary, ternary and quaternary subsystems, respectively.

For a multi-species substitutional solution phase, the binary interactions result in the following contribution to excess molar Gibbs energy of mixing:

$$g_{\text{bin}}^{\text{ex}} = \sum_{i} \sum_{j>i} x_i x_j L_{ij}. \quad \text{(Eq 10)}$$

The solution parameter $L_{ij}$ represents the interaction between the two species and is, in general, a function of both temperature and composition.

Redlich and Kister[6] proposed a symmetrical form of the interaction parameter, which is now widely used because of the ease of extrapolating it to ternary and higher-order systems. This is commonly referred to as the Redlich–Kister polynomial and is represented as follows:

$$L_{ij} = \sum_{v \geq 0} {}^{v}L_{ij} (x_i - x_j)^{v}, \quad \text{(Eq 11)}$$

where the parameters ${}^{v}L_{ij}$ are independent of composition but can be temperature dependent, and the number of terms used can be chosen to make an appropriate fit to the available experimental data. The superscript $v$ denotes the order of the interaction parameter terms.

While the Redlich–Kister polynomials are most commonly used to represent a solution parameter, a number of other forms have been proposed, such as simple polynomial form, Lagrange series, etc. Among these, the simple polynomial form is the most commonly used and results in the following:

$$L_{ij} = \sum_{u,v \geq 0} {}^{uv}Q_{ij} x_i{}^{u} x_j{}^{v}, \quad \text{(Eq 12)}$$

where parameters ${}^{uv}Q_{ij}$ are independent of composition but can be temperature dependent. The two formulations are identical in the case of binary systems and the interaction parameters can be easily converted from one form to another. However, in the case of higher order systems, the interpolations would depend on the series used and the interpolation method.

Considering ternary mixing, interaction requires an additional summation resulting in the following:

$$g^{\mathrm{ex}}_{\mathrm{ter}} = \sum_i \sum_{j>i} \sum_{k>j} x_i x_j x_k L_{ijk}. \quad \text{(Eq 13)}$$

Like the binary subsystems, the interaction parameters for the ternary subsystems can be determined experimentally or based on a number of analytical methods. According to Hillert,[7] in case of composition dependence, there is no unique way of predicting the binary contribution to ternary and higher order systems and as a result a number of different expressions have been proposed with preference given to the expression suggested by Redlich and Kister.[6] To interpolate ternaries from their binaries, a number of interpolation schemes have been proposed by Kohler,[8] Toop,[9] Colinet,[10] and Muggiano.[11] A combination of these models, most commonly Kohler–Toop and Muggiano-Toop, can be used to estimate the energies of higher order systems from their binary subsystems. Among the four interpolation methods, Kohler, Colinet and Muggiano methods are symmetric and treat all the binary subsystems in the same way, but the ternary excess terms are related to the binary excess terms through the composition paths depicted in Fig. 1. It must emphasised that the components in the illustrated figures refer to the species and not the system components. For example, in Fig. 1(a), the phase has three species *i, j* and *k*, which are denoted at the vertices of the triangle.

The composition of the ternary phase is denoted by point *p* and the points *a*, *b* and *c* represent the binary compositions obtained using the interpolation model in question. In the following discussion, the functional form $g_{ij}(\alpha;\beta)$ will be used to refer to the molar Gibbs energy contribution from a binary system, with $\alpha$ and $\beta$ representing the projected concentrations of the two species of the binary subsystem. For example, the excess Gibbs energy of mixing in the $i-j$ binary subsystem should be calculated at point *a* and is given as $g^{\mathrm{ex}}_{ij}(\alpha;\beta)$, where $\alpha$ and $\beta$ are the equivalent concentrations of species *i* and *j* in the binary subsystem, respectively, and $\alpha+\beta=1$.

- *Kohler*: The Kohler interpolation scheme shown in Fig. 1(a) is symmetric. On the line *ap*, the ratio $x_j/(x_i+x_j)$ remains constant and the binary contribution of the $i-j$ subsystem to the ternary can be computed by evaluating the binary excess Gibbs energy of mixing of the $i-j$ subsystem at point *a*.[13] For a multispecies phase, the ternary excess Gibbs energy is then given as the following:

$$g^{\mathrm{ex}} = \sum_i \sum_{j>i} (x_i+x_j)^2 \cdot g^{\mathrm{ex}}_{ij}\left(\frac{x_i}{x_i+x_j};\frac{x_j}{x_i+x_j}\right), \quad \text{(Eq 14)}$$

where the expression $g^{\mathrm{ex}}_{ij}(\alpha;\beta)$ denotes that excess Gibbs energy of mixing of binary subsystem $i-j$ evaluated at molar equivalent composition $\alpha$ and $\beta$ and the factor $(x_i+x_j)^2$ is a result of using the interpolation formula instead of the composition of the system.

- *Muggiano*: The Muggiano interpolation scheme is based on the fact that along the line *ap* shown in Fig. 1(b), the ratios $(1+x_i-x_j)/2$ and $(1-x_i+x_j)/2$ both remain constant.[13] The excess Gibbs energy of mixing takes the following form:

$$g^{\mathrm{ex}} = \sum_i \sum_{j>i} \frac{4x_i x_j}{(1+x_i-x_j)(1+x_j-x_i)} \cdot g^{\mathrm{ex}}_{ij}\left(\frac{1+x_i-x_j}{2};\frac{1+x_j-x_i}{2}\right). \quad \text{(Eq 15)}$$

- *Kohler–Toop*: The Kohler–Toop interpolation scheme shown in Fig. 1(c) is an asymmetrical model, which is often used when one species of the subsystem belongs to a group different from the others.[13] Since the mole fraction $x_i$ is constant along the line *ac*, and the line *bp* follows from Kohler interpolation, the excess molar Gibbs energy can be written as follows[14]

$$g^{\mathrm{ex}} = \frac{x_j}{1-x_i}\cdot g^{\mathrm{ex}}_{ij}(x_i;1-x_i) + \frac{x_k}{1-x_i}\cdot g^{\mathrm{ex}}_{ik}(x_i;1-x_i) + (1-x_i)^2 \cdot g^{\mathrm{ex}}_{jk}\left(\frac{x_j}{x_j+x_k};\frac{x_k}{x_j+x_k}\right). \quad \text{(Eq 16)}$$

The Kohler–Toop model depends on the choice of symmetric and asymmetric species and in the Eq 16, species *i* of Fig. 1(c) has been selected as the Kohler component.

An advantage of using Redlich–Kister polynomials is the fact that when using the Muggiano interpolation method, the binary terms can be used directly in the ternary extrapolations. This is an outcome of the fact that along the line *ap* shown in Fig. 1(b), the quantity $x_i-x_j$ remains constant.[13, 15] This results in what is commonly referred to as the Redlich–Kister–Muggiano polynomial model. Also, it must be mentioned that the composition independent parameter ${}^0L_{ij}$ scales the same way irrespective of the model used.

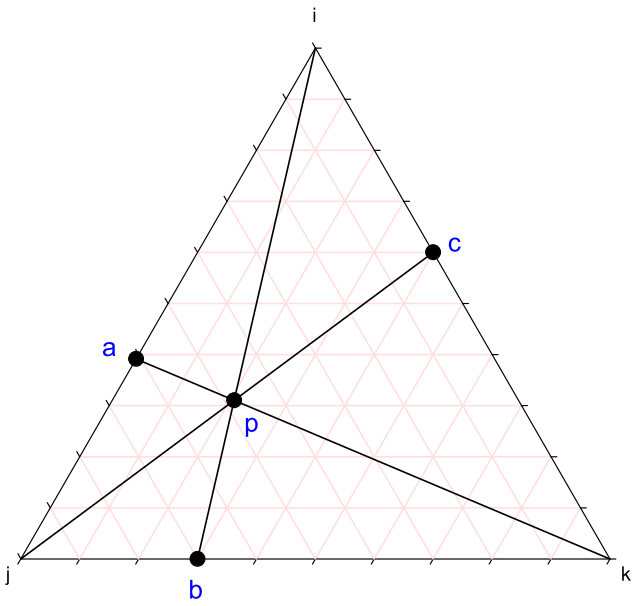


**(a)** Kohler interpolation scheme.

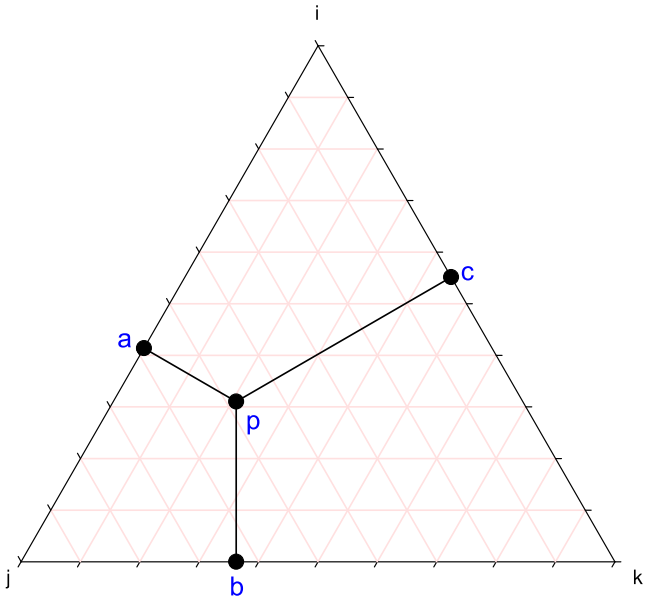


**(b)** Muggiano interpolation scheme.

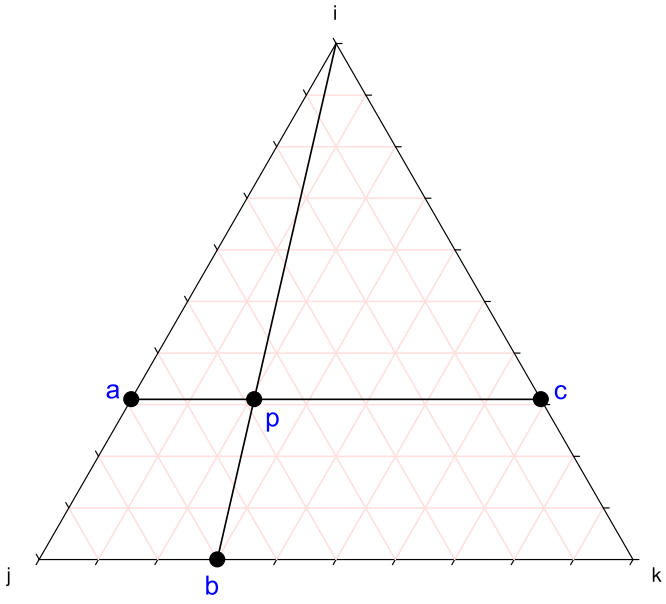


**(c)** Kohler-Toop interpolation scheme.

**Fig. 1** Commonly used interpolation models[12]

## 3 Simple Polynomial Solution Model with Kohler–Toop Interpolation

Substitutional solution models using the simple polynomial form of the interaction parameters often utilise the Kohler–Toop interpolation scheme. The choice of the interpolation scheme for a system of interest is based on the judgement of the model developer, with physical and thermodynamic factors such as the similarity of species playing key roles in the choice between the symmetric Muggiano or the asymmetric Kohler–Toop models. Chartrand and Pelton have provided a detailed description of the reasoning behind the preferability of the Kohler–Toop model in a number of cases.[13] While Redlich–Kister polynomials can also be used in place of simple polynomials, the latter has been the standard notation adopted when using the Kohler–

Toop interpolation model. A derivation for the partial molar excess Gibbs energy for this case follows.

### 3.1 Derivation of Partial Excess Gibbs Energy of Mixing for a Solution Model with Kohler–Toop Interpolation

#### *3.1.1 Derivation of Terms for a Subsystem Modelled by a Simple Polynomial Formulation*

In the substitutional solution model using simple polynomials, the molar excess Gibbs energy of mixing is generally given in terms of binary and ternary mixing parameters:

$$^{\mathrm{SP}}g_{ijk}^{\mathrm{ex}}(x_i;x_j;x_k) = \sum_{u,v,w\geq 0} {}^{uvw}Q_{ijk}x_i{}^{u}x_j{}^{v}x_k{}^{w}, \quad \text{(Eq 17)}$$

where the left-superscript SP indicates the Simple Polynomial formulation and the exponents $u$, $v$ and $w$ are integers.

Denoting the number of moles of the phase by $n$, where $n$ is equal to the sum of the number of moles of each species of the solution phase (i.e. $n = \sum_i n_i$) the integral excess Gibbs energy of mixing is:

$$^{\mathrm{SP}}G_{ijk}^{\mathrm{ex}}(\{n_i;n_j;n_k\},n_{\mathrm{interp}}) = n_{\mathrm{interp}}\cdot {}^{\mathrm{SP}}g_{ijk}^{\mathrm{ex}}\left(\frac{n_i}{n_{\mathrm{interp}}};\frac{n_j}{n_{\mathrm{interp}}};\frac{n_k}{n_{\mathrm{interp}}}\right). \quad \text{(Eq 18)}$$

Equation 18 makes explicit how one may interpolate into subsystems, which will become very useful in the following subsections. The first argument ($\{n_i;n_j;n_k\}$) is the list of molar quantities of species used in the excess mixing term, while the second argument ($n_{\mathrm{interp}}$) is the total number of moles to consider when interpolating into the desired subsystem. For the moment, one may consider the entire system by setting $n_{\mathrm{interp}} = n$ as the second argument.

$$\begin{aligned} ^{\mathrm{SP}}G_{ijk}^{\mathrm{ex}}(\{n_i;n_j;n_k\},n) &= n\cdot {}^{\mathrm{SP}}g_{ijk}^{\mathrm{ex}}\left(\frac{n_i}{n};\frac{n_j}{n};\frac{n_k}{n}\right)\\ &= n\cdot\sum_{u,v,w\geq 0} {}^{uvw}Q_{ijk}x_i{}^{u}x_j{}^{v}x_k{}^{w}\\ &= n\cdot\sum_{u,v,w\geq 0} {}^{uvw}Q_{ijk}\frac{n_i{}^{u}n_j{}^{v}n_k{}^{w}}{n^{u+v+w}}\\ &= \sum_{u,v,w\geq 0} {}^{uvw}Q_{ijk}\left(n_i{}^{u}n_j{}^{v}n_k{}^{w}\right)\left(n^{1-u-v-w}\right). \end{aligned} \quad \text{(Eq 19)}$$

The partial molar excess Gibbs energy of mixing of species $i$ resulting from parameters involving species $i,j$, and $k$, $\mu_{i(ijk)}^{\mathrm{ex}}$, is obtained by taking the partial derivative of Eq 19 with respect to the number of moles of the species, $n_i$, as per Eq 3:

$$^{\mathrm{SP}}\mu_{i(ijk)}^{\mathrm{ex}} = \sum_{u,v,w\geq 0} {}^{uvw}Q_{ijk}\left[\frac{un_i^{u-1}n_j^{v}n_k^{w}}{n^{u+v+w-1}} -(u+v+w-1)\frac{n_i^{u}n_j^{v}n_k^{w}}{n^{u+v+w}}\right]. \quad \text{(Eq 20)}$$

Substituting molar quantities, i.e. $x_i = \frac{n_i}{n}$, into Eq 20 gives:

$$\begin{aligned} ^{\mathrm{SP}}\mu_{i(ijk)}^{\mathrm{ex}} &= \sum_{u,v,w\geq 0} {}^{uvw}Q_{ijk}\left[\frac{u(nx_i)^{u-1}(nx_j)^{v}(nx_k)^{w}}{n^{u+v+w-1}} -(u+v+w-1)\frac{(nx_i)^{u}(nx_j)^{v}(nx_k)^{w}}{n^{u+v+w}}\right] \quad \text{(Eq 21)}\\ &= \sum_{u,v,w\geq 0} {}^{uvw}Q_{ijk}\left[\frac{ux_i^{u-1}x_j^{v}x_k^{w}n^{u+v+w-1}}{n^{u+v+w-1}} -(u+v+w-1)\frac{x_i^{u}x_j^{v}x_k^{w}n^{u+v+w}}{n^{u+v+w}}\right]. \end{aligned}$$

Simplifying, the following partial molar excess Gibbs energy of mixing of species $i$ in the subsystem is obtained:

$$^{\mathrm{SP}}\mu_{i(ijk)}^{\mathrm{ex}}(x_i;x_j;x_k) = \sum_{u,v,w\geq 0} {}^{uvw}Q_{ijk}\left[ux_i^{u-1}+(1-u-v-w)x_i^{u}\right]x_j^{v}x_k^{w}. \quad \text{(Eq 22)}$$

It is worth mentioning that the expressions for a three species phase can be directly used for a binary phase by setting the exponent $w$ equal to zero. Thus, for a binary phase, the following expression for the integral excess Gibbs energy of mixing is obtained:

$$^{\mathrm{SP}}G_{ij}^{\mathrm{ex}}(\{n_i;n_j\},n_{\mathrm{interp}}) = n_{\mathrm{interp}}\cdot {}^{\mathrm{SP}}g_{ij}^{\mathrm{ex}}\left(\frac{n_i}{n_{\mathrm{interp}}};\frac{n_j}{n_{\mathrm{interp}}}\right). \quad \text{(Eq 23)}$$

The molar excess Gibbs energy of mixing is:

$$^{\mathrm{SP}}g_{ij}^{\mathrm{ex}}(x_i;x_j) = \sum_{u,v>0} {}^{uv}Q_{ij}x_i^{u}x_j^{v}, \quad \text{(Eq 24)}$$

and the partial molar excess Gibbs energy is:

$$^{\mathrm{SP}}\mu_{i(ij)}^{\mathrm{ex}}(x_i;x_j) = \sum_{u,v>0} {}^{uv}Q_{ij}\left[ux_i^{u-1}+(1-u-v)x_i^{u}\right]x_j^{v}. \quad \text{(Eq 25)}$$

### 3.1.2 Derivation of Ternary Phase from Binary Subsystems of a Substitutional Solution Model Using Kohler Interpolation

When modelling the ternary phase by geometrically interpolating binary subsystems using Kohler interpolation (indicated in the following with left-superscript KO), the following expression is obtained by substituting Eq 24 into Eq 14 (and including ternary mixing terms as well):

$$\begin{aligned} {}^{\mathrm{KO}}g_{ijk}^{\mathrm{ex}} &= (x_i+x_j)^2 \cdot {}^{\mathrm{SP}}g_{ij}^{\mathrm{ex}}\left(\frac{x_i}{x_i+x_j};\frac{x_j}{x_i+x_j}\right) \\ &+ (x_i+x_k)^2 \cdot {}^{\mathrm{SP}}g_{ik}^{\mathrm{ex}}\left(\frac{x_i}{x_i+x_k};\frac{x_k}{x_i+x_k}\right) \\ &+ (x_j+x_k)^2 \cdot {}^{\mathrm{SP}}g_{jk}^{\mathrm{ex}}\left(\frac{x_j}{x_j+x_k};\frac{x_k}{x_j+x_k}\right) \\ &+ \sum_{u,v,w>0} {}^{uvw}Q_{ijk}x_i{}^u x_j{}^v x_k{}^w, \end{aligned} \quad \text{(Eq 26)}$$

where the binary subsystems are evaluated as described in section 2, and the summation in the last term is only over ternary parameters. In a ternary subsystem, this summation can be evaluated straightforwardly, and in subsystems with more species the procedure is described in section 3.1.4. For the moment, the focus will be on the evaluation of the binary terms within a ternary subsystem.

Owing to the symmetric nature of the preceding equation, the equations for partial molar excess Gibbs energies can be derived for a single binary subsystem and the contribution from each subsystem can be summed together. Considering the contribution of the $i-j$ binary subsystem:

$${}^{\mathrm{KO}}g_{ij}^{\mathrm{ex}} = (x_i+x_j)^2 \cdot {}^{\mathrm{SP}}g_{ij}^{\mathrm{ex}}\left(\frac{x_i}{x_i+x_j};\frac{x_j}{x_i+x_j}\right), \quad \text{(Eq 27)}$$

the integral excess Gibbs energy of mixing contribution of the subsystem can be written as follows:

$$\begin{aligned} {}^{\mathrm{KO}}G_{ij}^{\mathrm{ex}} &= n \cdot {}^{\mathrm{KO}}g_{ij}^{\mathrm{ex}} \\ &= \frac{(n_i+n_j)^2}{n} \cdot {}^{\mathrm{SP}}g_{ij}^{\mathrm{ex}}\left(\frac{x_i}{x_i+x_j};\frac{x_j}{x_i+x_j}\right) \end{aligned} \quad \text{(Eq 28)}$$

The interpolated integral excess Gibbs energy of the binary subsystem is weighted such that:

$${}^{\mathrm{SP}}G_{ij}^{\mathrm{ex}}\left(\{n_i;n_j\},n_i+n_j\right) = (n_i+n_j) \cdot {}^{\mathrm{SP}}g_{ij}^{\mathrm{ex}}\left(\frac{x_i}{x_i+x_j};\frac{x_j}{x_i+x_j}\right), \quad \text{(Eq 29)}$$

and the equation then becomes:

$${}^{\mathrm{KO}}G_{ij}^{\mathrm{ex}} = \frac{(n_i+n_j)}{n} \cdot {}^{\mathrm{SP}}G_{ij}^{\mathrm{ex}}\left(\{n_i;n_j\},n_i+n_j\right). \quad \text{(Eq 30)}$$

Taking the partial derivative of Eq 30 with respect to $n_i$:

$$\begin{aligned} {}^{\mathrm{KO}}\mu_{i(ij)}^{\mathrm{ex}} &= \frac{(n_i+n_j)}{n} \cdot {}^{\mathrm{SP}}g_{ij}^{\mathrm{ex}}\left(\frac{x_i}{x_i+x_j};\frac{x_j}{x_i+x_j}\right) \\ &+ \frac{(n_i+n_j)}{n} \cdot {}^{\mathrm{SP}}\mu_{i(ij)}^{\mathrm{ex}}\left(\frac{x_i}{x_i+x_j};\frac{x_j}{x_i+x_j}\right) \\ &- \frac{(n_i+n_j)^2}{n^2} \cdot {}^{\mathrm{SP}}g_{ij}^{\mathrm{ex}}\left(\frac{x_i}{x_i+x_j};\frac{x_j}{x_i+x_j}\right). \end{aligned} \quad \text{(Eq 31)}$$

The previous equation simplifies to the following expression, which is applicable to both species of the binary subsystem[1]:

$$\begin{aligned} {}^{\mathrm{KO}}\mu_{i(ij)}^{\mathrm{ex}} &= \left[{}^{\mathrm{SP}}\mu_{i(ij)}^{\mathrm{ex}}\left(\frac{x_i}{x_i+x_j};\frac{x_j}{x_i+x_j}\right) + (1-x_i-x_j)\right. \\ &\left. \cdot {}^{\mathrm{SP}}g_{ij}^{\mathrm{ex}}\left(\frac{x_i}{x_i+x_j};\frac{x_j}{x_i+x_j}\right)\right](x_i+x_j), \end{aligned} \quad \text{(Eq 32)}$$

where the term ${}^{\mathrm{SP}}\mu_{i(ij)}^{\mathrm{ex}}$ is the chemical potential of species $i$ in binary subsystem $i-j$ and can be calculated using Eq 25. For any remaining species (i.e., the species not part of the binary subsystem):

$${}^{\mathrm{KO}}\mu_{k(ij)}^{\mathrm{ex}} = -(x_i+x_j)^2 \cdot {}^{\mathrm{SP}}g_{ij}^{\mathrm{ex}}\left(\frac{x_i}{x_i+x_j};\frac{x_j}{x_i+x_j}\right). \quad \text{(Eq 33)}$$

In Eq 31, 32 and 33, the definitions of ${}^{\mathrm{SP}}g_{ij}^{\mathrm{ex}}$ and ${}^{\mathrm{SP}}\mu_{i(ij)}^{\mathrm{ex}}$ given in Eq 24 and 25 can be used directly. Therefore, in a ternary phase evaluated using Kohler interpolation, the total of the binary contributions to the chemical potential of species $i$ will be:

$${}^{\mathrm{KO}}\mu_{i(ijk)}^{\mathrm{ex}} = {}^{\mathrm{KO}}\mu_{i(ij)}^{\mathrm{ex}} + {}^{\mathrm{KO}}\mu_{i(ik)}^{\mathrm{ex}} + {}^{\mathrm{KO}}\mu_{i(jk)}^{\mathrm{ex}}. \quad \text{(Eq 34)}$$

### 3.1.3 Derivation of Ternary Phase from Binary Subsystems of a Substitutional Solution Model Using Kohler–Toop Interpolation

When modelling the ternary phase of a three species subsystem by geometrically interpolating binary subsystems

[1] Unless specified otherwise, all the expressions for chemical potentials account for the chain rule and the expressions from the referenced equations can be directly substituted.

using Kohler–Toop interpolation (indicated in the following by the left-superscript KT), the expression shown in Eq 16 is obtained:

$$
\begin{aligned}
&{}^{\mathrm{KT}}g_{ijk}^{\mathrm{ex}} \\
&\quad = \frac{x_j}{1-x_i} \cdot {}^{\mathrm{SP}}g_{ij}^{\mathrm{ex}}(x_i;\, 1-x_i) \\
&\qquad + \frac{x_k}{1-x_i} \cdot {}^{\mathrm{SP}}g_{ik}^{\mathrm{ex}}(x_i;\, 1-x_i) \\
&\qquad + (1-x_i)^2 \cdot {}^{\mathrm{SP}}g_{jk}^{\mathrm{ex}}\left(\frac{x_j}{x_j+x_k};\, \frac{x_k}{x_j+x_k}\right),
\end{aligned}
\tag{Eq 35}
$$

where the binary subsystems are evaluated as mentioned in section 2. Since the model is asymmetric, the expression for the partial molar excess Gibbs energy will depend on the choice of the Kohler component, which has been selected to be species $i$ in the previous equation.

Expressing the previous equation in terms of molar quantities and multiplying by the molar amount of the phase, $n$, the following ternary contribution to the integral Gibbs energy is obtained:

$$
\begin{aligned}
{}^{\mathrm{KT}}G_{ijk}^{\mathrm{ex}} = n\Bigg[&\frac{n_j}{n-n_i} \cdot {}^{\mathrm{SP}}g_{ij}^{\mathrm{ex}}(x_i;\, 1-x_i) \\
&+ \frac{n_k}{n-n_i} \cdot {}^{\mathrm{SP}}g_{ik}^{\mathrm{ex}}(x_i;\, 1-x_i) \\
&+ \left(\frac{n-n_i}{n}\right)^2 \cdot {}^{\mathrm{SP}}g_{jk}^{\mathrm{ex}}\left(\frac{x_j}{x_j+x_k};\, \frac{x_k}{x_j+x_k}\right)\Bigg].
\end{aligned}
\tag{Eq 36}
$$

The integral excess Gibbs energy of mixing contribution of the $ij$ pair and non-Kohler subsystems can be written as follows:

$$
{}^{\mathrm{SP}}G_{ij}^{\mathrm{ex}}(\{n_i;\, n-n_i\}, n) = n \cdot {}^{\mathrm{SP}}g_{ij}^{\mathrm{ex}}(x_i;\, 1-x_i), \tag{Eq 37}
$$

making use of this plus the earlier definition in Eq 29

$$
\begin{aligned}
{}^{\mathrm{KT}}G_{ijk}^{\mathrm{ex}} = &\frac{n_j}{n-n_i} \cdot {}^{\mathrm{SP}}G_{ij}^{\mathrm{ex}}(\{n_i;\, n-n_i\}, n) \\
&+ \frac{n_k}{n-n_i} \cdot {}^{\mathrm{SP}}G_{ik}^{\mathrm{ex}}(\{n_i;\, n-n_i\}, n) \\
&+ \frac{(n-n_i)^2}{n\cdot(n_j+n_k)} \cdot {}^{\mathrm{SP}}G_{jk}^{\mathrm{ex}}\left(\{n_i; n_j\}, n_i+n_j\right).
\end{aligned}
\tag{Eq 38}
$$

The partial molar excess Gibbs energy of species $j$ can be calculated by taking the partial derivative of Eq 36 with respect to $n_j$:

$$
\begin{aligned}
&{}^{\mathrm{KT}}\mu_{j(ijk)}^{ex} \\
&\quad = n\left(\frac{1}{n-n_i} - \frac{n_j}{(n-n_i)^2}\right) \\
&\qquad \cdot {}^{\mathrm{SP}}g_{ij}^{ex}(x_i;\, 1-x_i) \\
&\qquad + \frac{n_j}{n-n_i} \cdot {}^{\mathrm{SP}}\mu_{j(ij)}^{ex}(x_i;\, 1-x_i) \\
&\qquad - n\frac{n_k}{(n-n_i)^2} \cdot {}^{\mathrm{SP}}g_{ik}^{ex}(x_i;\, 1-x_i) \\
&\qquad + \frac{n_k}{n-n_i} \cdot {}^{\mathrm{SP}}\mu_{j(ik)}^{ex}(x_i;\, 1-x_i) \\
&\qquad + \left(\frac{2}{n-n_i} - \frac{1}{n} - \frac{1}{n_j+n_k}\right)\left(\frac{(n-n_i)^2}{n}\right) \\
&\qquad \cdot {}^{\mathrm{SP}}g_{jk}^{ex}\left(\frac{x_j}{x_j+x_k};\, \frac{x_k}{x_j+x_k}\right) \\
&\qquad + \frac{(n-n_i)^2}{n\cdot(n_j+n_k)} \\
&\qquad \cdot {}^{\mathrm{SP}}\mu_{j(jk)}^{ex}\left(\frac{x_j}{x_j+x_k};\, \frac{x_k}{x_j+x_k}\right) \\
&\quad = \left(\frac{1}{1-x_i} - \frac{x_j}{(1-x_i)^2}\right) \\
&\qquad \cdot {}^{\mathrm{SP}}g_{ij}^{ex}(x_i;\, 1-x_i) \\
&\qquad + \frac{x_j}{1-x_i} \cdot {}^{\mathrm{SP}}\mu_{j(ij)}^{ex}(x_i;\, 1-x_i) \\
&\qquad - \frac{x_k}{(1-x_i)^2} \cdot {}^{\mathrm{SP}}g_{ik}^{ex}(x_i;\, 1-x_i) \\
&\qquad + \frac{x_k}{1-x_i} \cdot {}^{\mathrm{SP}}\mu_{j(ik)}^{ex}(x_i;\, 1-x_i) \\
&\qquad + \left(2(1-x_i) - (1-x_i)^2 - \frac{(1-x_i)^2}{x_j+x_k}\right) \\
&\qquad \cdot {}^{\mathrm{SP}}g_{jk}^{ex}\left(\frac{x_j}{x_j+x_k};\, \frac{x_k}{x_j+x_k}\right) \\
&\qquad + \frac{(1-x_i)^2}{x_j+x_k} \\
&\qquad \cdot {}^{\mathrm{SP}}\mu_{j(jk)}^{ex}\left(\frac{x_j}{x_j+x_k};\, \frac{x_k}{x_j+x_k}\right).
\end{aligned}
\tag{Eq 39}
$$

Similarly, the partial molar excess Gibbs energy of mixing of species $k$ can be calculated by taking the partial derivative of Eq 36 with respect to $n_k$:

$$
\begin{aligned}
&{}^{\mathrm{KT}}\mu^{ex}_{k(ijk)} \\
&= -\frac{x_j}{(1-x_i)^2}\cdot {}^{\mathrm{SP}}g^{ex}_{ij}(x_i;\,1-x_i) \\
&\quad + \frac{x_j}{1-x_i}\cdot {}^{\mathrm{SP}}\mu^{ex}_{k(ij)}(x_i;\,1-x_i) \\
&\quad + \left(\frac{1}{1-x_i} - \frac{x_k}{(1-x_i)^2}\right) \\
&\quad \cdot {}^{\mathrm{SP}}g^{ex}_{ik}(x_i;\,1-x_i) \\
&\quad + \frac{x_k}{1-x_i}\cdot {}^{\mathrm{SP}}\mu^{ex}_{k(ik)}(x_i;\,1-x_i) \\
&\quad + \left(2(1-x_i) - (1-x_i)^2 - \frac{(1-x_i)^2}{x_j+x_k}\right) \\
&\quad \cdot {}^{\mathrm{SP}}g^{ex}_{jk}\left(\frac{x_j}{x_j+x_k};\frac{x_k}{x_j+x_k}\right) \\
&\quad + \frac{(1-x_i)^2}{x_j+x_k} \\
&\quad \cdot {}^{\mathrm{SP}}\mu^{ex}_{k(jk)}\left(\frac{x_j}{x_j+x_k};\frac{x_k}{x_j+x_k}\right).
\end{aligned}
\tag{Eq 40}
$$

Finally, the partial molar excess Gibbs energy of species $i$ can be calculated by taking the partial derivative of Eq 36 with respect to $n_i$:

$$
\begin{aligned}
&{}^{\mathrm{KT}}\mu^{ex}_{i(ijk)} \\
&= \frac{n_j}{n-n_i}\cdot {}^{\mathrm{SP}}\mu^{ex}_{i(ij)}(x_i;\,1-x_i) \\
&\quad + \frac{n_k}{n-n_i}\cdot {}^{\mathrm{SP}}\mu^{ex}_{i(ik)}(x_i;\,1-x_i) \\
&\quad - \frac{(n-n_i)^2}{n^2} \\
&\quad \cdot {}^{\mathrm{SP}}g^{ex}_{jk}\left(\frac{x_j}{x_j+x_k};\frac{x_k}{x_j+x_k}\right) \\
&= \frac{x_j}{1-x_i}\cdot {}^{\mathrm{SP}}\mu^{ex}_{i(ij)}(x_i;\,1-x_i) \\
&\quad + \frac{x_k}{1-x_i}\cdot {}^{\mathrm{SP}}\mu^{ex}_{i(ik)}(x_i;\,1-x_i) \\
&\quad - (1-x_i)^2 \\
&\quad \cdot {}^{\mathrm{SP}}g^{ex}_{jk}\left(\frac{x_j}{x_j+x_k};\frac{x_k}{x_j+x_k}\right).
\end{aligned}
\tag{Eq 41}
$$

In the previous equations, the definitions of ${}^{\mathrm{SP}}g^{\mathrm{ex}}_{ij}$ and ${}^{\mathrm{SP}}\mu^{\mathrm{ex}}_{i(ij)}$ given in Eq 24 and 25 can be used directly.

#### 3.1.4 Derivation of Terms of a Ternary Subsystem Using Kohler Interpolation

A multi-species phase can be extrapolated from the ternary phase following the same principle used for extrapolating the ternary from a binary. The molar excess Gibbs energy of mixing of such a phase can be represented as:

$$
\begin{aligned}
g^{\mathrm{ex}} &= \sum_{i,j,k\geq 0}(x_i+x_j+x_k)^3 \\
&\quad \cdot {}^{\mathrm{SP}}g^{\mathrm{ex}}_{ijk}\left(\frac{x_i}{x_i+x_j+x_k};\frac{x_j}{x_i+x_j+x_k};\frac{x_k}{x_i+x_j+x_k}\right),
\end{aligned}
\tag{Eq 42}
$$

and expanding this expression in terms of molar quantities instead of mole fractions:

$$
\begin{aligned}
g^{\mathrm{ex}} &= \sum_{i,j,k\geq 0}\left(\frac{n_i+n_j+n_k}{n}\right)^3 \\
&\quad \cdot \frac{{}^{\mathrm{SP}}G^{\mathrm{ex}}_{ijk}\left(\{n_i;n_j;n_k\},n_i+n_j+n_k\right)}{n_i+n_j+n_k}.
\end{aligned}
\tag{Eq 43}
$$

Evidently, the integral excess Gibbs energy of mixing of the phase is defined as:

$$
\begin{aligned}
G^{\mathrm{ex}} &= \sum_{i,j,k\geq 0}\left(\frac{n_i+n_j+n_k}{n}\right)^2 \\
&\quad \cdot {}^{\mathrm{SP}}G^{\mathrm{ex}}_{ijk}\left(\{n_i;n_j;n_k\},n_i+n_j+n_k\right).
\end{aligned}
\tag{Eq 44}
$$

As before, the focus can be on a single ternary subsystem for finding the relevant partial molar quantities. The partial molar excess Gibbs energy of mixing of species $i$ due to the $ijk$ ternary subsystem is the following:

$$
\begin{aligned}
&\mu^{\mathrm{ex}}_{i(ijk)} \\
&= 2\left(\frac{n_i+n_j+n_k}{n^2}\right) \\
&\quad \cdot {}^{\mathrm{SP}}G^{\mathrm{ex}}_{ijk}\left(\{n_i;n_j;n_k\},n_i+n_j+n_k\right) \\
&\quad + \left(\frac{n_i+n_j+n_k}{n}\right)^2 \\
&\quad \cdot {}^{\mathrm{SP}}\mu^{\mathrm{ex}}_{i(ijk)}\left(\frac{x_i}{x_i+x_j+x_k};\frac{x_j}{x_i+x_j+x_k};\frac{x_k}{x_i+x_j+x_k}\right) \\
&\quad - 2\frac{(n_i+n_j+n_k)^2}{n^3} \\
&\quad \cdot {}^{\mathrm{SP}}G^{\mathrm{ex}}_{ijk}\left(\{n_i;n_j;n_k\},n_i+n_j+n_k\right).
\end{aligned}
\tag{Eq 45}
$$

In a simplified form, the previous equation can be written as follows:

$$\begin{aligned}\mu^{\mathrm{ex}}_{i(ijk)} &= (x_i+x_j+x_k)^2\left[{}^{\mathrm{SP}}\mu^{\mathrm{ex}}_{i(ijk)}\left(\frac{x_i}{x_i+x_j+x_k};\right.\right.\\ &\left.\frac{x_j}{x_i+x_j+x_k};\frac{x_k}{x_i+x_j+x_k}\right)\\ &+2(1-x_i-x_j-x_k)\cdot{}^{\mathrm{SP}}g^{\mathrm{ex}}_{ijk}\\ &\left.\left(\frac{x_i}{x_i+x_j+x_k};\frac{x_j}{x_i+x_j+x_k};\quad\frac{x_k}{x_i+x_j+x_k}\right)\right]\end{aligned} \tag{Eq 46}$$

The partial molar excess Gibbs energy of mixing of species $m$ ($m \neq i,j,k$) is:

$$\begin{aligned}\mu^{\mathrm{ex}}_{m(ijk)} &= -2(x_i+x_j+x_k)^3\\ &\cdot{}^{\mathrm{SP}}g^{\mathrm{ex}}_{ijk}\left(\frac{x_i}{x_i+x_j+x_k};\frac{x_j}{x_i+x_j+x_k};\frac{x_k}{x_i+x_j+x_k}\right)\end{aligned} \tag{Eq 47}$$

In the preceding equations, the definitions of ${}^{\mathrm{SP}}g^{\mathrm{ex}}_{ijk}$ and ${}^{\mathrm{SP}}\mu^{\mathrm{ex}}_{i(ijk)}$ given in Eq 17 and 22 can be used directly.

## 4 Redlich–Kister Polynomial Model with Muggiano Interpolation

The substitutional solution model employing a Redlich–Kister polynomial formulation has several advantages over the simple polynomial formulation. These advantages have already been mentioned in the previous section. Starting with the Redlich–Kister formalism, the Muggiano interpolation is the simplest higher-order interpolation scheme and the resultant formalism, often called Redlich–Kister–Muggiano polynomial formalism, is widely used in thermodynamic modelling of symmetric phases. The derivations of the relevant terms for computing the chemical potential of a phase modelled using a Redlich–Kister polynomial with Muggiano interpolation are presented in the following discussion.

### 4.1 Derivation of Partial Excess Gibbs Energy of Mixing

#### *4.1.1 Derivation of Terms of a Multi-species Phase with only Binary Excess Mixing Terms*

If Redlich–Kister polynomials are used to represent interaction parameters, then the binary contribution to the molar excess Gibbs energy of mixing of a multi-species phase is simply:

$$g^{\mathrm{ex}}_{\mathrm{bin}} = \sum_i\sum_{j>i} x_i x_j \sum_v {}^{v}L_{ij}(x_i-x_j)^v. \tag{Eq 48}$$

The equations are simplified in comparison to the Kohler–Toop scheme, which requires special consideration when relating binary interaction parameters for the molar Gibbs energy of a phase.

The integral excess Gibbs energy of the phase, considering only binary contributions, is defined as follows:

$$\begin{aligned}G^{\mathrm{ex}}_{\mathrm{bin}} &= n\sum_i\sum_{j>i} x_i x_j \sum_v {}^{v}L_{ij}(x_i-x_j)^v\\ &= \sum_i\sum_{j>i}\frac{n_i n_j}{n}\sum_v {}^{v}L_{ij}\left(\frac{n_i-n_j}{n}\right)^v.\end{aligned} \tag{Eq 49}$$

For deriving the partial molar excess Gibbs energy of mixing of species $k$ in a multi-species phase, the binary contribution to the integral Gibbs energy of mixing can be subdivided into three cases based on the presence or absence of species $k$ in the binary subsystems. This results in the following form of Eq 49:

$$\begin{aligned}G^{\mathrm{ex}}_{\mathrm{bin}} = &\underbrace{\sum_{j>k}\frac{n_k n_j}{n}\sum_v {}^{v}L_{kj}\left(\frac{n_k-n_j}{n}\right)^v}_{i=k}\\ &+\underbrace{\sum_{i<k}\frac{n_i n_k}{n}\sum_v {}^{v}L_{ik}\left(\frac{n_i-n_k}{n}\right)^v}_{j=k}\\ &+\underbrace{\sum_i\sum_{j>i}\frac{n_i n_j}{n}\sum_v {}^{v}L_{ij}\left(\frac{n_i-n_j}{n}\right)^v}_{i,j\neq k}.\end{aligned} \tag{Eq 50}$$

Taking the partial derivative of Eq 50 with respect to $n_k$, the partial molar excess Gibbs energy of mixing can be given as follows:

$$\begin{aligned}\mu^{\mathrm{ex}}_{k(\mathrm{bin})} = &\underbrace{\sum_{j>k}\left[\left(\frac{n_j}{n}-\frac{n_k n_j}{n^2}\right)\sum_v {}^{v}L_{kj}\left(\frac{n_k-n_j}{n}\right)^v+\frac{n_k n_j}{n}\sum_v {}^{v}L_{kj}v\left(\frac{n_k-n_j}{n^2}\right)^{v-1}\left(\frac{1}{n}-\frac{n_k-n_j}{n^2}\right)\right]}_{i=k}\\ &+\underbrace{\sum_{i<k}\left[\left(\frac{n_i}{n}-\frac{n_i n_k}{n^2}\right)\sum_v {}^{v}L_{ik}\left(\frac{n_i-n_k}{n}\right)^v+\frac{n_i n_k}{n}\sum_v {}^{v}L_{ik}v\left(\frac{n_i-n_k}{n}\right)^{v-1}\left(-\frac{1}{n}-\frac{n_i-n_k}{n^2}\right)\right]}_{j=k}\\ &+\underbrace{\sum_i\sum_{j>i}\left[-\frac{n_i n_j}{n^2}\sum_v {}^{v}L_{ij}\left(\frac{n_i-n_j}{n}\right)^v-\frac{n_i n_j}{n}\sum_v {}^{v}L_{ij}v\left(\frac{n_i-n_j}{n}\right)^{v-1}\left(\frac{n_i-n_j}{n^2}\right)\right]}_{i,j\neq k},\end{aligned} \tag{Eq 51}$$

which simplifies to the following expression for the partial molar excess Gibbs energy of mixing of species $k$ when considering only binary contributions:

$$\mu^{\mathrm{ex}}_{k(\mathrm{bin})} = \underbrace{\sum_{j>k}\left[(x_j - x_k x_j)\sum_v {}^vL_{kj}(x_k - x_j)^v + x_k x_j(1-(x_k - x_j))\sum_v {}^vL_{kj}v(x_k - x_j)^{v-1}\right]}_{i=k} + \underbrace{\sum_{i<k}\left[(x_i - x_i x_k)\sum_v {}^vL_{ik}(x_i - x_k)^v - x_i x_k(1+(x_i - x_k))\sum_v {}^vL_{ik}v(x_i - x_k)^{v-1}\right]}_{j=k} - \underbrace{\sum_i\sum_{j>i}\left[x_i x_j\sum_v {}^vL_{ij}(1+v)(x_i - x_j)^v\right]}_{i,j\neq k}. \quad \text{(Eq 52)}$$

### 4.1.2 Derivation of Terms of a Multi-species Phase with only Ternary Excess Mixing Terms

Using Muggiano interpolation, the ternary contribution to the molar Gibbs energy of a multi-species solution phase can be represented by the following expression[13]:

$$g^{\mathrm{ex}}_{\mathrm{ter}} = \sum_i\sum_{j>i}\sum_{k>j} x_i x_j x_k \sum_l {}^0L_{l(ijk)}\left(\frac{1 - x_i - x_j - x_k}{3} + x_l\right), \quad \text{(Eq 53)}$$

where the interaction parameter ${}^0L_{l(ijk)}$ is only temperature dependent (i.e., only a zeroth-order interaction term, independent of composition) and the right superscript $l = i$, $j$ and $k$ denotes the species for which the parameter has been established.

The integral excess Gibbs energy of mixing is given as the following:

$$G^{\mathrm{ex}}_{\mathrm{ter}} = \sum_i\sum_{j>i}\sum_{k>j}\frac{n_i n_j n_k}{n^3}\sum_l {}^0L_{l(ijk)}\left(\frac{n - n_i - n_j - n_k}{3} + n_l\right). \quad \text{(Eq 54)}$$

For a general species $w$ of the multi-species phase, the partial molar excess Gibbs energy can be derived by taking the partial derivative of Eq 54 with respect to the molar quantity of $w$, $n_w$

$$\mu^{\mathrm{ex}}_{w(ter)} = \sum_i\sum_{j>i}\sum_{k>j}\left[\left\{\frac{1}{n^3}\left(\delta_{iw}n_j n_k + \delta_{jw}n_i n_k + \delta_{kw}n_i n_j\right) - \frac{3n_i n_j n_k}{n^4}\right\}\sum_l {}^0L^l_{ijk}\left(\frac{n - n_i - n_j - n_k}{3} + n_l\right) + \frac{n_i n_j n_k}{n^3}\sum_l {}^0L_{l(ijk)}\left(\frac{1 - \delta_{iw} - \delta_{jw} - \delta_{kw}}{3} + \delta_{lw}\right)\right], \quad \text{(Eq 55)}$$

where the Kronecker delta function $\delta_{ij}$ is defined as:

$$\delta_{ij} = \begin{cases} 0 & i \neq j \\ 1 & i = j. \end{cases}$$

Equation 55 simplifies into the following form valid for any species:

$$\mu^{\mathrm{ex}}_{w(\mathrm{ter})} = \sum_i\sum_{j>i}\sum_{k>j} x_i x_j x_k \left[\left(\sum_u \frac{\delta_{uw}}{x_u} - 3\right)\sum_l {}^0L_{l(ijk)}\left(\frac{1 - x_i - x_j - x_k}{3} + x_l\right) + \sum_l {}^0L^l_{ijk}\left(\frac{1 - \delta_{iw} - \delta_{jw} - \delta_{kw}}{3} + \delta_{lw}\right)\right], \quad \text{(Eq 56)}$$

where the species index $u = i$, $j$ and $k$.

### 4.1.3 Derivation of Terms of a Multi-species Phase with only Quaternary Excess Mixing Terms

In a multi-species phase modelled by the Redlich–Kister polynomials with Muggiano interpolation, the quaternary contribution to the molar Gibbs energy can be represented with the following equation:

$$g^{\mathrm{ex}}_{\mathrm{qua}} = \sum_i\sum_{j>i}\sum_{k>j}\sum_{l>k} x_i x_j x_k x_l L_{ijkl}, \quad \text{(Eq 57)}$$

where the interaction parameter $L_{ijkl}$ is only temperature dependent (i.e. only a zeroth-order interpolation term, independent of composition).[13]

The integral excess Gibbs energy of the phase can then be written as follows:

$$G^{\mathrm{ex}}_{\mathrm{qua}} = \sum_i\sum_{j>i}\sum_{k>j}\sum_{l>k}\left(\frac{n_i n_j n_k n_l}{n^3}\right)L_{ijkl}. \quad \text{(Eq 58)}$$

For a general species $v$ of the multi-species phase, the quaternary contribution to the partial molar excess Gibbs energy of mixing can be derived by taking the partial derivative of the previous equation with respect to the molar quantity of $v$, $n_v$:

$$\mu^{\mathrm{ex}}_{w(qua)} = \sum_i \sum_{j>i} \sum_{k>j} \sum_{l>k} \left[ \frac{1}{n^3} \left( \delta_{iw} n_j n_k n_l + \delta_{jw} n_i n_k n_l + \delta_{kw} n_i n_j n_l + \delta_{lw} n_i n_j n_k \right) - \frac{3 n_i n_j n_k n_l}{n^4} \right] L_{ijkl}. \quad \text{(Eq 59)}$$

The previous expression can be simplified using the definition of mole fractions:

$$\mu^{\mathrm{ex}}_{w(qua)} = \sum_i \sum_{j>i} \sum_{k>j} \sum_{l>k} x_i x_j x_k x_l \left( \sum_u \frac{\delta_{uw}}{x_u} - 3 \right) L_{ijkl}, \quad \text{(Eq 60)}$$

where the species index $u = i, j, k$ and $l$.

## 5 Compound Energy Formalism

The CEF was developed to account for the existence of multiple sublattices and the mixing of constituents within a sublattice. The CEF is applicable to an arbitrary number of sublattices with any number of constituents on each sublattice. It has been widely applied to the modelling of a variety of phases, such as interstitial solutions, intermetallic phases, etc.

Following the nomenclature of Hillert,[16] while there can be multiple sets of species with the same chemical formula, they can be distinguished as compound end members with different constituents on the sublattices. To reiterate earlier definitions, in the context of the CEF, a *compound end member* refers to a unique combination of constituents formed by picking one constituent from each sublattice. The total number of end members of a phase modelled by the CEF is the product of the number of constituents on each sublattice. The CEF is based on the principle that each compound end member has its own Gibbs energy of formation.

### 5.1 Gibbs Energy of Compound Energy Formalism Phases

In CEF, the molar Gibbs energy expressions are defined for each compound end member and excess Gibbs energy of mixing parameters are defined for interactions between the constituents. The molar Gibbs energy, $g$, of a solution phase modelled using the CEF model is generally given as[16]:

$$g = \sum_{k=1}^{N} g_k^{\circ} \prod_{s=1}^{N_s} y_{k(s)} + RT \left( \sum_{s=1}^{N_s} v_s \sum_{j=1}^{C_s} y_{j(s)} \ln \left( y_{j(s)} \right) \right) + g^{\mathrm{ex}}, \quad \text{(Eq 61)}$$

where $g_k^{\circ}$ is the reference molar Gibbs energy of the compound end member $k$, $y_{j(s)}$ represents the site fraction on sublattice $s$ corresponding to constituent $j$, $N$ and $N_s$ denote the number of compound end members and number of sublattices in the solution phase, respectively. The site fractions of constituents of an end member can be related to the mole fraction of the end member as $x_k = \prod_{s=1}^{N_s} y_{j(s)}$. The stoichiometry coefficient for sublattice $s$ is represented by $v_s$, the number of constituents on sublattice $s$ is $C_s$. Finally, the molar excess Gibbs energy of mixing of the solution phase is $g^{\mathrm{ex}}$ and is generally defined as follows:

$$g^{\mathrm{ex}} = \sum_{p=1}^{N_p} y_{j_p(s_p)} y_{k_p(s_p)} \left( \prod_{\substack{s=1 \\ s \neq s_p}}^{N_s} y_{l_p(s)} \right) \sum_{v=0}^{V_p} {}^{v}L_{j_p(s_p)k_p(s_p)} \left( y_{j_p(s_p)} - y_{k_p(s_p)} \right)^v, \quad \text{(Eq 62)}$$

where $N_p$ denotes the number of excess mixing terms, $s_p$ is the sublattice on which mixing is taking place, $j_p(s_p)$ and $k_p(s_p)$ are the constituents being mixed on that sublattice, $l_p(s)$ are the constituents corresponding to the mixed end members on all sublattices other than $s_p$, and ${}^{v}L_{jk}$ denotes the interaction parameter of order $v$. $V_p$ denotes the number of interaction parameters corresponding to the excess mixing term $p$.

Equation 61 can be represented in the following form which is more conducive to the subsequent mathematics and explicitly states the meaning of the first term in the previous equation:

$$g = \sum_{k=1}^{N} g_k^{\circ} \prod_{s=1}^{N_s} \sum_{j=1}^{C_s} \delta_{k(s)j(s)} y_{j(s)} + RT \left( \sum_{s=1}^{N_s} v_s \sum_{j=1}^{C_s} y_{j(s)} \ln \left( y_{j(s)} \right) \right) + g^{\mathrm{ex}}, \quad \text{(Eq 63)}$$

where $\delta_{k(s)j(s)}$ is a Kronecker delta term that is equal to unity when the constituent $j$ on sublattice $s$ matches that of end member $k$ on sublattice $s$ and is otherwise equal to zero.

### 5.2 Derivation of Chemical Potential

In models with multiple sublattices including the CEF, the chemical potentials are defined for the compound end members—not the species or constituents—because the reference Gibbs energies are defined for the compound end members.[16] Applying Eq 3 in this context, the chemical potential of compound end member $i$ in the solution phase represented by the CEF model is generally given as[17]:

$$\mu_i = g + \underbrace{\sum_{s=1}^{N_s}\sum_{j=1}^{C_s}\delta_{i(s)j(s)}\frac{\partial g}{\partial y_{j(s)}}}_{\text{constituents in end member}} \underbrace{\sum_{s=1}^{N_s}\sum_{j=1}^{C_s} y_{j(s)}\frac{\partial g}{\partial y_{j(s)}}}_{\text{all constituents}}. \quad \text{(Eq 64)}$$

#### 5.2.1 *Derivation of Partial Molar Reference Gibbs Energy and Partial Molar Ideal Gibbs Energy of Mixing Contributions to Chemical Potential*

Defining the derivative of the site fraction of constituent $k$ on a sublattice $a$ with respect to the site fraction of constituent $j$ on a sublattice $s$ as:

$$\frac{\partial y_{k(a)}}{\partial y_{j(s)}} = \delta_{as}\delta_{j(s)k(s)}, \quad \text{(Eq 65)}$$

one can compute the partial derivative of Eq 63 with respect to $y_{j(s)}$ for all constituents $j$ of compound end member $i$. Neglecting the partial excess Gibbs energy contribution, the following is obtained for a particular constituent:

$$\frac{\partial(g-g^{\text{ex}})}{\partial y_{j(s)}} = \sum_{k=1}^{N} g_k^{\circ}\left(\frac{\delta_{k(s)j(s)}}{y_{k(s)}}\right)\prod_{a=1}^{N_s} y_{k(a)} + RTv_s\left(1+\ln\left(y_{j(s)}\right)\right). \quad \text{(Eq 66)}$$

Substituting Eq 66 into Eq 64 yields the reference and ideal mixing contributions to the chemical potential of compound end member $i$[17]:

$$\begin{aligned}\mu_i^{\circ}+\mu_i^{\text{id}} &= (g-g^{\text{ex}}) + \sum_{s=1}^{N_s}\sum_{j=1}^{C_s}\delta_{i(s)j(s)}\left(\sum_{k=1}^{N} g_k^{\circ}\left(\frac{\delta_{k(s)j(s)}}{y_{k(s)}}\right)\prod_{a=1}^{N_s} y_{k(a)} + RTv_s\left(1+\ln\left(y_{j(s)}\right)\right)\right)\\ &\quad - \sum_{s=1}^{N_s}\sum_{j=1}^{C_s} y_{j(s)}\left(\sum_{k=1}^{N} g_k^{\circ}\left(\frac{\delta_{k(s)j(s)}}{y_{k(s)}}\right)\prod_{a=1}^{N_s} y_{k(a)} + RTv_s\left(1+\ln\left(y_{j(s)}\right)\right)\right),\end{aligned} \quad \text{(Eq 67)}$$

which simplifies to the following:

$$\begin{aligned}\mu_i^{\circ}+\mu_i^{\text{id}} &= (g-g^{\text{ex}}) + \sum_{s=1}^{N_s}\sum_{k=1}^{N} g_k^{\circ}x_k\left(\frac{\delta_{i(s)k(s)}}{y_{k(s)}}\right)\\ &\quad + RT\sum_{s=1}^{N_s} v_s\left(1+\ln\left(y_{i(s)}\right)\right)\\ &\quad - N_s\sum_{k=1}^{N} g_k^{\circ}x_k - RT\sum_{s=1}^{N_s} v_s\left(1+\sum_{j=1}^{C_s} y_{j(s)}\ln\left(y_{j(s)}\right)\right).\end{aligned} \quad \text{(Eq 68)}$$

Replacing the expression for $g-g^{\text{ex}}$ from Eq 61 into the preceding equation, the following is obtained:

$$\begin{aligned}\mu_i^{\circ}+\mu_i^{\text{id}} &= \sum_{k=1}^{N} g_k^{\circ}x_k\\ &\quad + RT\left(\sum_{s=1}^{N_s} v_s\sum_{j=1}^{C_s} y_{j(s)}\ln\left(y_{j(s)}\right)\right) + \sum_{s=1}^{N_s}\sum_{k=1}^{N} g_k^{\circ}x_k\left(\frac{\delta_{i(s)k(s)}}{y_{k(s)}}\right)\\ &\quad + RT\sum_{s=1}^{N_s} v_s\left(1+\ln\left(y_{i(s)}\right)\right)\\ &\quad - N_s\sum_{k=1}^{N} g_k^{\circ}x_k - RT\sum_{s=1}^{N_s} v_s\left(1+\sum_{j=1}^{C_s} y_{j(s)}\ln\left(y_{j(s)}\right)\right),\end{aligned} \quad \text{(Eq 69)}$$

which simplifies to the following expression for reference and ideal mixing contributions to chemical potential of compound end member $i$:

$$\begin{aligned}\mu_i^{\circ}+\mu_i^{\text{id}} &= \sum_{k=1}^{N} g_k^{\circ}x_k\left(1-N_s+\sum_{s=1}^{N_s}\frac{\delta_{i(s)k(s)}}{y_{i(s)}}\right)\\ &\quad + RT\sum_{s=1}^{N_s} v_s\ln\left(y_{i(s)}\right).\end{aligned} \quad \text{(Eq 70)}$$

The chemical potential of a compound end member therefore includes contributions from the reference molar Gibbs energies of all compound end members in that phase and the ideal mixing contribution to $\mu_i$ only considers the constituents associated with the compound end member $i$.

### 5.2.2 *Derivation of Partial Molar Excess Gibbs Energy of Mixing Contribution to Chemical Potential*

Considering only the composition-independent interaction parameters, Sundman and Ågren gave an expression for the partial molar excess Gibbs energy of mixing of an end member in a CEF phase.[17] However, a full derivation of partial molar excess Gibbs energy of mixing requires considering composition-dependent terms as well. Accounting for these interaction terms results in the following general expression:

$$\mu_i^{\text{ex}} = \sum_{p=1}^{N_p} y_{j_p(s_p)} y_{k_p(s_p)} \left( \prod_{\substack{s=1 \\ s \neq s_p}}^{N_s} y_{l_p(s)} \right) \sum_{v=0}^{V_p} {}^{v}L_{j_p(s_p)k_p(s_p)} (y_{j_p(s_p)} - y_{k_p(s_p)})^v \cdot \left( -(N_s + v) + \frac{\delta_{i(s_p)j_p(s_p)}}{y_{j_p(s_p)}} + \frac{\delta_{i(s_p)k_p(s_p)}}{y_{k_p(s_p)}} + \sum_{\substack{s=1 \\ s \neq s_p}}^{N_s} \frac{\delta_{i(s)l_p(s)}}{y_{l_p(s)}} + \frac{v\left(\delta_{i(s_p)j_p(s_p)} - \delta_{i(s_p)k_p(s_p)}\right)}{(y_{j_p(s_p)} - y_{k_p(s_p)})} \right) \quad \text{(Eq 71)}$$

where terms such as $\delta_{i(s_p)j_p(s_p)}$ are Kronecker deltas equal to unity when the constituent associated with compound end member $i$ on the mixing sublattice $s_p$ is the same as the corresponding constituent of mixing parameter $p$, $j_p(s_p)$. Equation 71 depends only on the constituents $j_p$ and $k_p$, and compound end member $i$. Therefore, this computation does not require looping over other end members and their constituents. Also, note that the indexing scheme used here differs from that of Sundman and Ågren.[17] Sundman et al. use the variables $z > 0$ and $b$ to represent the order of mixing where $z = b + 1$. To minimise confusion, $v \geq 0$ is used here.

## 6 Conclusion

Chemical potentials play a key role in the calculation of thermodynamic equilibrium of an isothermal, isobaric system. Explicit expressions for chemical potentials of the independent variables are required by Gibbs energy minimisers for the formulation of the constraint vector associated with the Hessian matrix of the undetermined Lagrange multipliers and to update the system. A large number of classes of thermodynamic models have been proposed to describe the excess Gibbs energy of mixing for a wide variety of solution phases. While several papers are available in the literature that have described the development of those classes of models, derivations of the chemical potentials ready for implementation in a Gibbs energy minimiser have been absent from the literature. This paper provides full derivations of the chemical potentials of the species in several commonly-used classes of thermodynamic models, such as the substitutional solution model with Kohler–Toop and Muggiano interpolation schemes, and compound energy formalism. These derivations will enable researchers in developing new thermodynamic equilibrium solvers and in integrating the models described in this paper into their pre-existing software.

## 7 Supplementary Materials

To aid the readers in exploring and verifying the equations presented, Mathematica notebooks are available as supplementary material. Readers without a Mathematica license can use the free Wolfram Player (https://www.wolfram.com/player/) to view and interact with the notebooks. A sample PDF output from the notebooks is also attached.

**Acknowledgments** This research was funded, in part, by the U.S. Department of Energy Nuclear Energy Advanced Modeling and Simulation program. This research was undertaken, in part, thanks to funding from the Canada Research Chairs program and the Discovery Grant Program of the Natural Sciences and Engineering Research Council of Canada.

## References

1. L. Kaufman, H. Bernstein, *Computer Calculation of Phase Diagrams—With Special Reference to Refractory Metals* (Academic Press, London, 1970).
2. W. White, S. Johnson, G. Dantzig, Chemical Equilibrium in Complex Mixtures. J. Chem. Phys. **28**(5), 751 (1958)
3. M. Piro, S. Simunovic, T. Besmann, B. Lewis, W. Thompson, The Thermochemistry Library Thermochimica. Comput. Mater. Sci. **67**, 266 (2013)
4. P. Bajpai, M. Poschmann, D. Andrš, C. Bhave, M. Tonks, M. Piro, in *TMS 2020 149th Annual Meeting and Exhibition Supplemental Proceedings* (Springer, 2020), pp. 1013–1025
5. J.J. Van Laar, Die schmelz-oder erstarrungskurven bei binären systemen, wenn die feste phase ein gemisch (amorphe feste lösung oder mischkristalle) der beiden komponenten ist. Z. Phys. Chem. **63**(1), 216 (1908)

6. O. Redlich, A.T. Kister, Algebraic Representation of Thermodynamic Properties and the Classification of Solutions. Ind. Eng. Chem. **40**(2), 345 (1948)
7. M. Hillert, Empirical Methods of Predicting and Representing Thermodynamic Properties of Ternary Solution Phases. Calphad **4**(1), 1 (1980). https://doi.org/10.1016/0364-5916(80)90016-4
8. F. Kohler, Estimation of the Thermodynamic Data for a Ternary System from the Corresponding Binary Systems. Monatshefte für Chemie - Chem. Mon. **91**(4), 738 (1960)
9. G.W. Toop, Predicting ternary activities using binary data. Trans. Metall. Soc. AIME **223**, 850 (1965)
10. C. Colinet, *Estimation Des Grandeurs Thermodynamiques Des Alliages Ternaries* (DES, Faculté Des Sciences, Université de Grenoble, France, 1967).
11. Y.M. Muggianu, M. Gambino, J.P. Bros, Enthalpies de formation des alliages liquides bismuth-étain-gallium à 723 K. choix d'une représentation analytique des grandeurs d'excès intégrales et partielles de mélange. J. Chim. Phys. **72**, 83 (1975)
12. M.H. Piro (ed.), *Advances in Nuclear Fuel Chemistry. Woodhead Publishing Series in Energy* (Woodhead Publishing, Sawston, 2020), pp. 159–182. https://doi.org/10.1016/B978-0-08-102571-0.00004-5
13. P. Chartrand, A. Pelton, On the Choice of Geometric Thermodynamic Models. J. Phase Equilib. **21**(2), 141 (2000)
14. I. Ansara, Comparison of Methods for Thermodynamic Calculation of Phase Diagrams. Int. Met. Rev. **24**(1), 20 (1979)
15. G. Eriksson, K. Hack, Chemsage—A Computer Program for the Calculation of Complex Chemical Equilibria. Metall. Mater. Trans. B **21B**, 1013 (1990)
16. M. Hillert, The Compound Energy Formalism. J. Alloys Compd. **320**(2), 161 (2001). https://doi.org/10.1016/S0925-8388(00)01481-X
17. B. Sundman, J. Ågren, A Regular Solution Model for Phases with Several Components and Sublattices, Suitable for Computer Applications. J. Phys. Chem. Solids **42**, 297 (1981)

Contents lists available at ScienceDirect

Calphad

journal homepage: www.elsevier.com/locate/calphad

# Recent developments for molten salt systems in Thermochimica

Max Poschmann [a], Parikshit Bajpai [b], Bernard W.N. Fitzpatrick [a], Markus H.A. Piro [a,b,*]

[a] Faculty of Energy Systems and Nuclear Science, Ontario Tech University, Oshawa, ON, Canada
[b] Faculty of Science, Ontario Tech University, Oshawa, ON, Canada

ARTICLE INFO

*Keywords:*
CALPHAD
Modified quasi-chemical model
Multi-physics
Thermochimica
Molten salt

ABSTRACT

The modified quasi-chemical model in the quadruplet approximation has been implemented in the open-source equilibrium thermodynamics library Thermochimica, enabling single point equilibrium calculations and sophisticated multi-physics simulations of molten salt nuclear reactor systems. Here, the derivations necessary to obtain the chemical potentials of the quadruplet species required for Gibbs energy minimization are provided. The implementation is verified via code-to-code benchmarking against FactSage. A scheme to increase computational efficiency of multi-physics simulations including Thermochimica is described and its effectiveness for molten salt systems demonstrated. Finally, a multi-physics simulation of a molten salt nuclear fuel system is presented as a demonstration problem: ORIGEN-S is used to calculate the isotopic evolution of a fuel-loaded FLiBe mixture with fission and activation products as Thermochimica predicts the phase evolution and number of moles of Cs in various phases.

## 1. Introduction

With the recent increase in world-wide interest in Molten Salt (nuclear) Reactor (MSR) designs [1], the need for efficient and accurate chemical thermodynamics calculations involving molten salts has grown rapidly. The MSR concept is being actively explored as a next generation nuclear reactor design in Canada, United States, Europe, and several other nation states in both large scale (e.g., approximately 1000 GWe) and small modular reactor platforms. Molten salts are also used in other engineering applications, including solar technologies. The Modified Quasi-chemical Model (MQM) [2–4] in the Quadruplet Approximation (MQMQA) [5,6] has proven to be an effective model for representing fluoride [7–12] and chloride [8,11–14] salt systems. Use of the MQMQA specifically within the FactSage [15] software in which it was first made available has been extremely popular in recent years [16–21]. Unlike other classes of thermodynamic models that focus on the mixing of constituents, the MQMQA focuses on the mixing of pairs (or quadruplets) of constituents to capture short-range ordering.

As a result of this rapidly growing interest, the MQMQA has been implemented in Thermochimica [22]. Thermochimica offers two features that distinguish it from other software: Thermochimica is a free, open-source library, and Thermochimica may be readily coupled to other software for the purposes of multi-physics simulations. In particular, Thermochimica has a history of use in multi-physics simulations of nuclear fuel materials [23–28]. Thus, implementation of MQMQA in Thermochimica enables the integration of Thermochimica into multi-physics simulations of MSRs. Due to widespread concerns over possible corrosion of MSR components by the salts themselves [29], thermochemical predictions for these systems are of particularly high importance. Through the use of Thermochimica, designers of MSR systems may be able to predict when corrosion of reactor components and formation of precipitate or gaseous species may occur, and seek combinations of chemistry and operating conditions that minimize these occurrences.

A critical step in implementing the MQMQA into Thermochimica, or any other Gibbs energy minimizer that uses explicit expressions for the chemical potentials, is the derivation of equations to represent the chemical potentials of individual species as input to the Hessian matrix. These equations have not been previously presented in the literature and are not trivial to derive. One objective of this paper is to provide a derivation of these equations, which will be helpful to others in implementing this model into their own programming. Another objective of this work is to demonstrate capabilities in using such calculations in a multi-physics code for subsequent engineering analyses.

In Section 2, the equations required to implement the MQMQA in thermodynamic software are derived. In Section 3, the implementation of these equations in Thermochimica is verified. In Section 4, a method for accelerating multi-physics simulations employing Thermochimica through re-initialization is described. In Section 5 an application of the

* Corresponding author.
*E-mail address:* markus.piro@ontariotechu.ca (M.H.A. Piro).

https://doi.org/10.1016/j.calphad.2021.102341
Received 30 April 2021; Received in revised form 10 August 2021; Accepted 12 August 2021

MQMQA in Thermochimica to a multi-physics simulation of a molten salt nuclear fuel system is demonstrated. In Section 6 concepts for improvement and future applications are laid out.

## 2. Derivation of chemical potentials within the modified quasi-chemical model

Thermochimica [22] is an open-source equilibrium thermodynamics software library that solves for a unique combination of phases and concentrations that minimizes the Gibbs energy of an input system. This is performed using the Gibbs Energy Minimization (GEM) method [30]. The approach of the GEM method is to optimize the system such that the residuals in mass balance equations and the total Gibbs energy are simultaneously minimized, subject to the constraints of the Gibbs Phase Rule and conservation of mass [30,31]. Upon successful optimization of the chemical system, many thermochemical properties are available, including the mass of stable phases, the concentrations of all species in every stable solution phase, the Gibbs energy of the system, and the chemical potentials of all system components and stable species in the system. Some of these quantities may be used directly in the context of multi-physics simulations, while others might feed into parametrizations of necessary thermophysical properties.

The Gibbs energy of a solution phase depends on its composition, and a number of models and parameters have been proposed to model different phases. These models include ideal solution models, models for a single sublattice and models for multiple sublattices (e.g., Compound Energy Formalism (CEF) [32]). Despite the large number of models available to represent the Gibbs energy of a phase, the general representative expression is as follows:

$$G = G^{\circ} + G^{\mathrm{id}} + G^{\mathrm{ex}} + G^{\mathrm{phys}}, \tag{1}$$

where the Gibbs energy of the phase, $G$, is a sum of the reference Gibbs energy of its species, $G^{\circ}$, which depends only on temperature, hydrostatic pressure and composition of individual species, the ideal mixing term of Gibbs energy, $G^{\mathrm{id}} = -TS^{id}$, which assumes random mixing of constituents with $S^{id}$ denoting the entropy of mixing, and a term to account for non-ideal mixing energy, $G^{\mathrm{ex}}$. The term $G^{\mathrm{phys}}$ captures the various physical phenomena that contribute to the Gibbs energy of the phase (e.g., magnetic contributions), and is not used within the existing MQMQA formalism.

The chemical potential of species $i$ is by definition the partial derivative of the integral Gibbs energy of the system with respect to the number of moles of that species at constant temperature, $T$, and pressure, $P$. Mathematically, this is represented as:

$$\mu_i = \left(\frac{\partial G}{\partial n_i}\right)_{T,P,n_{j\neq i}}, \tag{2}$$

where $n_i$ represents the number of moles of species $i$. One can obtain an expanded expression for chemical potential of $i$ by substituting Eq. (1) into Eq. (2) above, which gives the following:

$$\mu_i = \underbrace{\left(\frac{\partial G^{\circ}}{\partial n_i}\right)_{T,P,n_{j\neq i}}}_{\mu_i^{\circ}} + \underbrace{\left(\frac{\partial G^{\mathrm{id}}}{\partial n_i}\right)_{T,P,n_{j\neq i}}}_{\mu_i^{\mathrm{id}}} + \underbrace{\left(\frac{\partial G^{\mathrm{ex}}}{\partial n_i}\right)_{T,P,n_{j\neq i}}}_{\mu_i^{\mathrm{ex}}}, \tag{3}$$

where the contributions to the integral Gibbs energy are obtained as the product of number of moles of a phase and the respective molar Gibbs energy contribution (i.e., $G^{\circ} = ng^{\circ}$, $G^{\mathrm{id}} = ng^{\mathrm{id}}$ and $G^{\mathrm{ex}} = ng^{\mathrm{ex}}$), with $g^{\circ}$, $g^{\mathrm{id}}$ and $g^{\mathrm{ex}}$ denoting the molar reference Gibbs energy, the molar ideal Gibbs energy of mixing and the molar excess Gibbs energy of mixing, respectively. The partial derivative terms are referred to as the partial reference molar Gibbs energy, partial molar ideal Gibbs energy of mixing and partial molar excess Gibbs energy of mixing and are denoted by $\mu_i^{\circ}$, $\mu_i^{\mathrm{id}}$, and $\mu_i^{\mathrm{ex}}$ respectively.

The MQMQA is a thermodynamic model for treating Short-Range Order (SRO) with two sublattices. The MQMQA is fundamentally different from other classes of thermodynamic models in that the focus is not on the mixing of chemical species or constituents on a lattice, but rather the mixing of species as quadruplets to capture SRO of both First-Nearest-Neighbors (FNN) and Second-Nearest-Neighbors (SNN) in liquid or solid solutions. The details of the evolution of the modified quasichemical model from pair approximation for species mixing on only one sublattice to the current quadruplet approximation on two sublattices are provided by Pelton et al. [2,3,5], Chartrand et al. [4], and Lambotte et al. [6].

### 2.1. Gibbs energy of modified quasichemical model phases

The integral Gibbs energy of a solution phase modeled by MQMQA can be expanded in terms of the site fractions of constituents, $X_i$, equivalent site fractions of constituents, $Y_i$, FNN pair fractions, $X_{i/k}$, SNN quadruplet fractions, $X_{ij/kl}$, and the molar quantities corresponding to these fractions. As the quadruplets are taken to be independent components of the phase, it is necessary to express all of these quantities in terms of the molar quantities of the quadruplets, $n_{ij/kl}$. In the subscript notation used throughout, a single subscript (i.e. $i$) indicates a cation or anion constituent, a subscript pair ($i/k$) indicates a pair consisting of cation constituent $i$ and anion constituent $k$, and a quartet ($ij/kl$) indicates a quadruplet composed of cation constituents $i$ and $j$, and anion constituents $k$ and $l$. The quadruplet fractions are:

$$X_{ij/kl} = \frac{n_{ij/kl}}{\sum_{ab/xy} n_{ab/xy}}. \tag{4}$$

The molar quantity of a pair $i/k$ is:

$$n_{i/k} = \sum_{ab/xy} n_{ab/xy} \frac{(\delta_{ai} + \delta_{bi})(\delta_{xk} + \delta_{yk})}{\zeta_{i/k}}, \tag{5}$$

where $\delta$ is the Kronecker delta function, and $\zeta_{i/k}$ is the FNN to SNN ratio for the pair $i/k$. Then, the mole fraction of a pair is:

$$X_{i/k} = \frac{n_{i/k}}{\sum_{a/x} n_{a/x}}. \tag{6}$$

Next are the site molar quantities, $n_i$. Since the site fractions are specific to each sublattice, the calculation of each is explicitly shown (i.e. $n_i^{\mathrm{1st}}$ and $n_k^{\mathrm{2nd}}$). In the following discussion, the distinction will not be carried through, and the convention will be that if a constituent $i$ is on the first sublattice, then $X_i$ is implicitly $X_i^{\mathrm{1st}}$. That said,

$$n_i^{\mathrm{1st}} = \sum_{ab/xy} n_{ab/xy} \left( \frac{\delta_{ai}}{Z^a_{ab/xy}} + \frac{\delta_{bi}}{Z^b_{ab/xy}} \right), \tag{7}$$

where $Z^i_{ij/kl}$ is the coordination number of constituent $i$ within the quadruplet $ij/kl$, and

$$n_k^{\mathrm{2nd}} = \sum_{ab/xy} n_{ab/xy} \left( \frac{\delta_{xk}}{Z^x_{ab/xy}} + \frac{\delta_{yk}}{Z^y_{ab/xy}} \right). \tag{8}$$

Then, the site fractions are:

$$X_i^{\mathrm{1st}} = \frac{n_i^{\mathrm{1st}}}{\sum_a n_a^{\mathrm{1st}}}, \tag{9}$$

and

$$X_k^{\mathrm{2nd}} = \frac{n_k^{\mathrm{2nd}}}{\sum_x n_x^{\mathrm{2nd}}}. \tag{10}$$

The site-equivalent fractions ($Y_i$) are calculated similar to the site molar quantities ($n_i$), and the same convention will be used here to distinguish between sublattices. They are then:

$$Y_i^{\mathrm{1st}} = \sum_{ab/xy} X_{ab/xy} \left( \frac{\delta_{ai} + \delta_{bi}}{2} \right), \tag{11}$$

and

$$Y_k^{\mathrm{2nd}} = \sum_{ab/xy} X_{ab/xy} \left( \frac{\delta_{xk} + \delta_{yk}}{2} \right). \tag{12}$$

The coordination-equivalent fractions ($F_i$), which are identical to the site-equivalent fractions ($Y_i$) when all $\zeta_{i/k}$ are equal, are defined as [6]:

$$F_i^{1\text{st}} = \sum_{a/x} \delta_{ai} X_{a/x}, \tag{13}$$

and

$$F_k^{2\text{nd}} = \sum_{a/x} \delta_{xk} X_{a/x}. \tag{14}$$

The reference Gibbs energy term is given as follows:

$$G^\circ = \sum_{ij/kl} n_{ij/kl} g^\circ_{ij/kl}, \tag{15}$$

where $g^\circ_{ij/kl}$ denotes the reference molar Gibbs energy of the quadruplet. The configurational entropy terms can be written as the following:

$$\Delta S = -R \left[ \sum_i n_i \ln(X_i) + \sum_{i/k} n_{i/k} \ln\left(\frac{X_{i/k}}{F_i F_k}\right) + \sum_{ij/kl} n_{ij/kl} \ln\left(\frac{X_{ij/kl}}{C_{ij/kl}(X_{i/k}X_{i/l}X_{j/k}X_{j/l})^{\phi}/(Y_iY_jY_kY_l)^{\psi}}\right)\right], \tag{16}$$

where $R$ is the ideal gas constant, $C_{ij/kl} = (2-\delta_{ij})(2-\delta_{kl})$ with $\delta$ being the Kronecker delta function, and the exponents $\phi$ and $\psi$ take the values 1 and 1, or 3/4 and 1/2, depending on whether the original or the updated implementation of MQMQA is used [6]. The excess Gibbs energy term takes the following form:

$$G^{\text{ex}} = \frac{1}{2}\left[ \sum_{ij/kl} n_{ij/kl} \Delta g_{ij/kl} + \sum_{\substack{ij/kl \\ l=k}} \left( \frac{Z^k_{ij/kl}}{2} \sum_{\substack{m \\ m\neq k}} \frac{n_{ij/km}}{Z^k_{ij/km}} \right) \Delta g_{ij/kl} + \sum_{\substack{ij/kl \\ j=i}} \left( \frac{Z^i_{ij/kl}}{2} \sum_{\substack{m \\ m\neq i}} \frac{n_{im/kl}}{Z^i_{im/kl}} \right) \Delta g_{ij/kl} \right]. \tag{17}$$

In the preceding expressions, sums over $i$ are for all constituents, sums over $i/k$ are for all FNN pairs, and sums over $ij/kl$ are for all FNN quadruplets. The empirical mixing parameter used to fit the Gibbs energy of formation of quadruplets, $\Delta g_{ij/kl}$, can take a variety of forms, and indeed even be composed of many of these forms. Because each $\Delta g_{ij/kl}$ contains an unknown number (possibly zero) of terms of various forms, which eventually will be summed, it is convenient to handle each of these terms independently. It should be noted that by definition for quadruplets with $i = j$ and $k = l$, the excess mixing energy is necessarily zero (as no mixing is occurring). For all other quadruplets:

$$\Delta g_{ij/kl} = \sum_{\alpha=1}^{N^{\text{ex}}_{ij/kl}} \Delta g_{ij/kl,\alpha}, \tag{18}$$

where $N^{\text{ex}}_{ij/kl}$ is the number of excess energy terms corresponding to the $ij/kl$ quadruplet.

As described by Pelton [33], the calculation of excess mixing energy terms within the MQMQA depends on the symmetry of the ternary subsystems. These calculations are aided by the use of the variables $\xi_{ij/k}$ and $\chi_{ij/kk}$. They have been generalized to allow for the existence in the system of multiple constituents on both sublattices and to specify which of these constituents the mixing term corresponds to. $\xi_{ij/k}$ is defined as follows:

$$\xi_{ij/k} = \sum_{a=\{i,\nu\}} Y_{a/k}, \tag{19}$$

where $\nu$ represents all constituents that form asymmetrical $i-j-\nu$ ternary subsystems in which $j$ is the asymmetric constituent. $Y_{i/k}$ is a modification of $Y_i$ from Eq. (11) such that only contributions from quadruplets containing species $k$ on the second sublattice are included, such that:

$$Y_{i/k} = \sum_{ab/xy} X_{ab/xy} \left( \frac{(\delta_{ai}+\delta_{bi})(\delta_{xk}+\delta_{yk})}{4} \right). \tag{20}$$

$\chi_{ij/kk}$ is defined as follows in the original implementation [5]:

$$\chi_{ij/kk} = \frac{\sum_{a=\{i,\nu\}} \sum_{b=\{i,\nu\}} X_{ab/kk}}{\sum_{a=\{i,j,\nu,\gamma\}} \sum_{b=\{i,j,\nu,\gamma\}} X_{ab/kk}} = \frac{\sum_{a=\{i,\nu\}} \sum_{b=\{i,\nu\}} n_{ab/kk}}{\sum_{a=\{i,j,\nu,\gamma\}} \sum_{b=\{i,j,\nu,\gamma\}} n_{ab/kk}}, \tag{21}$$

or in the updated implementation [6,33]:

$$\chi_{ij/kk} = \frac{\sum_{a=\{i,\nu\}} \sum_{b=\{i,\nu\}} \sum_x \sum_y \frac{\delta_{kx}+\delta_{ky}}{2} X_{ab/xy}}{\sum_{a=\{i,j,\nu,\gamma\}} \sum_{b=\{i,j,\nu,\gamma\}} \sum_x \sum_y \frac{\delta_{kx}+\delta_{ky}}{2} X_{ab/xy}} = \frac{\sum_{a=\{i,\nu\}} \sum_{b=\{i,\nu\}} \sum_x \sum_y \frac{\delta_{kx}+\delta_{ky}}{2} n_{ab/xy}}{\sum_{a=\{i,j,\nu,\gamma\}} \sum_{b=\{i,j,\nu,\gamma\}} \sum_x \sum_y \frac{\delta_{kx}+\delta_{ky}}{2} n_{ab/xy}}, \tag{22}$$

where $\gamma$ represents all constituents that form asymmetrical $i-j-\gamma$ ternary subsystems in which $i$ is the asymmetric constituent. The sums over $x$ and $y$ are for all constituents on the second sublattice. These equations can be reversed to apply to the second sublattice, but for the sake of brevity from here on only mixing on the first sublattice will be shown explicitly. In Eq. (21), it can be observed that because the numerator and denominator involve the same powers of $X_{ij/kl}$, the mole fractions can be replaced with the molar quantities.

There are numerous possibilities for the form of each $\Delta g_{ij/kl,\alpha}$. These include binary mixing terms proportional to the quadruplet fractions:

$$\Delta g_{ij/kk,\alpha} = g_{ij/kk,\alpha} \cdot \chi^{p_\alpha}_{ij/kk} \chi^{q_\alpha}_{ji/kk}, \tag{23}$$

binary mixing proportional to equivalent site fractions:

$$\Delta g_{ij/kk,\alpha} = g_{ij/kk,\alpha} \cdot \frac{\xi^{p_\alpha}_{ij/k} \xi^{q_\alpha}_{ji/k}}{(\xi_{ij/k}+\xi_{ji/k})^{p_\alpha+q_\alpha}}, \tag{24}$$

ternary mixing proportional to the quadruplet fractions:

$$\Delta g_{ij(m)/kk,\alpha} = g_{ij(m)/kk,\alpha} \cdot \chi^{p_\alpha}_{ij/kk} \chi^{q_\alpha}_{ji/kk} \cdot \begin{cases} \left(\frac{Y_{m/k}}{\xi_{ji/k}}\right)\left(1-\frac{Y_{j/k}}{\xi_{ji/k}}\right)^{r_\alpha-1} & m \in \gamma \\ \left(\frac{Y_{m/k}}{\xi_{ij/k}}\right)\left(1-\frac{Y_{i/k}}{\xi_{ij/k}}\right)^{r_\alpha-1} & m \in \nu \\ Y_{m/k}\left(1-\xi_{ij/k}-\xi_{ji/k}\right)^{r_\alpha-1} & m \notin \{\nu,\gamma\}, \end{cases} \tag{25}$$

and ternary mixing proportional to equivalent site fractions:

$$\Delta g_{ij(m)/kk,\alpha} = g_{ij(m)/kk,\alpha} \cdot \frac{\xi^{p_\alpha}_{ij/k} \xi^{q_\alpha}_{ji/k}}{(\xi_{ij/k}+\xi_{ji/k})^{p_\alpha+q_\alpha}} \cdot \begin{cases} \left(\frac{Y_{m/k}}{\xi_{ji/k}}\right)\left(1-\frac{Y_{j/k}}{\xi_{ji/k}}\right)^{r_\alpha-1} & m \in \gamma \\ \left(\frac{Y_{m/k}}{\xi_{ij/k}}\right)\left(1-\frac{Y_{i/k}}{\xi_{ij/k}}\right)^{r_\alpha-1} & m \in \nu \\ Y_{m/k}\left(1-\xi_{ij/k}-\xi_{ji/k}\right)^{r_\alpha-1} & m \notin \{\nu,\gamma\}, \end{cases} \tag{26}$$

where in the above equations $p_\alpha$, $q_\alpha$, and $r_\alpha$ are integer exponents chosen for the excess mixing term $\alpha$.

In the types of mixing terms described in Eqs. (23)–(26), there is a restriction of having only one constituent involved on either the first or second sublattice. Expressions for mixing on the first sublattice are shown. Note that the terms preceding the cases in Eqs. (25) and (26) correspond to Eqs. (23) and (24), and that the terms within the cases are identical for the two forms of ternary mixing. The cases $m \in \gamma$, $m \in \nu$, and $m \notin \{\nu,\gamma\}$ correspond to the ternary system $i-j-m$ being

asymmetric with $i$ as the asymmetric constituent, asymmetric with $j$ as the asymmetric constituent, and either asymmetric with $m$ as the asymmetric constituent or symmetric, respectively. $m$ cannot be equal to either of $i$ and $j$, as this would not indicate a ternary subsystem.

### 2.2. Derivation of chemical potential equations

In the MQMQA, the chemical potentials are defined as partial derivatives in terms of the molar quantities of the various quadruplets (analogous to the compound end members in the CEF). Following the procedure employed to compute the Gibbs energies, the chemical potentials are computed as sums of derivatives of the various energetic contributions:

$$\begin{aligned}\mu_{ij/kl} &= \left(\frac{\partial G}{\partial n_{ij/kl}}\right)_{T,P,n_{(ab/xy)\neq(ij/kl)}} \\ &= \left(\frac{\partial G^{\circ}}{\partial n_{ij/kl}} - T\frac{\partial \Delta S}{\partial n_{ij/kl}} + \frac{\partial G^{\mathrm{ex}}}{\partial n_{ij/kl}}\right)_{T,P,n_{(ab/xy)\neq(ij/kl)}}.\end{aligned} \tag{27}$$

The following sub-sections will derive each of the terms in Eq. (27).

#### 2.2.1. Derivation of the reference Gibbs energy and entropic contributions to chemical potential equations

The partial molar reference Gibbs energy is defined as follows:

$$\frac{\partial G^{\circ}}{\partial n_{ij/kl}} = g^{\circ}_{ij/kl}. \tag{28}$$

The entropic contributions to chemical potentials are greatly simplified by the cancellation of the derivatives of the terms within logarithms, which results in:

$$\begin{aligned}\frac{\partial \Delta S}{\partial n_{ij/kl}} = R\Bigg[&\sum_m \frac{\partial n_m}{\partial n_{ij/kl}}\ln(X_m) + \sum_{m/z}\frac{\partial n_{m/z}}{\partial n_{ij/kl}}\ln\left(\frac{X_{m/z}}{F_m F_z}\right) \\ &+\ln\left(\frac{X_{ij/kl}}{C_{ij/kl}(X_{i/k}X_{i/l}X_{j/k}X_{j/l})^{\phi}/(Y_iY_jY_kY_l)^{\psi}}\right)\Bigg],\end{aligned} \tag{29}$$

where the sum over $m$ is over all constituents, and the sum over $m/z$ is over all pairs. This leaves only the values of the partial derivatives $\frac{\partial n_m}{\partial n_{ij/kl}}$ and $\frac{\partial n_{m/z}}{\partial n_{ij/kl}}$ to be determined as follows:

$$\frac{\partial n_m}{\partial n_{ij/kl}} = \frac{\delta_{im}}{Z^i_{ij/kl}} + \frac{\delta_{jm}}{Z^j_{ij/kl}} + \frac{\delta_{km}}{Z^k_{ij/kl}} + \frac{\delta_{lm}}{Z^l_{ij/kl}}. \tag{30}$$

While the previous expression is general, it is worth noting that $m$ can never be equal to $i$ or $j$ and $k$ or $l$ at the same time, as the constituent is on either the first sublattice or the second. Finally,

$$\frac{\partial n_{m/z}}{\partial n_{ij/kl}} = \frac{(\delta_{im}+\delta_{jm})(\delta_{kz}+\delta_{lz})}{\zeta_{m/z}}, \tag{31}$$

where $\zeta_{m/z}$ is the ratio of FNN to SNN for the FNN pair $m/z$.

#### 2.2.2. Derivation of the partial molar excess Gibbs energy contribution to chemical potential

Due to the dependence of excess mixing Gibbs energy terms on the mole fractions of phase components, the derivative of each term with respect to molar amounts of all quadruplets are non-zero, unless if all exponents are zero. This results in many cases for the derivatives, as within each form there are cases for the quadruplets explicitly involved in the mixing, and for the rest that are implicitly involved. Fortunately, as will be shown, these derivatives can be written compactly in terms of the excess mixing energies themselves. It is crucial not to forget the product rule resulting from Eq. (17), in which molar quantities are multiplied by the sums of individual excess mixing terms:

$$\begin{aligned}\frac{\partial G^{\mathrm{ex}}}{\partial n_{ab/xy}} = \frac{1}{2}\Bigg[&\sum_{ij/kl}\left\{\frac{\partial n_{ij/kl}}{\partial n_{ab/xy}}\Delta g_{ij/kl} + n_{ij/kl}\frac{\partial \Delta g_{ij/kl}}{\partial n_{ab/xy}}\right\} \\ &+\sum_{\substack{ij/kl\\ l=k}}\left\{\left(\frac{Z^k_{ij/kl}}{2}\sum_{\substack{m\\ m\neq k}}\frac{\frac{\partial n_{ij/km}}{\partial n_{ab/xy}}}{Z^k_{ij/km}}\right)\Delta g_{ij/kl}\right. \\ &\left.+\left(\frac{Z^k_{ij/kl}}{2}\sum_{\substack{m\\ m\neq k}}\frac{n_{ij/km}}{Z^k_{ij/km}}\right)\frac{\partial \Delta g_{ij/kl}}{\partial n_{ab/xy}}\right\} \\ &+\sum_{\substack{ij/kl\\ j=i}}\left\{\left(\frac{Z^i_{ij/kl}}{2}\sum_{\substack{m\\ m\neq i}}\frac{\frac{\partial n_{im/kl}}{\partial n_{ab/xy}}}{Z^i_{im/kl}}\right)\Delta g_{ij/kl}\right. \\ &\left.+\left(\frac{Z^i_{ij/kl}}{2}\sum_{\substack{m\\ m\neq i}}\frac{n_{im/kl}}{Z^i_{im/kl}}\right)\frac{\partial \Delta g_{ij/kl}}{\partial n_{ab/xy}}\right\}\Bigg].\end{aligned} \tag{32}$$

$\frac{\partial n_{ij/kl}}{\partial n_{ab/xy}}$ is equal to 1 if $i=a$, $j=b$, $k=x$, and $l=y$, and is 0 otherwise. Thus, the foregoing expression simplifies to the following:

$$\begin{aligned}\frac{\partial G^{\mathrm{ex}}}{\partial n_{ab/xy}} = \frac{1}{2}\Bigg[&\Delta g_{ab/xy} + \sum_{ij/kl}\left\{n_{ij/kl}\frac{\partial \Delta g_{ij/kl}}{\partial n_{ab/xy}}\right\} \\ &+\left(\frac{Z^x_{ab/xx}}{2Z^x_{ab/xy}} + \frac{Z^y_{ab/yy}}{2Z^y_{ab/xy}}\right)\Delta g_{ab/xy} \\ &+\sum_{\substack{ij/kl\\ l=k}}\left\{\left(\frac{Z^k_{ij/kl}}{2}\sum_{\substack{m\\ m\neq k}}\frac{n_{ij/km}}{Z^k_{ij/km}}\right)\frac{\partial \Delta g_{ij/kl}}{\partial n_{ab/xy}}\right\} \\ &+\left(\frac{Z^a_{aa/xy}}{2Z^a_{ab/xy}} + \frac{Z^b_{bb/xy}}{2Z^b_{ab/xy}}\right)\Delta g_{ab/xy} \\ &+\sum_{\substack{ij/kl\\ j=i}}\left\{\left(\frac{Z^i_{ij/kl}}{2}\sum_{\substack{m\\ m\neq i}}\frac{n_{im/kl}}{Z^i_{im/kl}}\right)\frac{\partial \Delta g_{ij/kl}}{\partial n_{ab/xy}}\right\}\Bigg].\end{aligned} \tag{33}$$

By substituting Eq. (18) into Eq. (33), $\Delta g_{ij/kl}$ can be replaced by $\sum_{\alpha=1}^{N^{\mathrm{ex}}_{ij/kl}}\Delta g_{ij/kl,\alpha}$. Thus, in all cases, the quantity of interest remains $\frac{\partial \Delta g_{ij/kl,\alpha}}{\partial n_{ab/xy}}$. The possible forms for $\Delta g_{ij/kl,\alpha}$ will be approached in the same order as before. Starting with binary mixing based on quadruplet fractions:

$$\begin{aligned}\frac{\partial(\Delta g_{ij/kk,\alpha})}{\partial n_{ab/xy}} = &\frac{\Delta g_{ij/kk,\alpha}}{\sum_{cd/vw} n_{cd/vw}}\cdot\frac{\delta_{xk}\delta_{yk}}{\sum_{c=\{i,j,v,\gamma\}}\sum_{d=\{i,j,v,\gamma\}}X_{cd/kk}} \\ &\times\Bigg[\frac{\left(\sum_{e=i,v}\delta_{ae}\right)\left(\sum_{e=i,v}\delta_{be}\right)p_{\alpha}}{\chi_{ij/kk}} \\ &+\frac{\left(\sum_{e=j,\gamma}\delta_{ae}\right)\left(\sum_{e=j,\gamma}\delta_{be}\right)q_{\alpha}}{\chi_{ji/kk}} \\ &-\left(\sum_{e=i,v}\delta_{ae}+\sum_{e=j,\gamma}\delta_{ae}\right)\left(\sum_{e=i,v}\delta_{be}+\sum_{e=j,\gamma}\delta_{be}\right) \\ &\times\left(p_{\alpha}+q_{\alpha}\right)\Bigg].\end{aligned} \tag{34}$$

In these equations, advantage has been taken of the equal powers of the mole fractions $X_{ij/kl}$ terms in the numerator and denominator to transform these to the molar quantities $n_{ij/kl}$ prior to differentiation.

Eq. (34) is convenient for computational purposes because the derivative of the excess energy term can be expressed relatively compactly in terms of the excess energy term itself. Furthermore, all quantities can be written in terms of $X_{ij/kl}$ except the denominator of the leading fraction, which will cancel with a similar term in Eq. (33).

Next, one can apply the same procedure to binary mixing based on equivalent site fractions:

$$\begin{aligned}\frac{\partial(\Delta g_{ij/kk,\alpha})}{\partial n_{ab/xy}} = \frac{\Delta g_{ij/kk,\alpha}}{\sum_{cd/vw} n_{cd/vw}} \Bigg[ &\left( \sum_{e=\{i,\nu\}} \frac{(\delta_{ae}+\delta_{be})(\delta_{xk}+\delta_{yk})}{4} \right) \\ &\times \left( \frac{p_\alpha}{\xi_{ij/k}} - \frac{p_\alpha + q_\alpha}{\xi_{ij/k}+\xi_{ji/k}} \right) \\ &+ \left( \sum_{e=\{j,\gamma\}} \frac{(\delta_{ae}+\delta_{be})(\delta_{xk}+\delta_{yk})}{4} \right) \\ &\times \left( \frac{q_\alpha}{\xi_{ji/k}} - \frac{p_\alpha + q_\alpha}{\xi_{ij/k}+\xi_{ji/k}} \right) \Bigg],\end{aligned} \tag{35}$$

which has similar properties to Eq. (34).

As shown in Eqs. (25) and (26), the ternary mixing terms include three possible cases. To compute the derivatives of Eqs. (25) and (26), one must first differentiate these three cases. First, the case in which $m \in \gamma$ results in:

$$\begin{aligned}&\frac{\partial}{\partial n_{ab/xy}} \left[ \left( \frac{Y_{m/k}}{\xi_{ji/k}} \right) \left( 1 - \frac{Y_{j/k}}{\xi_{ji/k}} \right)^{r_\alpha - 1} \right] \\ &= \left( \frac{1}{\sum_{cd/vw} n_{cd/vw}} \right) \left( \frac{Y_{m/k}}{\xi_{ji/k}} \right) \left( 1 - \frac{Y_{j/k}}{\xi_{ji/k}} \right)^{r_\alpha - 1} \\ &\quad \cdot \left[ \left( \frac{(\delta_{am}+\delta_{bm})(\delta_{xk}+\delta_{yk})}{4Y_{m/k}} \right) - \left( \sum_{e=\{j,\gamma\}} \frac{(\delta_{ae}+\delta_{be})(\delta_{xk}+\delta_{yk})}{4\xi_{ji/k}} \right) \right. \\ &\quad - \left( \frac{r_\alpha - 1}{\xi_{ji/k}} \right) \left( 1 - \frac{Y_{j/k}}{\xi_{ji/k}} \right)^{-1} \left\{ \left( \frac{(\delta_{aj}+\delta_{bj})(\delta_{xk}+\delta_{yk})}{4} \right) \right. \\ &\quad \left. \left. - Y_{j/k} \left( \sum_{e=\{j,\gamma\}} \frac{(\delta_{ae}+\delta_{be})(\delta_{xk}+\delta_{yk})}{4\xi_{ji/k}} \right) \right\} \right]\end{aligned} \tag{36}$$

Similarly, the case in which $m \in \nu$ results in:

$$\begin{aligned}&\frac{\partial}{\partial n_{ab/xy}} \left[ \left( \frac{Y_{m/k}}{\xi_{ij/k}} \right) \left( 1 - \frac{Y_{i/k}}{\xi_{ij/k}} \right)^{r_\alpha - 1} \right] \\ &= \left( \frac{1}{\sum_{cd/vw} n_{cd/vw}} \right) \left( \frac{Y_{m/k}}{\xi_{ij/k}} \right) \left( 1 - \frac{Y_{i/k}}{\xi_{ij/k}} \right)^{r_\alpha - 1} \\ &\quad \cdot \left[ \left( \frac{(\delta_{am}+\delta_{bm})(\delta_{xk}+\delta_{yk})}{4Y_{m/k}} \right) - \left( \sum_{e=\{i,\nu\}} \frac{(\delta_{ae}+\delta_{be})(\delta_{xk}+\delta_{yk})}{4\xi_{ij/k}} \right) \right. \\ &\quad - \left( \frac{r_\alpha - 1}{\xi_{ij/k}} \right) \left( 1 - \frac{Y_{i/k}}{\xi_{ij/k}} \right)^{-1} \left\{ \left( \frac{(\delta_{ai}+\delta_{bi})(\delta_{xk}+\delta_{yk})}{4} \right) \right. \\ &\quad \left. \left. - Y_{i/k} \left( \sum_{e=\{i,\nu\}} \frac{(\delta_{ae}+\delta_{be})(\delta_{xk}+\delta_{yk})}{4\xi_{ij/k}} \right) \right\} \right]\end{aligned} \tag{37}$$

The case in which $m \notin \{\nu, \gamma\}$ results in:

$$\begin{aligned}\frac{\partial}{\partial n_{ab/xy}} \left[ Y_{m/k} \left( 1 - \xi_{ij/k} - \xi_{ji/k} \right)^{r_\alpha - 1} \right] &= \left( \frac{Y_{m/k} \left( 1 - \xi_{ij/k} - \xi_{ji/k} \right)^{r_\alpha - 1}}{\sum_{cd/vw} n_{cd/vw}} \right) \\ &\cdot \left[ -(r_\alpha) + \left( \frac{(\delta_{am}+\delta_{bm})(\delta_{xk}+\delta_{yk})}{4} \right) \left( \frac{1}{Y_{m/k}} \right) \right. \\ &+ (r_\alpha - 1) \left\{ 1 - \xi_{ij} - \xi_{ji} \right\}^{-1} \\ &\cdot \left\{ 1 - \sum_{e=\{i,\nu\}} \left( \frac{(\delta_{ae}+\delta_{be})(\delta_{xk}+\delta_{yk})}{4} \right) \right. \\ &\left. \left. - \sum_{e=\{j,\gamma\}} \left( \frac{(\delta_{ae}+\delta_{be})(\delta_{xk}+\delta_{yk})}{4} \right) \right\} \right]\end{aligned} \tag{38}$$

With all the necessary pieces in place, the derivatives for ternary excess energy terms can be formed by combining Eqs. (36), (37), and (38) with Eq. (34) (for the quadruplet fraction formulation) and with Eq. (35) (for the site fraction formulation). Taking the quadruplet fraction case first: Eq. (37) is given in Box I where the cases in the last term were described below equation (26). In the second line of Eq. (39), the term $\delta_{xk}\delta_{yk}$ is replaced with $\frac{1}{2}(\delta_{xk}+\delta_{yk})$ for the updated implementation of MQMQA [6,33]. Finally, the site fraction case: Eq. (38) is given in Box II.

The equations presented here are in a form suitable for direct implementation into software, and have been incorporated in Thermochimica in as similar a manner as is possible within the Fortran language. This is intended to enhance readability of the Thermochimica source code to enable verification, modification, use, and comparison with other software in which the MQMQA is implemented. In the following sections, we will demonstrate verification, modification, and use of the MQMQA in Thermochimica.

$$\frac{\partial \Delta g_{ij(m)/kk,\alpha}}{\partial n_{ab/xy}} = \frac{\Delta g_{ij(m)/kk,\alpha}}{\sum_{cd/vw} n_{cd/vw}}$$

$$\cdot \left[ \frac{\delta_{xk}\delta_{yk}}{\sum_{c=\{i,j,\nu,\gamma\}} \sum_{d=\{i,j,\nu,\gamma\}} X_{cd/kk}} \left[ \frac{\left(\sum_{e=i,\nu} \delta_{ae}\right)\left(\sum_{e=i,\nu} \delta_{be}\right) p_\alpha}{\chi_{ij/kk}} + \frac{\left(\sum_{e=ij,\gamma} \delta_{ae}\right)\left(\sum_{e=j,\gamma} \delta_{be}\right) q_\alpha}{\chi_{ji/kk}} \right.\right.$$

$$\left.\left. - \left(\left(\sum_{e=i,\nu} \delta_{ae}\right) + \left(\sum_{e=ij,\gamma} \delta_{ae}\right)\right)\left(\left(\sum_{e=i,\nu} \delta_{be}\right) + \left(\sum_{e=j,\gamma} \delta_{be}\right)\right)(p_\alpha + q_\alpha) \right] \right.$$

$$+ \left\{ \begin{array}{ll} \left(\frac{(\delta_{am}+\delta_{bm})(\delta_{xk}+\delta_{yk})}{4Y_{m/k}}\right) - \left(\sum_{e=\{j,\gamma\}} \frac{(\delta_{ae}+\delta_{be})(\delta_{xk}+\delta_{yk})}{4\xi_{ji/k}}\right) & \\ - \left(\frac{r_\alpha - 1}{\xi_{ji/k}}\right)\left(1 - \frac{Y_{j/k}}{\xi_{ji/k}}\right)^{-1} \left\{ \left(\frac{(\delta_{aj}+\delta_{bj})(\delta_{xk}+\delta_{yk})}{4}\right) - Y_{j/k}\left(\sum_{e=\{j,\gamma\}} \frac{(\delta_{ae}+\delta_{be})(\delta_{xk}+\delta_{yk})}{4\xi_{ji/k}}\right)\right\} & m \in \gamma \\ \left(\frac{(\delta_{am}+\delta_{bm})(\delta_{xk}+\delta_{yk})}{4Y_{m/k}}\right) - \left(\sum_{e=\{i,\nu\}} \frac{(\delta_{ae}+\delta_{be})(\delta_{xk}+\delta_{yk})}{4\xi_{ij/k}}\right) & \\ - \left(\frac{r_\alpha - 1}{\xi_{ij/k}}\right)\left(1 - \frac{Y_{i/k}}{\xi_{ij/k}}\right)^{-1} \left\{ \left(\frac{(\delta_{ai}+\delta_{bi})(\delta_{xk}+\delta_{yk})}{4}\right) - Y_{i/k}\left(\sum_{e=\{i,\nu\}} \frac{(\delta_{ae}+\delta_{be})(\delta_{xk}+\delta_{yk})}{4\xi_{ij/k}}\right)\right\} & m \in \nu \\ -(r_\alpha) + \left(\frac{(\delta_{am}+\delta_{bm})(\delta_{xk}+\delta_{yk})}{4}\right)\left(\frac{1}{Y_{m/k}}\right) + (r_\alpha - 1)\left\{1 - \xi_{ij} - \xi_{ji}\right\}^{-1} & \\ \quad \cdot \left\{1 - \sum_{e=\{i,\nu\}} \left(\frac{(\delta_{ae}+\delta_{be})(\delta_{xk}+\delta_{yk})}{4}\right) - \sum_{e=\{j,\gamma\}} \left(\frac{(\delta_{ae}+\delta_{be})(\delta_{xk}+\delta_{yk})}{4}\right)\right\} & m \notin \{\nu, \gamma\} \end{array} \right\}, \tag{39}$$

**Box I.**

$$\frac{\partial \Delta g_{ij(m)/kk,\alpha}}{\partial n_{ab/xy}} = \frac{\Delta g_{ij(m)/kk,\alpha}}{\sum_{cd/vw} n_{cd/vw}}$$

$$\cdot \left[ \left( \sum_{e=\{i,\nu\}} \frac{(\delta_{ae} + \delta_{be})(\delta_{xk} + \delta_{yk})}{4} \right) \left( \frac{p_\alpha}{\xi_{ij/k}} - \frac{p_\alpha + q_\alpha}{\xi_{ij/k} + \xi_{ji/k}} \right) \right.$$

$$\left. + \left( \sum_{e=\{j,\gamma\}} \frac{(\delta_{ae} + \delta_{be})(\delta_{xk} + \delta_{yk})}{4} \right) \left( \frac{q_\alpha}{\xi_{ji/k}} - \frac{p_\alpha + q_\alpha}{\xi_{ij/k} + \xi_{ji/k}} \right) \right.$$

$$+ \left\{ \begin{array}{ll} \left(\frac{(\delta_{am}+\delta_{bm})(\delta_{xk}+\delta_{yk})}{4Y_{m/k}}\right) - \left(\sum_{e=\{j,\gamma\}} \frac{(\delta_{ae}+\delta_{be})(\delta_{xk}+\delta_{yk})}{4\xi_{ji/k}}\right) & \\ - \left(\frac{r_\alpha - 1}{\xi_{ji/k}}\right)\left(1 - \frac{Y_{j/k}}{\xi_{ji/k}}\right)^{-1} \left\{ \left(\frac{(\delta_{aj}+\delta_{bj})(\delta_{xk}+\delta_{yk})}{4}\right) - Y_{j/k}\left(\sum_{e=\{j,\gamma\}} \frac{(\delta_{ae}+\delta_{be})(\delta_{xk}+\delta_{yk})}{4\xi_{ji/k}}\right)\right\} & m \in \gamma \\ \left(\frac{(\delta_{am}+\delta_{bm})(\delta_{xk}+\delta_{yk})}{4Y_{m/k}}\right) - \left(\sum_{e=\{i,\nu\}} \frac{(\delta_{ae}+\delta_{be})(\delta_{xk}+\delta_{yk})}{4\xi_{ij/k}}\right) & \\ - \left(\frac{r_\alpha - 1}{\xi_{ij/k}}\right)\left(1 - \frac{Y_{i/k}}{\xi_{ij/k}}\right)^{-1} \left\{ \left(\frac{(\delta_{ai}+\delta_{bi})(\delta_{xk}+\delta_{yk})}{4}\right) - Y_{i/k}\left(\sum_{e=\{i,\nu\}} \frac{(\delta_{ae}+\delta_{be})(\delta_{xk}+\delta_{yk})}{4\xi_{ij/k}}\right)\right\} & m \in \nu \\ -(r_\alpha) + \left(\frac{(\delta_{am}+\delta_{bm})(\delta_{xk}+\delta_{yk})}{4}\right)\left(\frac{1}{Y_{m/k}}\right) + (r_\alpha - 1)\left\{1 - \xi_{ij} - \xi_{ji}\right\}^{-1} & \\ \quad \cdot \left\{1 - \sum_{e=\{i,\nu\}} \left(\frac{(\delta_{ae}+\delta_{be})(\delta_{xk}+\delta_{yk})}{4}\right) - \sum_{e=\{j,\gamma\}} \left(\frac{(\delta_{ae}+\delta_{be})(\delta_{xk}+\delta_{yk})}{4}\right)\right\} & m \notin \{\nu, \gamma\} \end{array} \right\}. \tag{40}$$

**Box II.**

## Declaration of competing interest

The authors declare that they have no known competing financial interests or personal relationships that could have appeared to influence the work reported in this paper.

## Acknowledgments

The authors thank O. Beneš (JRC) and T.M. Besmann (UofSC) for technical discussions. This research was funded, in part, by the U.S. Department of Energy Nuclear Energy Advanced Modeling and Simulation program. This research was undertaken, in part, thanks to funding from the Canada Research Chairs program and the Discovery Grant Program of the Natural Sciences and Engineering Research Council of Canada.

## Appendix A

### A.1. Extended derivations

Some steps omitted from the derivations in the main text are included below for curious readers.

Eq. (34):

$$
\begin{aligned}
\frac{\partial(\Delta g_{ij/kk,\alpha})}{\partial n_{ab/xy}} &= g_{ij/kk,\alpha}\frac{\partial}{\partial n_{ab/xy}}\left[\chi_{ij/kk}^{p_\alpha}\chi_{ji/kk}^{q_\alpha}\right]\\
&= g_{ij/kk,\alpha}\frac{\partial}{\partial n_{ab/xy}}\left[\left(\frac{\sum_{c=\{i,\nu\}}\sum_{d=\{i,\nu\}}X_{cd/kk}}{\sum_{c=\{i,j,\nu,\gamma\}}\sum_{d=\{i,j,\nu,\gamma\}}X_{cd/kk}}\right)^{p_\alpha}\right.\\
&\quad\left.\times\left(\frac{\sum_{c=\{j,\gamma\}}\sum_{d=\{j,\gamma\}}X_{cd/kk}}{\sum_{c=\{i,j,\nu,\gamma\}}\sum_{d=\{i,j,\nu,\gamma\}}X_{cd/kk}}\right)^{q_\alpha}\right]\\
&= g_{ij/kk,\alpha}\frac{\partial}{\partial n_{ab/xy}}\left[\frac{\left(\sum_{c=\{i,\nu\}}\sum_{d=\{i,\nu\}}n_{cd/kk}\right)^{p_\alpha}\left(\sum_{c=\{j,\gamma\}}\sum_{d=\{j,\gamma\}}n_{cd/kk}\right)^{q_\alpha}}{\left(\sum_{c=\{i,j,\nu,\gamma\}}\sum_{d=\{i,j,\nu,\gamma\}}n_{cd/kk}\right)^{p_\alpha+q_\alpha}}\right]\\
&= g_{ij/kk,\alpha}\delta_{xk}\delta_{yk}\left[\frac{\left(\sum_{e=i,\nu}\delta_{ae}\right)\left(\sum_{e=i,\nu}\delta_{be}\right)p_\alpha}{\sum_{c=\{i,\nu\}}\sum_{d=\{i,\nu\}}n_{cd/kk}}+\frac{\left(\sum_{e=j,\gamma}\delta_{ae}\right)\left(\sum_{e=j,\gamma}\delta_{be}\right)q_\alpha}{\sum_{c=\{j,\gamma\}}\sum_{d=\{j,\gamma\}}n_{cd/kk}}\right.\\
&\quad\left.-\frac{\left(\sum_{e=i,\nu}\delta_{ae}+\sum_{e=j,\gamma}\delta_{ae}\right)\left(\sum_{e=i,\nu}\delta_{be}+\sum_{e=j,\gamma}\delta_{be}\right)(p_\alpha+q_\alpha)}{\sum_{c=\{i,j,\nu,\gamma\}}\sum_{d=\{i,j,\nu,\gamma\}}n_{cd/kk}}\right]\\
&\quad\cdot\left[\frac{\left(\sum_{c=\{i,\nu\}}\sum_{d=\{i,\nu\}}n_{cd/kk}\right)^{p_\alpha}\left(\sum_{c=\{j,\gamma\}}\sum_{d=\{j,\gamma\}}n_{cd/kk}\right)^{q_\alpha}}{\left(\sum_{c=\{i,j,\nu,\gamma\}}\sum_{d=\{i,j,\nu,\gamma\}}n_{cd/kk}\right)^{p_\alpha+q_\alpha}}\right]\\
&= \Delta g_{ij/kk,\alpha}\frac{\delta_{xk}\delta_{yk}}{\sum_{c=\{i,j,\nu,\gamma\}}\sum_{d=\{i,j,\nu,\gamma\}}n_{cd/kk}}\left[\frac{\left(\sum_{e=i,\nu}\delta_{ae}\right)\left(\sum_{e=i,\nu}\delta_{be}\right)p_\alpha}{\chi_{ij/kk}}\right.\\
&\quad\left.+\frac{\left(\sum_{e=j,\gamma}\delta_{ae}\right)\left(\sum_{e=j,\gamma}\delta_{be}\right)q_\alpha}{\chi_{ji/kk}}-\left(\sum_{e=i,\nu}\delta_{ae}+\sum_{e=j,\gamma}\delta_{ae}\right)\right.\\
&\quad\left.\times\left(\sum_{e=i,\nu}\delta_{be}+\sum_{e=j,\gamma}\delta_{be}\right)(p_\alpha+q_\alpha)\right]\\
&= \frac{\Delta g_{ij/kk,\alpha}}{\sum_{cd/vw}n_{cd/vw}}\cdot\frac{\delta_{xk}\delta_{yk}}{\sum_{c=\{i,j,\nu,\gamma\}}\sum_{d=\{i,j,\nu,\gamma\}}X_{cd/kk}}\left[\frac{\left(\sum_{e=i,\nu}\delta_{ae}\right)\left(\sum_{e=i,\nu}\delta_{be}\right)p_\alpha}{\chi_{ij/kk}}\right.\\
&\quad\left.+\frac{\left(\sum_{e=j,\gamma}\delta_{ae}\right)\left(\sum_{e=j,\gamma}\delta_{be}\right)q_\alpha}{\chi_{ji/kk}}-\left(\sum_{e=i,\nu}\delta_{ae}+\sum_{e=j,\gamma}\delta_{ae}\right)\right.\\
&\quad\left.\times\left(\sum_{e=i,\nu}\delta_{be}+\sum_{e=j,\gamma}\delta_{be}\right)(p_\alpha+q_\alpha)\right].
\end{aligned}
\tag{A.1}
$$

Eq. (35) is given in Box III.

Eq. (36) is given in Box IV.

Eq. (38):

$$
\begin{aligned}
&\frac{\partial}{\partial n_{ab/xy}}\left[Y_{m/k}\left(1-\xi_{ij/k}-\xi_{ji/k}\right)^{r_\alpha-1}\right]\\
&\quad=\frac{\partial}{\partial n_{ab/xy}}\left[Y_{m/k}\left(1-\sum_{e=\{i,\nu\}}Y_{e/k}-\sum_{e=\{j,\gamma\}}Y_{e/k}\right)^{r_\alpha-1}\right]\\
&\quad=\frac{\partial}{\partial n_{ab/xy}}\left[\left(\sum_{cd/vw}X_{cd/vw}\left(\frac{(\delta_{cm}+\delta_{dm})(\delta_{vk}+\delta_{wk})}{4}\right)\right)\right.\\
&\qquad\left\{1-\left(\sum_{e=\{i,\nu\}}\sum_{cd/vw}X_{cd/vw}\left(\frac{(\delta_{ce}+\delta_{de})(\delta_{vk}+\delta_{wk})}{4}\right)\right)\right.\\
&\qquad\left.\left.-\left(\sum_{e=\{j,\gamma\}}\sum_{cd/vw}X_{cd/vw}\left(\frac{(\delta_{ce}+\delta_{de})(\delta_{vk}+\delta_{wk})}{4}\right)\right)\right\}^{r_\alpha-1}\right]\\
&\quad=\frac{\partial}{\partial n_{ab/xy}}\left[\left(\frac{1}{\sum_{cd/vw}n_{cd/vw}}\right)^{r_\alpha}\left(\sum_{cd/vw}n_{cd/vw}\left(\frac{(\delta_{cm}+\delta_{dm})(\delta_{vk}+\delta_{wk})}{4}\right)\right)\right.\\
&\qquad\left\{\sum_{cd/vw}n_{cd/vw}-\left(\sum_{e=\{i,\nu\}}\sum_{cd/vw}n_{cd/vw}\left(\frac{(\delta_{ce}+\delta_{de})(\delta_{vk}+\delta_{wk})}{4}\right)\right)\right.\\
&\qquad\left.\left.-\left(\sum_{e=\{j,\gamma\}}\sum_{cd/vw}n_{cd/vw}\left(\frac{(\delta_{ce}+\delta_{de})(\delta_{vk}+\delta_{wk})}{4}\right)\right)\right\}^{r_\alpha-1}\right]\\
&\quad=\left(\frac{Y_{m/k}\left(1-\xi_{ij/k}-\xi_{ji/k}\right)^{r_\alpha-1}}{\sum_{cd/vw}n_{cd/vw}}\right)\\
&\qquad\cdot\left[-(r_\alpha)+\left(\frac{(\delta_{am}+\delta_{bm})(\delta_{xk}+\delta_{yk})}{4}\right)\left(\frac{1}{Y_{m/k}}\right)\right.\\
&\qquad+(r_\alpha-1)\left\{1-\xi_{ij}-\xi_{ji}\right\}^{-1}\\
&\qquad\cdot\left\{1-\sum_{e=\{i,\nu\}}\left(\frac{(\delta_{ae}+\delta_{be})(\delta_{xk}+\delta_{yk})}{4}\right)\right.\\
&\qquad\left.\left.-\sum_{e=\{j,\gamma\}}\left(\frac{(\delta_{ae}+\delta_{be})(\delta_{xk}+\delta_{yk})}{4}\right)\right\}\right]
\end{aligned}
\tag{A.4}
$$

## Appendix B. Supplementary data

Supplementary material related to this article can be found online at https://doi.org/10.1016/j.calphad.2021.102341.

$$
\begin{aligned}
\frac{\partial(\Delta g_{ij/kk,\alpha})}{\partial n_{ab/xy}} &= g_{ij/kk,\alpha}\frac{\partial}{\partial n_{ab/xy}}\left[\frac{\xi_{ij/k}^{p_\alpha}\xi_{ji/k}^{q_\alpha}}{(\xi_{ij/k}+\xi_{ji/k})^{p_\alpha+q_\alpha}}\right] \\
&= g_{ij/kk,\alpha}\frac{\partial}{\partial n_{ab/xy}}\left[\frac{\left(\sum_{e=\{i,\nu\}} Y_{e/k}\right)^{p_\alpha}\left(\sum_{e=\{j,\gamma\}} Y_{e/k}\right)^{q_\alpha}}{\left(\sum_{e=\{i,\nu\}} Y_{e/k}+\sum_{e=\{j,\gamma\}} Y_{e/k}\right)^{p_\alpha+q_\alpha}}\right] \\
&= g_{ij/kk,\alpha}\frac{\partial}{\partial n_{ab/xy}}\left[\left(\sum_{e=\{i,\nu\}}\sum_{cd/vw} X_{cd/vw}\left(\frac{(\delta_{ce}+\delta_{de})(\delta_{vk}+\delta_{wk})}{4}\right)\right)^{p_\alpha}\cdot\left(\sum_{e=\{j,\gamma\}}\sum_{cd/vw} X_{cd/vw}\left(\frac{(\delta_{ce}+\delta_{de})(\delta_{vk}+\delta_{wk})}{4}\right)\right)^{q_\alpha}\right. \\
&\qquad \left.\Big/\left(\sum_{e=\{i,\nu\}}\sum_{cd/vw} X_{cd/vw}\left(\frac{(\delta_{ce}+\delta_{de})(\delta_{vk}+\delta_{wk})}{4}\right)+\sum_{e=\{j,\gamma\}}\sum_{cd/vw} X_{cd/vw}\left(\frac{(\delta_{ce}+\delta_{de})(\delta_{vk}+\delta_{wk})}{4}\right)\right)^{p_\alpha+q_\alpha}\right] \\
&= g_{ij/kk,\alpha}\frac{\partial}{\partial n_{ab/xy}}\left[\left(\sum_{e=\{i,\nu\}}\sum_{cd/vw} n_{cd/vw}\left(\frac{(\delta_{ce}+\delta_{de})(\delta_{vk}+\delta_{wk})}{4}\right)\right)^{p_\alpha}\cdot\left(\sum_{e=\{j,\gamma\}}\sum_{cd/vw} n_{cd/vw}\left(\frac{(\delta_{ce}+\delta_{de})(\delta_{vk}+\delta_{wk})}{4}\right)\right)^{q_\alpha}\right. \\
&\qquad \left.\Big/\left(\sum_{e=\{i,\nu\}}\sum_{cd/vw} n_{cd/vw}\left(\frac{(\delta_{ce}+\delta_{de})(\delta_{vk}+\delta_{wk})}{4}\right)+\sum_{e=\{j,\gamma\}}\sum_{cd/vw} n_{cd/vw}\left(\frac{(\delta_{ce}+\delta_{de})(\delta_{vk}+\delta_{wk})}{4}\right)\right)^{p_\alpha+q_\alpha}\right] \\
&= \Delta g_{ij/kk,\alpha}\left[\left(\sum_{e=\{i,\nu\}}\frac{(\delta_{ae}+\delta_{be})(\delta_{xk}+\delta_{yk})}{4}\right)\left(\frac{p_\alpha}{\sum_{e=\{i,\nu\}}\sum_{cd/vw} n_{cd/vw}\left(\frac{(\delta_{ce}+\delta_{de})(\delta_{vk}+\delta_{wk})}{4}\right)}-\frac{p_\alpha+q_\alpha}{\sum_{e=\{i,\nu\}}\sum_{cd/vw} n_{cd/vw}\left(\frac{(\delta_{ce}+\delta_{de})(\delta_{vk}+\delta_{wk})}{4}\right)+\sum_{e=\{j,\gamma\}}\sum_{cd/vw} n_{cd/vw}\left(\frac{(\delta_{ce}+\delta_{de})(\delta_{vk}+\delta_{wk})}{4}\right)}\right)\right. \\
&\qquad \left.+\left(\sum_{e=\{j,\gamma\}}\frac{(\delta_{ae}+\delta_{be})(\delta_{xk}+\delta_{yk})}{4}\right)\left(\frac{q_\alpha}{\sum_{e=\{j,\gamma\}}\sum_{cd/vw} n_{cd/vw}\left(\frac{(\delta_{ce}+\delta_{de})(\delta_{vk}+\delta_{wk})}{4}\right)}-\frac{p_\alpha+q_\alpha}{\sum_{e=\{i,\nu\}}\sum_{cd/vw} n_{cd/vw}\left(\frac{(\delta_{ce}+\delta_{de})(\delta_{vk}+\delta_{wk})}{4}\right)+\sum_{e=\{j,\gamma\}}\sum_{cd/vw} n_{cd/vw}\left(\frac{(\delta_{ce}+\delta_{de})(\delta_{vk}+\delta_{wk})}{4}\right)}\right)\right] \\
&= \frac{\Delta g_{ij/kk,\alpha}}{\sum_{cd/vw} n_{cd/vw}}\left[\left(\sum_{e=\{i,\nu\}}\frac{(\delta_{ae}+\delta_{be})(\delta_{xk}+\delta_{yk})}{4}\right)\left(\frac{p_\alpha}{\xi_{ij/k}}-\frac{p_\alpha+q_\alpha}{\xi_{ij/k}+\xi_{ji/k}}\right)+\left(\sum_{e=\{j,\gamma\}}\frac{(\delta_{ae}+\delta_{be})(\delta_{xk}+\delta_{yk})}{4}\right)\left(\frac{q_\alpha}{\xi_{ji/k}}-\frac{p_\alpha+q_\alpha}{\xi_{ij/k}+\xi_{ji/k}}\right)\right],
\end{aligned}
\tag{A.2}
$$

**Box III.**

$$
\begin{aligned}
&\frac{\partial}{\partial n_{ab/xy}}\left[\left(\frac{Y_{m/k}}{\xi_{ji/k}}\right)\left(1-\frac{Y_{j/k}}{\xi_{ji/k}}\right)^{r_\alpha-1}\right]=\frac{\partial}{\partial n_{ab/xy}}\left[\left(\frac{Y_{m/k}}{\sum_{e=\{j,\gamma\}} Y_{e/k}}\right)\left(1-\frac{Y_{j/k}}{\sum_{e=\{j,\gamma\}} Y_{e/k}}\right)^{r_\alpha-1}\right] \\
&=\frac{\partial}{\partial n_{ab/xy}}\left[\left(\frac{\sum_{cd/vw} X_{cd/vw}\left(\frac{(\delta_{cm}+\delta_{dm})(\delta_{vk}+\delta_{wk})}{4}\right)}{\sum_{e=\{j,\gamma\}}\sum_{cd/vw} X_{cd/vw}\left(\frac{(\delta_{ce}+\delta_{de})(\delta_{vk}+\delta_{wk})}{4}\right)}\right)\cdot\left(1-\frac{\sum_{cd/vw} X_{cd/vw}\left(\frac{(\delta_{cj}+\delta_{dj})(\delta_{vk}+\delta_{wk})}{4}\right)}{\sum_{e=\{j,\gamma\}}\sum_{cd/vw} X_{cd/vw}\left(\frac{(\delta_{ce}+\delta_{de})(\delta_{vk}+\delta_{wk})}{4}\right)}\right)^{r_\alpha-1}\right] \\
&=\frac{\partial}{\partial n_{ab/xy}}\left[\left(\frac{\sum_{cd/vw} n_{cd/vw}\left(\frac{(\delta_{cm}+\delta_{dm})(\delta_{vk}+\delta_{wk})}{4}\right)}{\sum_{e=\{j,\gamma\}}\sum_{cd/vw} n_{cd/vw}\left(\frac{(\delta_{ce}+\delta_{de})(\delta_{vk}+\delta_{wk})}{4}\right)}\right)\cdot\left(1-\frac{\sum_{cd/vw} n_{cd/vw}\left(\frac{(\delta_{cj}+\delta_{dj})(\delta_{vk}+\delta_{wk})}{4}\right)}{\sum_{e=\{j,\gamma\}}\sum_{cd/vw} n_{cd/vw}\left(\frac{(\delta_{ce}+\delta_{de})(\delta_{vk}+\delta_{wk})}{4}\right)}\right)^{r_\alpha-1}\right] \\
&=\left(\frac{Y_{m/k}}{\xi_{ji/k}}\right)\left(1-\frac{Y_{j/k}}{\xi_{ji/k}}\right)^{r_\alpha-1}\left[\left(\frac{\frac{(\delta_{am}+\delta_{bm})(\delta_{xk}+\delta_{yk})}{4}}{\sum_{cd/vw} n_{cd/vw}\left(\frac{(\delta_{cm}+\delta_{dm})(\delta_{vk}+\delta_{wk})}{4}\right)}\right)-\left(\frac{\sum_{e=\{j,\gamma\}}\frac{(\delta_{ae}+\delta_{be})(\delta_{xk}+\delta_{yk})}{4}}{\sum_{e=\{j,\gamma\}}\sum_{cd/vw} n_{cd/vw}\left(\frac{(\delta_{ce}+\delta_{de})(\delta_{vk}+\delta_{wk})}{4}\right)}\right)-\left(\frac{r_\alpha-1}{\sum_{e=\{j,\gamma\}}\sum_{cd/vw} n_{cd/vw}\left(\frac{(\delta_{ce}+\delta_{de})(\delta_{vk}+\delta_{wk})}{4}\right)}\right)\right. \\
&\qquad \left.\cdot\left(1-\frac{\sum_{cd/vw} n_{cd/vw}\left(\frac{(\delta_{cj}+\delta_{dj})(\delta_{vk}+\delta_{wk})}{4}\right)}{\sum_{e=\{j,\gamma\}}\sum_{cd/vw} n_{cd/vw}\left(\frac{(\delta_{ce}+\delta_{de})(\delta_{vk}+\delta_{wk})}{4}\right)}\right)^{-1}\times\left\{\left(\frac{(\delta_{aj}+\delta_{bj})(\delta_{xk}+\delta_{yk})}{4}\right)-\left(\sum_{cd/vw} n_{cd/vw}\left(\frac{(\delta_{cj}+\delta_{dj})(\delta_{vk}+\delta_{wk})}{4}\right)\right)\cdot\left(\frac{\sum_{e=\{j,\gamma\}}\frac{(\delta_{ae}+\delta_{be})(\delta_{xk}+\delta_{yk})}{4}}{\sum_{e=\{j,\gamma\}}\sum_{cd/vw} n_{cd/vw}\left(\frac{(\delta_{ce}+\delta_{de})(\delta_{vk}+\delta_{wk})}{4}\right)}\right)\right\}\right] \\
&=\left(\frac{1}{\sum_{cd/vw} n_{cd/vw}}\right)\left(\frac{Y_{m/k}}{\xi_{ji/k}}\right)\left(1-\frac{Y_{j/k}}{\xi_{ji/k}}\right)^{r_\alpha-1}\times\left[\left(\frac{(\delta_{am}+\delta_{bm})(\delta_{xk}+\delta_{yk})}{4Y_{m/k}}\right)-\left(\sum_{e=\{j,\gamma\}}\frac{(\delta_{ae}+\delta_{be})(\delta_{xk}+\delta_{yk})}{4\xi_{ji/k}}\right)\right. \\
&\qquad \left.-\left(\frac{r_\alpha-1}{\xi_{ji/k}}\right)\left(1-\frac{Y_{j/k}}{\xi_{ji/k}}\right)^{-1}\left\{\left(\frac{(\delta_{aj}+\delta_{bj})(\delta_{xk}+\delta_{yk})}{4}\right)-Y_{j/k}\left(\sum_{e=\{j,\gamma\}}\frac{(\delta_{ae}+\delta_{be})(\delta_{xk}+\delta_{yk})}{4\xi_{ji/k}}\right)\right\}\right]
\end{aligned}
\tag{A.3}
$$

**Box IV.**

## References


[1] J. Serp, M. Allibert, O. Beneš, S. Delpech, O. Feynberg, V. Ghetta, D. Heuer, D. Holcomb, V. Ignatiev, J.L. Kloosterman, L. Luzzi, E. Merle-Lucotte, J. Uhlíř, R. Yoshioka, D. Zhimin, The molten salt reactor (MSR) in generation IV: overview and perspectives, Prog. Nucl. Energy 77 (2014) 308–319.

[2] A. Pelton, S. Degterov, G. Eriksson, C. Robelin, Y. Dessureault, The modified quasichemical model I – binary solutions, Metall. Mater. Trans. B 31B (2000) 651–659.

[3] A. Pelton, P. Chartrand, The modified quasichemical model II – multicomponent solutions, Metall. Mater. Trans. A 32A (2001) 1355–1360.

[4] P. Chartrand, A. Pelton, The modified quasichemical model III – two sublattices, Metall. Mater. Trans. A 32 (2001) 1397–1407.

[5] A. Pelton, P. Chartrand, G. Eriksson, The modified quasichemical model IV – two-sublattice quadruplet approximation, Metall. Mater. Trans. A 32 (2001) 1409–1416.

[6] G. Lambotte, P. Chartrand, Thermodynamic optimization of the ($Na_2O$ + $SiO_2$ + NaF + $SiF_4$) reciprocal system using the modified quasichemical model in the quadruplet approximation, J. Chem. Thermodyn. 43 (2011) 1678–1699.

[7] P. Chartrand, A.D. Pelton, Thermodynamic evaluation and optimization of the LiF-NaF-KF-$MgF_2$-$CaF_2$ system using the modified quasi-chemical model, Metall. Mater. Trans. A 32 (6) (2001) 1385–1396.

[8] P. Chartrand, A.D. Pelton, Thermodynamic evaluation and optimization of the Li, Na, K, Mg, Ca//F, Cl reciprocal system using the modified quasi-chemical model, Metall. Mater. Trans. A 32 (6) (2001) 1417–1430.

[9] O. Beneš, J. Van der Meer, R. Konings, Modelling and calculation of the phase diagrams of the LiF–NaF–RbF–$LaF_3$ system, CALPHAD 31 (2) (2007) 209–216.

[10] M. Beilmann, O. Beneš, R. Konings, T. Fanghänel, Thermodynamic investigation of the (LiF+ NaF+ $CaF_2$+ $LaF_3$) system, J. Chem. Thermodyn. 43 (10) (2011) 1515–1524.

[11] O. Beneš, P. Souček, Molten salt reactor fuels, in: M.H. Piro (Ed.), Advances in Nuclear Fuel Chemistry, in: Woodhead Publishing Series in Energy, Woodhead Publishing, 2020, pp. 249–271.

[12] J. McMurray, T. Besmann, J. Ard, B. Fitzpatrick, M. Piro, J. Jerden, M. Williamson, B. Collins, B. Betzler, A. Qualls, Multi-Physics Simulations for Molten Salt Reactor Evaluation: Chemistry Modeling and Database Development, Tech. Rep. ORNL/SPR-2018/864, Oak Ridge National Laboratory, Oak Ridge, TN, 2018.

[13] K. Wang, Z. Fei, J. Wang, Z. Wu, C. Li, L. Xie, Thermodynamic description of the AgCl–$CoCl_2$–$InCl_3$–KCl system, Mater. Chem. Phys. 163 (2015) 73–87.

[14] J.W. McMurray, S.S. Raiman, Thermodynamic modeling of the K-KCl and Mg-$MgCl_2$ binary systems using the CALPHAD method, Sol. Energy 170 (2018) 1039–1042.

[15] C. Bale, P. Chartrand, S. Degterov, G. Eriksson, K. Hack, R. Mahfoud, J. Melançon, A. Pelton, S. Peterson, FactSage thermochemical software and databases, CALPHAD 26 (2) (2002).

[16] G. Lambotte, P. Chartrand, Thermodynamic evaluation and optimization of the $Al_2O_3$–$SiO_2$–$AlF_3$–$SiF_4$ reciprocal system using the modified quasichemical model, J. Am. Ceram. Soc. 94 (11) (2011) 4000–4008.

[17] G. Lambotte, P. Chartrand, Thermodynamic modeling of the ($Al_2O_3$+ $Na_2O$),($Al_2O_3$+ $Na_2O$+ $SiO_2$), and ($Al_2O3$+ $Na_2O$+ $AlF_3$ + NaF) systems, J. Chem. Thermodyn. 57 (2013) 306–334.

[18] K. Wang, P. Chartrand, A thermodynamic description for water, hydrogen fluoride and hydrogen dissolutions in cryolite-base molten salts, Phys. Chem. Chem. Phys. 20 (25) (2018) 17324–17341.

[19] D. Shishin, E. Jak, S.A. Decterov, Thermodynamic assessment of slag–matte–metal equilibria in the Cu-Fe-OS-Si system, J. Phase Equilib. Diffus. 39 (5) (2018) 456–475.

[20] D. Shishin, T. Hidayat, J. Chen, P.C. Hayes, E. Jak, Combined experimental and thermodynamic modelling investigation of the distribution of antimony and tin between phases in the Cu-Fe-OS-Si system, CALPHAD 65 (2019) 16–24.

[21] D. Shishin, T. Hidayat, J. Chen, P.C. Hayes, E. Jak, Integrated experimental study and thermodynamic modelling of the distribution of arsenic between phases in the Cu-Fe-OS-Si system, J. Chem. Thermodyn. 135 (2019) 175–182.

[22] M. Piro, S. Simunovic, T. Besmann, B. Lewis, W. Thompson, The thermochemistry library THERMOCHIMICA, Comput. Mater. Sci. 67 (2013) 266–272.

[23] M. Piro, J. Banfield, K. Clarno, S. Simunovic, T. Besmann, B. Lewis, W. Thompson, Coupled thermochemical, isotopic evolution and heat transfer simulations in highly irradiated $UO_2$ nuclear fuel, J. Nucl. Mater. 441 (2013) 240–251.

[24] S. Simunovic, S.L. Voit, T.M. Besmann, Oxygen Diffusion Model using the Thermochimica Module in MOOSE/BISON, Tech. Rep. ORNL/TM-2014/293, Oak Ridge National Laboratory, Oak Ridge, TN (United States), 2014.

[25] S. Simunovic, T.M. Besmann, S.L. Voit, Benchmark Problem for Calculating Oxygen Potential in High Burnup LWR Fuel using the Thermochimica Module in MOOSE/BISON, Tech. Rep. ORNL/TM-2014/529, Oak Ridge National Laboratory, Oak Ridge, TN (United States), 2014.

[26] S. Simunovic, T.M. Besmann, Coupling of Thermochemistry Solver Thermochimica with MOOSE/BISON, Tech. Rep. ORNL/TM-2015/322, Oak Ridge National Laboratory, Oak Ridge, TN (United States), 2015, p. 25.

[27] S. Simunovic, T.M. Besmann, E. Moore, M. Poschmann, M.H. Piro, K.T. Clarno, J.W. McMurray, W.A. Wieselquist, Modeling and simulation of oxygen transport in high burnup LWR fuel, J. Nucl. Mater. (2020) 152194.

[28] M. Poschmann, M.H. Piro, T.M. Besmann, K.T. Clarno, S. Simunovic, Thermochemically-informed mass transport model for interdiffusion of U and Zr in irradiated U-Pu-Zr fuel with fission products, J. Nucl. Mater. 554 (2021) 153089.

[29] L.C. Olson, J.W. Ambrosek, K. Sridharan, M.H. Anderson, T.R. Allen, Materials corrosion in molten LiF–NaF–KF salt, J. Fluor. Chem. 130 (1) (2009) 67–73.

[30] W.B. White, S.M. Johnson, G.B. Dantzig, Chemical equilibrium in complex mixtures, J. Chem. Phys. 28 (5) (1958) 751–755.

[31] M.H.A. Piro, J. Banfield, K.T. Clarno, S. Simunovic, T.M. Besmann, B.J. Lewis, W.T. Thompson, Coupled thermochemical, isotopic evolution and heat transfer simulations in highly irradiated $UO_2$ nuclear fuel, J. Nucl. Mater. 441 (1–3) (2013) 240–251.

[32] M. Hillert, The compound energy formalism, J. Alloys Compd. 320 (2) (2001) 161–176.

[33] A.D. Pelton, Phase Diagrams and Thermodynamic Modeling of Solutions, Academic Press, 2018.

[34] T.M. Besmann, J. Ard, S. Utlak, J.W. McMurray, R.A. Lefebvre, Status of the Salt Thermochemical Database, Tech. Rep. ORNL/SPR-2019/1208, Oak Ridge National Laboratory, Oak Ridge, TN (United States), 2019.

[35] M.H.A. Piro, M. Poschmann, P. Bajpai, On the interpretation of chemical potentials computed from equilibrium thermodynamic codes: Applications to molten salts, J. Nucl. Mater. 526 (2019) 151756.

[36] G. Eriksson, W.T. Thompson, A procedure to estimate equilibrium concentrations in multicomponent systems amd related applications, CALPHAD 13 (4) (1989) 389–400.

[37] M. Piro, S. Simunovic, Performance enhancing algorithms for computing thermodynamic equilibria, CALPHAD 39 (2012) 104–110.

[38] M. Poschmann, M. Piro, S. Simunovic, Acceleration of Thermochimica Calculations in Bison, Report ORNL/TM-2020/1473, Oak Ridge National Laboratory, Oak Ridge, TN (United States), 2020.

[39] D. Gaston, C. Newman, G. Hansen, D. Lebrun-Grandie, MOOSE: A parallel computational framework for coupled systems of nonlinear equations, Nucl. Eng. Des. 239 (10) (2009) 1768–1778.

[40] M. Rosenthal, R. Briggs, P. Kasten, Molten Salt Reactor Program Semiannual Progress Report. For Period Ending February 29, 1968, Tech. Rep. ORNL-4254, Oak Ridge National Laboratory, Oak Ridge, TN (United States), 1968.

[41] O. Hermann, R. Westfall, ORIGEN-S: SCALE System Module to Calculate Fuel Depletion, Actinide Transmutation, Fission Product Buildup and Decay, and Associated Radiation Source Terms, Tech. Rep. ORNL/NUREG/CSD-2/V2/R6, Oak Ridge National Laboratory, 1998.

[42] M. Chadwick, M. Herman, P. Obložinský, M. Dunn, Y. Danon, A. Kahler, D. Smith, B. Pritychenko, G. Arbanas, R. Arcilla, R. Brewer, D. Brown, R. Capote, A. Carlson, Y. Cho, H. Derrien, K. Guber, G. Hale, S. Hoblit, S. Holloway, T. Johnson, T. Kawano, B. Kiedrowski, H. Kim, S. Kunieda, N. Larson, L. Leal, J. Lestone, R. Little, E. McCutchan, R. MacFarlane, M. MacInnes, C. Mattoon, R. McKnight, S. Mughabghab, G. Nobre, G. Palmiotti, A. Palumbo, M. Pigni, V. Pronyaev, R. Sayer, A. Sonzogni, N. Summers, P. Talou, I. Thompson, A. Trkov, R. Vogt, S. van der Marck, A. Wallner, M. White, D. Wiarda, P. Young, ENDF/B-VII.1 nuclear data for science and technology: Cross sections, covariances, fission product yields and decay data, Nucl. Data Sheets 112 (12) (2011) 2887–2996, Special Issue on ENDF/B-VII.1 Library.

[43] M. Poschmann, B.W. Fitzpatrick, S. Simunovic, M.H. Piro, Recent development of thermochimica for simulations of nuclear materials, in: TMS 2020 149th Annual Meeting & Exhibition Supplemental Proceedings, Springer, 2020, pp. 1003–1012.

[44] D. Schwen, L.K. Aagesen, J.W. Peterson, M.R. Tonks, Rapid multiphase-field model development using a modular free energy based approach with automatic differentiation in MOOSE/MARMOT, Comput. Mater. Sci. 132 (2017) 36–45.

[45] P. Bajpai, M. Poschmann, D. Andrš, C. Bhave, M. Tonks, M. Piro, Development of a new thermochemistry solver for multiphysics simulations of nuclear materials, in: TMS 2020 149th Annual Meeting & Exhibition Supplemental Proceedings, Springer International Publishing, Cham, 2020, pp. 1013–1025.

[46] D.J. Diamond, N.R. Brown, R. Denning, S. Bajorek, Phenomena Important in Molten Salt Reactor Simulations, Tech. Rep. BNL-114869-2017-INRE DE-SC0012704, Brookhaven National Lab.(BNL), Upton, NY (United States), 2018.

[47] J. McFarlane, P.A. Taylor, D.E. Holcomb, W. Poore III, Review of Hazards Associated with Molten Salt Reactor Fuel Processing Operations, Tech. Rep. ORNL/TM-2019/1195, Oak Ridge National Lab.(ORNL), Oak Ridge, TN (United States), 2019.

[48] J.A. Turner, K. Clarno, M. Sieger, R. Bartlett, B. Collins, R. Pawlowski, R. Schmidt, R. Summers, The virtual environment for reactor applications (VERA): design and architecture, J. Comput. Phys. 326 (2016) 544–568.

[49] A.M. Graham, Z. Taylor, B.S. Collins, R.K. Salko, M. Poschmann, Multiphysics coupling methods for molten salt reactor modeling and simulation in VERA, Nucl. Sci. Eng. (2021) 1–22.

# 5

# Equilibrium Thermodynamics

*The foundations of thermodynamic equilibrium calculations were laid down by American chemical physicist Josiah Willard Gibbs who originally published his work* On the Equilibrium of Heterogeneous Substances *in a relatively obscure American journal, the Transactions of the Connecticut Academy of Arts and Sciences, in several parts, during the years 1875 to 1878. Thermodynamic equilibrium computations in isothermal, isobaric systems are aimed at identifying a unique combination of phases and species which minimises the integral Gibbs energy of the system while satisfying the necessary underlying conditions. Thermodynamics requires that a favourable change in a system must decrease the Gibbs energy of the system while respecting the mass constraints of the system components and the Gibbs' phase rule must be satisfied.*

## **5.1.** Phase Equilibrium in Heterogeneous Systems

A heterogeneous system is defined as one where the thermodynamic properties may have different values in different parts of the system when the system is at equilibrium. While a continuous variation of these properties is possible, equilibrium thermodynamics in the context of this work only concerns discontinuous variations where the properties have different values in different portions of the systems but are homogeneous within each portion. A practical example of such a scenario is that of multiple phases being present in a system with the properties in phase being homogeneous and the different phases are in equilibrium with each other [169].

In a system at thermodynamic equilibrium, with $C$ components, there are $C + 2$ natural variables with 2 representing the variables temperature, $T$, and pressure, $P$. For an isothermal,

isobaric system, the equilibrium conditions result in:

$$dG_{\text{sys}} = 0, \tag{5.1}$$

$$dG_{\text{sys}} = -SdT - Vd(-P) + \sum_i \mu_j dn_j. \tag{5.2}$$

As a result, the equilibrium state is defined by a minimum in the integral Gibbs energy of the system at constant $T$, $P$ and $n_i$. In doing so one must respect the mass balance and charge neutrality constraints. In the present context, this also implies that the chemical potential of each component must be homogenous in all phases stable at equilibrium and gives the common tangent construction for phases at equilibrium:

$$\mu_i^{\phi_1} = \mu_i^{\phi_2} = \mu_i^{\phi_2} = \cdots, \tag{5.3}$$

where $\phi_1$, $\phi_2$, etc. denote the phases stable at equilibrium. The above arguments can be generalised into the necessary and sufficient conditions for equilibrium which are used in the development of the Gibbs energy minimiser.

## 5.2. Conditions of Phase Equilibrium

A thermodynamic equilibrium solver must respect both the necessary and sufficient conditions for thermodynamic equilibrium. Rooted in the fundamental laws of thermodynamics, the necessary conditions ensure that the Gibbs energy of the system is at a local equilibrium. Satisfying the sufficient condition, while respecting the constraints, verifies that an alternative phase assemblage yielding a lower Gibbs energy is not possible and guarantees a global minimum.

### 5.2.1. Necessary conditions

The necessary conditions for phase equilibrium, which include mass conservation, Gibbs' phase rule and a generalisation of the common tangent construction, are summarised as follows:

1. **Conservation of mass**

   The law of conservation of mass requires that the linear equations representing mass constraints be satisfied. For component $j$, the mass balance equation can be written as:

$$b_j = \sum_{\phi=1}^{\Phi} n_\phi \sum_{i=1}^{N_\phi} \nu_{ij} x_i, \tag{5.4}$$

where $\nu_{ij}$ represents the stoichiometric coefficient of system components $j$ in phase species $i$. In an electrochemical system where the electrons form a system component with zero moles overall in the system, the mass balance constraint includes the charge neutrality constraint but it can be explicitly written as:

$$b_{e^-} = \sum_{i=1}^{N_\phi} x_i \nu_{ie^-} = 0. \tag{5.5}$$

2. **Gibbs' phase rule**

   Thermodynamic equilibrium conditions also require that Gibbs' phase rule be satisfied. Gibbs' phase rule determines the *degree of freedom* of the system, i.e., the number of phases that can be stable at equilibrium in relation to the state variables [159]. In general, the phase rule can be written as:

$$F = C - \Phi + 2 + \Xi, \tag{5.6}$$

   where $F$ represents the degrees of freedom, $C$ denotes the number of components in the system, $\Phi$ denotes the number of phases and $\Xi$ denotes the number of ionic phases. However, for isothermal, isobaric systems with no charged species, the phase rule takes the following simplified form :

$$F = C - \Phi, \tag{5.7}$$

   which implies that the number of phases that can co-exist at equilibrium cannot exceed the number of components in a closed isothermal, isobaric system.

3. **Gibbs' criterion**

   Ensuring that the Gibbs phase rule and mass balance constraints are satisfied is relatively straightforward but special attention must be paid to ensuring that the integral Gibbs energy of the system is at a minimum. The equilibrium criteria established by Gibbs requires that at equilibrium $dG_{\text{sys}} = 0$ [159]. Thus, differentiating equation (4.24):

$$dG_{\text{sys}} = \sum_{\phi=1}^{\Phi} \sum_{i=1}^{N_\phi} (dn_i \mu_i + n_i d\mu_i) = 0. \tag{5.8}$$

   The chemical potentials are related through the *Gibbs-Duhem equation* which, at constant

temperature and pressure, can be written as [170]:

$$\sum_{\phi=1}^{\Phi}\sum_{i=1}^{N_\phi}(n_i d\mu_i) = 0. \tag{5.9}$$

Substituting the Gibbs-Duhem equation in equation (5.8) gives:

$$dG_{\text{sys}} = \sum_{\phi=1}^{\Phi}\sum_{i=1}^{N_\phi}(dn_i\mu_i) = 0. \tag{5.10}$$

The chemical potentials of the species can be written in terms of the chemical potentials of the system components. Therefore, substituting equation (5.4) into equation (4.25), differentiating with respect to $n_i$ at constant temperature and pressure and equating to zero gives:

$$dG_{\text{sys}} = \sum_{\phi=1}^{\Phi}\sum_{i=1}^{N_\phi} dn_i \sum_{j=1}^{C}\nu_{ij}\Gamma_j = 0, \tag{5.11}$$

and rearranging the above results in:

$$\sum_{\phi=1}^{\Phi}\sum_{i=1}^{N_\phi} dn_i \left(\mu_i - \sum_{j=1}^{C}\nu_{ij}\Gamma_j\right) = 0. \tag{5.12}$$

Since both $\nu_{ij}$ and $\mu_i$ are unique for every species, the chemical potentials of species or phase in the system can be related to chemical potentials of system component at equilibrium through the following equation [31]:

$$\mu_{i(\phi)} = \sum_{j=1}^{C}\nu_{ij}\Gamma_j. \tag{5.13}$$

Equation (4.22) is known as *Gibbs' criterion* and ensuring that it is satisfied for all species in the system is equivalent to satisfying the equilibrium criterion that the Gibbs energy of the system be at a local minimum. This is useful in developing a convergence criterion for thermodynamic equilibrium calculations.

### 5.2.2. Sufficient conditions

The linear equality in equation (4.22) justifies the selection of stable species and making sure that no metastable species gets added to the system. However, satisfying the linear equation

is insufficient to conclude that the system is at a *global* minimum since $g_\phi^{ex}$ can be non-convex [110]. The driving force of a phase, $\Delta G_\phi$, is used to determine whether a system involving that phase is more stable than the previous system, which is defined as:

$$\Delta G_\phi = \min_{\lambda} \sum_{i=1}^{N_\lambda} x_i \left( \mu_i - \sum_{j=1}^{C} \nu_{ij} \Gamma_j \right), \tag{5.14}$$

which is subject to the following linear equality and inequality constraints:

$$\sum_{i=1}^{N_\phi} x_i = 1, \; x_i > 0, \; \forall i \in \phi. \tag{5.15}$$

## 5.3. Computing Phase Equilibria

Accurate and computationally efficient determination of equilibrium from the conditions mentioned in the previous section require careful consideration of the numerical methods employed in the solver. Over the years, numerous strategies have been developed to solve the equilibrium thermodynamics problems but the two most relevant methods are the *Gibbs Energy Minimisation* by White, Johnson and Dantzig [32], which is based on the method of steepest descent of second order, and the *Partitioning of Gibbs Energy* method, which was also proposed by White [48] but is substantially different than GEM.

The goal of both GEM and PGE approaches is to predict a unique combination of phases and species that minimise the integral Gibbs energy of an isothermal, isobaric system at a given composition. As in equation (4.24), the integral Gibbs energy of a multicomponent multiphase system can be represented as:

$$G = RT \left( \sum_{\lambda=1}^{\Lambda} n_\lambda \sum_{i=1}^{N_\lambda} x_{i(\lambda)} \tilde{\mu}_{i(\lambda)} + \sum_{\omega=1}^{\Omega} n_\omega \tilde{\mu}_\omega \right), \tag{5.16}$$

where the symbols represent their usual variables mentioned before. As the conditions that must be satisfied at thermodynamic equilibrium have already been mentioned, the numerical procedures for both the approaches can now be elaborated.

### 5.3.1. Method of Lagrange multipliers

White et al. [32] established a second order steepest descent method for minimising Gibbs energy, which is based on the method of Lagrange multipliers for constrained optimisation. The GEM approach simultaneously optimises the mass balance constraint and Gibbs' criterion

while fixing the system size through the Gibbs phase rule. The dimensionless form of Gibbs energy of the system can be expressed as a quadratic approximation obtained by the Taylor series expansion as follows:

$$\begin{aligned}\tilde{Q}^{m+1} = \tilde{G}^{m} &+ \sum_{\omega=1}^{\Omega} \Delta_{\omega} \frac{\partial \tilde{G}^{m}}{\partial n_{\omega}^{m}}\bigg|_{n_{\omega}^{m}=n_{\omega}^{m+1}} \\ &+ \sum_{\lambda=1}^{\Lambda}\sum_{i=1}^{N_{\lambda}} \Delta_{i} \frac{\partial \tilde{G}^{m}}{\partial n_{i(\lambda)}^{m}}\bigg|_{n_{i(\lambda)}^{m}=n_{i(\lambda)}^{m+1}} \\ &+ \frac{1}{2}\sum_{\omega=1}^{\Omega} \Delta_{\omega}^{2} \frac{\partial^{2} \tilde{G}^{m}}{\partial (n_{\omega}^{m})^{2}}\bigg|_{n_{\omega}^{m}=n_{\omega}^{m+1}} \\ &+ \frac{1}{2}\sum_{\lambda=1}^{\Lambda}\sum_{i=1}^{N_{\lambda}}\sum_{l=1}^{N_{\lambda}} \Delta_{i}\Delta_{l} \frac{\partial^{2} \tilde{G}^{m}}{\partial n_{i(\lambda)}^{m} \partial n_{l(\lambda)}^{m}}\bigg|_{n_{i(\lambda)}^{m}=n_{i(\lambda)}^{m+1}},\end{aligned} \tag{5.17}$$

where the superscripts $m$ and $m+1$ denote the iteration at which the Gibbs energy is calculated and the deltas are represented as follows:

$$\Delta_{i} = n_{i(\lambda)}^{m+1} - n_{i(\lambda)}^{m}, \tag{5.18}$$

$$\Delta_{\lambda} = n_{\lambda}^{m+1} - n_{\lambda}^{m}, \tag{5.19}$$

$$\Delta_{\omega} = n_{\omega}^{m+1} - n_{\omega}^{m}. \tag{5.20}$$

While the first order partial derivatives are equal to the chemical potentials, as shown in equation (4.20), the second order derivatives are as follows:

$$\frac{\partial^{2} \tilde{G}^{m}}{\partial (n_{\omega}^{m})^{2}} = 0, \tag{5.21}$$

$$\frac{\partial^{2} \tilde{G}^{m}}{\partial (n_{i(\lambda)}^{m})^{2}} = \frac{1}{n_{i(\lambda)}^{m}} - \frac{1}{n_{\lambda}^{m}}, \tag{5.22}$$

$$\frac{\partial^{2} \tilde{G}^{m}}{\partial n_{i(\lambda)}^{m} \partial n_{l\neq i(\lambda)}^{m}} = -\frac{1}{n_{\lambda}^{m}}. \tag{5.23}$$

Substituting equations (4.20) and (5.21)–(5.23) into the second order approximation of

Gibbs energy given by equation (5.17), one gets the following objective function:

$$\tilde{Q}^{m+1} = \tilde{G}^{m} + \sum_{\omega=1}^{\Omega} \tilde{\mu}_{\omega}^{m} + \sum_{\lambda=1}^{\Lambda} \sum_{i=1}^{N_\lambda} \Delta_i \tilde{\mu}_{i(\lambda)}^{m} + \frac{1}{2} \sum_{\lambda=1}^{\Lambda} \sum_{i=1}^{N_\lambda} n_{i(\lambda)}^{m} \left( \frac{\Delta_i}{n_{i(\lambda)}} - \frac{\Delta_\lambda}{n_\lambda^m} \right)^2, \tag{5.24}$$

which must be minimised subject to the mass balance constraints. In order to solve the constrained optimisation problem, the method of Lagrange multipliers can be used and the resulting Lagrangian function is defined as:

$$\mathcal{L} = \tilde{Q}^{m+1} - \sum_{j=1}^{C} \pi_j^{m+1} \left( b_j - b_j^m \right), \tag{5.25}$$

where $\pi_j$ denote the dimensionless undetermined Lagrange multipliers[1]. The Gibbs energy of the system and the mass balance residuals can be simultaneously minimised by equating the gradient of the Lagrangian function to zero:

$$\nabla \mathcal{L} = 0. \tag{5.26}$$

The elements of the gradient vector are found by taking the partial derivatives of equation (5.25) with respect to the number of moles of species $n_{i(\lambda)}$ and $n_\omega$:

$$\frac{\partial \mathcal{L}}{\partial n_{i(\lambda)}} = \tilde{\mu}_{i(\lambda)} - \sum_{j=1}^{C} \nu_{ij} \pi_j^{m+1} + \left( \frac{n_{i(\lambda)}^{m+1}}{n_{i(\lambda)}^{m}} - \frac{n_\lambda^{m+1}}{n_\lambda^m} \right), \tag{5.27}$$

$$\frac{\partial \mathcal{L}}{\partial n_\omega} = \tilde{\mu}_\omega - \sum_{j=1}^{C} \nu_{\omega j} \pi_j^{m+1}, \tag{5.28}$$

$$\frac{\partial \mathcal{L}}{\partial \pi_j} = b_j - b_j^m. \tag{5.29}$$

By rearranging the preceeding equations and substituting the mass balance constraint, the following equation is obtained:

$$b_j = \sum_{\lambda=1}^{\Lambda} \sum_{i=1}^{N_\lambda} \left( -\tilde{\mu}_{i(\lambda)}^{m} + \frac{n_\lambda^{m+1}}{n_\lambda^m} + \sum_{k=1}^{C} \nu_{ik} \pi_k^{m+1} \right) n_{i(\lambda)}^{m} \nu_{ij} + \sum_{\omega=1}^{\Omega} n_\omega^m \nu_{ij}. \tag{5.30}$$

[1] While $\lambda$ is commonly used to denote Lagrange multipliers, $\pi$ is used here to avoid confusion with the solution phase index $\lambda$.

Upon rearranging, the commonly used form proposed by Eriksson and Rosén [38] is obtained:

$$\sum_{j=1}^{C} \underbrace{\sum_{\lambda=1}^{\Lambda}\sum_{i=1}^{N_\lambda} n_{i(\lambda)}\nu_{ij}\nu_{ik}}_{r_{jk}} \pi_j^{m+1} + \sum_{\lambda=1}^{\Lambda}\underbrace{\sum_{i=1}^{N_\lambda} n_{i(\lambda)}\nu_{ij}}_{\phi_{j\lambda}^m} \underbrace{\left(\frac{n_\lambda^{m+1}}{n_\lambda^m} - 1\right)}_{\pi_\lambda^{m+1}} + \sum_{\omega=1}^{\Omega} n_\omega^{m+1}\nu_{\omega j} = b_j + \sum_{\lambda=1}^{\Lambda}\sum_{i=1}^{N_\lambda}\left(\tilde{\mu}_{i(\lambda)}^{m+1} - 1\right) n_{i(\lambda)}^m \nu_{ij}. \quad (5.31)$$

The chemical potentials of the species in solution phases can be related to system component potentials by the following:

$$\sum_{j=1}^{C} \pi_j^{m+1}\phi_{j\lambda}^m = \sum_{i=1}^{N_\lambda} \tilde{\mu}_{i(\lambda)}^m n_{i(\lambda)}^m, \quad (5.32)$$

and the chemical potentials of stoichiometric phases constrain the system component potentials through the following relationship:

$$\tilde{\mu}_\omega = \sum_{j=1}^{C} \nu_{\omega j}\pi_j^{m+1}. \quad (5.33)$$

Together, equations (5.31)–(5.33) results in the following system of linear equations:

$$\mathbf{H}\mathbf{u} = \kappa \quad (5.34)$$

where the unknown vector $\mathbf{u} \in \mathbb{R}^N$ and the vector of constraints $\kappa \in \mathbb{R}^N$ with the number of unknowns $N = E + \Lambda + \Omega$. The two can be expanded as:

$$\mathbf{u} = \begin{bmatrix} \pi_{j=1}^{m+1} \\ \vdots \\ \pi_{j=E}^{m+1} \\ \pi_{\lambda=1}^{m+1} \\ \vdots \\ \pi_{\lambda=\Lambda}^{m+1} \\ n_{\omega=1}^{m+1} \\ \vdots \\ n_{\omega=\Omega}^{m+1} \end{bmatrix}, \kappa = \begin{bmatrix} b_{j=1} + \sum_{\lambda=1}^{\Lambda}\sum_{i=1}^{N_\lambda}\left(\tilde{\mu}_{i(\lambda)}^m - 1\right) n_{i(\lambda)}^m \nu_{ij=1} \\ \vdots \\ b_{j=E} + \sum_{\lambda=1}^{\Lambda}\sum_{i=1}^{N_\lambda}\left(\tilde{\mu}_{i(\lambda)}^m - 1\right) n_{i(\lambda)}^m \nu_{ij=E} \\ \sum_{i=1}^{N_\lambda} \tilde{\mu}_{i(\lambda=1)}^m n_{i(\lambda=1)}^m \\ \vdots \\ \sum_{i=1}^{N_\lambda} \tilde{\mu}_{i(\lambda=\Lambda)}^m n_{i(\lambda=\Lambda)}^m \\ \tilde{\mu}_{\omega=1} \\ \vdots \\ \tilde{\mu}_{\omega=\Omega} \end{bmatrix}. \quad (5.35)$$

The Hessian matrix, $\mathbf{H}$, is given as follows:

$$\mathbf{H} = \begin{bmatrix} r_{11} & \cdots & r_{1E} & \phi_{11} & \cdots & \phi_{1\Lambda} & \nu_{11} & \cdots & \nu_{1\Omega} \\ \vdots & \ddots & \vdots & \vdots & \ddots & \vdots & \vdots & \ddots & \vdots \\ r_{E1} & \cdots & r_{EE} & \phi_{E1} & \cdots & \phi_{E\Lambda} & \nu_{E1} & \cdots & \nu_{E\Omega} \\ \phi_{11} & \cdots & \phi_{1E} & 0 & \cdots & 0 & 0 & \cdots & 0 \\ \vdots & \ddots & \vdots & \vdots & \ddots & \vdots & \vdots & \ddots & \vdots \\ \phi_{\Lambda 1} & \cdots & \phi_{\Lambda E} & 0 & \cdots & 0 & 0 & \cdots & 0 \\ \nu_{11} & \cdots & \nu_{1E} & 0 & \cdots & 0 & 0 & \cdots & 0 \\ \vdots & \ddots & \vdots & \vdots & \ddots & \vdots & \vdots & \ddots & \vdots \\ \nu_{\Omega 1} & \cdots & \nu_{\Omega E} & 0 & \cdots & 0 & 0 & \cdots & 0 \end{bmatrix}, \tag{5.36}$$

where the terms $r_{jk}$ and $\phi_{j\lambda}$ are defined in equation (5.31) and $\nu_{\omega j}$ represents the stoichiometric coefficient of system component $j$ in stoichiometric compound $\omega$.

While solving equation (5.34) gives the mole numbers of stoichiometric phases directly, the mole numbers of the species of solution phases must be computed using the following rearranged form of equation (5.27):

$$n_{i(\lambda)}^{m+1} = n_{i(\lambda)}^{m+1} \left( -\tilde{\mu}_{i(\lambda)}^{m} + \frac{n_{\lambda}^{m+1}}{n_{\lambda}^{m} - \sum_{j=1}^{C} \nu_{ij} \pi_{j}^{m+1}} \right). \tag{5.37}$$

### 5.3.2. Partitioning of Gibbs energy

PGE is based on finding the roots of the mass balance residual by expressing the mole fraction as a function of system component potentials. The expression for chemical potential of a solution species from equation (4.22) can be substituted into equation (5.13) and upon rearranging one gets:

$$x_{i(\lambda)} = \exp \left( -\tilde{\mu}_{i(\lambda)}^{\circ} - \tilde{\mu}_{i(\lambda)}^{\text{ex}} + \sum_{j=1}^{C} \nu_{ij} \tilde{\Gamma}_{j} \right). \tag{5.38}$$

Substituting the previous equation into the mass balance equation (5.4), one can formally relate the mass balance equations to the element potentials and results in the following:

$$b_{k}^{m} = \sum_{\lambda=1}^{\Lambda} n_{\lambda}^{m} \sum_{i=1}^{N_{\lambda}} \nu_{ik} \exp \left( -\tilde{\mu}_{i(\lambda)}^{\circ} - \tilde{\mu}_{i(\lambda)}^{\text{ex}} + \sum_{j=1}^{C} \nu_{ij} \tilde{\Gamma}_{j}^{m} \right) + \sum_{\omega=1}^{\Omega} n_{\omega}^{m} \nu_{\omega k}, \tag{5.39}$$

where the superscript $m$ denotes that the mass of element $k$ is the estimated mass at iteration $m$ and not the true total amount of the element in the system which will be denoted by $b_k$

without the iteration index. At convergence, the two will be equal and the sum of the mole fractions of the species $x_{i(\lambda)}$ will be equal to unity.

The PGE method surmises to partitioning the Gibbs energy of the system among elements by manipulating $\tilde{\Gamma}_j^m$ together with $n_\lambda^m$ and $n_\omega^m$ in order to reduce the residuals of the mass balance equations to zero. While doing this, one must ensure that the Gibbs criterion given by equation (5.13) is always satisfied. Mathematically this is equivalent to finding the roots of the system of non-linear equations of mass balance. The residual of mass balance $\Delta b_k^m$ at iteration $m$ can be defined as:

$$\Delta b_k^m = \sum_{\lambda=1}^{\Lambda} n_\lambda^m \sum_{i=1}^{N_\lambda} \nu_{ik} \exp\left(-\tilde{\mu}_{i(\lambda)}^\circ - \tilde{\mu}_{i(\lambda)}^{\text{ex}} + \sum_{j=1}^{C} \nu_{ij} \tilde{\Gamma}_j^m\right) + \sum_{\omega=1}^{\Omega} n_\omega^m \nu_{\omega k} - b_k. \tag{5.40}$$

The subsidiary condition satisfying the requirement for the sum of all mole fraction to be equal to unity results in the following residual for each phase $\lambda$:

$$\Delta x_\lambda^m = x_\lambda^m - 1, \tag{5.41}$$

where $x_\lambda^m$ denotes the sum of mole fractions of all species of phase $\lambda$ at iteration $m$ (i.e. $x_\lambda^m = \sum_{i=1}^{N_\lambda} x_{i(\lambda)}$).

Finally, the chemical potentials of the stoichiometric phases constrain the adjustments applied to the element potentials through the Gibbs criterion and results in the following residual equation:

$$\Delta \tilde{\mu}_\omega = \sum_{k=1}^{C} \nu_{\omega k} \tilde{\Gamma}_k - \tilde{\mu}_\omega^\circ. \tag{5.42}$$

Together, the residual equations (5.40)–(5.42) result in the following system of equation with the objective of finding roots $\mathbf{u}$ of the residual vector $\epsilon$:

$$\epsilon(\mathbf{u}) = 0, \tag{5.43}$$

where $\epsilon \in \mathbb{R}^N$, $\mathbf{u} \in \mathbb{R}^N$ and $N$ is the number of non-linear equations and corresponding unknown variables ($N = E + \Lambda + \Omega$). The residual vector, $\epsilon$, can be expanded as:

$$\epsilon(\mathbf{u}) = \begin{bmatrix} \Delta b_{k=1}^m & \dots & \Delta b_{k=E}^m & \Delta x_{\lambda=1}^m & \dots & \Delta x_{\lambda=\Lambda}^m & \Delta \tilde{\mu}_{\omega=1} & \dots & \Delta \tilde{\mu}_{\omega=\Omega} \end{bmatrix}^T, \tag{5.44}$$

where superscript $T$ denotes the transpose. The unknown system variable vector takes the

following form:

$$\mathbf{u} = \begin{bmatrix} \tilde{\Gamma}^m_{k=1} & \dots & \tilde{\Gamma}^m_{k=E} & n^m_{\lambda=1} & \dots & n^m_{\lambda=\Lambda} & n^m_{\omega=1} & \dots & n^m_{\omega=\Omega} \end{bmatrix}^T. \tag{5.45}$$

The roots of equation (5.43) can be found using the Newton-Raphson method. Given $\epsilon : \mathbb{R}^N \to \mathbb{R}^N$ continuously differentiable and starting with an initial estimate $\mathbf{u}^0$, the Newton-Raphson method for a system of nonlinear equations requires solving the following at each iteration $m$ [171]:

$$\mathbf{J}(\mathbf{u}^m)\mathbf{s}^m = -\epsilon(\mathbf{u}^m), \tag{5.46}$$

$$\mathbf{u}^{m+1} = \mathbf{u}^m + \alpha^m \mathbf{s}^m, \tag{5.47}$$

where $\alpha^m$ is a scaling factor selected using an appropriate line search algorithm and $\mathbf{s}^m$ is the Newton step representing the adjustment to the system variables and is given by:

$$\mathbf{s}^m = \begin{bmatrix} d\tilde{\Gamma}^m_{k=1} & \dots & d\tilde{\Gamma}^m_{k=E} & dn^m_{\lambda=1} & \dots & dn^m_{\lambda=\Lambda} & dn^m_{\omega=1} & \dots & dn^m_{\omega=\Omega} \end{bmatrix}^T. \tag{5.48}$$

The Jacobian matrix[2] is defined as:

$$\mathbf{J} = \begin{bmatrix} \partial b^m_1/\partial \tilde{\Gamma}^m_1 & \dots & \partial b^m_1/\partial \tilde{\Gamma}^m_E & \partial b^m_1/\partial n^m_{\lambda=1} & \dots & \partial b^m_1/\partial n^m_{\lambda=\Lambda} & \partial b^m_1/\partial n^m_{\omega=1} & \dots & \partial b^m_1/\partial n^m_{\omega=\Omega} \\ \vdots & \ddots & \vdots & \vdots & \ddots & \vdots & \vdots & \ddots & \vdots \\ \partial b^m_E/\partial \tilde{\Gamma}^m_1 & \dots & \partial b^m_E/\partial \tilde{\Gamma}^m_E & \partial b^m_E/\partial n^m_{\lambda=1} & \dots & \partial b^m_E/\partial n^m_{\lambda=\Lambda} & \partial b^m_E/\partial n^m_{\omega=1} & \dots & \partial b^m_E/\partial n^m_{\omega=\Omega} \\ \partial b^m_1/\partial n^m_{\lambda=1} & \dots & \partial b^m_1/\partial n^m_{\lambda=\Lambda} & 0 & \dots & 0 & 0 & \dots & 0 \\ \vdots & \ddots & \vdots & \vdots & \ddots & \vdots & \vdots & \ddots & \vdots \\ \partial b^m_E/\partial n^m_{\lambda=1} & \dots & \partial b^m_E/\partial n^m_{\lambda=\Lambda} & 0 & \dots & 0 & 0 & \dots & 0 \\ \partial b^m_1/\partial n^m_{\omega=1} & \dots & \partial b^m_E/\partial n^m_{\omega=1} & 0 & \dots & 0 & 0 & \dots & 0 \\ \vdots & \ddots & \vdots & \vdots & \ddots & \vdots & \vdots & \ddots & \vdots \\ \partial b^m_1/\partial n^m_{\omega=\Omega} & \dots & \partial b^m_E/\partial n^m_{\omega=\Omega} & 0 & \dots & 0 & 0 & \dots & 0 \end{bmatrix}, \tag{5.49}$$

[2] It must be noted the Jacobian matrix from the partitioning of Gibbs energy method is equivalent to the Hessian matrix resulting from the Gibbs energy minimisation approach.

where the partial derivatives are defined as follows:

$$\frac{\partial b_j^m}{\partial \tilde{\Gamma}_k^m} = \sum_{\lambda=1}^{\Lambda} n_\lambda^m \sum_{i=1}^{N_\lambda} x_{i(\lambda)}^m \nu_{ij} \nu_{ik} \tag{5.50}$$

$$\frac{\partial b_j^m}{\partial n_\lambda^m} = \sum_{i=1}^{N_\lambda} x_{i(\lambda)}^m \nu_{ij} \tag{5.51}$$

$$\frac{\partial b_j^m}{\partial n_\omega^m} = \nu_{\omega j}. \tag{5.52}$$

At every iteration step, the direction vector is computed and the system is adjusted until the convergence criteria are achieved.

### 5.3.3. Convergence criteria

A number of different methods can be proposed to judge the convergence of a thermodynamic equilibrium solver, the most obvious being ensuring that the relative change in Gibbs energy between two iterations is within a specified tolerance. Another approach that makes better use of principles of thermodynamic equilibrium is based on equation (4.22) and requires that the chemical potentials of all species lie on or above the Gibbs plane formed by chemical potentials of system components.

1. **Tolerance of $G_{\text{sys}}^m$**
   The most obvious method of ensuring convergence is to ensure that the normalised absolute difference of Gibbs energy, $\Psi_G$, between subsequent iterations is within a specified tolerance. Mathematically, this can be expressed as:

   $$\Psi_G = \left| \frac{G_{\text{sys}}^m - G_{\text{sys}}^{m-1}}{G_{\text{sys}}^m} \right| < \epsilon, \tag{5.53}$$

   where $\epsilon$ denotes the specified tolerance and the superscripts refer to iteration $m$ and $m-1$ respectively. Using the interpretation of Lagrange multipliers in the GEM [32], one can obtain a similar estimate of convergence. Since the Lagrange multipliers, $\pi_j$, denote the chemical potentials, they can be related to Gibbs energy of the system, $G_{sys}$. This can be mathematically expressed as:

   $$\Psi_\pi = \left| \frac{\pi_j^m - \pi_j^{m-1}}{\pi_j^m} \right| < \epsilon. \tag{5.54}$$

   Though intuitive, this approach to judging convergence suffers from two potential is-

sues. The first issue is commonly observed in iterative solutions of non-linear systems where numerical stagnation can occur when significant numerical dampening is required to maintain the stability of numerical algorithm. In GEM for large chemical components, numerical dampening is often required and false convergence can result when the approach to minimum Gibbs energy becomes extremely slow. The second issue relates to insignificant contribution to the Gibbs energy of the system by minor species. These minor species can often be incorrect by several orders of magnitude and though they don't contribute to Gibbs energy significantly, they might be of significant chemical or radiological importance and the false sense of convergence can then lead to significant problems [172].

2. **Gibbs' Criterion**

   The Gibbs criteria for judging convergence relies on the relationship between chemical potentials and Gibbs energies. To utilise this concept, the chemical potentials can be expressed per gram-atom as:

$$\hat{\mu}_i = \frac{\mu_i}{a_{i(T)}}, \tag{5.55}$$

   where $\hat{\mu}_i$ [$\mathrm{J\,g^{-1}\,at^{-1}}$] is the chemical potential and $a_{i(T)}$ is the total number of atoms in the formula mass. This method of defining chemical potentials allows an equivalent comparison of chemical potentials of compounds with different numbers of atoms per molar mass.

   At equilibrium, all $\hat{\mu}_i$ must lie on a hyper-plane at equilibrium in the $C$-dimensional Euclidean space, where $C$ represents the number of system components. This plane is called the *Gibbs plane* and an example of it is shown in Figure 5.1 for a three dimensional space.

   The chemical potential of any point on the Gibbs plane can be expressed as a linear combination of chemical potentials of system components and this interpolated potential can be denoted by $\hat{\mu}_{i(\phi)}(\Gamma)$. The absolute difference between $\hat{\mu}_{i(\phi)}(\Gamma)$ and $\hat{\mu}_{i(\phi)}$, $\Psi_\Gamma$ can then be used as convergence criterion:

$$\Psi_\Gamma = \left|\hat{\mu}_{i(\phi)}(\Gamma) - \hat{\mu}_{i(\phi)}\right| < \epsilon, \tag{5.56}$$

   i.e., all the species in equilibrium must lie on the Gibbs plane. If a phase lies below the Gibbs plane, adding it to the phase assemblage would yield a lower Gibbs energy of the system and such a system would not be at a global minimum. The Gibbs criteria is easily extendable to electrochemical equilibrium and can be conveniently implemented in

a thermodynamic equilibrium solver [172].

### 5.3.4. Choice of numerical algorithm

Both GEM and PGE have advantages and disadvantages and the choice of the algorithm must be based on the applications and excess mixing models used in them. For Yellowjacket–GEM, the Gibbs energy minimisation method was selected and the reasoning behind it has been explained by Bajpai et al. [51]. While the paper, presented on the following pages, was written primarily for the thermochemistry library Thermochimica, the goal was also to pre-emptively justify the choice of the algorithm for Yellowjacket–GEM. The article shows how PGE can have considerable convergence issues when applied to highly non-ideal solution phases and thus doesn't work well for this work despite its apparent numerical advantage previously shown by Piro et al. [50].

Computational Materials Science 198 (2021) 110659

Contents lists available at ScienceDirect

Computational Materials Science

journal homepage: www.elsevier.com/locate/commatsci

Corrigendum

# Corrigendum to "The thermochemistry library Thermochimica"

Parikshit Bajpai [a], Markus H.A. Piro [a,b,*]

[a] Faculty of Science, Ontario Tech University, Oshawa, ON, Canada
[b] Faculty of Energy Systems and Nuclear Sciences, Ontario Tech University, Oshawa, ON, Canada

ARTICLE INFO

*Keywords*
Gibbs energy minimisation
Partitioning of gibbs energy
Thermochimica
Yellowjacket

ABSTRACT

The CALPHAD method has been highly relied upon for material design and development and a number of software packages have been developed for computing thermodynamic equilibrium. While Gibbs Energy Minimisation (GEM) has been the most commonly used algorithm for thermodynamic equilibrium calculations, an alternative technique namely Partitioning of Gibbs Energy Minimisation (PGE) was advanced and applied to the thermochemistry library Thermochimica due to some of its numerical advantages. The PGE approach, however, has considerable convergence issues when applied to highly non-ideal solution phases and therefore was eventually abandoned in Thermochimica. This corrigendum illustrates the convergence issues and their underlying cause with the aim of informing the readers about the reasoning for adopting GEM in place of PGE in Thermochimica and may help their own decision making in selecting an algorithm for their own software.

## 1. Introduction

Recent trends in material design and development have relied heavily on the CALPHAD method [1] and over the years a number of software packages have been developed for computing thermodynamic equilibrium, such as Thermo-Calc [2], FactSage [3], PANDAT [4], pyCalphad [5], OpenCalphad [6], Thermochimica [7], Yellowjacket [8], etc. While most thermochemical equilibrium solvers rely on the Gibbs Energy Minimisation (GEM) approach, originally developed by White et al. [9], Piro et al. advanced a numerical procedure called the Partitioning of Gibbs Energy (PGE) in Thermochimica, which built upon the concepts presented by White [10] in combination with that of Eriksson and Thompson [11]. In initial developments of Thermochimica, the PGE method was applied in place of the GEM method due to some numerical advantages that improved the rate of convergence and reduced numerical instabilities for some applications. These advantages include the fact that PGE does not require any numerical dampening to ensure that the mole fractions of the various solution species remain positive as compared to GEM where numerical dampening becomes necessary. This issue will become clearer in the next section. GEM also requires additional corrections to be applied in order to improve the estimates of mole fractions of dilute species. While such corrections can compromise the mass balance constraints in GEM, they are inherently satisfied in PGE, thereby simplifying the numerical process.

Despite its numerical advantages, a significant challenge is experienced when PGE is applied to a broader range of applications that results in considerable convergence issues. Ultimately, the PGE method was abandoned in Thermochimica in favour of the more widely used GEM technique, which offers greater robustness over a wide range of applications. This corrigendum is intended to better inform the readers about the reasoning behind adopting the GEM method in place of PGE, which may help their own decision making in developing their own software. In the current context, for the sake of simplicity, the discussion will focus on species in single-sublattice phases. However, the concepts readily apply to the compound end members and/or quadruplets in multi-sublattice phases.

## 2. Discussion

From a theoretical point view, both GEM and PGE methods should yield the same set of predictions of thermodynamic equilibria: a unique combination of phases and species that are stable in a closed isothermal-isobaric system of fixed composition. The distinction between GEM and PGE lies not in the mathematical content of the equilibrium conditions but rather in the numerical algorithms adopted to solve the problem. At a high level, GEM is an optimisation method, whereas the PGE approach is based on finding the roots of a system of nonlinear equations [12]. To highlight the differences between the two approaches, the conditions for

DOI of original article: https://doi.org/10.1016/j.commatsci.2012.09.011.
* Corresponding author at: Faculty of Science, Ontario Tech University, Oshawa, ON, Canada.
*E-mail addresses:* parikshit.bajpai@ontariotechu.net (P. Bajpai), markus.piro@ontariotechu.ca (M.H.A. Piro).

https://doi.org/10.1016/j.commatsci.2021.110659
Received 29 April 2021; Accepted 14 June 2021
Available online 1 July 2021

thermodynamic equilibrium are first summarized:

1. The conservation of mass must be satisfied:

$$b_j = \sum_{\lambda=1}^{\Lambda} n_\lambda \sum_{i=1}^{N_\lambda} x_{i(\lambda)} \nu_{ij} + \sum_{\omega=1}^{\Omega} n_\omega \nu_{\omega j}. \tag{1}$$

where $b_j$ denotes the molar amount of component $j$ in the system[1], $n_\lambda$ and $n_\omega$ are the molar amounts of solution phase $\lambda$ and stoichiometric phase $\omega$, respectively. $x_{i(\lambda)}$ represents the mole fraction of species $i$ in solution phase $\lambda$, and $\nu_{ij}$ and $\nu_{\omega j}$ are the stoichiometry coefficients of component $j$ in species $i$ and stoichiometric phase $\omega$, respectively. Note that this equation also applies to ionic charge to ensure charge neutrality constraints are respected.

2. The Gibbs phase rule must be respected:

$$F = C - \Phi + 2 - \Xi. \tag{2}$$

where $F$ denotes the degree of freedom of the system, $C$ represents the number of system components and $\Phi = \lambda + \Omega$ is the number of phases present at equilibrium. $\Xi$ represents the number of ionic phases[2]. Under isothermal-isobaric conditions, the Gibbs phase rule is reduced to $F = C - \Phi - \Xi$, where $F \geqslant 0$.

3. The Gibbs energy of the system must be at a global minimum. The *necessary condition* corresponding to a local minimum requires that the chemical potentials of any species must be represented by a linear function of the system component potentials as [12–14]:

$$\widetilde{\mu}_{i(\lambda)} = \sum_{j=1}^{C} \nu_{ij} \widetilde{\Gamma}_j, \tag{3}$$

where $\widetilde{\mu}_{i(\lambda)}$ represents the dimensionless chemical potential of species $i$ and $\widetilde{\Gamma}_j$ represents the dimensionless chemical potential[3] of component $j$. The *sufficient condition* for global minimum requires that all the metastable phases abide by the following condition [15–17]:

$$\pi_\lambda = \min_{\lambda} \sum_{i=1}^{N_\lambda} x_{i(\lambda)} \left( \mu_{i(\lambda)} - \sum_{j=1}^{C} \nu_{ij} \widetilde{\Gamma}_j \right) \geqslant 0, \tag{4}$$

that is, the driving force of all the phases believed to be metastable must be positive and all stable phases are zero.

In addition to the above conditions, the following constraints must be respected:

A. The number of moles of any phase cannot be negative.
B. The sum of mole fractions of all species in a solution phase must equal unity.

It must be mentioned that both GEM and PGE are methods for computing local minima and to compute the global minimum, they must be coupled with a global optimisation routine, some of which have been analysed by Piro and Simunovic [17].

The fundamental premise of GEM is to define the quantities of all species and phases as the *independent* variables, and their corresponding chemical potentials as *dependent* variables (i.e., $\mu_i = f(\mathbf{x})$). In contrast, the PGE method defines the chemical potentials as independent variables, and the quantities of species and phases as the dependent variables (i.e., $x_i = f(\boldsymbol{\mu})$). In GEM, the estimated quantities of all species and phases are iteratively altered to progressively minimize the Gibbs energy of the system. In other words, the GEM approach optimises equilibrium conditions 1 and 3 while constraining equilibrium condition 2 [9,18,19].

Thus, the mass balance residuals and residuals of chemical potentials of each phase with respect to the system components are simultaneously minimised in GEM [7]. The number of moles of each solution species is updated with a linear function, which is then used to compute the conjugate chemical potential terms. One must often dampen this calculation to prevent the computation of the logarithm of a negative number. In contrast, the PGE method defines the chemical potentials of all species and phases by a set chemical potentials of the system components, which are then used to compute the mole fractions of individual species and iteratively attempts to satisfy the mass balance equations in Eq. (1). Thus, PGE constrains equilibrium conditions 2 and 3 while iteratively satisfying equilibrium condition 1 [7]. Furthermore, since the PGE method defines the mole fraction as an exponential function, rather than a linear function involving the natural logarithm, it will always be positive as long as the chemical potentials are real. This feature reduces the need for numerical dampening in PGE.

The distinguishing feature of PGE is in solving a system of non-linear equations to find the roots of the mass balance equations, which requires representing the mole fraction of any species as an exponential function involving the system component potentials. One can formulate an explicit function for species in an ideal solution phase; however, for non-ideal solution phases requiring an excess Gibbs energy of mixing contribution, this is not always a straightforward mathematical operation. The Gibbs energy of a non-ideal solution phase is generally given as:

$$G_\lambda = G_\lambda^\circ + G_\lambda^{\mathrm{id}} + G_\lambda^{\mathrm{ex}}, \tag{5}$$

where $G_\lambda$ is the Gibbs energy of the solution phase $\lambda$ and the superscripts $\circ$, id and ex denote the reference, ideal mixing and excess mixing contributions, respectively. The chemical potential of species $i$ in solution phase $\lambda$ is generally given as:

$$\mu_{i(\lambda)} = \left( \frac{\partial G_\lambda}{\partial n_{i(\lambda)}} \right)_{T,P,n_{j \neq i}} \tag{6}$$

For a species in an ideal solution phase, the reference and ideal mixing contributions result in linear contributions to the chemical potentials, yielding:

$$\widetilde{\mu}_{i(\lambda)} = \widetilde{\mu}_{i(\lambda)}^\circ + \ln(x_{i(\lambda)}) \tag{7}$$

Recall that $\widetilde{\mu}_{i(\lambda)}$ represents the dimensionless chemical potential, which is why $RT$ is not used in the foregoing equation.

Substituting Eq. 3 for $\widetilde{\mu}_{i(\lambda)}$ in Eq. (7), and re-arranging to solve for $x_{i(\lambda)}$ gives:

$$x_{i(\lambda)} = \exp\left( -\widetilde{\mu}_{i(\lambda)}^\circ + \sum_{j=1}^{C} \nu_{ij} \widetilde{\Gamma}_j \right) \tag{8}$$

For the case of a non-ideal solution phase, an excess Gibbs energy of mixing term is added, which is a model-specific function that involves mole fractions of the species within that phase, $x_{i(\lambda)}$ [20]. Similar to Eq. (8), the mole fraction of a species in a non-ideal phase is represented in PGE as a function of the system component potentials as follows:

$$x_{i(\lambda)} = \exp\left( -\widetilde{\mu}_{i(\lambda)}^\circ - \widetilde{\mu}_{i(\lambda)}^{\mathrm{ex}} + \sum_{j=1}^{C} \nu_{ij} \widetilde{\Gamma}_j \right) \tag{9}$$

Technically, the equation for $x_{i(\lambda)}$ in Eq. (9) is *not a function* because $\widetilde{\mu}_{i(\lambda)}^{\mathrm{ex}}$ is itself a function of $x_{j(\lambda)}, \forall j$. Therefore, one can only define an

[1] Note that a system component may be a chemical element, an integer combination of chemical elements, or an electron corresponding to an ionic phase.

[2] Note that $\Xi$ is the conjugate variable to the increase in $C$ corresponding to ionic phases.

[3] Dividing by $RT$, where $R$ is the ideal constant and $T$ the absolute temperature, reduces computational expense and is standard practice.

explicit function for $x_{i(\lambda)}$ in PGE when solution phase $\lambda$ is ideal; however, this cannot be done when $\lambda$ is non-ideal. For any non-ideal solution phase $\lambda$, replacing the expressions of chemical potentials in Eq. (9), one gets an implicit expression of the form $x_{i(\lambda)} = f(\boldsymbol{\mu}(\boldsymbol{x}))$. In PGE, the preceding expression is used to construct the mass balance residuals, which must be near zero (within tolerance) when the conditions of equilibrium are satisfied [7]. The roots, including $x_{i(\lambda)}$, of the non-linear system of equations so formed must then be solved, which significantly impacts the performance and stability of PGE. At this stage, one faces a difficult choice of options due to several reasons.

Firstly, since the residual equations are not explicit, solving the system of equations in order to find the mole fractions of the species requires solving an additional non-linear problem within PGE. One is faced with the question of how to evaluate the roots of an implicit expression in a closed-form sense. In Thermochimica, multiple approaches were explored to find the roots. One of these approaches was to solve for the mole fractions, $x_{i(\lambda)}$, at each step while computing the partial molar excess terms using the mole fractions from the previous global iteration. Though the use of this approach temporarily makes the residual equation explicit, it does not guarantee convergence especially in highly non-linear phases. Another approach was to use a linear averaged approximation of the mole fraction $\left(x^{m+1} = 0.5(x^{m} + x^{\text{temp}})\right)$ or a non-linear averaged approximation $\left(x^{m+1} = \sqrt{x^{m} x^{\text{temp}}}\right)$ but without any assurance of convergence. A more involved attempt used a nested non-linear root finding algorithm but it was often unfruitful despite adding significantly to the computational expense.

Secondly, and more critically, there might be cases where the residual equations result in a system with no roots. Such a situation cannot be dealt with using any algorithm and causes the PGE method to fail. Finally, the last issue relates to existence of multiple roots. Such a scenario can arise, for example, in systems with miscibility gaps and the roots calculated using the PGE algorithm are virtually indistinguishable and can therefore result in misleading predictions of equilibrium conditions. These predicaments are further amplified as one moves to more complicated non-linear models and higher order systems. In general, such models act as significant impediments to the applicability of PGE for determining phase equilibrium in systems where highly non-linear non-ideal phases are involved.

GEM, on the other hand, does not require a set of explicit functions of the mole fractions of the species $x_{i(\lambda)}$. Since the Gibbs energy and mass balance residual are simultaneously minimised in GEM, it instead requires an explicit function of chemical potentials as a function of $x_{i(\lambda)}$. Even without any rearrangement, the chemical potentials of species are explicit functions of mole fractions ($\widetilde{\mu}_{i(\lambda)} = f(\mathbf{x})$). As a result, the roots of the resulting system of linearised equations[4] can be directly evaluated. Therefore, GEM does not suffer from the shortcomings of PGE and is directly applicable to all sorts of mixing models. While applying GEM, one does not need to focus on sidestepping the numerous hurdles faced by PGE when dealing with highly non-linear phases and despite the numerical disadvantages discussed by Piro et al. [7], it is much more robust and with the aid of a good initial estimate and proper line search methods it converges easily for a much broader range of models compared to PGE.

## 3. Summary

In summary, the PGE method has been found to offer marginal benefits to GEM in handling systems containing stoichiometric and ideal solution phases. However, PGE experiences a great predicament when involving non-ideal solution phases whereby one can no longer define mole fractions as explicit functions of chemical potentials because excess Gibbs energy expressions are also functions of mole fractions. In contrast, the GEM method avoids this shortfall as it reverses the selection of dependent and independent variables, whereby the chemical potentials of solution species can be written as explicit functions of the mole fraction of solution species. In practice, the GEM method has proven to be quite robust in a number of complex thermodynamic systems involving highly non-linear excess Gibbs energy models.

[4] The linearised system follows from the method of Lagrange multipliers used to solve the constrained optimisation problem and derivation of such a system of equations has been presented by, for example, White et al. [9], Eriksson and Rosen [18], etc.

## Declaration of Competing Interest

The authors declare that they have no known competing financial interests or personal relationships that could have appeared to influence the work reported in this paper.

## Acknowledgements

This research was undertaken, in part, thanks to funding from the Canada Research Chairs (950–231328) and Discovery Grant programs of the Natural Sciences and Engineering Research Council of Canada.

## References

[1] P. Spencer, A brief history of CALPHAD, Calphad 32 (1) (2008) 1–8.
[2] J.-O. Andersson, T. Helander, L. Höglund, P. Shi, B. Sundman, Thermo-Calc & DICTRA, computational tools for materials science, Calphad 26 (2) (2002) 273–312.
[3] C. Bale, P. Chartrand, S. Degterov, G. Eriksson, K. Hack, R. Mahfoud, J. Melançon, A. Pelton, S. Peterson, "FactSage thermochemical software and databases," Calphad, vol. 26, no. 2, 2002.
[4] W. Cao, S.-L. Chen, F. Zhang, K. Wu, Y. Yang, Y. Chang, R. Schmid-Fetzer, W. Oates, "PANDAT software with panengine, panoptimizer and panprecipitation for multi-component phase diagram calculation and materials property simulation," Calphad, vol. 33, no. 328–342, 2009.
[5] R. Otis, M. Emelianenko, Z.-K. Liu, An improved sampling strategy for global energy minimization of multi-component systems, Comput. Mater. Sci. 130 (2017) 282–291.
[6] B. Sundman, U.R. Kattner, M. Palumbo, S.G. Fries, OpenCalphad - a free thermodynamic software, Integrating Mater. Manuf. Innovation 4 (1) (2015) 1.
[7] M. Piro, S. Simunovic, T. Besmann, B. Lewis, W. Thompson, The thermochemistry library Thermochimica, Comput. Mater. Sci. 67 (2013) 266–272.
[8] P. Bajpai, M. Poschmann, D. Andrš, C. Bhave, M. Tonks, M. Piro, "Development of a new thermochemistry solver for multiphysics simulations of nuclear materials," in TMS 2020 149th Annual Meeting & Exhibition Supplemental Proceedings, pp. 1013–1025, Springer, 2020.
[9] W. White, S. Johnson, G. Dantzig, Chemical equilibrium in complex mixtures, J. Chem. Phys. 28 (5) (1958) 751–755.
[10] W. White, Numerical determination of chemical equilibrium and the partitioning of free energy, J. Chem. Phys. 46 (11) (1967) 4171–4175.
[11] G. Eriksson, W. Thompson, A procedure to estimate equilibrium concentrations in multicomponent systems and related applications, Calphad 13 (4) (1989) 389–400.
[12] F. van Zeggeren, S. Storey, The Computation of Chemical Equilibria, Cambridge University Press, 2011.
[13] M. Piro, T. Besmann, S. Simunovic, B. Lewis, W. Thompson, Numerical verification of equilibrium thermodynamic computations in nuclear fuel performance codes, J. Nucl. Mater. 414 (3) (2011) 399–407.
[14] M. Zemansky, R. Dittman, Heat and thermodynamics. McGraw-Hill, 6th ed., 1981.
[15] M. Hillert, Some viewpoints on the use of a computer for calculating phase diagrams, Physica 103B (1981) 31–40.
[16] H. Lukas, S. Fries, B. Sundman, Computational Thermodynamics: The Calphad Method, Cambridge University Press, 2007.
[17] M. Piro, S. Simunovic, Global optimization algorithms to compute thermodynamic equilibria in large complex systems with performance considerations, Comput. Mater. Sci. 118 (2016) 87–96.
[18] G. Eriksson, E. Rosén, General equations for the calculation of equilibria in multiphase systems, Chemica Scripta 4 (1973) 193–194.
[19] W.R. Smith, R.W. Missen, Chemical Reaction Equilibrium Analysis: Theory and Applications, John Wiley and Sons, 1982.
[20] P. Bajpai, M. Poschmann, M. Piro, Derivations of partial molar excess gibbs energy of mixing expressions for common thermodynamic models, J. Phase Equilibria Diffusion (2021).

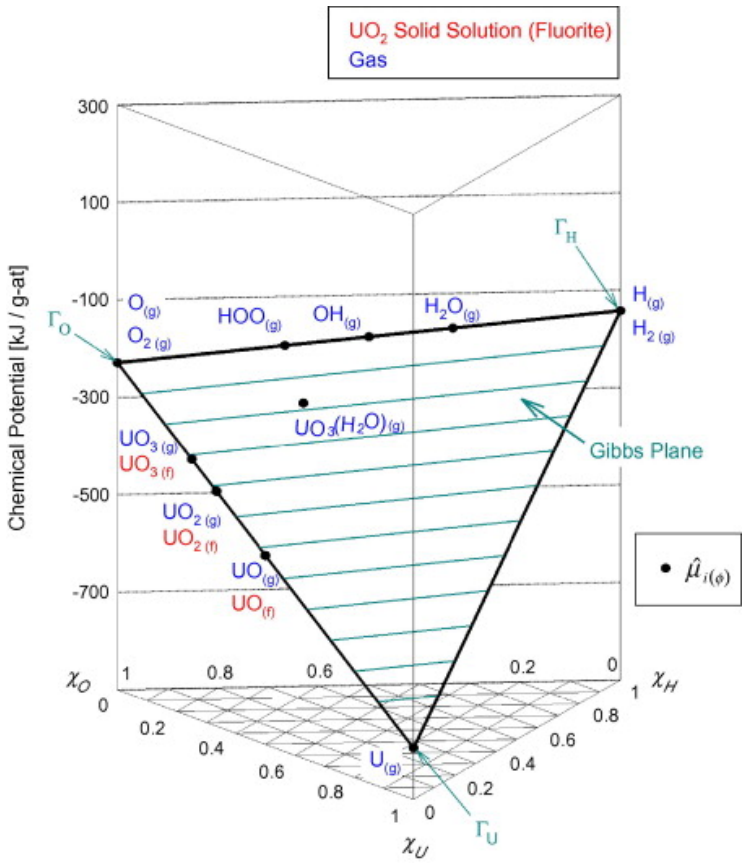


Figure 5.1: The Gibbs criteria is satisfied when the chemical potentials for all species represented per gram-atom lie on the Gibbs Plane within an acceptable tolerance [172].

## 5.4. Global Energy Minimisation

Global minimisation of Gibbs energy is crucial to accurately predicting the stable phase assemblage using equilibrium thermodynamic softwares. An example application is the detection of miscibility gaps in phases containing regions of compositional instability. In a miscibility gap, the same phase can appear with different compositions and finding the global minimum from among the many local minima can be a daunting challenge. For multi-component systems, the topology of the energy surfaces tends to become quite complex particularly when there are multiple non-ideal phases in the system. This significantly complicates the interaction of the Gibbs energy surface with the Gibbs hyperplane and an inadequate numerical approach may lead to a false sense of thermodynamic equilibrium despite being far from the true equilibrium. To illustrate how an inadequate solver may yield a false equilibrium, the following scenarios can be considered:

1. In the fictive binary system shown in Figure 5.2, a solution phase $\alpha$ and a stoichiometric phase $A_3B_2$ can possibly coexist. While the stoichiometric phase $A_3B_2$ and solution phase

$\alpha$ are predicted to be stable, as represented by the dashed tangent line, they are in fact metastable and a miscibility gap would yield a lower value of the integral Gibbs energy of the system, $G_{sys}$.

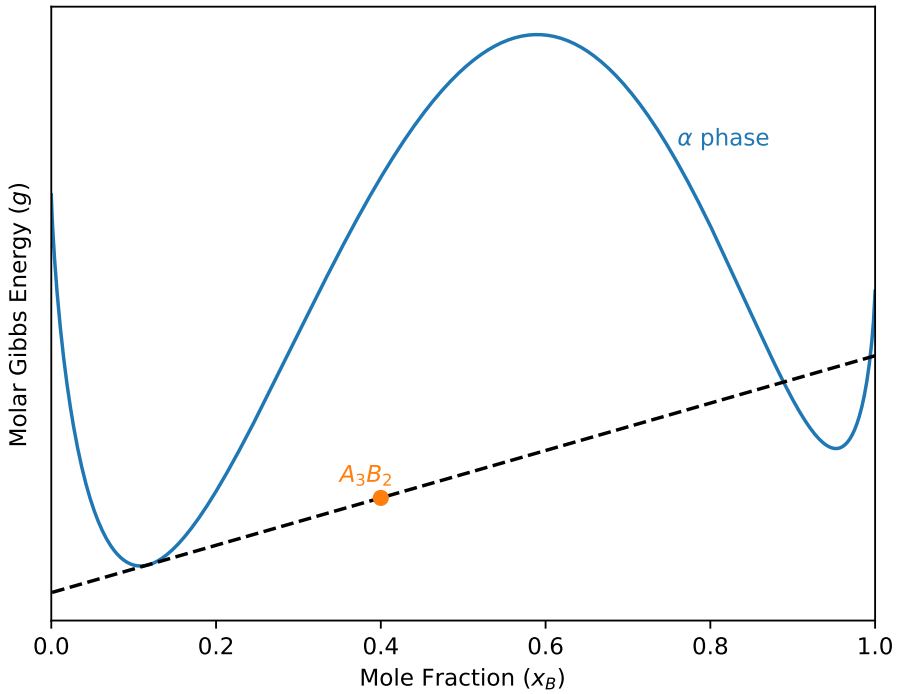


Figure 5.2: Fictive system with miscibility gap showing a possible false positive from thermodynamic equilibrium solver (after Piro and Simunovic [110]).

2. In the fictive binary system shown in Figure 5.3 which can have three possible solution phases, the $\delta$ phase is believed to be metastable but one must confirm that the combination of $\beta$ and $\gamma$ is most stable or if a different combination is more stable. However, it can be seen that inserting the $\delta$ phase into the system and replacing one of the other two phases would yield a lower value of the integral Gibbs energy of the system, $G_{sys}$.

As previously mentioned in Section 5.2, satisfying the necessary conditions, specifically the Gibbs' Criterion, is equivalent to finding a local minimum but one must demonstrate that the driving force, $\Delta G$, is non-negative for all phases to be metastable. Throughout the iterative process, the driving force for all the metastable phases should be calculated to determine if a particular phase needs to be added to the system. At this point, two similar but distinct approaches to the problem of identifying phases with negative driving force can be adopted. In the first approach, the goal is only to find out whether or not a phase has a negative driving force while in the second approach the goal is to determine the minimum value of the driving force

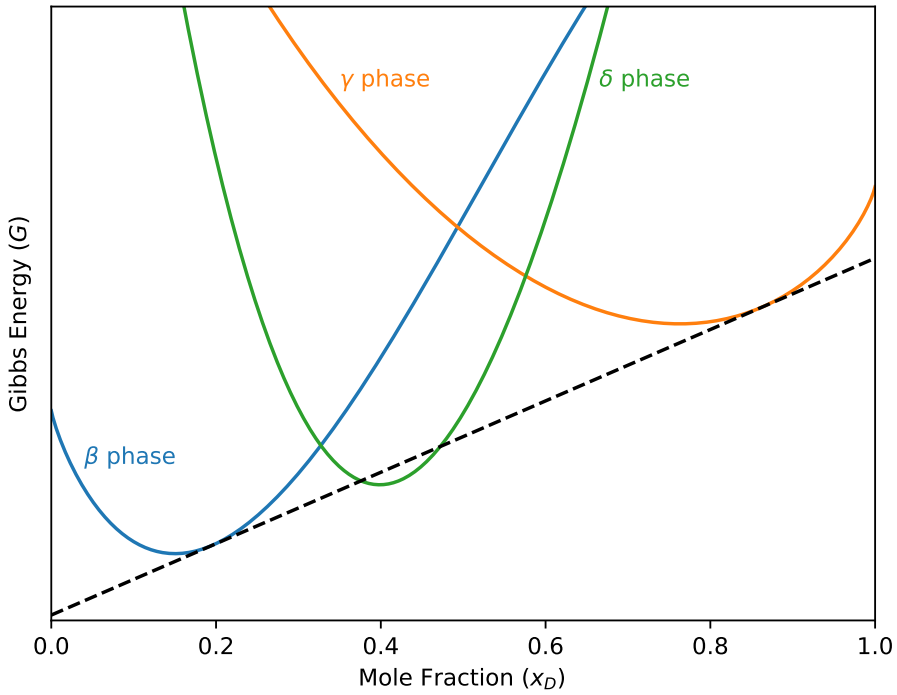


Figure 5.3: Fictive system with three possible phases showing a false positive from thermodynamic equilibrium solver wherein a wrong phase is believed to be present at equilibrium (after Piro and Simunovic [110]).

subject to the equality and inequality constraints mentioned previously. While the first approach can be computationally cheaper, the second approach can provide additional information about the state of the system. For instance, when multiple phases have a negative driving force, the phase with the most negative driving force can be added to the system.

Since the driving force function can be non-convex, finding the most negative driving force is essentially a constrained global optimisation problem. The domain space of the problem is defined by the number of species in the solution phase and, because the mole fractions of the species must lie in $(0, 1)$, the search space is box constrained. Using the sufficient conditions previously mentioned, the Lagrangian function of the driving force of solution phase $\phi$ can be defined as:

$$\mathcal{L}_\phi = \sum_{i=1}^{N_\phi} x_i \left( \tilde{\mu}_i - \sum_{j=1}^{C} \nu_{ij} \tilde{\Gamma}_j \right) - \pi_\phi \left( \sum_{i=1}^{N_\phi} x_i - 1 \right) - \pi_{e^-} \left( \sum_{i=1}^{N_\phi} \nu_{ie^-} x_i - 1 \right), \qquad (5.57)$$

where the first Lagrange multiplier, $\pi_\phi$, imposes the constraint on mole fractions and the second multiplier, $\pi_{e^-}$, extends the constraints to handle ionic phases where the charge neutrality constraint must also be satisfied. The natural constraint on mole fractions implies $x_i \in (0, 1)$ and the unknowns in the above expression, $x_i$, $\pi_\phi$ and $\pi_{e^-}$, must lie in $\mathbb{R}^{N_\phi+2}$. For phases

without any ionic components, the dimension of the above problem reduces by one. The Lagrangian function has a minimum value when $\nabla\mathcal{L} = 0$. Differentiating $\mathcal{L}$ with respect to $x_i$:

$$\frac{\partial\mathcal{L}}{\partial x_i} = \tilde{\mu}_i - \sum_{j=1}^{C} \nu_{ij}\tilde{\Gamma}_j - \lambda_\phi, \tag{5.58}$$

which shows that the undetermined Lagrange multiplier, $\lambda_\phi$, is the same as the driving force of the phase, $\Delta G_\phi$. Differentiating with respect to $\lambda_\phi$ yields:

$$\frac{\partial\mathcal{L}}{\partial\pi_\phi} = 1 - \sum_{i=1}^{N_\phi} x_i, \tag{5.59}$$

and taking the derivative with respect to $\lambda_{e^-}$ results in:

$$\frac{\partial\mathcal{L}}{\partial\pi_{e^-}} = 1 - \sum_{i=1}^{N_\phi} \nu_{ie^-} x_i. \tag{5.60}$$

The system of non-linear equations above can be solved using many different non-linear solution methods such as by taking the second order Taylor expansion of the Lagrangian function. The global optimisation algorithms used in Yellowjacket–GEM will be discussed in further details in Chapter 6.

## 5.5. Summary

Based on the fundamental laws of thermodynamics, achieving thermochemical equilibrium in a system requires satisfaction of several conditions. While satisfying the necessary conditions is relatively straightforward, special care must be taken to ensure that the sufficient condition is satisfied. This is because, as previously mentioned, the necessary conditions result in identification of a local minimum which may or may not correspond to the true global minimum. The aforementioned conditions are used in thermodynamic equilibrium solvers to find a unique combination of phases that are stable in the system. In such solvers, one must also carefully consider the role of the numerical algorithm and the convergence criteria to be adopted as these choices can have a significant impact on both computational performance and robustness of the solver.

# 6

# Computational Implementation

*The principles of thermodynamic equilibrium set the background for solving phase equilibrium problem in multicomponent system but being able to solve the resulting optimisation problem requires the use of efficient algorithms and high-quality software implementations. While many of the algorithms employed in Yellowjacket–GEM embody the concepts previously presented in open literature, there remains a scope for improving the efficiency and capabilities of some of these algorithms through careful implementation and/or building upon them. The top level architecture of the thermodynamic equilibrium solver has been outlined in Figure 6.1. The program essentially consists of parsing and input modules to read the required thermodynamic data and system information followed by initialisation routines which provide the initial assemblage to a non-linear solver. The assemblage from the non-linear solver is then checked to ensure global minimum is achieved at which stage the outputs are produced.*

## 6.1. Thermodynamic Database

Calculation of thermodynamic equilibrium requires a thermodynamic database, which includes Gibbs energy functions for the different phases and species that can exist in the system. These thermodynamic databases are developed using the well established CALPHAD method [173] and are available in different formats, the most commonly used being ThermoCalc (`*.tdb`) and ChemSage (`*.dat`) datafile formats, which are generated by the commercial software ThermoCalc and FactSage, respectively. An example of a typical ChemSage format datafile is shown in Figure 6.2 and consists of a header block followed by information blocks for every

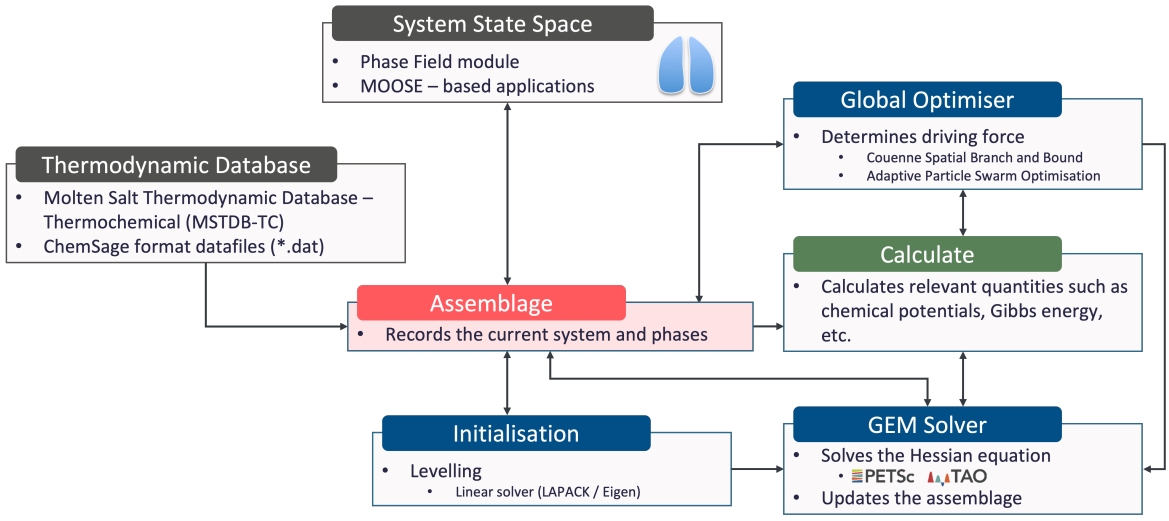


Figure 6.1: Top-level architecture of Yellowjacket–GEM.

possible phase in the system.

A datafile parser for Yellowjacket–GEM has been developed in C++ and it performs the extraction of Gibbs energy functions from ChemSage format (`*.dat`) thermodynamic files and creates an in-memory thermodynamic database class, `Database`, that can be conveniently accessed by any part of the code throughout rest of the solve. All the data structure objects inherit from a single base class allowing the rest of the code to track the phases conveniently without having to track the model-specific details. Moreover, in multiphysics simulations, it allows a single database instance to be created at the start of the simulations instead of the need of reading the datafile every time the information is needed. In Yellowjacket–GEM, the MSTDB-TC [175, 176], is natively supported but any ChemSage format datafile can be supplied by the user.

The `Database` class includes a number of utility functions for post-processing and cleaning up the raw database constructed after parsing. A peculiarity of ChemSage datafiles is how they denote phases that can have a miscibility gap. In ChemSage, such phases are denoted by adding a duplicate entry for a phase that is considered to have miscibility gaps. This has several disadvantages. First, this creates unnecessary duplication of thermodynamic data and can have memory and performance implications for large databases. Second, the decision about miscibility gap should be enforced using physical rules rather than basing them upon the database or user inputs. As an example, since a phase with more than one miscibility gap is not only plausible but also observed in many physical systems, a phase being duplicated once doesn't reveal any information about the number of such possible gaps and can be a source of confusion. In post-processing, such duplicate entries are deleted, but to not lose the information

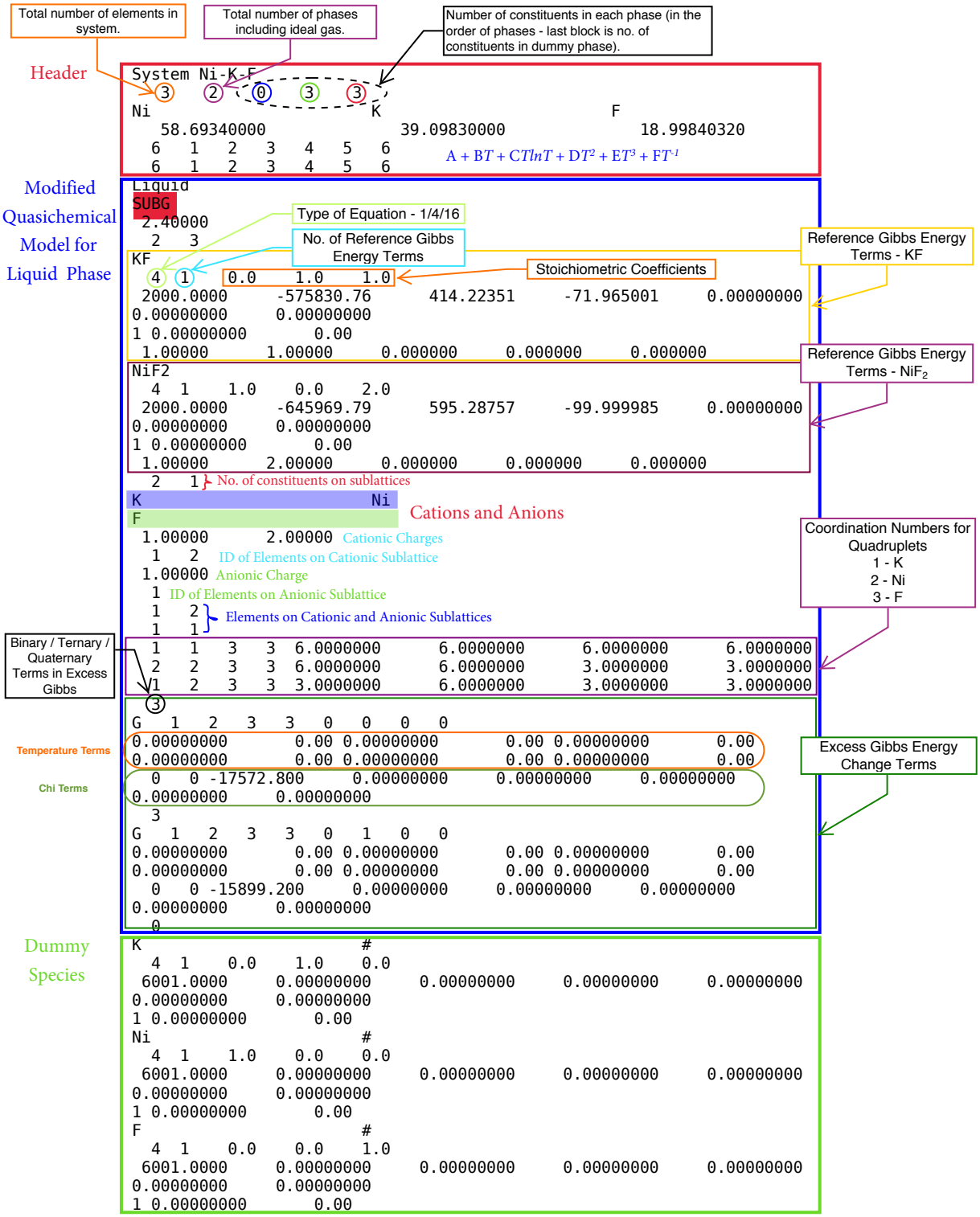


Figure 6.2: A marked-up example of a ChemSage format datafile of the Ni−K−F system [174].

completely, a flag is raised in the thermodynamic phase whose duplicate was deleted. For multi-sublattice phases, the post-processor also maps all the sublattice constituents to the system components, and, for phase represented by MQMQA, it calculates the default coordination numbers for the quadruplets that are not included in the datafile.

## 6.2. System State-Space

Thermochemical equilibrium calculations are isothermal, isobaric point calculations and require the temperature and pressure, as well as the composition, of the system to be specified. In Yellowjacket–GEM, this information is provided by MOOSE or MOOSE-based applications such as the Phase Field module. To facilitate such data transfer, a MOOSE UserObject, namely `GEMUserObject`, has been developed. The MOOSE UserObject system is built for developing and running custom algorithms that may not fit well within any other system in MOOSE. Examples include complex calculations that may result values that don't associate in a one to one manner with elements, nodes, or sides. `GEMUserObject` allows the thermodynamic equilibrium solver to be called by other codes and the invocation requires that the temperature, pressure and composition be specified as required parameters. The UserObject is also responsible for passing back the return values to the calling code and some of the common variables that are often requested include the Gibbs energy, chemical potentials, stable phases and their speciation.

## 6.3. Initialisation

Much like any other optimisation problem, the choice of initial estimate plays a critical role in reducing the amount of computational time required for the solution to converge to a minimum. This requirement of initial estimates of the stable phases and their speciation creates a significant challenge. Many early softwares created for the purpose of estimating thermodynamic equilibrium, for example SOLGASMIX, required the user to input an initial estimate but this relied on the user's intuition and was often very inconvenient for them, especially when working with complex systems and/or systems where finding estimates from intuition was not straightforward. A bigger problem was that it could often result in initial estimates that were far from the real stable assemblage of phases and would increase the computational cost substantially, often even compromising the convergence itself.

Yellowjacket–GEM implements *levelling* from Eriksson and Thompson [46] as the standard initialisation routine and it is described in the following text.

### 6.3.1. Levelling

The levelling algorithm was developed to accelerate the rate of convergence by eliminating the phases and species that have an insignificant contribution in the final phase assemblage. The algorithm is based on a temporary treatment of all species and phases in the system as pure stoichiometric phases. Mathematically, this amounts to temporarily converting the non-linear optimisation problem into a linear optimisation problem. The algorithm for the computational implementation has been illustrated in Figure 6.3.

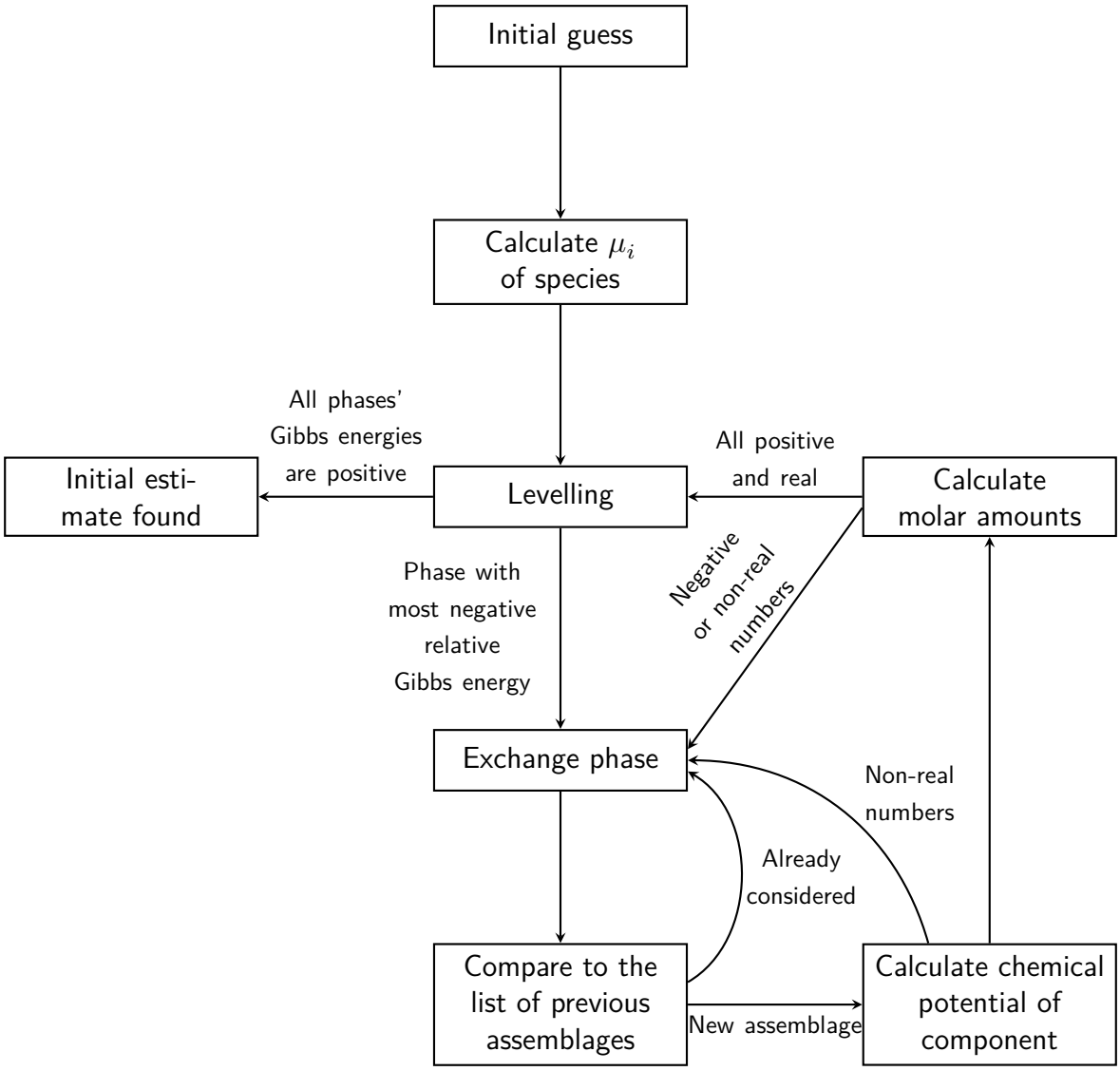


Figure 6.3: Levelling algorithm for finding the initial estimate of stable phase assemblage. After Loukusa [91].

Since the Gibbs energy is a relative thermodynamic function and the Gibbs energies of each component element are not related to one another [46], it is possible to numerically alter the

Gibbs energy of each phase while preserving the elemental differences. Levelling is performed by representing the set of Gibbs energies relative to the collection of phases assumed to be most stable and uses a relative Gibbs energy function called the *absolute Gibbs energy* by Eriksson and Thompson and is the Gibbs energy of the pure species per atom in the species as shown in equation (6.1)

$$\hat{G}_i = \frac{G_j}{\sum_{j=1}^{C} \nu_{ij}}. \tag{6.1}$$

The levelling process determines the combination of phases yielding the lowest Gibbs energy by evaluating a combination of Gibbs energies on a relative basis. A phase that has a negative relative Gibbs energy with respect to the assemblage indicates that a phase in the assemblage must be replaced by the current phase to achieve a lower integral Gibbs energy. Mathematically, levelling is achieved through an iterative process that systematically adjusts fixed combinations of phases, subject to the linear equality and inequality mass balance constraints, to progressively minimise the Gibbs energy of the system [47]. At iteration $m+1$, the adjustment to be applied to the relative Gibbs energy of phase $i$ is defined by [46]:

$$\begin{aligned} d\hat{G}_i^{m\to m+1} &= \sum_{j=1}^{C} c_{ij} d\Gamma_j^{m\to m+1}, \\ \hat{G}_i^{m+1} &= \hat{G}_i^{m} - d\hat{G}_i^{m\to m+1}, \end{aligned} \tag{6.2}$$

where $c_{ij}$ denotes the atomic fraction of element $j$ in species $i$ and $d\Gamma_j^{m\to m+1}$ is the adjustment applied to the chemical potential of element $j$, which in turn is determined by the most stable phases found at iteration $m$. In matrix form, the overall mass balance constraint can be represented as [47]

$$\nu^T \mathbf{n} = \mathbf{b}, \tag{6.3}$$

where $\nu^T \in \mathbb{R}^{C\times\Phi}$ represents the stoichiometric matrix, $\mathbf{n} \in \mathbb{R}^{\Phi}$ denotes the column vector of the number of moles of each phase, and $\mathbf{b} \in \mathbb{R}^{C}$ is the column vector with the total mass of each element in the system. When equation 6.3 is used in levelling, $\Phi = C$.

The initial guess for the levelling method is the most chemically stable form of each element and the stoichiometric matrix $\nu^T$ in equation (6.3) becomes a diagonal matrix. Subsequently, provided all elements of vector $\mathbf{b}$ are positive, all the elements of $\mathbf{n}$ must also be positive. However, the diagonality of the stoichiometric matrix is not preserved over subsequent iteration and it assumes a non-symmetric sparse form. In fact, the matrix $\nu^T$ might become rank deficient if proper care is not taken while selecting the phase assemblage.

In levelling, since the number of phases in the system is equal to the number of elements,

the element potentials can then be uniquely determined from the current estimated phase assemblage by solving the following system of linear equations:

$$\nu^T \Gamma = \mu, \tag{6.4}$$

where $\Gamma \in \mathbb{R}^C$ and $\mu \in \mathbb{R}^\Phi$.

The next step in levelling is updating the phase assemblage in accordance with equation (6.2). A species with a positive $\hat{G}_i^{m+1}$ would yield a thermodynamically less stable assemblage and is left out along with phases with insignificant contributions to final equilibrium while the phase with the most negative $\hat{G}_i^{m+1}$ is introduced into the assemblage by replacing a phase in the previous assemblage. The phase assemblage at this stage must meet three requirements. First, the number of moles of all phase in $\mathbf{n}$ must be non-negative and real. Second, all the elements of the vector $\Gamma$ must be real. Finally, the phase assemblage must not have been previously considered. If the phase assemblage does not meet any of these requirements, the phase with the second lowest relative Gibbs energy must be considered, and so on.

While the criteria for the phase to be added in the system was well established by Eriksson and Thompson, a criterion to select the phase to be replaced wasn't proposed and, typically, local iterations were performed to systematically traverse through the candidate phases until a particular combination yielded an entire set of non-negative and real mole numbers [46]. The number of these local iterations rapidly grows with the number of elements in the system and an alternative named *Euclidean norm* was proposed by Piro and Simunovic [47]. This method has been described in Section 6.3.2.

Once the new phase has been exchanged with one of the existing phases and its acceptability has been determined, levelling step is repeated until no phases with negative absolute Gibbs energy remain in the system. At this stage, the assemblage can be passed on to a non-linear solver as the initial estimate.

An example of the levelling method is presented in Figure 6.4. In the illustration, in the first iteration, the phase with the most negative Gibbs energy is paired with another phase that together has non-negative molar quantities. At the end of iteration 0, choosing solid $UO_2$ as the phase with the most negative relative Gibbs energy and arbitrarily choosing solid $UO_3$ to pair it with, the equivalent Gibbs energies of pure uranium and pure oxygen are computed and followed by the element potentials $\Gamma_{\mathrm{U}}$ and $\Gamma_{\mathrm{O}}$ (represented by the dashed red line). The levelling procedure is then applied and the relative Gibbs energies of the terms are calculated.

At the start of iteration 1, the relative Gibbs energy of solid $U_3O_8$ is negative with respect to the combination of solid $UO_2$ and solid $UO_3$, indicating it must be introduced in the assemblage. The internal linear solver then determines the phase that must be replaced and the iterative

process continues with the updated phase assemblage.

At the end of the levelling procedure, the assemblage has the lowest Gibbs energy with all other phases being positive with respect to the assemblage. The Gibbs energy of the pure stoichiometric system is thereby minimised. For the example presented in Figure 6.4, the levelling solver converges in only 3 iterations. According to Eriksson and Thompson [46], the computational expense using levelling can be up to two to five times lower than the general equilibrium calculations.

Mathematically, the levelling process always respects the Gibbs phase rule, mass balance and the Gibbs' criterion and the number of iterations required to achieve convergence is typically close to the number of system components. This results in significant computational advantage when considering exceeding large number of possible phase combinations as the number of components in the system grow making levelling an excellent choice as an initialisation routine.

### 6.3.2. Euclidean norm

The Euclidean norm method was proposed by Piro and Simunovic [47], to strategically rank the best candidate phases to accommodate a new phase change. The Gibbs phase rule requires that when the thermodynamic degree of freedom $F$ equals zero, a phase must be removed in order to introduce a new phase. Determining whether a candidate phase is feasible is the most expensive task within the global iteration cycles as it requires solution of a simultaneous equation to ensure that the Hessian matrix is non-singular [47]. If there are multiple candidate phases, this iterative process must be repeated for each candidate.

The Euclidean norm method systematically ranks the best candidates to be withdrawn from the system without having to perform an exhaustive search. The method is based on the principle that the best candidate phase to be withdrawn from the current assemblage has the most similar atomic composition to the phase that has to be added to the system. The atomic fractions in phase $\phi$ are represented by the following equation:

$$c_{\phi j} = \frac{\sum_{i=1}^{N_\phi} \nu_{ij}}{\sum_{i=1}^{N_\phi} \sum_{k=1}^{C} x_i \nu_{ik}}, \tag{6.5}$$

Denoting the atom fraction of the element $j$ in the new phase that is to be introduced into the system with $c^*_{\phi j}$, the difference between this phase and the phases currently in the assemblage is given by the Euclidean norm of each phase $\phi$

$$\|c_\phi\|_2 = \sqrt{\sum_{j=1}^{C} \left(c_{\phi j} - c^*_{\phi j}\right)^2}. \tag{6.6}$$

The phase with the lowest Euclidean norm has the most similar composition to the phase to be introduced in the assemblage. In case the resulting assemblage does not meet the criterion to be a valid assemblage, the phase with the second lowest Euclidean norm can be introduced and so on.

## 6.4. Non-linear solver

The linear solver can often provide estimates close to the final assemblage of the system and in certain circumstances, such as for systems with only stoichiometric species, it might be able to predict the equilibrium assemblage. However, almost always, further computations are required to arrive at the final assemblage especially in cases where the phases have more than one species with significant contribution to the Gibbs energy. This situation arises more often than not and a non-linear solver is required to handle the non-linearities arising from the logarithmic term in the compositional component of the chemical potentials.

For the sake of completeness of the argument, the conditions for equilibrium are restated below:

1. The mass balance constraint must be satisfied.
2. The Gibbs' phase rule must be satisfied.
3. The integral Gibbs energy must be at a global minimum.

The following subsidiary conditions arise from the constraints

A. The number of moles of any species must be positive.
B. The sum of mole fractions must be one (inherent in the Gibbs energy method).

### 6.4.1. Numerical implementation

The system of non-linear equations can be solved using the Newton-Raphson method. The Newton-Raphson method depends on solving equation (5.36) and is an $O(N^3)$ operation where $N$ is the size of the system. An integral component of the solver is an appropriate line-search algorithm to determine how far the system should progress along the direction vectors. The functional norm of the Lagrangian is an effective choice to ensure convergence and is defined

as [177]:

$$\begin{aligned}\|f\|^2 = &\sum_{j=1}^{C}\left(\sum_{\lambda=1}^{\Lambda} n_\lambda \sum_{i=1}^{N_\lambda} x_{i(\lambda)}\nu_{ij} + \sum_{\omega=1}^{\Omega} n_\omega \nu_{\omega,j} - b_j\right)^2 \\ &+ \sum_{\lambda=1}^{\Lambda}\left(\sum_{i=1}^{N_\lambda} x_{i(\lambda)}\left|\mu_{i(\lambda)} - \sum_{j=1}^{C}\nu_{ij}\Gamma_j\right|\right)^2 + \sum_{\omega=1}^{\Omega}\left(g_\omega - \sum_{j=1}^{C}\nu_{\omega,j}\Gamma_j\right)^2,\end{aligned} \tag{6.7}$$

where the first term on the right represents the mass balance residuals, the second represents the absolute sum of chemical potential residuals of solution species and the third represents the chemical potential residuals of stoichiometric phases. By enforcing the Wolfe/Armijo condition [45], a sufficient step length is decided.

Each iteration step in the minimisation problem involves approximately solving the subproblem:

$$\min_{\alpha} f\left(\mathbf{x}^m + \alpha \mathbf{p}^m\right), \tag{6.8}$$

where $\mathbf{x}^m$ is the best estimate at iteration $m$, $\mathbf{p}^m$ denotes the search direction vector and $\alpha$ represents the step size.

The Wolfe conditions are a set of inequalities for performing inexact line search and provide an efficient way of computing an acceptable step length $\alpha$ that reduces the objective function sufficiently, rather than minimising the objective function over $\alpha \in \mathbb{R}^+$ exactly.

A step length $\alpha^m$ is said to satisfy the Wolfe conditions, restricted to the direction $\mathbf{p}^m$, if the following two inequalities hold:

$$f\left(\mathbf{x}^m + \alpha^m \mathbf{p}^m\right) \leq f\left(\mathbf{x}^m\right) + c_1 \alpha^m \left(\mathbf{p}^m\right)^T \nabla f\left(\mathbf{x}^m\right), \tag{6.9}$$

$$-\left(\mathbf{p}^m\right)^T \nabla f\left(\mathbf{x}^m + \alpha^m \mathbf{p}^m\right) \leq -c_2 \left(\mathbf{p}^m\right)^T \nabla f\left(\mathbf{x}^m\right), \tag{6.10}$$

with $0 < c_1 < c_2 < 1$. The first inequality, known as the Armijo condition ensures that the step length $\alpha^m$ decreases $f$ sufficiently, and the second inequality known as the curvature condition ensures that the slope has been reduced sufficiently. Together, the two inequalities provide upper and lower bounds for the step lengths [45].

Yellowjacket–GEM uses the state-of-the-art non-linear solvers in PETSc to solve the non-linear system. The `SNESNEWTONLS` is a Newton based nonlinear solver that uses line search and has been used as the default solver in this work.

### 6.4.2. Adding/Removing phases

Updating the estimated phase assemblage plays a significant role in the convergence of thermodynamic solvers. Inadequate strategies for updating the assemblage might lead to inefficient global iterations (i.e., iterations in which changes are made to the system such as addition/removal of phases while the Newton iterations described above can be referred to as local iteration since they are aimed at finding the minimum of a problem with a fixed system) and might even prevent convergence. Though the number of phases that can be added into or removed from the system is constrained by the Gibbs' phase rule, proper care must be taken to ensure that any change to the system drives it towards convergence and not hold it back. To ensure that the phase assemblage updating does not result in undesired behaviour, the strategy proposed by Piro [177] has been adopted. This strategy has been illustrated in Figure 6.5.

In conjunction with the global optimisation algorithms used to detect the presence of miscibility gaps (discussed in Section 6.5), the phase handling strategy can also be used for managing miscibility gaps. Once the existence of miscibility gaps has been identified, each minimum of Gibbs energy can be treated as a separate "phase" and the same rules as other phases apply in terms of adding these phases into the assemblage.

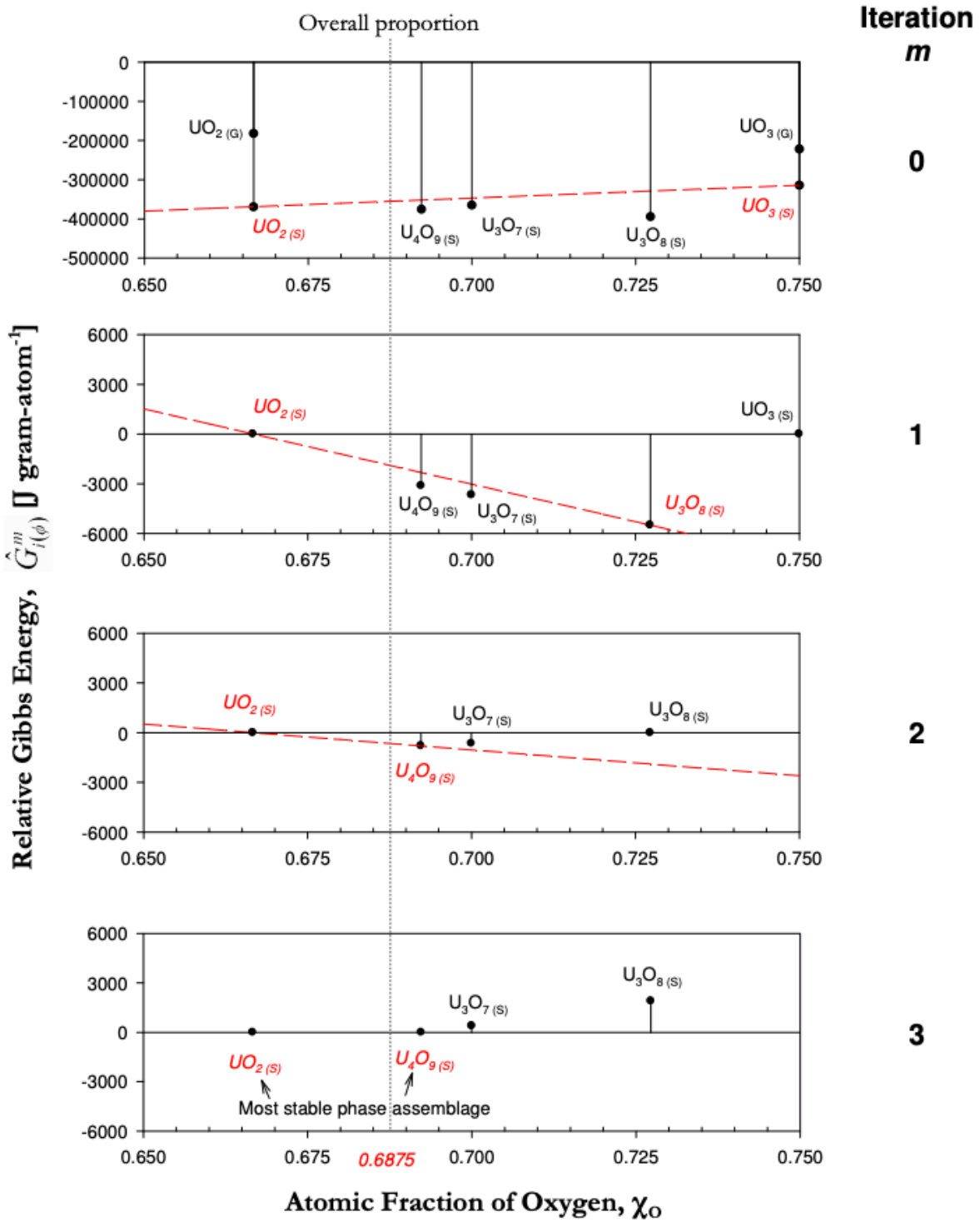


Figure 6.4: Illustration of the levelling process for a binary system of U−O at each iteration (1 mol U, 2.2 mol O, 298.15 K, 1 atm). From Piro et al. [49].

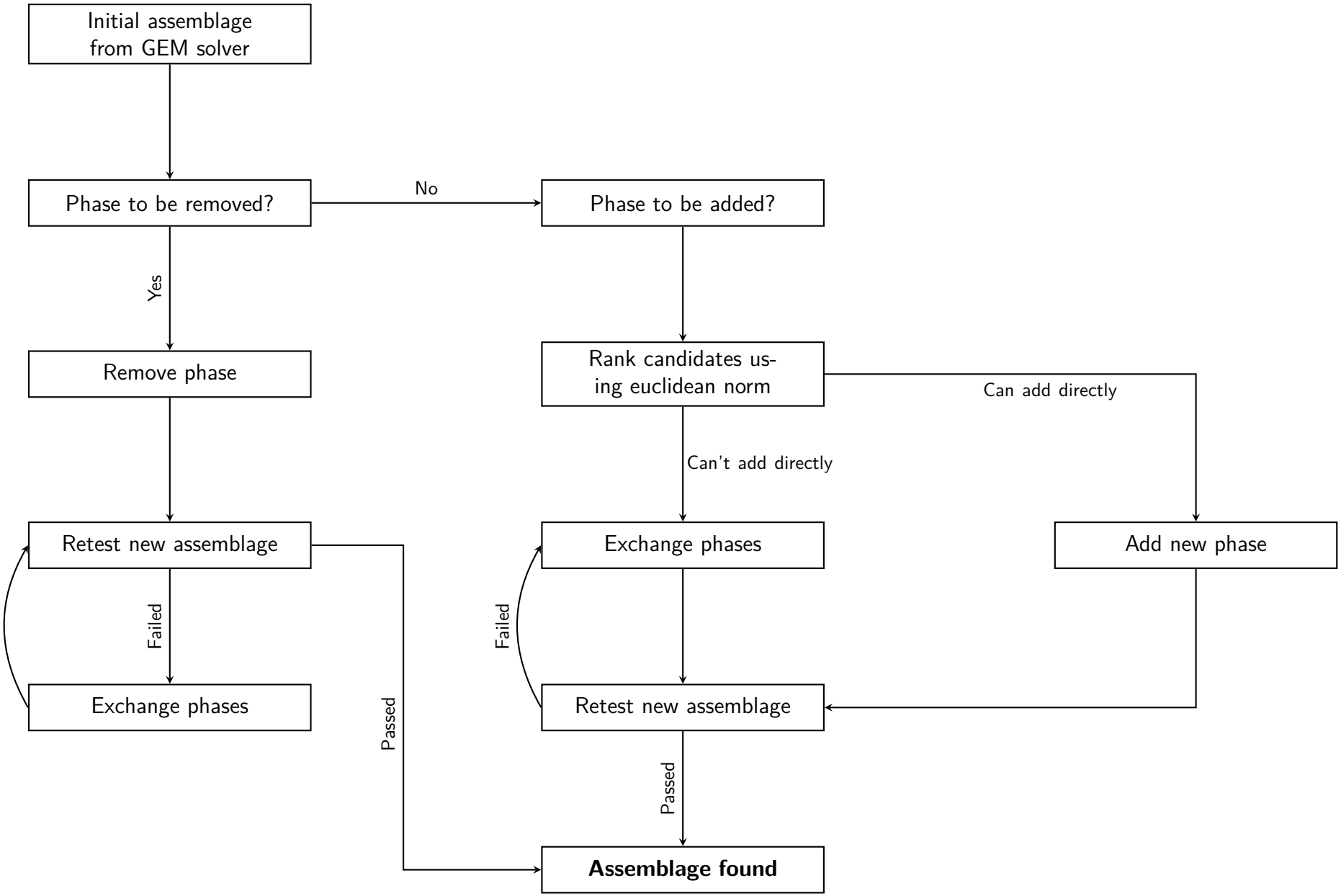


Figure 6.5: Illustration of the methodology for updating the phase assemblage. Adapted from Piro [177].

### 6.4.3. Convergence criterion

The convergence of the solver is tested in accordance with conditions for convergence described in Chapter 5. The relative error of the mass balance and Gibbs' criterion is calculated and the solver converges when both of these are within the specified tolerance. In addition, it must be tested that the mole numbers are not negative for any species in the system. The charge neutrality constraint must also be respected. To minimise the computational cost, it is also possible to test convergence only when the functional norm has been satisfied to a specified tolerance.

Two issues that can prevent convergence were foreseen for a thermodynamic equilibrium solver. First, when the objective function has multiple roots, for example due to miscibility gap, and second when the slope of the objective function is extremely small or zero. These two issues can result in non-real numbers or divergence and possible failure of the iterative solver. The numerical dampening through Wolfe/Armijo conditions and the use of levelling as an initialisation method helps in avoiding the ill-behaviour and promotes numerical stability and enhances performance characteristics. The proposed algorithm of the thermodynamic solver with both local and global iterations has been presented in Figure 6.6.

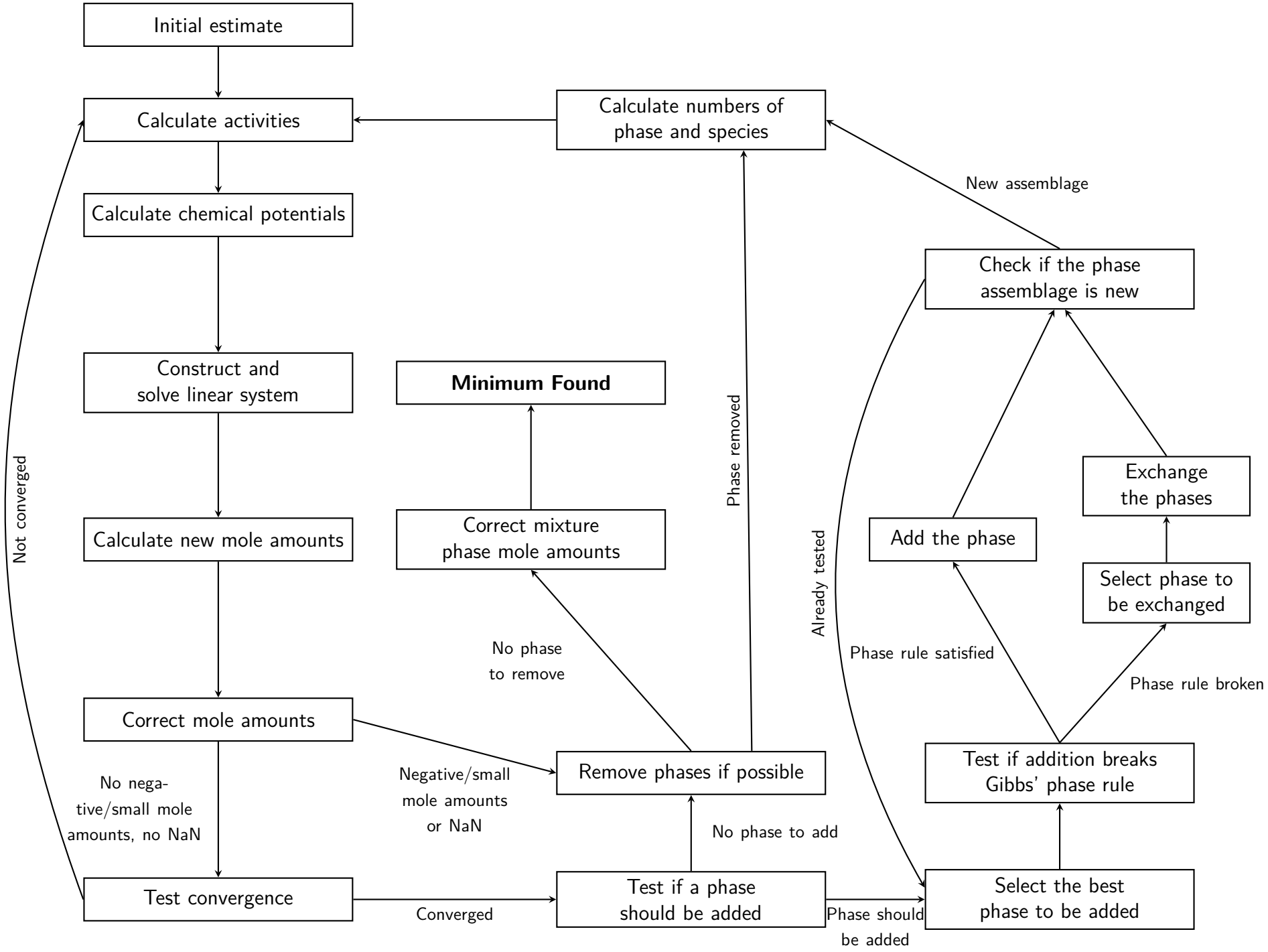


Figure 6.6: Illustration of the Gibbs energy minimisation algorithm. After Loukusa [91].

### 6.4.4. Interpreting the results

Though the developed algorithms are relatively very robust, there are certain classes of problems where the rank-deficiency in the stoichiometric matrices is inherent. In such cases, special care must be taken in interpreting the results computed by thermodynamic equilibrium codes. The author of this thesis co-authored a letter to the editor of Journal of Nuclear Materials explaining how one must be careful in interpreting the chemical potentials for molten salts systems. The letter by Piro et al. [167] illustrates the case of a rank-deficient stoichiometric matrix in a model represented by MQMQA and shows how the chemical potential results can be misinterpreted. The author of this thesis contributed to the discussion presented in the work and co-authored the manuscript. The article follows on the next pages.

Journal of Nuclear Materials 526 (2019) 151756

Contents lists available at ScienceDirect

Journal of Nuclear Materials

journal homepage: www.elsevier.com/locate/jnucmat

# On the interpretation of chemical potentials computed from equilibrium thermodynamic codes: Applications to molten salts

*Keywords:*
Molten salt
MSR
Modified quasi-chemical model
Thermodynamic

In an earlier Letter to the Editor of the Journal of Nuclear Materials (JNM) [1], situations were explored whereby the chemical potentials computed by an equilibrium thermodynamics code could potentially be misleading. The intent of that letter was to acknowledge specific situations that may unintentionally lead to the misinterpretation of results that may be well understood by a specialist, but may perhaps be less obvious to a non-specialist. A closely related situation may also arise from the results produced by thermodynamic calculations involving the Modified Quasi-chemical Model (MQM), which is a sophisticated model often used to represent molten salts. With the increasing interest in Molten Salt Reactor (MSR) research [2], particularly with thermodynamic modelling and related multi-physics simulations, it seems prudent to have a follow-up discussion regarding the interpretation of chemical potentials computed by equilibrium thermodynamic codes in the context of molten salts. This Letter to the Editor of JNM is intended to better inform the user of such thermodynamic software using models specific to molten salts who may be a non-specialist. Furthermore, these matters may be of important interest when integrating thermodynamic calculations in multi-physics codes to prevent numerical instabilities.

In one particular scenario explored by Piro et al. [1], the fictive A-B system was considered with 2 mol of A and 3 mol of B. For this specific situation, only the $A_2B_3$ phase is stable at equilibrium. As shown in Fig. 1, the system is homogeneous and the lowest common tangent line (representing the equilibrium state, also called the "Gibbs Plane" [3]) is tangent to this phase; however, the line is not uniquely defined. This is shown graphically in Fig. 1, whereby a line cannot be uniquely defined by a single point. The tangent line could conceivably be drawn between $A_2B_3$ and either $B_{(s)}$ or $\alpha$ (with zero moles); however, there is no basis for selecting zero moles of one phase or the other.

For this particular scenario, the system is under-determined when the system components[1] are taken as A and B. One may be under the false impression that the chemical potentials of A and B have been determined, whereas these are in fact undefined due to the misidentification of the system components – for this particular situation, the system components A and B should be re-defined to a single system component: $A_2B_3$. As the International Union of Pure and Applied Chemistry defines the term 'component': "The number of components in a given system is the minimum number of independent species necessary to define the composition in all the phases of a system" [4]. Since the minimum number of species required to define this system is one (i.e., $A_2B_3$), the system components should be re-defined from A and B to $A_2B_3$ for this particular scenario.

Due to the mathematical nature of the MQM model, one can easily misinterpret calculated chemical potentials of some components for similar reasons. The MQM class of models, which has been advanced primarily by Pelton et al. [5–8], has been used with great success to model various fluoride [9–12] and chloride salts [9,13] for nuclear applications. This model is currently implemented in FACTSAGE [14] and THERMOCHIMICA [15]. The fundamental premise of this model is to shift focus from the interaction of species to the interaction of pairs of species (or quadruplets) in an effort to capture short range ordering. For example, if one has a solution model comprised of species C and D, then one would be concerned with interactions of C–C, D-D, and C-D pairs. Equilibrium calculations are centred on the chemical potentials of the pairs (or quadruplets) rather than the species.[2] Furthermore, the model involves two sublattices, which do not include vacancies; therefore, every phase component (or 'compound end member') is necessarily a compound and not a pure element. The importance of this feature of the model is that the representation of the phase in composition space is limited by the compounds – not the elements – and will be further explained in the following paragraphs.

One can model a familiar material of interest to the MSR community, LiF–$BeF_2$ (aka. "FLiBe"), with MQM. The model produced by Beneš and Konings [16] assigns the species as LiF and $BeF_2$, which produces the following pairs: LiF–LiF, $BeF_2$–$BeF_2$, and LiF–$BeF_2$. A thermodynamic database of the Li–Be–F system may include other phases in addition to this molten salt, such as various stoichiometric solid phases and an ideal gas mixture. Some of these non-salt species may not necessarily correspond to LiF or $BeF_2$,

[1] The terms 'phase component' and 'system component' are used here to differentiate a component of a phase (synonymous with 'species' or 'compound end member') from a component of a system, which may be a pure element, a compound, or electron (corresponding to an ionic phase).

[2] Note that internal to a Gibbs energy minimizer, the number of moles of the pairs are used as independent variables rather than those of the species. This is an important point to enable effective execution of equilibrium calculations, as explained by Pelton et al. [5].

https://doi.org/10.1016/j.jnucmat.2019.151756

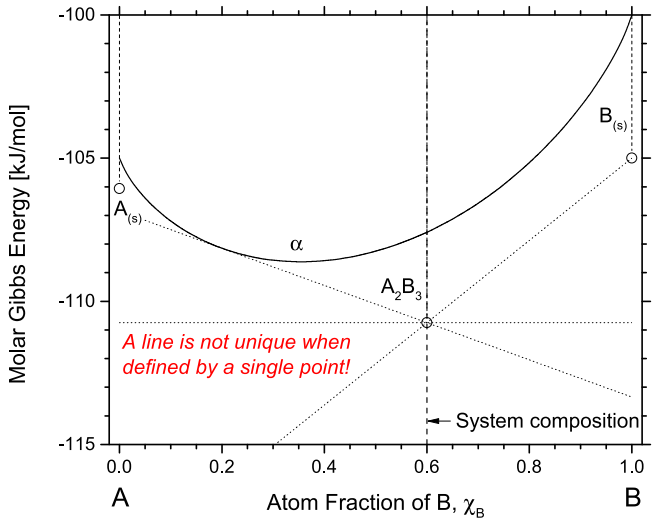


**Fig. 1.** The fictive A-B system is shown with the overall composition identified, which intersects the $A_2B_3$ phase. The lowest common tangent line intersects this phase, but is not uniquely defined. Copied from Piro et al. [1].

which may include the pure elements (e.g., $F_{2(g)}$).

Suppose one were to define the system components by the chemical elements (i.e., Li, Be, and F) while assigning mass quantities to the system that precisely correspond to LiF and $BeF_2$, and a specified temperature and pressure that together yield a homogeneous system with only a molten salt being stable. This would be a typical calculation using an equilibrium solver. The composition space of this system is illustrated in Fig. 2. In this situation, there are three phase components (i.e., LiF—LiF, $BeF_2$—$BeF_2$, and LiF—$BeF_2$) and three system components (i.e., Li, Be, and F); however, one cannot uniquely define the Gibbs Plane because the three points are co-linear in three dimensional space. In more mathematical terms, the Hessian matrix is rank deficient.

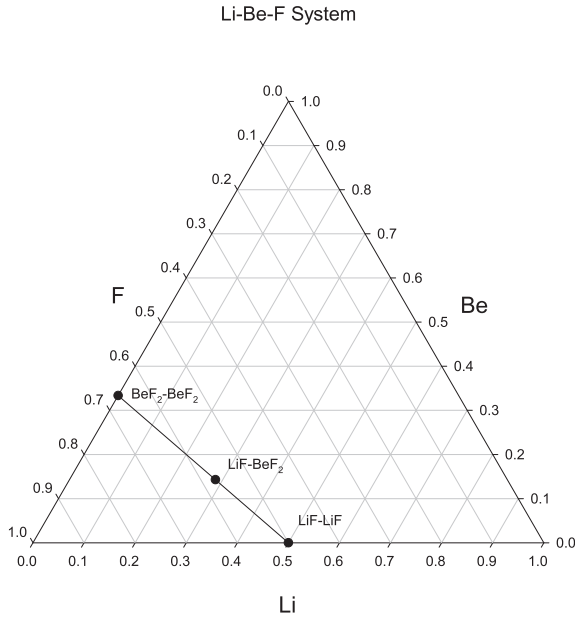


**Fig. 2.** A ternary plot of the Li—Be—F system with the three pair fractions corresponding to LiF—$BeF_2$ are indicated. A three dimensional Gibbs plane cannot be defined by three points because they are colinear.

Since the Gibbs Plane is used to define all chemical potentials in the system and it is not uniquely defined for this scenario, not all chemical potentials in the system are uniquely defined. The only uniquely defined chemical potentials in this system lie on the LiF—$BeF_2$ line and anything outside from that is not unique. Of particular interest to the MSR community, the fluorine potential — and the corresponding thermochemical activity of fluorine — is not uniquely defined for this situation. This scenario is analogous to the one shown in Fig. 1, whereby one could potentially compute a fluorine potential, but it would not be uniquely defined. The issue here is that the user may receive from the software a numerical value of the chemical potential or thermochemical activity of fluorine that is meaningless and misleading. A more mathematically rigorous proof is provided in the Appendix, which shows that the Hessian matrix used in Gibbs energy minimization is underdetermined for this situation. It may be possible to still computationally solve the Hessian, but that would only be possible due to very minor machine imprecisions.

Note that one would have a uniquely defined system for this situation if the system components were instead defined as LiF and $BeF_2$. Alternatively, one could also have a uniquely defined system if there was a slight surplus or deficit of one of the chemical elements, which would effectively shift the system off the line shown in Fig. 2. In that situation, conservation of mass would require another phase to be stable in addition to the salt. Graphically, one could interpret that situation as a three-dimensional Gibbs plane defined by three points that are co-linear (corresponding to the salt, akin to Fig. 2) in addition to some additional point(s) (representing a secondary phase).

To summarize, the MQM model has been effectively used to capture the thermodynamic behaviour of various salts for MSR applications. To avoid potentially misinterpreting calculated chemical potentials and other thermodynamic quantities, which may be non-unique, recommendations are made to the user to be conscientious of the appropriateness of selecting the system components. If the overall system composition can be defined by a reduced set of compounds that do not correspond directly to the chemical elements, then the user should define them as such. While these matters may be familiar and clear to a thermodynamics specialist, the intent of this letter is to assist non-specialists in interpreting and executing such calculations, particularly those involved with MSR research.

## Acknowledgements

This research was undertaken, in part, thanks to funding from the Canada Research Chairs (950—231328) program of the Natural Sciences and Engineering Research Council of Canada.

## Appendix

Mathematically, Gibbs energy minimization is a constrained non-convex optimization problem with the objective of determining a unique combination of system potentials that yields a minimum in Gibbs energy of the system while satisfying mass balance constraints and the Gibbs phase rule under isothermal isobaric conditions. The objective is often achieved using the method of Lagrange multipliers that simultaneously minimizes the integral Gibbs energy and the residuals of mass balance equations. This results in a system of linearized equations that can be written in matrix form as [17]:

$$\mathbf{H} \cdot \boldsymbol{\pi} = \boldsymbol{\zeta} \tag{1}$$

where $\boldsymbol{\pi}$ and $\boldsymbol{\zeta}$ denote the unknown and constraint vectors respectively, and the Hessian matrix ($\mathbf{H}$) can be written as [17,18]:

$$\mathbf{H} = \begin{bmatrix} r_{j=1,k=1} & \cdots & r_{j=1,k=C} & \phi_{j=1,\lambda=1} & \cdots & \phi_{j=1,\lambda=\Lambda} & \nu_{j=1,\omega=1} & \cdots & \nu_{j=1,\omega=\Omega} \\ \vdots & \ddots & \vdots & \vdots & \ddots & \vdots & \vdots & \ddots & \vdots \\ r_{j=C,k=1} & \cdots & r_{j=C,k=C} & \phi_{j=C,\lambda=1} & \cdots & \phi_{j=C,\lambda=\Lambda} & \nu_{j=C,\omega=1} & \cdots & \nu_{j=C,\omega=\Omega} \\ \phi_{\lambda=1,j=1} & \cdots & \phi_{\lambda=1,j=C} & 0 & \cdots & 0 & 0 & \cdots & 0 \\ \vdots & \ddots & \vdots & \vdots & \ddots & \vdots & \vdots & \ddots & \vdots \\ \phi_{\lambda=\Lambda,j=1} & \cdots & \phi_{\lambda=\Lambda,j=C} & 0 & \cdots & 0 & 0 & \cdots & 0 \\ \nu_{\omega=1,j=1} & \cdots & \nu_{\omega=1,j=C} & 0 & \cdots & 0 & 0 & \cdots & 0 \\ \vdots & \ddots & \vdots & \vdots & \ddots & \vdots & \vdots & \ddots & \vdots \\ \nu_{\omega=\Omega,j=1} & \cdots & \nu_{\omega=\Omega,j=C} & 0 & \cdots & 0 & 0 & \cdots & 0 \end{bmatrix} \tag{2}$$

where $C$ is the number of system components, $\lambda$ is an index of a solution phase, of which there are $\Lambda$ in the system, $\omega$ is an index of a stoichiometric phase, of which there are $\Omega$ in the system, $\nu_{i,j}$ is the stoichiometric coefficient of component $j$ in species $i$, and $r_{j,k}$ and $\phi_{j,\lambda}$ can be expressed as follows:

$$r_{j,k} = \sum_{\lambda=1}^{\Lambda} \sum_{i=1}^{N_\lambda} n_{i(\lambda)} \nu_{i,j} \nu_{i,k}, \tag{3}$$

$$\phi_{j,\lambda} = \sum_{i=1}^{N_\lambda} n_{i(\lambda)} \nu_{i,j}. \tag{4}$$

$N_\lambda$ is the number of species in phase $\lambda$, and $n_{i(\lambda)}$ is the number of moles of species $i$ in solution phase $\lambda$. Clearly, $r_{j,k} = r_{k,j}$ and $\phi_{j,\lambda} = \phi_{\lambda,j}$, which yields a symmetric matrix for $\mathbf{H}$.

The example of the FLiBe system discussed above is used to illustrate the under-determined nature of the Hessian matrix with improperly chosen system components. Consider a homogeneous system in which the only phase present is a solution phase represented by the MQM model. Suppose the system composition falls somewhere along the $BeF_2 - LiF$ composition line illustrated in Fig. 2, and thus the phase components are LiF–LiF, $BeF_2$–$BeF_2$, and LiF–$BeF_2$, and the system components are Li, Be, and F. For this case $C = 3$, $\Lambda = 1$, $N_1 = 3$, and $\Omega = 0$. This results in a $4 \times 4$ Hessian matrix as follows:

$$\mathbf{H} = \begin{bmatrix} r_{1,1} & r_{1,2} & r_{1,3} & \phi_{1,1} \\ r_{1,2} & r_{2,2} & r_{2,3} & \phi_{2,1} \\ r_{1,3} & r_{2,3} & r_{3,3} & \phi_{3,1} \\ \phi_{1,1} & \phi_{2,1} & \phi_{3,1} & 0 \end{bmatrix}. \tag{5}$$

The stoichiometry matrix $\boldsymbol{\nu}$ is:

$$\boldsymbol{\nu} = \begin{bmatrix} 2 & 0 & 2 \\ 0 & 2 & 4 \\ 1 & 1 & 3 \end{bmatrix}. \tag{6}$$

where the rows represent LiF–LiF, $BeF_2$–$BeF_2$, and LiF–$BeF_2$, and the columns represent Li, Be, and F. Taking the current estimate of the number of moles of each species to be the arbitrary values $n_1$, $n_2$, and $n_3$, $\mathbf{H}$ is then:

$$\mathbf{H} = \begin{bmatrix} 4n_1 + n_3 & n_3 & 4n_1 + 3n_3 & 2n_1 + n_3 \\ n_3 & 4n_2 + n_3 & 8n_2 + 3n_3 & 2n_2 + n_3 \\ 4n_1 + 3n_3 & 8n_2 + 3n_3 & 4n_1 + 16n_2 + 9n_3 & 2n_1 + 4n_2 + 3n_3 \\ 2n_1 + n_3 & 2n_2 + n_3 & 2n_1 + 4n_2 + 3n_3 & 0 \end{bmatrix}. \tag{7}$$

This Hessian is rank-deficient, with the first three columns linearly dependent, and thus has a determinant of 0. Therefore, any attempt to solve the corresponding system of linear equations will fail. Note that in practice it is possible that the system of equations can be solved with a sufficient numerical error associated with machine precision, which will yield some mathematically meaningless results. In this case, one must rely heavily on the quality and robustness of the linear equation solver employed.

If one were to instead take the system components as LiF and $BeF_2$, $C$ is reduced to 2, and the Hessian is of the $3 \times 3$ form:

$$\mathbf{H} = \begin{bmatrix} r_{1,1} & r_{1,2} & \phi_{1,1} \\ r_{1,2} & r_{2,2} & \phi_{2,1} \\ \phi_{1,1} & \phi_{2,1} & 0 \end{bmatrix}. \tag{8}$$

In this case, the stoichiometry matrix is:

$$\boldsymbol{\nu} = \begin{bmatrix} 2 & 0 \\ 0 & 2 \\ 1 & 1 \end{bmatrix}. \tag{9}$$

where the rows represent LiF–LiF, $BeF_2$–$BeF_2$, and LiF–$BeF_2$, and the columns LiF and $BeF_2$. The Hessian is then:

$$\mathbf{H} = \begin{bmatrix} 4n_1 + n_3 & n_3 & 2n_1 + n_3 \\ n_3 & 4n_2 + n_3 & 2n_2 + n_3 \\ 2n_1 + n_3 & 2n_2 + n_3 & 0 \end{bmatrix}. \tag{10}$$

This matrix is non-singular, and its determinant is:

$$\mathrm{Det}(\mathbf{H}) = -4(n_1 + n_2 + n_3)(4n_1 n_2 + n_1 n_3 + n_2 n_3). \tag{11}$$

This determinant is always non-zero, as the values $n_1$, $n_2$, and $n_3$ must all be greater than zero and real. This example illustrates how an under-determined system of equations representing a phase represented in MQM form can be converted to a full-rank system by reducing the number of system components to a more appropriate form.

## References


[1] M. Piro, M. Welland, M. Stan, On the interpretation of chemical potentials computed from equilibrium thermodynamic codes, J. Nucl. Mater. 464 (2015) 48–52.

[2] J. McMurray, T. Besmann, J. Ard, B. Fitzpatrick, M. Piro, J. Jerden, M. Williamson, B. Collins, B. Betzler, A. Qualls, Multi-physics simulations for molten salt reactor evaluation: Chemistry modeling and database development, in: Tech. Rep. ORNL/SPR-2018/864, Oak Ridge National Laboratory, Oak Ridge, TN, 2018.

[3] M. Piro, T. Besmann, S. Simunovic, B. Lewis, W. Thompson, Numerical verification of equilibrium thermodynamic computations in nuclear fuel performance codes, J. Nucl. Mater. 414 (3) (2011) 399–407.

[4] Compendium of Chemical Terminology, Gold Book. No. Version 2.3.3, International Union of Pure and Applied Chemistry, 2014.

[5] A. Pelton, S. Degterov, G. Eriksson, C. Robelin, Y. Dessureault, The modified

quasichemical model I — binary solutions, Metall. Mater. Trans. B 31B (2000) 651–659.
[6] A. Pelton, P. Chartrand, The modified quasichemical model II — multicomponent solutions, Metall. Mater. Trans. A 32A (2001) 1355–1360.
[7] P. Chartrand, A. Pelton, The modified quasichemical model III — two sublattices, Metall. Mater. Trans. A 32 (6) (2001) 1397–1407.
[8] A. Pelton, P. Chartrand, G. Eriksson, The modified quasichemical model IV — two-sublattice quadruplet approximation, Metall. Mater. Trans. A 32A (2001) 1409–1416.
[9] O. Beneš, Thermodynamics of Molten Salts for Nuclear Applications, PhD thesis, Institute of Chemical Technology, Prague, Czech Republic, 2008.
[10] O. Beneš, M. Beilmann, R. Konings, Thermodynamic assessment of the LiF-NaF-$ThF_4$-$UF_4$ system, J. Nucl. Mater. 405 (2010) 186–198.
[11] E. Capelli, O. Beneš, R. Konings, Thermodynamics of soluble fission products cesium and iodine in the molten salt reactor, J. Nucl. Mater. 501 (2018) 238–252.
[12] O. Beneš, P. Soucek, 7: molten salt reactor fuels, in: M. Piro (Ed.), Advances in Nuclear Fuel Chemistry, Elsevier, 2019.
[13] K. Johnson, M. Kahn, J. Leary, Phase equilibria in fused salt systems: binary systems of plutonium(III) chloride with the chlorides of magnesium, calcium, strontium, and barium, J. Phys. Chem. 65 (1961) 1461–1462.
[14] C. Bale, P. Chartrand, S. Degterov, G. Eriksson, K. Hack, R. Mahfoud, J. Melançon, A. Pelton, S. Peterson, FactSage thermochemical software and databases, Calphad 26 (2) (2002).
[15] M. Piro, S. Simunovic, T. Besmann, B. Lewis, W. Thompson, The thermochemistry library thermochimica, Comput. Mater. Sci. 67 (2013) 266–272.
[16] O. Beneš, R. Konings, 3.13 - molten salt reactor fuel and coolant, in: R.J. Konings (Ed.), Comprehensive Nuclear Materials, Elsevier, Oxford, 2012, pp. 359–389.
[17] M. Piro, Computation of Thermodynamic Equilibria Pertinent to Nuclear Materials in Multi-Physics Codes, PhD thesis, Royal Military College of Canada, 2011.
[18] W. White, S. Johnson, G. Dantzig, Chemical equilibrium in complex mixtures, J. Chem. Phys. 28 (5) (1958) 751–755.

M.H.A. Piro*, M. Poschmann
*Faculty of Energy Systems and Nuclear Sciences, Ontario Tech University, Oshawa, ON, Canada*

P. Bajpai
*Faculty of Science, Ontario Tech University, Oshawa, ON, Canada*

* Corresponding author.
*E-mail address:* markus.piro@ontariotechu.ca (M.H.A. Piro).

8 August 2019
Available online 20 August 2019

## 6.5. Global Optimisation

As described in Section 5.4, computing the minimum driving force of a thermodynamic system requires solving a non-convex constrained optimisation problem. The conditions for thermodynamic equilibrium discussed in Section 5.2 require that the chemical potentials of all the species must lie on or above the Gibbs plane, which passes through the element potentials $\Gamma_j$. Thus metastable phases must lie above the Gibbs plane and the difference between the Gibbs plane and the plane tangent to a metastable phase is referred to as the *driving force* [7] or *tangent plane distance function* [7, 109]. The driving force for phase $\phi$ is represented by $\Delta G_\phi$ and is computed as [110]:

$$\Delta G_\phi = \min_{\lambda} \sum_{i=1}^{N_\lambda} x_i \left( \mu_i - \sum_{j=1}^{C} \nu_{ij} \Gamma_j \right), \tag{6.11}$$

which is subject to conservation of mass and the following linear equality and inequality constraints:

$$\sum_{i=1}^{N_\phi} x_i = 1, \; x_i > 0, \; \forall i \in \phi. \tag{6.12}$$

The sufficient condition for equilibrium requires that the driving force $\Delta G_\phi$ computed with equation (6.11) is positive for all phases believed to be metastable and zero for all the stable phases. According to Hillert [178], the driving force of metastable phases can be evaluated at each iteration to determine whether or not it should be added into the system. However, this function can be non-convex and requires the evaluation of a global minimum. Though the open literature on computing these methods appears rather exhaustive, few authors have discussed generalised global minimisation schemes for the phase equilibria problem. The majority of articles focus either on relatively small systems, such as liquid-vapour equilibria, or are aimed at only a handful of calculations. Some notable exceptions to this include those of Hillert [178], Lukas et al.[179], Sundman [120], Piro and Simunovic [110], and Otis et al. [121]. Even amongst these, only Piro and Simunovic [110] systematically explore optimisation algorithms and the others only look at sampling strategies. Since both robustness and computational efficiency of Yellowjacket–GEM are of concern, a number of global optimisation methods were tested through a set of carefully constructed test problems representative of some common scenarios in equilibrium thermodynamics. Though no global optimisation method can guarantee the ability to find the true global minimum, sufficient confidence can be achieved for the problem under consideration under well-defined parameters.

### 6.5.1. Test Problems

To objectively test the reliability and performance of various global optimisation algorithms, the methods must be benchmarked against a set of test problems representative of the requirements from the solver. While most of the open literature focusses on a single problem and tries to optimise the algorithm for the problem, such an approach is not ideal for the development of Yellowjacket–GEM. Instead the focus here has been to select an algorithm that can work reasonably well for wide variety of problems with a large number of components. The reasoning behind such an approach is that a wide variety of excess mixing models are encountered in computational thermodynamics applied to nuclear materials. To test the algorithms under consideration, eight test cases representing different thermodynamic models and system sizes, and are summarised in Table 6.1.

Table 6.1: Summary of test cases used for comparing global optimisation algorithms.

| **Label** | $C$ | **Problem Description** |
|---|---|---|
| A | 2 | Fictive binary system with a miscibility gap and a stoichiometric phase from Piro and Simunovic [110]. |
| B | 2 | Pd−Rh binary system with a shallow Face Centered Cubic (FCC) miscibility gap phase from Kaye et al. [180]. |
| C | 2 | Fictive binary system with three convex phases with one phase having a negative driving force from Piro and Simunovic [110]. |
| D | 3 | Pu−U−O ternary system from Guéneau et al. [181] containing an ideal gas phase, a non-ideal liquid phase, many stoichiometric phases and a $(U_y Pu_{1-y})O_{2\pm x}$ fluorite phase. Involves a multi-sublattice model and a charge balance constraint. |
| E | 3 | Al−Cr−Co ternary system used as reference problem by Otis et al. [121]. |
| F | 5 | Hexagonal Close Packed (HCP) phase in the quinary system containing noble metal fission products Mo−Pd−Tc−Ru−Rh from Kaye et al. [180]. |
| G | 10 | Fictive high-dimensional systems with minefield of miscibility gaps based on |
| H | 30 | Piro and Simunovic [110]. |

1. *Problem A*

   A fictive binary A−B system based on Piro and Simunovic [110] has been considered as the first test problem. As shown previously in Section 5.4, it consists of solution phase $\alpha$ and a stoichiometric phase $A_3B_2$ which can possibly coexist and while the stoichiometric phase $A_3B_2$ and solution phase $\alpha$ are initially predicted to be stable, as represented by the dashed tangent line in Figure 6.7, they are in fact metastable and a miscibility gap would yield a lower value of the integral Gibbs energy of the system, $G_{\text{sys}}$. The $\alpha$ phase

is represented by a substitutional solution model with the reference Gibbs energies of the components being $g^{\circ}_{\mathrm{A}} = -100$ J mol$^{-1}$, $g^{\circ}_{\mathrm{B}} = -300$ J mol$^{-1}$ and the excess energy given by $g^{\mathrm{ex}}_{\alpha} = 21000 x_{\mathrm{A}} x_{\mathrm{B}} + 7000 x_{\mathrm{A}} x_{\mathrm{B}}^2$. The temperature of the system was fixed at $T = 1000$ K and the pressure at $P = 1$ atm.

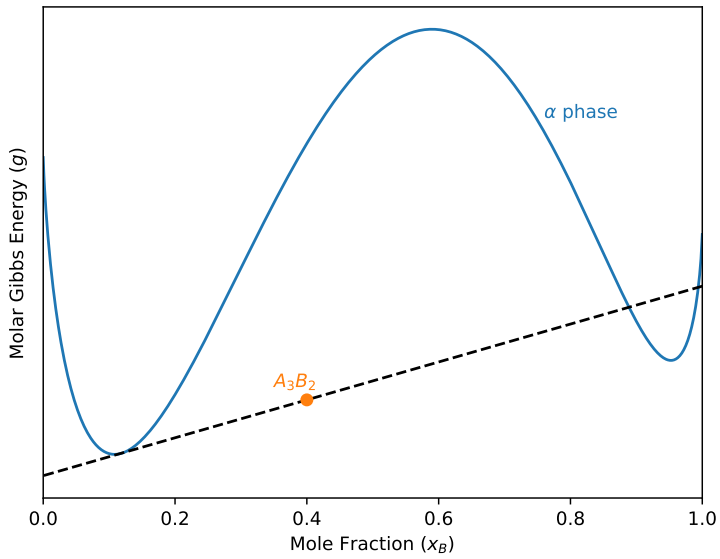


Figure 6.7: Fictive system with miscibility gap showing a possible false positive from thermodynamic equilibrium solver.

2. *Problem B*

   The binary Pd−Rh system from Kaye et al. [180] has been selected as the second test problem. It consists of a shallow miscibility gap in the FCC phase which is assumed to be properly identified by the solver but the global optimisation algorithm must confirm that the driving force, $\Delta G_{\mathrm{FCC}}$, of the miscibility gap phase is indeed zero. The phase is represented by a substitutional solution model with the reference Gibbs energies of the components being $g^{\circ}_{\mathrm{Pd}} = -16480 + 9.02T$ J mol$^{-1}$, $g^{\circ}_{\mathrm{Rh}} = -26568 + 11.88T$ J mol$^{-1}$ and the excess energy given by $g^{\mathrm{ex}}_{\mathrm{FCC}} = x_{\mathrm{Pd}} x_{\mathrm{Rh}} \left(21247 + 2199 x_{\mathrm{Rh}} - (2.74 - 0.56 x_{\mathrm{Rh}})T\right)$. The temperature of the system was fixed at $T = 1100$ K and the pressure at $P = 1$ atm.

3. *Problem C*

   Another fictive binary system from Piro and Simunovic [110] with components C−D can have three possible solution phases, the $\delta$ phase as shown in figure 6.9. At temperature $T = 1100$ K, pressure $P = 1$ atm and composition $x_{\mathrm{D}} = 0.6$, the $\delta$ phase is believed to be metastable but one must confirm that the combination of $\beta$ and $\gamma$ is most stable

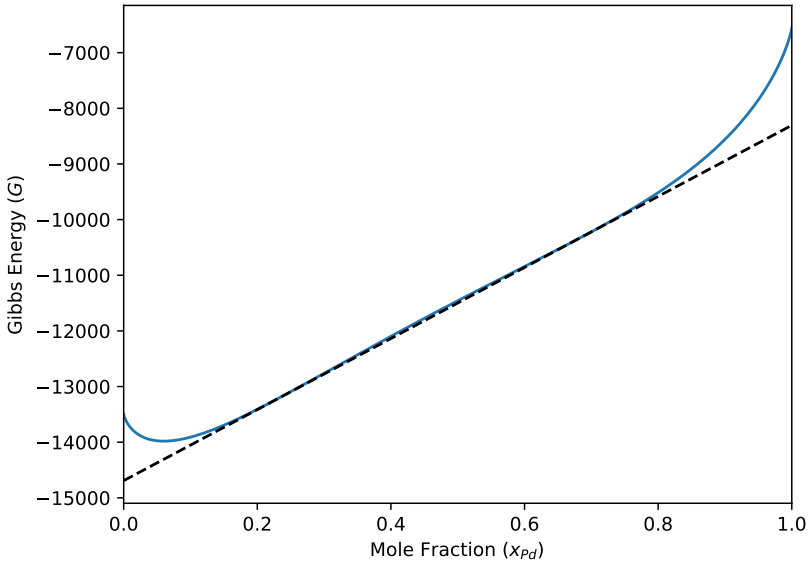


Figure 6.8: FCC phase miscibility gap in Pd−Rh binary system from Kaye et al. [180] shows a correctly identified miscibility gap which must be verified by the global optimisation algorithm.

or if a different combination is more stable. However, it can be seen that inserting the $\delta$ phase into the system and replacing one of the other two phases would yield a lower value of the integral Gibbs energy of the system, $G_{\text{sys}}$. For this system, $g^{\circ}_{\mathrm{C}(\beta)} = 0$ J mol$^{-1}$, $g^{\circ}_{\mathrm{D}(\beta)} = 12471$ J mol$^{-1}$, $g^{\circ}_{\mathrm{C}(\gamma)} = 16628$ J mol$^{-1}$, $g^{\circ}_{\mathrm{D}(\gamma)} = 4157$ J mol$^{-1}$, $g^{\circ}_{\mathrm{C}(\delta)} = 26604$ J mol$^{-1}$ and $g^{\circ}_{\mathrm{D}(\delta)} = 33256$ J mol$^{-1}$. The molar Gibbs energies of mixing are $g^{\text{ex}}_{\beta} = 41570x_{\mathrm{C}}x_{\mathrm{D}} - 58198x_{\mathrm{C}}x^2_{\mathrm{D}}$, $g^{\text{ex}}_{\gamma} = -5238x_{\mathrm{C}}x_{\mathrm{D}}$ and $g^{\text{ex}}_{\delta} = -59445x_{\mathrm{C}}x_{\mathrm{D}} - 74826x_{\mathrm{C}}x^2_{\mathrm{D}}$.

4. *Problem D*

   Mixed OXide fuel (MOX) is a nuclear fuel that is manufactured by mixing plutonium dioxide recovered from used reactor fuel with depleted uranium dioxide and the Pu−U−O ternary system from Guéneau et al. [181, 182] has been selected as a test problem. The thermodynamic assessment of the system contains an ideal gas, a non-ideal liquid, and a $(\mathrm{U}_y\,\mathrm{Pu}_{1-y})\mathrm{O}_{2\pm x}$ fluorite phase modelled using CEF with three sublattices and is an ionic phases where the first sublattice contains actinoid cations and the second and third sublattices contain oxygen anions mixing with vacancies. The global optimisation algorithm must respect the charge neutrality constraint thus distinguishing this problem from others. The system composition, as in [110], is $0.93$ mol of U, $0.07$ mol of Pu and $2$ mol of O maintained at temperature $T = 1000$ K and hydrostatic pressure $P = 1$ atm. The global optimisation algorithm must verify that the $(\mathrm{U}_y\,\mathrm{Pu}_{1-y})\mathrm{O}_{2\pm x}$ fluorite phase is only stable phase at equilibrium. The expressions for reference Gibbs energies and mixing parameters can be found in [181].The expressions for reference Gibbs energies and mixing

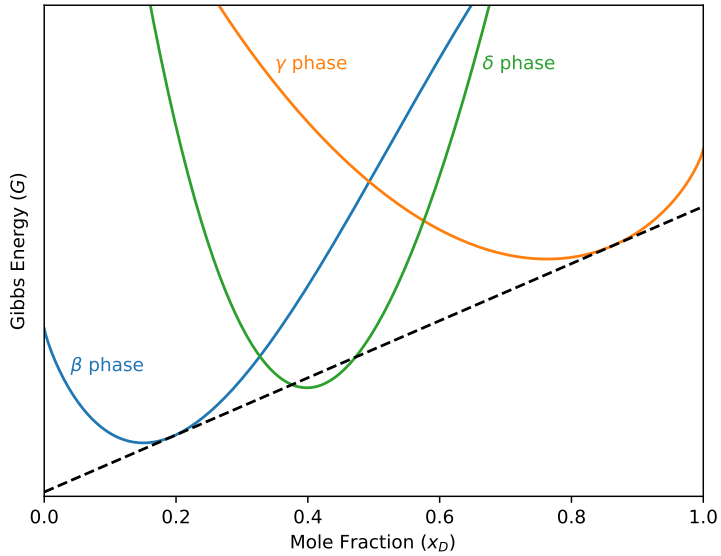


Figure 6.9: Fictive system with three phases showing a false positive from thermodynamic equilibrium solver wherein a wrong phase is believed to be present at equilibrium.

parameters can be found in [183].

5. *Problem E*

   Otis et al. [121] showed that the Al–Co–Cr ternary system modelled by Liu et al. [183] poses a challenge to thermodynamic equilibrium codes. In particular, it was shown that at temperature $T = 1523$ K, a ternary miscibility gap can be ignored when considering the metastable Body Centered Cubic (BCC) phase only. The phase was modelled with a three-sublattice CEF model with the elements mixing on the first and second sublattices. Considering the challenges posed by the BCC phase in the system, the system was selected as a test problem with the system containing $0.5$ mol of Al, $0.2$ mol of Co and $0.3$ mol of Cr at $T = 1000$ K and $P = 1$ atm. The global optimisation algorithm must identify the existence of a miscibility gap. The expressions for reference Gibbs energies and mixing parameters can be found in [183].

6. *Problem F*

   The quinary Mo–Pd–Tc–Ru–Rh system from Kaye et al. [180] is considered as the sixth test problem for comparing global optimisation algorithms. The system is relevant to nuclear reactor accident simulations as the components are noble metal fission products and their behaviour is critical to source term analyses. The system includes ideal gas, non-ideal liquid and four solid solution phases with FCC, BCC, HCP and tetragonal crystal structures in addition to several stoichiometric phases. The liquid and solid solution

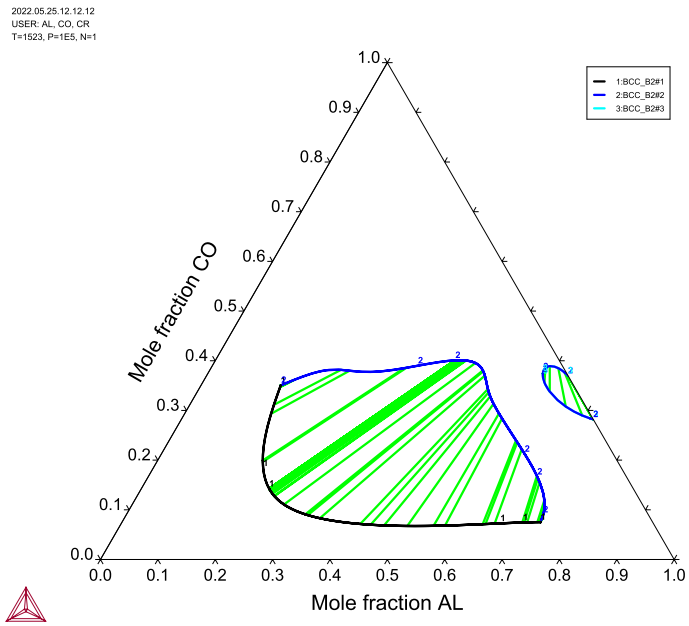


Figure 6.10: Al−Co−Cr phase diagram calculated with ThermoCalc version 2018b with an increased point density. With only BCC phase enabled, the existence of the miscibility gaps is shown in the central portion but as shown by Otis et al. [121], the miscibility gap is lost using the default ThermoCalc parameters.

phases were all modelled using substitutional solution models and, as in [110], the system contains $1$ mol of each component and is maintained at a temperature $T = 1000$ K and hydrostatic pressure $P = 1$ atm. Examining the HCP phase only, the HCP–$Mo_9Pd_{11}$ phase combination is assumed to be stable and the global optimisation algorithms must identify the presence of a miscibility gap which yields a lower integral Gibbs energy of the system. The stable phase assemblage should be HCP–HCP miscibility gap co-existing with $Mo_9Pd_{11}$. The expressions for reference Gibbs energies and mixing parameters can be found in [180].

7. *Problems G & H*

   The cases until now considered relatively simpler and smaller systems, which are easily visualisable and verifiable but a true representation of nuclear materials must consider a large number of system components. The last two test problems have been designed to test the global optimisation methods for a very large number of species. The fictive phases constructed for the high-dimensional tests are modelled using a three-sublattice CEF model with the first sublattice consisting of a large number of cations and the other two sublattices consisting of two anionic constituents mixing together. This results in two problems with 100 end members and 400 end members and is representative of irradiated molten salts. The fictive phases were constructed following the methodology

of Piro and Simunovic [110]. The phases were assumed to have 10 and 30 components with 1-4 constituents per component. The cations were assigned a charge of $+2$ or $+3$ and the anions were assigned a charge of -1 (halides) or 0 (vacancy). The reference molar Gibbs energy of each end member was $g_i^\circ = \mathcal{U}(200, 450)$ kJ mol$^{-1}$. As in [110], excess mixing parameters were created such that one cation would mix with the following cation in the list of constituents on the first sublattice with a mixing parameters ${}^0L = \mathcal{U}(-100000, 100000)$ and ${}^1L = \mathcal{U}(-1000, 1000)$.

### 6.5.2. Grid sampling

Sampling from an equispaced grid has been widely adopted in thermodynamic equilibrium codes as a strategy for testing equilibria by performing numerous evaluations of the objective function at regular intervals in the domain [74, 120, 184–186]. The method was developed in the 1970s and 1980s as a brute force method to verify global minimum for phase diagram construction problems and does not scale well for large systems. As shown in Figure 6.11, in the grid construction method, the surface of $\Delta G_\phi$ is discretised with each point treated as a stoichiometric compound and the ensemble of these compounds collectively approximates the driving force surface [110]. In the example figure, the arbitrary binary system consists of a solution phase and a stoichiometric phase and the domain for the solution phase has been sampled at nine equispaced grid points.

The discretisation of the grid plays a key role in the efficacy of this method and it has been shown by Chen et al. [186] that the grid must be sufficiently resolved to avoid missing critical features such as the minimum between grid points $\alpha_8$ and $\alpha_9$ in Figure 6.11. However, this requirement leads to performance concerns as too small a grid leads to an increase in the computational cost while too large a grid can lead to a false sense of having achieved a global minimum. Piro and Simunovic [110] have demonstrated how uniformly spaced grid for a phase $\phi$ in $N_\phi$ dimensional Euclidean phase (each dimension corresponds to a species in phase $\phi$) can result in an enormously large number of grid points depending on the grid size. In the example with nine grid points, it becomes clear from Figure 6.11 that global minimum would not be found but increasing the number of grid points will lead to an exponential increase in the cost. In conclusion, the rapid increase in the computational cost with the reduction in grid size and a questionable performance in terms of reaching a global maximum tilts the scales against this method. Despite the fact, this method was tested with three separate grid spacings ($\delta = 0.1$, $0.01$, and $0.001$) to serve as benchmarks and to numerically show the rapid increase in computational time.

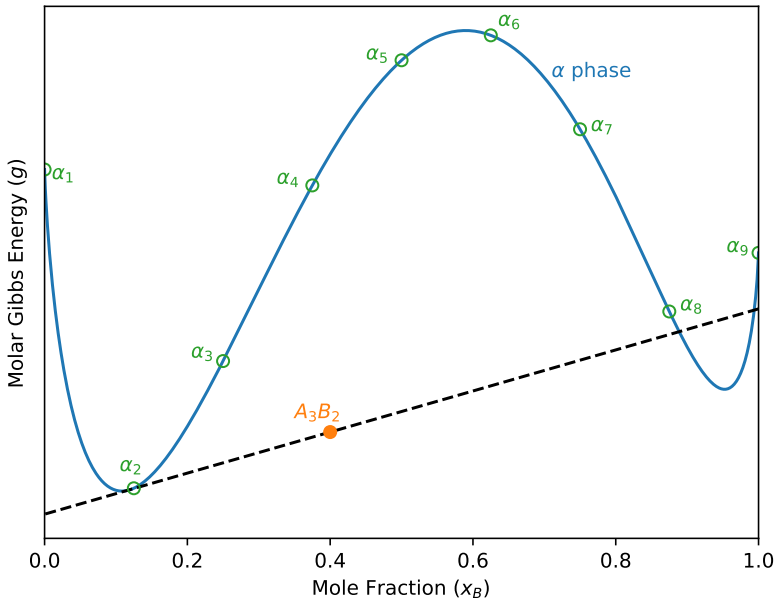


Figure 6.11: Demonstration of the grid construction method for fictive binary system in test problem A. The domain has been sampled at nine equispaced grid points and the pure stoichiometric phase $A_3B_2$ is found to be in equilibrium with the solution phase giving a false positive.

### 6.5.3. Spatial branch & bound (sBB)

The Branch & Bound (BB or B&B), attributed to Land and Doig [187] who introduced it in 1960 for discrete programming, is a widely used algorithmic paradigm for finding optimal solutions to optimisation problems. As illustrated in 6.12, the algorithm systematically enumerates all the candidate solutions by sequentially pruning out non-feasible solution candidates through a recursive approach of partitioning the domain and finding an upper and a lower bound for each subdomain. In 1969, Falk and Soland [188] proposed one of the first BB algorithms that could be applied to an continuous objective function with separable concave portions with a closed and convex set of constraints and a bounded feasibility region. The BB algorithm involves two procedures to solve global optimisation problems:

1. *Branching*: The domain $S$ is partitioned into two or more smaller disjoint domains $S_1, S_2, \ldots$, such that $S = S_1 \cup S_2 \cup \ldots$ Thus, the partitioned objective function can be considered a convex approximation of the objective function within the subdomain $S_i$.

2. *Bounding*: The upper and lower bound of the objective function are found within a subset of the domain $S$. In the classical Branch and Bound method, a subdomain can be removed from the analysis if the lower bound of the objective function in it is greater than the upper bound of the objective function in any other subdomain.

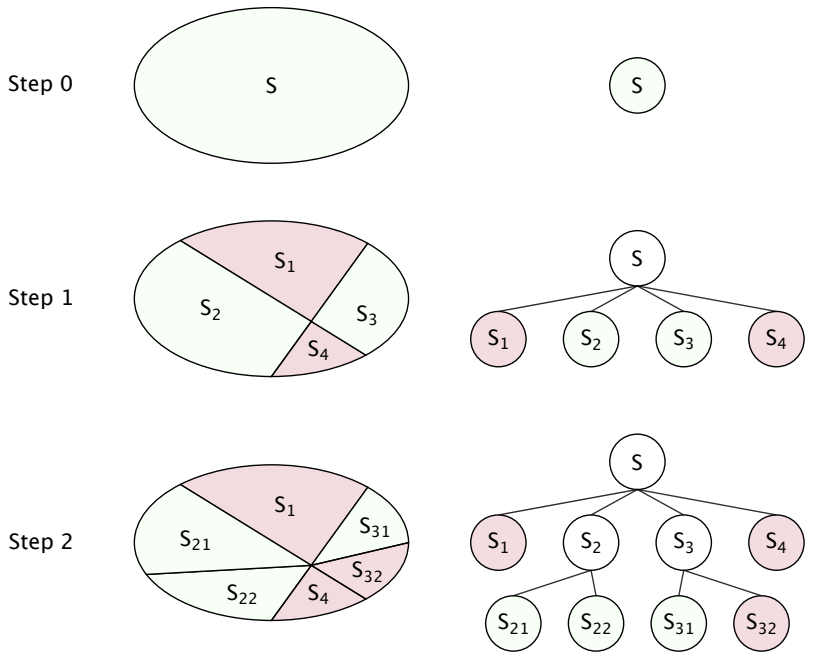


Figure 6.12: Illustration of the Branch & Bound (BB) class of algorithms. At each step, the domain is partitioned into a set of unexplored subdomains (denoted as nodes in a dynamic tree) which represent potential regions of optimal solution. By estimating the upper and lower bound on each subdomain, regions of infeasibility can be eliminated.

McDonald and Floudas [189] applied the BB algorithm to solve thermochemical equilibrium problems and Piro and Simunovic [110] proposed a modified version of the classical BB for the thermochemistry library Thermochimica which uses a different initialisation procedure and relaxation scheme for the bounds. Furthermore, instead of relying on pruning, every subdomain is evaluated till stopping criteria are met and if necessary, recursive partitioning technique is applied. The approach adopted by Piro and Simunovic [110] partitions the domain for each phase $\phi$ into $N_\phi$ subdomains and the driving force $\Delta G_\phi$ given by equation (5.57) is minimised in each subdomain. Their approach results in a Hessian which can be represented as a symmetric arrow matrix and by exploiting the structure of this matrix, the combination of $x_i$ that minimises $\Delta G_\phi$ can be easily determined. To solve the matrix, Gaussian elimination can be performed on the just the bottom row followed by back substitution. Furthermore, instead of storing a Hessian, the diagonal vector and a scalar representing the far right column can be stored. However, the implementation of this method warrants the use of an appropriate line search algorithm to ensure that the Wolfe conditions are satisfied and that the local system stays within the feasible region $0 < x_i < 1$ . In addition, the step length must be suitably constrained to avoid missing any local minimums [110]. While the method works reasonably well, there are situations where it fails to correctly identify the true global minimum.

One of the best known methods for solving non-convex Non-Linear Programming (NLP) problems is the *Spatial Branch & Bound (sBB)* [190, 191]. The branching, as already mentioned, is done by taking a continuous variable $v_i \in [v_i^l, v_i^u]$ and choosing $\beta$ $(v_i^l \leq \beta \leq v_i^u)$ to create two subproblems with domains $[v_i^l, \beta]$ and $[\beta, v_i^u]$. When solving either subproblem, the original lower and upper bounds can be replaced by tighter bounds by taking the advantage of the reduced domain. This process, from McCormick [192], is called *spatial branching*. In this work, a *Symbolic Reformulation sBB* [190, 193, 194] has been used through the Couenne (Convex Over and Under ENvelopes for Nonlinear Estimation) open-source software [195, 196]. Couenne has been developed to solve global optimisation problems $(\mathbf{P})$ of the form [195]:

$$\begin{aligned} \min \quad & f(x) & & \\ \text{s.t.} \quad & g_j(x) \leq 0 & & \forall j \in M \\ & x_i^l \leq x_i \leq x_i^u & & \forall i \in N_0 \\ & x_i \in \mathbb{Z} & & \forall i \in N_i^0 \subseteq N_0, \end{aligned} \tag{6.13}$$

where $f : \mathbb{R}^n \to \mathbb{R}$ and, $\forall j \in M$, $g_j : \mathbb{R}^n \to \mathbb{R}$ are multivariate functions, $n = |N_0|$ is the number of variables, and $x = (x_i)_{i \in N_0}$ is the n-vector variables. In the context of equilibrium thermodynamics, the problem in the form conformant to the above equation is as follows:

$$\begin{aligned} \min \Delta G_\phi(x_i) &= \sum_{i=0}^{N_\phi} \left( \tilde{\mu}_i - \sum_{j=1}^{C} \nu_{ij} \tilde{\Gamma}_j \right) & & \\ \text{s.t.} \quad & \sum_{i=1}^{N_\phi} x_i = 1 & & \forall i \in N_\phi \\ & \sum_{i=1}^{N_\phi} \nu_{ie^-} x_i = 0 & & \forall i \in N_\phi \\ & 0 \leq x_i \leq 1 & & \forall i \in N_\phi. \end{aligned} \tag{6.14}$$

Couenne implements linearisation, branching, heuristics and bound reduction and reformulates the problem by introducing a set of auxiliary variables. The reformulation of problem represented

by equation (6.13) results in the following form $(\mathbf{P}')$ [195]:

$$\begin{aligned} \min \quad & x_{n+q} \\ \text{s.t.} \quad & x_i = \vartheta_i(x) && \forall i \in \{n+1, n+2, \dots, n+q\} \\ & x_i^l \leq x_i \leq x_i^u && \forall i \in N \\ & x_i \in \mathbb{Z} && \forall i \in N_i \subseteq N, \end{aligned} \tag{6.15}$$

where $N = \{1, 2, \dots, n+q\}$ is the new variable index set which is a union of the original index set $\{1, 2, \dots, n\}$ and the auxiliary index set $\{n+1, n+2, \dots, n+q\}$. $N_i$ denotes the index set of integer variables and the value of the last auxiliary variable, $x_{n+q}$, is the value of the objective function.

sBB algorithms rely on the generation of rigorous lower and upper bounds for the objective function value over any given variable subdomain. Generation of a upper bound is relatively simple as any feasible point of problem $(\mathbf{P})$ serves as an upper bound to the function at global minimum. In practice, it is best to chose the local minimiser of equation (6.13) as the upper bound. When the reformulated problem $(\mathbf{P}')$ is in factorable form, the feature can be used to derive valid bounds and exact solution or one can use linear and quadratic approximations of $f$ and $g_j$. Detailed descriptions of sBB algorithms are found in literature [194, 197] and the specifics to implementation in Couenne are described in [195] but the method, illustrated in Algorithm 1, is briefly described here.

1. *Reformulation*

   A general method for allowing the formation of convex relaxation for any continuous twice differentiable function was given in [198–200] and a tighter relaxation framework was developed by Smith and Pantelides [194]. The goal of reformulation is to construct an equivalent formulation $(P')$ to problem $(P)$ such that it contains only linear constraints and special non-linear definitions. Since convex relations of many transcendental functions (such as logarithms, exponentials, etc.) exist and most algebraic expressions, including the ones encountered in equilibrium thermodynamics, are made up of binary operations of arithmetic and the unary operators, it is possible to construct convex relaxations of any algebraic expression. For doing this, additional variables can be introduced in the problem. For example, in test problem A, the non-linear terms in the excess mixing part can be reformulated as a linear problem by introducing variables $w_1 = x_A x_B$ and $w_2 = x_A x_B^2$. Such a process can be generalised and automated using the standard binary tree representation of algebraic expressions [190]. The reformulated problem $(P')$ is equivalent to the original problem $(P)$ but all the non-linearities are described by sets

**Algorithm 1:** sBB algorithm for the Mixed Integer Non-Linear Programming (MINLP) problem $(\mathbf{P})$ [195].

**Input:** Problem $(\mathbf{P})$

Define set $L$ of subproblems, $L \leftarrow \{\mathbf{P}\}$;
Define upper bound $z^u$ for $\mathbf{P}$, $z^u \leftarrow \infty$;
**while** $L \neq \emptyset$ **do**
  Choose $\mathbf{P}_k \in L$;
  $L \leftarrow L \setminus \{\mathbf{P}_l\}$;
  Apply bound tightening to $\mathbf{P}_k$ ; /* Bound tightening */
  **if** $\mathbf{P}_k$ *is feasible after bound tightening* **then**
    Generate a linear relaxation $\mathbf{LP}_k$ of $\mathbf{P}_k$ ; /* Linearisation */
    **repeat**
      Solve $\mathbf{LP}_k$ to get an optimum $\bar{x}^k$ with objective value $\bar{z}^k$;
      Refine linearisation $\mathbf{LP}_k$;
    **until** $\bar{x}^k$ *is feasible for* $\mathbf{P}_k$ *or* $\bar{z}^k$ *does not improve*;
    **if** $\bar{x}^k$ *is feasible for* $\mathbf{P}_k$ **then**
      $z^u \leftarrow \min\{z^u, \bar{z}^k\}$;
    **end**
    Find a local optimum $\hat{z}^k$ of $\mathbf{P}_k$ ; /* Upper bound calculation */
    $z^u \leftarrow \min\{z^u, \hat{z}^k\}$;
    **if** $\bar{z}^k \leq z^u - \epsilon$ **then**
      Choose a variable $x_i$ ; /* Branching variable selection */
      Choose a branching point $x_i^b$ ; /* Branching point selection */
      Create subproblems:
        $\mathbf{P}_{k-}$ with $x_i \leq x_i^b$,
        $\mathbf{P}_{k+}$ with $x_i \geq x_i^b$;
      $L \leftarrow L \cup \{\mathbf{P}_{k-}, \mathbf{P}_{k+}\}$;
    **end**
  **end**
**end**

**Output:** $z_{\text{out}} \leftarrow z^u$, an optimal solution of $(\mathbf{P})$

corresponding to bilinear product, linear fractional, simple exponentiation and univariate function terms. Because the two problems are equivalent, a convex relaxation of $(P')$ is also a valid relaxation of $(P)$. Hence, reformulation allows constructing a convex relaxation of any problem and the sBB determined optimal solution of $(P')$ is also the optimal solution to $(P)$.

2. *Linearisation*

   If one considers the constraint $x_j = \vartheta_j(x)$ created during reformulation and set $B =$

$[x^l, x^u]$ defining bounds on the variables, a $\vartheta_j$-linearisation is a system of linear inequalities $A^j x \geq b^j$ such that $X_{\mathsf{LP}} := x \in B : A^j x \geq b^j \supseteq x \in B : x_j = \vartheta_j(x)$. If a $\vartheta_j$-linearisation is created for each constraint $x_j$, a linear problem $\mathbf{LP}_k := \min x_{n+q} : Ax \geq b$ is a linear relaxation of $\mathbf{P}_k$ where $\mathbf{P}_k$ is a root node of $\mathbf{P}$ obtained through branching. The optimal solution $\bar{x}$ of $\mathbf{LP}_k$ provides a lower bound for the problem. If the solution of $\mathbf{LP}_k$ becomes infeasible for $\mathbf{P}_k$, the lower bound can be improved by either branching or refinement of $\mathbf{LP}_k$, i.e. by amending linearisation inequalities [195]. Couenne uses a variant of the projection error rule for refinement [195].

3. *Bound tightening*
   According to Smith and Pantelides [194], sBB can achieve convergence without any bound tightening but the rate of convergence can be improved by using it. The goal of bound tightening is to reduce the interval $[x_i^l, x_i^u]$ without causing the optimal value of the problem to change and it allows reduction of the feasible set and an improved linearisation. One way of propagating the effects of constraints to variable bounds in Optimality-Based Bounds Tightening (OBBT) [190, 197, 201] but Faster-Feasibility Bounds Tightening (FBBT) are also available albeit resulting in weaker bounds [190, 197, 202, 203]. In OBBT, two convex optimisation problems are solved:

$$x_i^l = \min_x x_i, \quad \text{subject to convex relaxation constraints,} \quad x^l \leq x \leq x^u, \tag{6.16}$$

$$x_i^u = \max_x x_i, \quad \text{subject to convex relaxation constraints,} \quad x^l \leq x \leq x^u. \tag{6.17}$$

   FBBT can be applied to every variable $x_i$ separately and when feasible the convex relaxation constraints can be updated but at each iteration it will solve $2N$ optimisation problems making it extremely expensive and suitable only for initial bound tightening steps [194]. FBBT, on the other hand, considers each constraint of the reformulated problem individually [202]. At any sBB node $k$, if the local minimum $\hat{x}^k \in [x^l, x^u]$ of the convex relaxed problem $\mathbf{CP}_k$ is known, FBBT is applied to fictitious bounding box $B \cap x \in \mathbb{R}^{n+q} : x_i \leq \tilde{x}_i$, where $\tilde{x}_i \in (x_i^l, \hat{x}_i^k)$ is suitably chosen. If the resulting problem become infeasible or if its lower bound becomes larger than the best upper bound, then $[\tilde{x}_i^k, x_i^u]$ is a valid tightening . On the other hand, if $\tilde{x}_i \in (\hat{x}_i^k, x_i^u)$ is chosen and FBBT applied to the analogous bounding box results in infeasibility, then $[x_i^l, \tilde{x}_i^k]$ is valid.

4. *Branching*
   Branching is critical to the performance of sBB and an effective strategy can help minimise the size of the sBB tree. The goal of branching is to choose a branch variable and

corresponding branch point to be use to partition the domain. In doing so, the goal must be to improve the lower bound of the resulting subproblems and to eliminate as large an infeasible region as possible. In doing so, one must also try to keep the sBB balanced and together the three requirements are often conflicting and the implementations can be optimised to emphasise on one aspect or the other. Branching may be required when the lower bound $\bar{x}^k_{n+q}$ of an sBB node $\mathbf{P}_k$ is smaller than the best known feasible solution and the relaxation $\mathbf{LP}_k$ cannot be further refined. To objectively select the branching variable and point, Belotti et al. [195] define the $\vartheta_i$-*infeasibility* of auxiliary variable $x_i$ at node $k$ as $U_i\left(\bar{x}^k\right) = \left|\bar{x}^k_i - \vartheta_i\left(\bar{x}^k\right)\right| / \left(1 + \left\|\nabla\vartheta_i(\bar{x}^k)\right\|_2\right)$. The scaling of the error term in numerator with the norm of the gradient avoids selecting a variable $x_i$ with a small bound interval $[x^l_i, x^u_i]$ but with a large $\left|\bar{x}^k_i - \vartheta_i\left(\bar{x}^k\right)\right|$ as it is unlikely to improve linearisation if used for branching.

(a) Branching variable selection

In Couenne, integer variables have higher priority than continuous variable but since the driving force function results in a strictly NLP problem, continuous variables become the only candidate for branching. Defining the *dependence set*, $D(x_i)$, as the set of variables in $\vartheta_i(x)$ (these are the variables in $x$ that $x_i$ directly depends on), the infeasibility of variable $x_i$ can be propagated to $D(x_i)$. In Couenne, Belotti et al. [195] define the non-linear infeasibility as:

$$\Omega^N_i(\bar{x}^k) = \mu_1 \sum_{j\in E(i)} U_j(\bar{x}^k) + \mu_2 \max_{j\in E(i)} U_j(\bar{x}^k) + \mu_3 \min_{j\in E(i)} U_j(\bar{x}^k),$$

where for variable $x_i$, the set $E(i) = j \in N \ : \ x_i \in D(x_j)$. Parameter $\mu_k \geq 0$, $k = 1, 2, 3$[1] and $\mu_1 + \mu_2 > 0$ ensures that $\bar{x}^k$ is infeasible if and only if $\Omega^N_i(\bar{x}^k) > 0$ for at least one variable $x_i$. In Couenne $(\mu_1, \mu_2, \mu_3) = (0.1, 1.3, 0.8)$ [195]. The strategy, however, can often be ineffective and Couenne also has implementations of *Violation Transfer* proposed by Tawarmalani and Sahinidis [204] and an extension of the *reliability branching* technique introduced by Achterberg et al. [205]. In violation transfer, violations of non-convexities by the current solution are assigned to problem variables followed by transfer of violations to $D(x_i)$. The violations are then weighted to account for branching priorities and potential for convex relaxation improvement. The variable that leads to the maximum weighted violation is selected as the branching variable [204]. Since, the reliability branching strategy was not used

[1]Parameters $\mu_k$ defined here have no correlation to the chemical potential $\mu_i$.

in Yellowjacket–GEM, a discussion of it is omitted and can be found in [196].

(b) Branching point selection

For a continuous variable $x_i$ appearing in a single expression $x_j = \vartheta_j(x_i)$, the goal of sBB is to keep the resulting tree balanced. This makes areas of the linearisations a reasonable metric for selecting the branching point as shown in Figure 6.13. In Couenne, three branching point selection strategies are implemented.

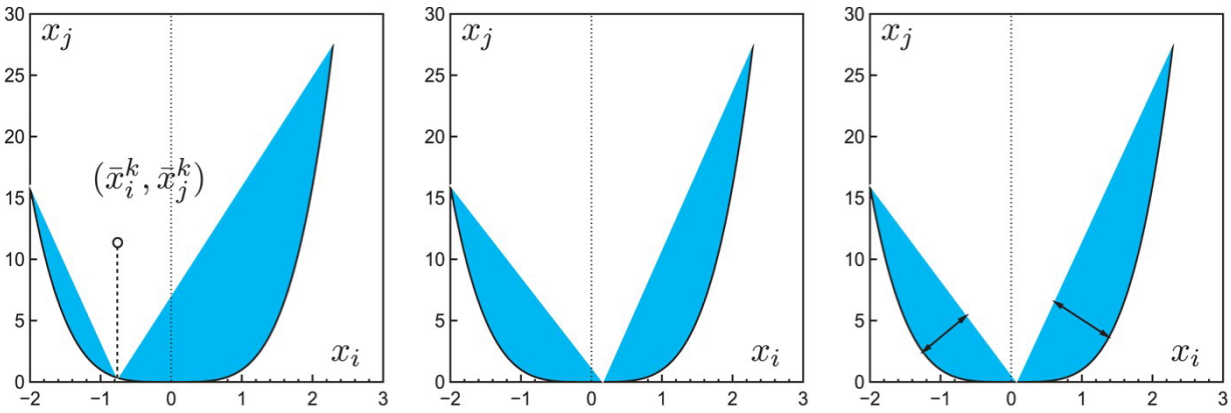


Figure 6.13: Strategies for selecting a branching point as implemented in Couenne: (a) branching on current LP solution $\bar{x}_i^k$, (b) Convex combination of LP point $\bar{x}_i^k$ and midpoint of bound interval, (c) Balancing the areas of the two resulting linearisations. Figure from Belotti et al. [195].

In the *LP-based strategy*, the branching point is set so that $\bar{x}^k$ can become infeasible in both the subproblems. While simple to implement, as shown in subfigure (a) of Figure 6.13, it can result in unbalanced subproblems. To avoid this, for variable $x_i \in [x_i^l, x_i^u]$, the branching point can be set as a convex combination of $\bar{x}_i^k$ and the midpoint of bound interval, $x_i^m = (x_i^l + x_i^u)/2$ (see subfigure (b) of Figure 6.13). Hence, a selection strategy guaranteeing a minimum distance from variable bounds is as follows [191]:

$$x_i^b = \max\left\{x_i^l + b, \min\left\{x_i^u - b, \alpha \bar{x}_i^k + (1-\alpha)\, x_i^m\right\}\right\},$$

where $0 < \alpha < 1$ and $b = \beta(x_i^u - x_i^l)$ for $0 < \beta < 0.5$ and $\alpha$ and $\beta$ are set to $0.25$ and $0.2$ respectively [195] and the strategy tries to balance the half-intervals of $x_i$. Alternatively, if a local minimum $\hat{x}^k$ is known, $\hat{x}_i^k$ can be chosen as a branching point since the resulting convexification will return a solution $\bar{x}^k$ that is very close to $\hat{x}^k$ [202].

In *expression-based strategies*, one can aim to reduce the sum of the areas of the

resulting convexifications as shown in subfigure (c) of Figure 6.13. Several methods for such strategy can be adopted [206, 207] but a balanced strategy implemented in Couenne finds the branching point using a binary search on the interval $[x_i^l, x_i^u]$ that minimises the difference between the maximum area $u'(x_i)$ and maximum area $u''(x_i)$ [195]:

$$x_i^b \in \arg\min \left| \max_{x_i \in [x_i^l, x_i^b]} u'(x_i) - \max_{x_i \in [x_i^b, x_i^u]} u''(x_i) \right|,$$

where $u'$ and $u''$ are the distance between the upper envelope line of $\vartheta_j$ and $(x_i, \vartheta_j(x_i))$ on the subdomains LP' and LP'' resulting from branching. The method balances the maximum distance between the points on $\vartheta_j(\cdot)$ and the upper envelope [196].

Together, the reformulation of the problem and the sBB algorithm result in a rigorous solution framework for global optimisation problem. Since the driving force functions are smooth and differentiable, they are well formulated for the method. Though the reformulation results in an increase in the size of the problem, it doesn't become a major issue for determining the minimum of the driving force.

### 6.5.4. Particle swarm optimisation

PSO is a stochastic search algorithm inspired by the flocking behaviour of birds. First proposed by Kennedy and Eberhart [208, 209], PSO is a population based method that relies on the premise of social sharing of information among a bird flock seeking food. PSO is relatively simple to describe and implement and its apparent competence in finding optimal solutions in complex search spaces has made it a widely studied search algorithm [210]. In PSO, a population of candidate solutions, dubbed particles, moves around the search space as a function of the position and velocity of the particle and the movement of each particle is influenced by its best known local position and guided towards the best global position as other particles find better solutions.

At each iteration $t$, the velocity vector of particle $i$ in the swarm gets updated according to the following equation [211]:

$$\mathbf{v}_i^{t+1} = \omega \mathbf{v}_i^t + \psi_1 R_{1_i}^{\ t} \left(\mathbf{p}_i^t - \mathbf{x}_i^t\right) + \psi_2 R_{2_i}^{\ t} \left(\mathbf{g}^t - \mathbf{x}_i^t\right), \tag{6.18}$$

where $\mathbf{v}_i^t$ and $\mathbf{x}_i^t$ are the velocity and position at iteration $t$. The inertia weight is given by $\omega$ and $\psi_1$ and $\psi_2$ are real acceleration coefficients known as cognitive weight and inertia weight

respectively. Together, the weights control the impact of global and individual best positions on the particle's velocity and trajectory. Kennedy and Eberhart [209] originally assigned the same value of 2 to social and cognition parts but fine-tuning the parameters is critical to performance and convergence of PSO, particularly when dealing with multimodal problems [212–214]. $R_1$ and $R_2$ are uniformly distributed vectors used to maintain an adequate level of diversity in the swarm population and $\mathbf{p}_i^t$ and $\mathbf{g}^t$ represent the best known position of particle $i$ and the global best position of the swarm at iteration $t$. In turn, the position of each particle $i$ at every iteration $t$ can be updated according to the following equation [211]:

$$\mathbf{x}_i^{t+1} = \mathbf{x}_i^t + \mathbf{v}_i^t. \tag{6.19}$$

**Algorithm 2:** PSO algorithm for objective function $f : \mathbb{R}^n \to \mathbb{R}$

**Input:** Objective function $f$, Search space $\mathbf{x}_i = [\mathbf{x}_i^l, \mathbf{x}_i^u]$, Number of particles $N_p$

**for** *Particle* $i \in \{1, 2, \dots, N_p\}$ **do**
  Initialise initialise position, $\mathbf{x}_i \leftarrow \mathcal{U}\left(\mathbf{x}_i^l, \mathbf{x}_i^u\right)$;
  Initialise particle's best known position, $\mathbf{p}_i \leftarrow \mathbf{x}_i$;
  **if** $f(\mathbf{p}_i) < f(\mathbf{g})$ **then**
    Update global best position, $\mathbf{g}_i \leftarrow \mathbf{p}_i$;
  **end**
  Initialise the particle velocity, $\mathbf{v}_i \leftarrow \mathcal{U}\left(-\left|\mathbf{x}_i^u - \mathbf{x}_i^l\right|, \left|\mathbf{x}_i^u - \mathbf{x}_i^l\right|\right)$;
**end**
**while** *Termination criteria is not met* **do**
  **for** *Particle* $i \in \{1, 2, \dots, N_p\}$ **do**
    Pick random vectors, $\mathbf{R}_1, \mathbf{R}_2 \leftarrow \mathcal{U}\left(0, 1\right)^n$;
    Update particle velocity, $\mathbf{v}_i^{t+1} \leftarrow \omega \mathbf{v}_i^t + \psi_1 {R_1}_i^t \left(\mathbf{p}_i^t - \mathbf{x}_i^t\right) + \psi_2 {R_2}_i^t \left(\mathbf{g}^t - \mathbf{x}_i^t\right)$;
    Update particle position, $\mathbf{x}_i^{t+1} = \mathbf{x}_i^t + \mathbf{v}_i^t$;
    **if** $f(\mathbf{x}_i^{t+1}) < f(\mathbf{p}_i)$ **then**
      Update particle's best known position, $\mathbf{p}_i^t \leftarrow \mathbf{x}_i^{t+1}$;
      **if** $f(\mathbf{p}_i^t) < f(\mathbf{g})$ **then**
        Update global best position, $\mathbf{g}^t \leftarrow \mathbf{p}_i^t$;
      **end**
    **end**
  **end**
**end**

**Output:** $x_{\text{out}} \leftarrow \mathbf{g}^t$, an optimal solution of $f$

The PSO algorithm, illustrated Algorithm 2, has several advantages compared to other continuous optimisation methods. First, PSO is a problem independent algorithm, which only

needs the objective function to evaluate the fitness of each candidate solution. In doing so, PSO does not make any assumptions about the continuity and differentiability of the objective function. Second, also doesn't need solution of linear or non-linear systems of equation which can often be expensive. Third, the evolution of particles is random and therefore the gradients of the objective function need not be calculated. Lastly, PSO does not need a good initial estimate or a-priori knowledge of the objective function search space [210]. These factors have led PSO to gain a widespread appeal and it has shown good performance in several domains like function optimisation, artificial neural network training, fuzzy system control, etc. Unfortunately, for complex multimodal problems, the conventional PSO algorithm can get trapped in local optima, considerably compromising the convergence rate. This leads to poor performance and accuracy, and imposes restrictions on applicability to a wide range of practical problems [215, 216]. While a priori tuning can help improve performance, it is a time-intensive process but also assume that the optimal parameter configuration does not change over time. However, as shown by Leonard and Engelbrecht [217], the parameter values well-suited for exploration are not well-suited for exploitation and vice-versa. To achieve the two fold characteristic of good convergence speed and to avoid stagnating in local optima, several variations of PSO have been developed [218–222]. Another limitation of PSO is in constrained optimisation problem as it lacks an explicit constraint-handling mechanism. Several methods such as penalty function, feasibility-based rules method and the constraint-preserving method have been proposed with the penalty method being the most commonly used [223, 224]. While detailed discussions on handling these problems are available in open literature, the specific approach in the context of this work is discussed in the following text.

1. *Constraint handling*

   As previously stated, several strategies have been explored to impose the constraints in PSO. One of the simplest constraint-handling mechanism is that of resetting the particles that escape the feasible region [225–227]. Minimisation of a non-stationary multi-stage assignment penalty function was proposed by Parsopoulos and Vrahatis [228] and the results were promising albeit at the cost of a very complex process for determining penalty. In the feasibility-based approaches such as that by Pulido and Coello [229], a candidate solution is chosen leader based on Deb's comparison rules [230]. The constraint handling strategy implemented in Yellowjacket–GEM is based on the method by Hu and Eberhart. [225]. To make the solution more plausible, all the equality constraints are modified into inequality constraints to a specified tolerance, i.e., the constraints on sum of mole

fractions and the charge neutrality constraints are reformulated as:

$$\left| \sum_{i=1}^{N_\phi} x_i - 1 \right| < \epsilon_1, \tag{6.20}$$

$$\left| \sum_{i=1}^{N_\phi} \nu_{ie^-} x_i \right| < \epsilon_2. \tag{6.21}$$

The initialisation step is then modified to impose the constraints and once a feasible initial solution is found, the algorithm can progress. At every iteration $t$, each particle is checked for feasibility. If the updated position $x_i^{t+1}$ results in the bounds being violated, the step length is updated based on the following equation:

$$\mathbf{x}_i^{t+1} = \mathbf{x}_i^t + \alpha \mathbf{v}_i^t, \tag{6.22}$$

where $\alpha \in \mathcal{U}(0.1, 0.9)$ is a randomly generated constriction vector used to scale the step length. Handling the constraints, however is less straightforward. Once the position of each particle has been updated, the feasibility of each particle is verified and if it is found to violate the feasibility condition, Deb's comparison rules [230] are applied as follows:

(a) If all candidate solutions are infeasible, the candidate closest to feasibility is selected as the best candidate and the remaining particles are restored to previous feasible position. The best known position of these particles is not changed.

(b) If some candidates are feasible, their personal best is updated and the global best solution is selected from the feasible particles. The particles in infeasible regions are restored to the previous feasible solution.

(c) If all candidates are feasible, the same process as usual is followed.

2. *Particle initialisation*

One of the parameters in PSO that can potentially affect the convergence rate is the number of particles and their initial positions. While the particle position $x_i$ is often initialised randomly from a uniform sampling in $[x_i^l, x_i^u]$, it has been shown by Woronow [231] that, when compared to normalised exponential distribution, normalised uniform distributions produce a poorer coverage of composition space. Otis et al. [121] employed a set of different sampling strategies such as Halton sequence, Sobol sequence and their variations to come come up with an efficient sampling strategy for PyCalphad. Furthermore, Piro and Simunovic [110] found that PSO often fails to capture the optimal

solutions located close to the domain edges and special considerations must be taken when the optimal solution may exist close to the boundaries. To best see the effect of particles' initial position on the performance of PSO, a number of different options were tested. First, the number of particles, $N_p$, was selected from a finite set $\{N_\phi, 2N_\phi\}$ and second, the particles were initialised using both normalised uniform and normalised exponential sampling. In addition, when $N_p = 2N_\phi$, a hybrid strategy was also used where $N_\phi$ particles were initialised using the sampling methods while the remaining $N_\phi$ particles were fixed at the corners of the domain. The reasoning behind this approach is that the particles closer to the edges should enable the space closer to the edges to be properly explored. Also, more advanced sampling methods were not selected as, with well-tuned hyperparameters, PSO is expected to efficiently scan the domain unlike when only sampling is used and one must make sure that the features are not missed if the samples are not well picked.

3. *Particle dynamics*

   Parameter tuning can have a significant impact on the performance of PSO and a large number of *Adaptive Particle Swarm Optimisation (APSO)* algorithms have been proposed in literature to overcome the problem of a priori tuning of the parameters. A comparative analysis of many such algorithms has been performed by Harrison et al. [216]. Amongst one of the promising APSO algorithms is *APSO based on Velocity Information (APSO-VI)* proposed by Xu [215] which adapts the inertia weight based on the current velocity of the particles. The concept of APSO-VI is borrowed from Yasuda et al. [232] and aims to evolve the velocity to be close to an *ideal* velocity. In APSO-VI the average velocity of swarm is defined as [215]:

$$\bar{v}^t = \frac{1}{nN_p} \sum_{i=1}^{N_p} \sum_{j=1}^{n} \left| v_{ij}^t \right|, \tag{6.23}$$

   where $n$ and $N_p$ represent the problem dimension and the number of particles in the swarm respectively. The size of the average velocity reflects the size of the particle search space and to better explore the search space, one should maintain a larger average velocity with longer time, during the early stage of the optimisation. On the other hand, during the latter stage, it is important to keep a small average velocity to find the optimum solution efficiently [215]. One can then define an ideal velocity at iteration $t$, which decreases

with time, as follows:

$$v_{\text{ideal}}^{t} = v_s \left( \frac{1 + \cos\left(\frac{\pi t}{T_{\text{end}}}\right)}{2} \right), \tag{6.24}$$

where $v_s = (x^u - x^l)/2$ is the initial ideal velocity, $T$ is the maximum number of iterations and $T_{\text{end}} = 0.95T$ is the time in which 95% of search is completed. As visualised in Figure 6.14, the ideal velocity profile matches the requirements for an effective exploration of the search space. The inertia weight can then be dynamically adapted at each iteration

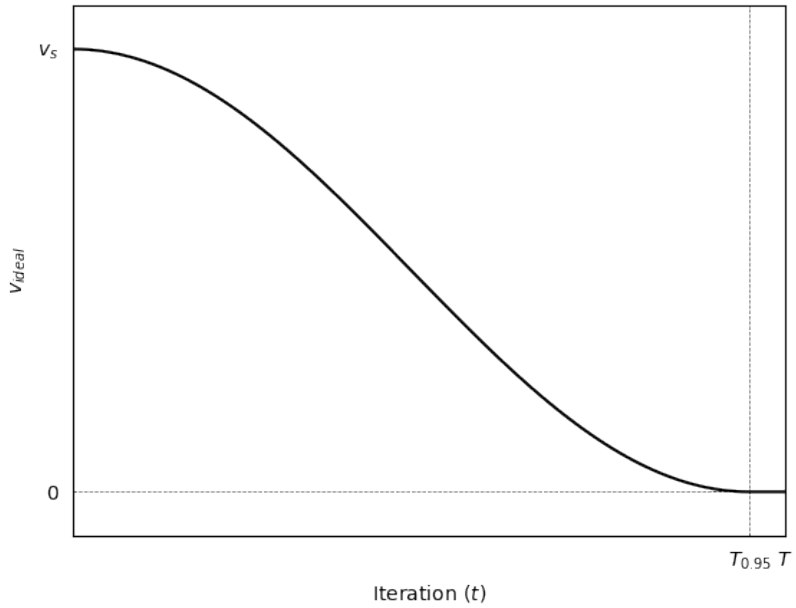


Figure 6.14: Schematic of ideal velocity profile in APSO-VI.

based on the average velocity in relation to the ideal velocity [216] using:

$$\omega^{t+1} = \begin{cases} \max\{\omega^t - \Delta\omega,\, \omega_{\text{min}}\} & \text{if } \bar{v}^t \geq v_{\text{ideal}}^{t+1} \\ \min\{\omega^t - \Delta\omega,\, \omega_{\text{max}}\} & \text{if } \bar{v}^t < v_{\text{ideal}}^{t+1} \end{cases}, \tag{6.25}$$

where $\omega_{\text{min}}$ and $\omega_{\text{max}}$ are the minimum and maximum inertia weights and $\Delta\omega$ is the inertia weight step size. It has been shown by Harrison et al. [233] that decreasing the ideal velocity decrease the inertia weight such that it remains within convergent range. Xu fixed the parameters $\omega_{\text{min}} = 0.3$, $\omega_{\text{max}} = 0.9$, $\Delta\omega = 0.1$, and $\psi_1 = \psi_2 = 1.49$ [215] and, in this work, APSO-VI has been adopted, albeit with slightly different parameter values. In Yellowjacket–GEM, the APSO-VI hyperparameters were selected to be $\omega_{\text{min}} = 0.2$,

$\omega_{\text{max}} = 0.9$, $\Delta\omega = 0.1$, $\psi_1 = 1.5$ and $\psi_2 = 2$. These values provided good convergence rates while reasonably exploring the search space and are similar to those previously used in thermodynamic equilibrium application such as by Piro and Simunovic [110] and Myint et al. [131].

### 6.5.5. Implementation and analysis

All global optimisation methods have their advantages and disadvantages and no global optimisation method is universally superior to others. While the deterministic methods are good at converging to a local minimum, they are often prone to high computational expense. The stochastic methods, on the other hand, tend to cover the search space more effectively but face difficulty at finding the global minimum [110]. The global optimisation methods discussed in literature have mostly been problem centric and there has been a lack of a comprehensive and rigorous analysis of these methods applied to a variety of thermodynamic equilibrium problems. Since the global optimisation methods are critical to the performance of Yellowjacket–GEM, an experimental approach was adopted to select a method to be used. While the goal of the global minimiser can be restricted to identifying whether or not a phase has a negative driving force, in terms of comparison, the aim was to correctly identify the minimum of driving force in each of the eight test cases described in Section 6.5.1.

Since, the convergence criteria for Couenne and the APSO-VI implementation differ, they must be clarified. In Couenne, the convergence is based on the feasibility tolerance. If a constraint $g_i(x) \leq 0$ within this tolerance, it is deemed satisfied [196]. The Couenne solve requires several options to be specified. The ones of particular concern here were that related to branching for which violation transfer was selected and FBBT was applied to bound tightening. Since OBBT is computationally expensive, it was disabled and Couenne was allowed to use heuristics through interior point optimisation. The tolerance was left to the default value of $1 \times 10^{-6}$.

In APSO-VI, the convergence criterion is more complicated due to the stochastic nature of the algorithm. Guaranteeing that all the particles will converge to the same value is impossible without significantly compromising performance. Apart from a preset maximum number of iterations $T = 100$, the algorithm is deemed to converge if 95% of the particles converge to a small distance of the global best position. For this, the Euclidean distance of each particle from the best known global solution is calculated using $S_i^t = \|x_i^t - g^t\|$ and if $S_i^t \leq 1 \times 10^{-6}$ for $0.95N_p$ particles, the algorithm is terminated as converged. For calculating the Euclidean distance, only feasible solutions are considered and if a feasible global best is not identified, the algorithm is marked as failed.

For comparison, each implementation of the method was executed a hundred times on a 2020 M1 MacBook Air with 8 GB of memory. The methods were alternated in ABC...ABC... pattern to avoid bias and the total time for all the runs was considered. The average time of all the times in the interquartile range was selected as the performance metric while the number of times the algorithm correctly identified the minimum or absence of negative driving force was the metric of reliability. No runs were discarded for the reliability metric. The results of a comparative analysis are shown in figures 6.15 and 6.16. The results demonstrate that the equispaced grid sampling method is only effective with very small resolutions leading to a very rapid increase in the computational cost. On the other hand, the APSO is a lot more robust but they do show that a larger number of particles can better scan the space. Despite their efficiency, the robustness of the APSO is slightly lower than the sBB algorithm which converges to the correct results for each test case but does so at the cost of increase in computational time.

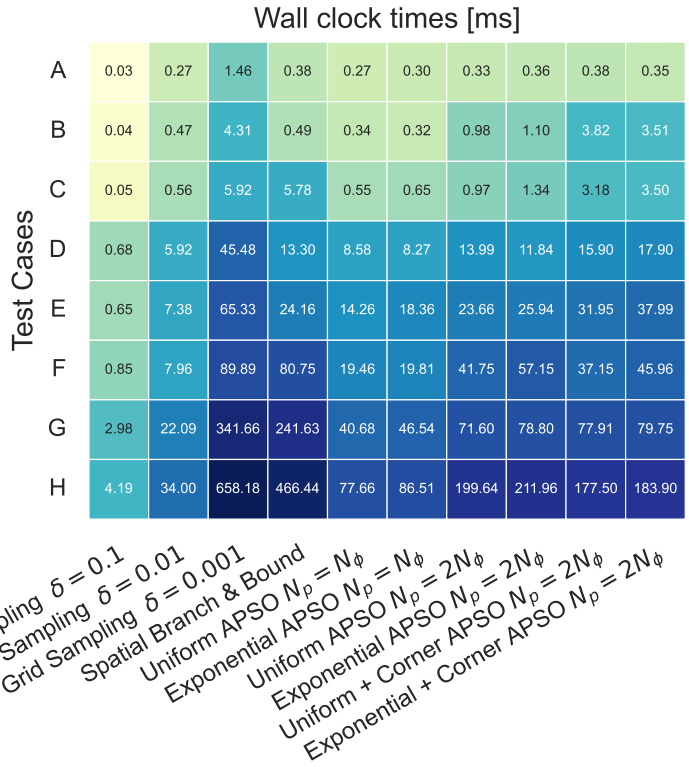


Figure 6.15: Comparison of computational performance of various global optimisation algorithms for the test cases. The wall clock time is the average time of the results in interquartile range for 100 calculations of each method and case combination.

The grid sampling method was able to find the minimum in all the test cases albeit only

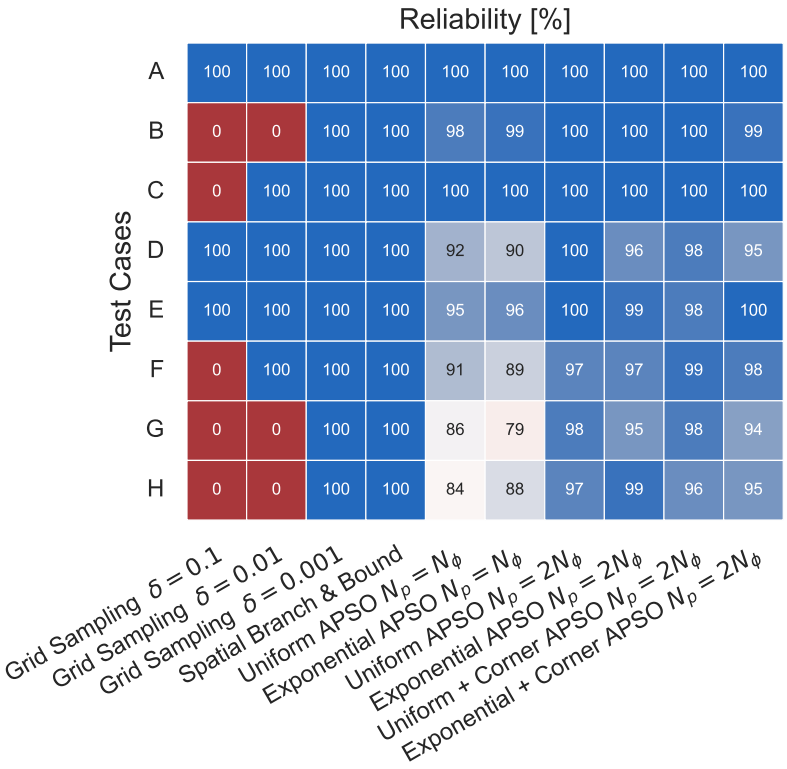


Figure 6.16: Comparison of reliability of various global optimisation algorithms for the test cases. The reliability is the number of times the correct results were shown by a method out of the 100 calculations.

when the grid resolution was increased to $\delta = 0.001$ and with a significant impediment on performance. In particular, one must be careful about the charge neutrality constraints with this approach. When dealing with ionic phases, many of the samples using this strategy will result in infeasibility due to the charge neutrality constraint getting violated. This could potentially compromise the method's reliability as a feasible point satisfying the charge constraint might never be found. In the implementation here, the objective function was evaluated at every sample point despite some of them being infeasible.

Among the tested options, sBB proves to be the most reliable though at a cost to performance. This is expected for the well behaved driving force functions. One way of reducing the computational cost of sBB is to terminate the solver as soon as an upper bound becomes negative or a feasible solution with negative driving force has been identified. This however has not been implemented in Yellowjacket–GEM. The stochastic methods on the other hand exhibit fairly good computational performance though with a slightly lower reliability. In the experiments, the loss of reliability is attributable to reaching maximum iterations and in a small number of cases to converging to an infeasible value. Moreover, the impact of the number of

particles in the swarm is clearly visible. With $N_p = N_\phi$, the space is not sufficiently scanned leading to a lower overall reliability. In such a scenario, increasing the number of particles seems to be the best choice but one must take cognisance of the fact that this can increase the computational time and might also require adjusting the convergence criteria. Initialising the particles on the corners did not have as big an impact as the number of particles. This can be attributed to the test cases itself where the optimal solution in most cases was not close to any edge and therefore no significant benefit was obtained from the particles scanning the space closer to the boundaries. Lastly, grid sampling can work for smaller systems given that the resolution is sufficiently small but it is not suitable for systems with large number of components as the cost increases rapidly and with no a priori knowledge of the required resolution, there is no way of knowing whether the solution is indeed a global minimum or not.

In the context of Yellowjacket, both the sBB and APSO algorithms have been integrated into the code and the user will have the option of specifying the desired method. In cases where reliability is of the utmost importance and the system is deemed too complex, one could select sBB as the global optimisation algorithm. On the other hand, in cases where the system is deemed to be not very complicated or where there is a possibility of a posteriori checking the results and / or augmenting global optimisation results with other information such as that from the grain information available in phase field, APSO can be used to reduce computational cost.

Though several other global optimisation algorithms exist, only the aforementioned models were selected based on the literature review. Among the stochastic methods, only PSO appears to have been reasonably successful for general thermodynamic equilibrium problems. Other methods such as genetic algorithm, tabu search and others have, to the author's best knowledge, only been applied to simple systems such as liquid-vapour equilibrium and even in those applications the reliability has sometimes been questionable. Among the deterministic methods, the usually high cost has meant that an even lesser number of applications are found for thermodynamic equilibrium problems. In addition, one must also consider the state of algorithms and libraries available. As an example, unlike other algorithms, sBB has numerous libraries which have been built on years of research and development and meet the requirements of rigorous testing and benchmarking.

## 6.6. Software Quality Assurance (SQA)

A key thrust area of the Yellowjacket–GEM development was to meet the SQA standards required from all MOOSE-based applications. Not only must one make sure that the results are physically representative, but the code itself must meet criteria for readability, uniformity and

understandability but also avoid vulnerability and bugs. Yellowjacket–GEM has been developed following industry standard development practices and procedures to ensure conformance to the MOOSE quality requirements. The key concepts worth mentioning are code review, source code control and continuous integration. MOOSE requires that any new code be reviewed by at least one reviewer other than the developer and the code can only be merged upon being approved. The main goal of the review process is to identify defects, improve code quality, finding better solutions to problems and ensuring coding guidelines are followed. The source code is maintained using the Git version control system and is hosted on INL's GitLab. Not only does it allow keeping a history of all the changes in the codebase but also enforces MOOSE syntax guidelines through Git hooks. MOOSE and hence Yellowjacket–GEM use ClangFormat for all C++ code. Yellowjacket–GEM also uses Continuous Integration (CI) using MOOSE's Continuous Integration, Verification, Enhancement and Testing tool (CIVET) [234] and MOOSE's gold file based testing harness. Upon every commit to the repository, CIVET runs a suite of unit tests that verify the functionality of every separable code piece and also regression tests that test the whole code against known good results. Upon the completion of tests, a comprehensive report is generated that shows if the new code has breaks an existing functionality. The report also highlights the total and differential code coverage which is the percentage of code (lines and functions) that is hit in the tests. The last SQA process used in Yellowjacket–GEM is code documentation. Every code is well documented through both in-code documentation and more detailed documentation pages that detail the different models, solvers and provide examples. Together, code review, version control, CI and documentation fulfil the SQA requirements of MOOSE-based applications.

## 6.7. Summary

A number of algorithms for different parts of a thermodynamic equilibrium solver were presented in this chapter. Many of these algorithms have already been implemented in other codes available in the literature and GEM and levelling are well-matured algorithms. This is evident from the fact that most of the development efforts since the original GEM method have relied on auxiliary operations such as initialisation, etc. However, this does not mean that improvements can not be made. The development of an advanced thermodynamic solver leaves the door open for incremental gains on many of these algorithms. The development of non-linear solver leverages state-of-the-art non-linear solvers available in PETSc and uses recent developments in algorithms for phase handling to minimise common pitfalls in many thermodynamic equilibrium codes. Finally, two of the major areas that stand to benefit from this work are global optimisation methods and integration with the multiphysics framework MOOSE. The rigorous, experimental

approach to global optimisation methods applicable to thermodynamic equilibrium provides measurable estimates for reliability, efficiency and robustness. The algorithms discussed here have been implemented in Yellowjacket–GEM thus bringing native thermodynamic equilibrium capability to MOOSE.

# 7

# Demonstration Problems

*Thermodynamics plays a central role in driving several physical phenomena and in nuclear reactor modelling, it is often used in conjunction with other codes, such as a phase-field model or a fuel performance code. Another very useful application of the thermodynamic equilibrium is to study the behaviour of nuclear fuels and materials under severe accident conditions such as in predicting the impact of oxygen potential on the onset temperature of fuel volatilisation. Though the goal of this work was to develop the capability to use thermodynamic equilibrium calculations in modelling nuclear materials, the tool was used to perform several calculations which can demonstrate its capability. It must be emphasised that such calculations are purely intended to demonstrate the capability of the tool developed as part of this research and are not aimed at modelling real-world problems and phenomena. Several such examples are presented in this chapter. The first example is a benchmarking exercise where the results of Yellowjacket–GEM for a molten salt system are compared to the results from FactSage. The second example reproduces a phase-diagram already reported in literature followed by an example of phase evolution of oxide fuel. The next couple of examples show how thermochemical equilibrium calculations may be relevant to severe accident modelling in CANada Deuterium Uranium (CANDU) reactors and source term modelling in MSRs. The last example demonstrates a simple coupling between Yellowjacket–GEM and the MOOSE phase field module to model leaching of Ni by a molten $LiF–NiF_2$ salt.*

## 7.1. MQMQA Calculation Comparison of Yellowjacket–GEM with FactSage

To ensure the accuracy of results, a significant effort was put into verification of Yellowjacket–GEM results by benchmarking with the commercial code FactSage. For this, a representative system was selected (the system composition is the same as that used by Poschmann et al. [68]) and the relative differences in the mole fractions of each quadruplet were compared between Yellowjacket–GEM and FactSage. The calculations were performed at $1500\,\mathrm{K}$ and $1\,\mathrm{atm}$ and, as shown in Figure 7.1, the results are in excellent agreement with FactSage and the maximum relative difference is of the order of $1 \times 10^{-5}$. The Gibbs energy predicted by both Yellowjacket–GEM and FactSage is $-2.9787 \times 10^{11}$ J.

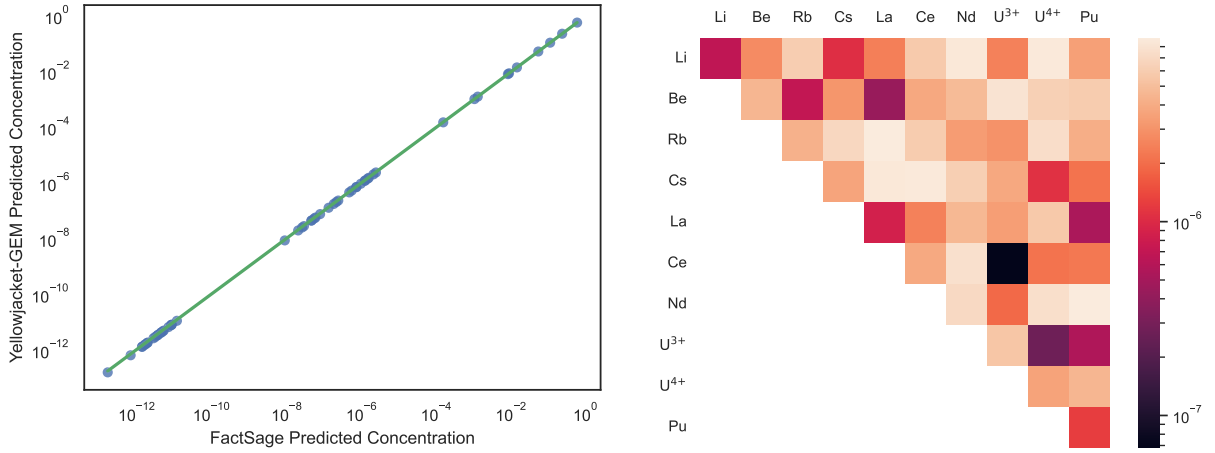


(a) Start of simulation

(b) Relative differences

Figure 7.1: Comparison of output species concentration predictions from Yellowjacket–GEM and FactSage for an MSRs system. The figure on the left shows the comparison between values from the two softwares with the green line indicating same values. A more detailed heatmap is shown on the right with each block denoting the relative difference in mole fractions for a quadruplet.

## 7.2. Phase Diagram Construction

Thermodynamic equilibrium calculations form the basis of phase diagram calculations. To demonstrate such applications, the phase diagram of the NaF – CsF binary system was calculated using Yellowjacket–GEM. This binary system has been recently re-evaluated experimentally by Lipkina et al. [235] and the phase diagram generated here was compared to the experimental results. The calculations from Yellowjacket–GEM are shown in Figure 7.2 and show excellent agreement with the experimental data for the eutectic points. There is, however, a departure

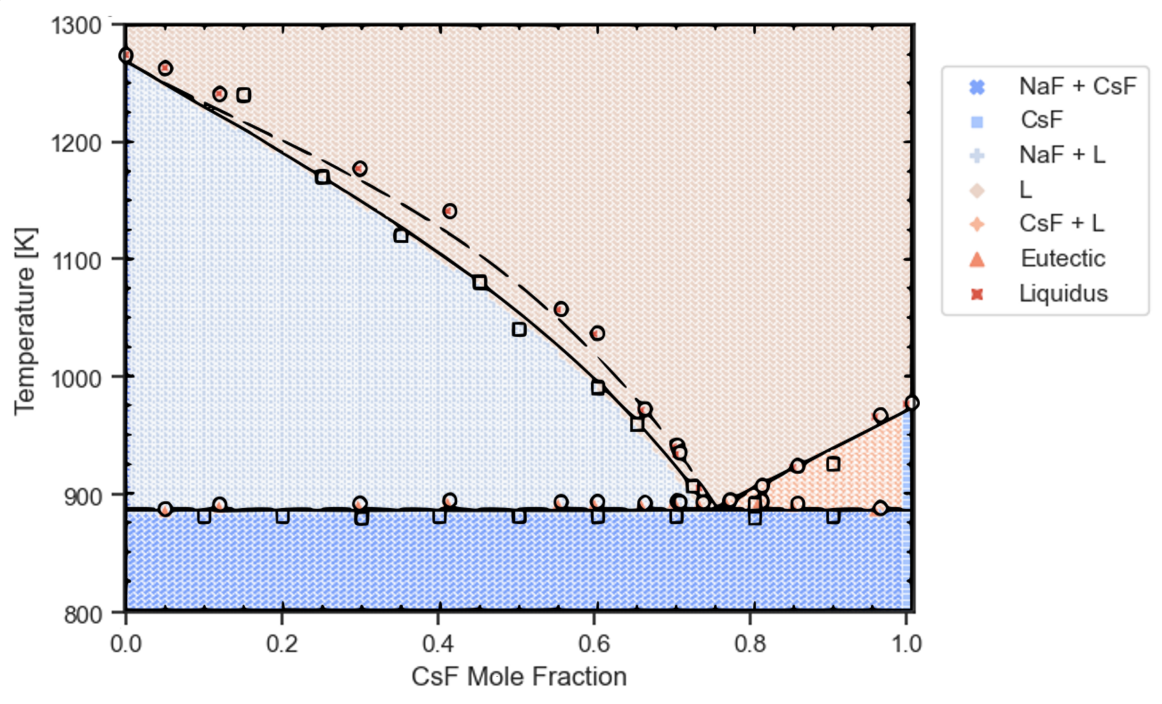


Figure 7.2: Yellowjacket prediction of a NaF – CsF phase diagram (coloured regions) with the phase diagram from Lipkina et al. [235] overlayed on top.

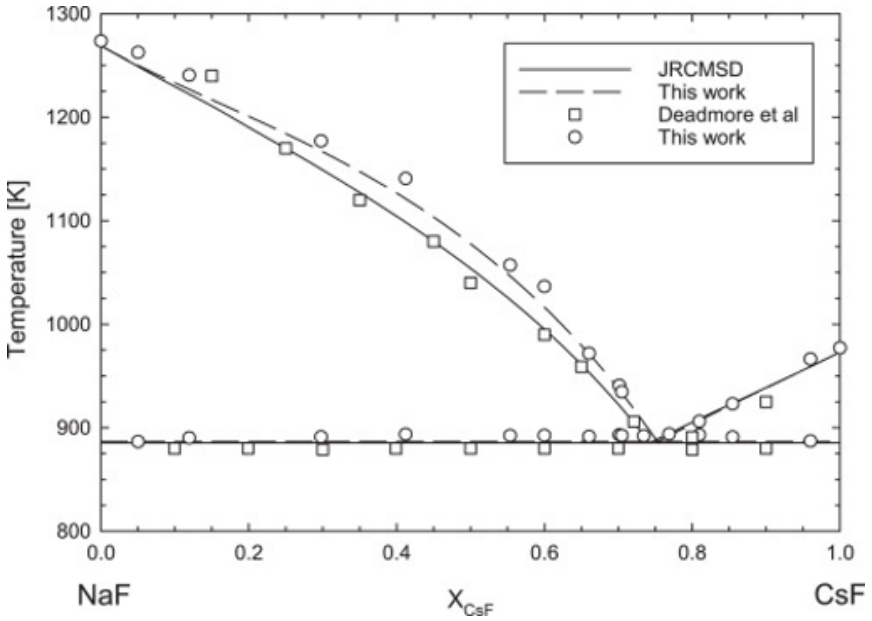


Figure 7.3: Reference NaF – CsF phase diagram from Lipkina et al. [235].

between the liquidus points calculated by Lipkina et al. and the ones predicted by Yellowjacket–GEM. This is a direct consequence of the database used in the calculations (MSTDB-TC) as it has not been updated to reflect the recent experimental results. In fact, as shown by the solid black line, the calculations match the results of the previously available experimental data. The example not only highlights the capability of Yellowjacket–GEM but also shows a need for the re-evaluation of the NaF – CsF thermodynamic model currently used in the databases.

## 7.3. CANDU Fuel Phase Evolution

Severe accident scenarios are amongst the phenomena that benefit most from the use of thermodynamic equilibrium calculations [236]. Piro performed thermodynamic investigations on irradiated uranium dioxide CANDU reactor fuel under conditions representative of severe accident scenarios [237]. Piro considered two cases of irradiated fuel interacting with the atmosphere. In the first case, the fuel was in contact with hydrogen gas while in the second case the irradiated fuel was in contact with air and steam. Piro used TAF-ID [182, 238] and varied the ratio of fuel to total atmospheric gas as well as the temperature and hydrostatic pressure. Here, a couple of similar simulations are performed albeit only for the case with a single fuel to atmosphere ratio and the database used is a modified version of TAF-ID obtained by translating the TAF-ID tdb file into ChemSage format. For the simulation, the same composition as that used by Piro was selected and the values are reported in Table 7.1. In the table, $b_{\mathrm{O}}$, $b_{\mathrm{H}}$ and $b_{\mathrm{N}}$ are variables which depend on the hydrogen to steam molar ratio $H = n_{\mathrm{H_2}}/n_{\mathrm{H_2O}}$, air to steam molar ratio $A = n_{\mathrm{air}}/n_{\mathrm{H_2O}}$, and fission product (Cesium in this case) to atmosphere molar ratio $R = b_{\mathrm{Cs}}/n_{\mathrm{gas}}$. The calculations show that under the given conditions, the main phase is O2ZRU_C [1] with other phases evolving as the system temperature changes. It must again be emphasised that the simulation is only representative of the capabilities developed as part of Yellowjacket–GEM and must not be considered as a safety case simulation.

Using $H = 10^5$ and $R = 10^{-4}$ for the case of fuel in contact with hydrogen, $b_{\mathrm{O}} = 2029.07449$ and $b_{\mathrm{H}} = 14900.00$. With the hydrostatic pressure $P = 1$ atm, the temperature of the system was varied from $1000\,\mathrm{K}$ to $3000\,\mathrm{K}$ in steps of $50\,\mathrm{K}$. The phase evolution predicted by Yellowjacket–GEM is shown in Figure 7.4. One must note that the database used here is not TAF-ID so the results will be different from the ones predicted by Piro [237].

In addition to comparing phase distributions under the varying system parameters, one is often interested in the oxidation states of different phases as they affect the material properties. Thermodynamic equilibrium calculations can be used to compute the oxygen-to-metal ratio $(O/M)$ of the phases. The same calculations as those used for the phase evolution were used

[1] O2ZRU_C denotes the fluorite phase. The name used in the database has been used here for consistency.

Table 7.1: Input mass parameters for CANDU reactor fuel under a severe accident condition. Adopted from Piro [237].

| **Element** | **Moles [mol]** |
|---|---|
| O | $b_{\mathrm{O}}$ |
| U | 1014.5 |
| Np | 0.096 |
| Pu | 2.754 |
| Ce | 0.824 |
| Y | 0.215 |
| Te | 0.138 |
| La | 0.332 |
| Zr | 1.442 |
| Ba | 0.389 |
| Ru | 0.899 |
| Mo | 1.15 |
| Sr | 0.421 |
| I | 0.077 |
| Nd | 0.859 |
| Nb | 0.043 |
| Am | 0.0064 |
| Cs | 0.745 |
| Rh | 0.166 |
| H | $b_{\mathrm{H}}$ |
| N | $b_{\mathrm{N}}$ |

to calculate the $(O/M)$ ratio and its evolution for the O2ZRU_C phase is shown in Figure 7.5.

## 7.4. Vapour Pressure Evolution in an MSR

Safety case demonstrations for MSRs are significantly different from water-cooled reactors. Since the fuel is already molten, there are no thresholds for a major release of radioactive material with severe core damage in MSRs accidents. The consequences of a primary system breach depend on the size and breach location and how much of the fuel salt or fission gases are leaked into a confined space. A small breach can result in significant fuel salt release and the high salt temperature can lead to a high pressure in the confined space [239]. Predicting vapour pressures is important for such safety demonstrations, but also for design and development of off-gas treatment system. Yellowjacket–GEM can predict the changes in vapour pressure of elements in gas phase, which can be used in source-term analyses and other simulations. The

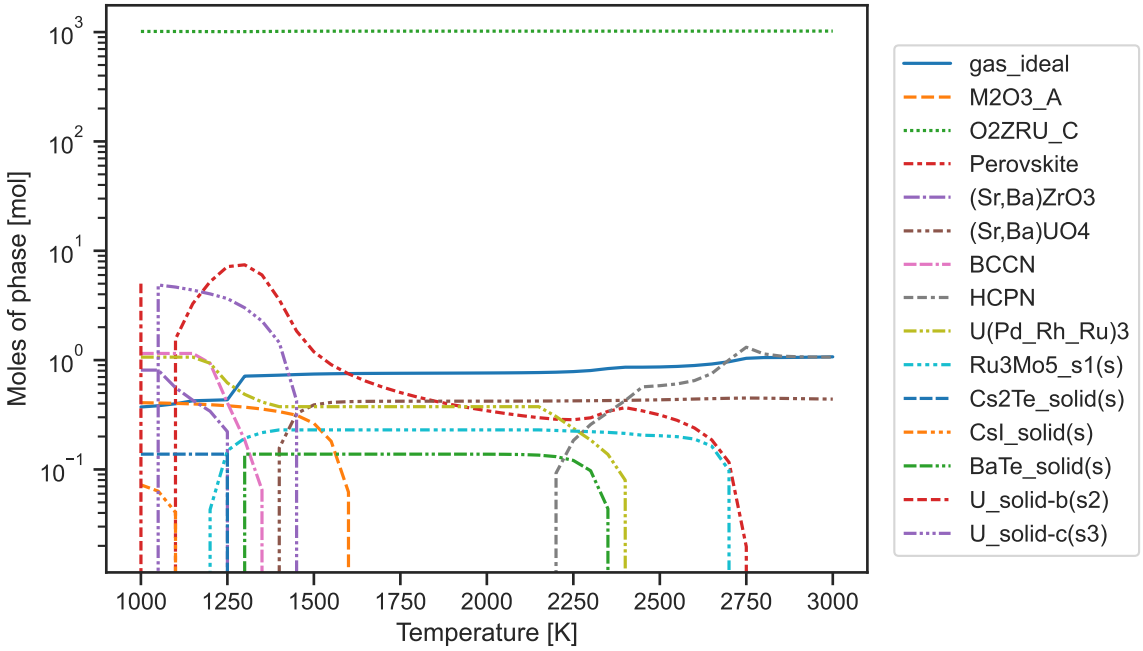


Figure 7.4: Predicted phase distribution with respect to temperature $H = 10^5$, $R = 10^{-4}$, and $P = 1$ atm.

role of a thermodynamic equilibrium solver in such cases can be demonstrated by the evolution of a fictive system representative of a molten salt system (FLiBe) with some dissolved fissile material (U) and some fission products (Nd, Ce, La, Cs, Rb). The system composition was adopted from Poschmann et al. [68] and is reported in Table 7.2.

Table 7.2: Input mass parameters for MSR fuel vapour pressure evolution. From Poschmann et al. [68].

| **Element** | **Moles [mol]** |
|---|---|
| Pu | $1.9780 \times 10^{-1}$ |
| U | $9.9695 \times 10^{3}$ |
| Nd | $3.3553 \times 10^{-1}$ |
| Ce | $4.2081 \times 10^{-1}$ |
| La | $1.4912 \times 10^{-1}$ |
| Cs | $4.2326 \times 10^{-1}$ |
| Rb | $8.1960 \times 10^{-2}$ |
| F | $4.4 \times 10^{5}$ |
| Be | $1.0 \times 10^{5}$ |
| Li | $2.0216 \times 10^{5}$ |

The system was assumed to undergo an unmitigated increase in temperature. The phase evolution, vapour pressure of species in the gas phase and element potential change as a function of temperature are shown in figures 7.6, 7.7 and 7.8. To reiterate, one must note that the

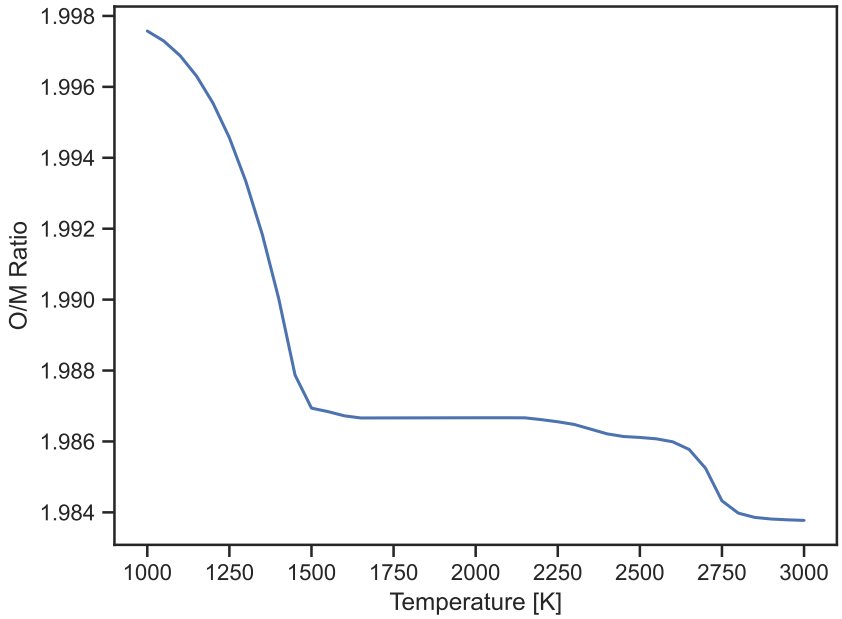


Figure 7.5: Predicted oxygen-to-metal ratio $(O/M)$ for O2ZRU_C phase with respect to temperature $H = 10^5$, $R = 10^{-4}$, and $P = 1$ atm.

results are purely for capability demonstration and must not be treated as physically relevant. However, they do exhibit cases where one might find the use of Yellowjacket–GEM relevant.

## 7.5. GEM - Phase Field Coupling

The objective of Yellowjacket development was to allow concurrent coupling of GEM with the phase field module in MOOSE. To achieve this a two step process was adopted. The first step was an offline coupling where Yellowjacket–GEM calculations are used to pre-tabulate the Gibbs energy and chemical potential data. This data was then used to generate interpolated functions of Gibbs energy and chemical potentials using the `PiecewiseLinearInterpolationMaterial` object in MOOSE. The interpolated functions were used as material properties in the phase field calculation. In doing so, one must also account for the difference between the Gibbs energies required by the phase field model and those calculated by Yellowjacket–GEM. The thermodynamic equilibrium calculations compute the Gibbs energy from the MQMQA and are in the following form given by equation (4.42). On the other hand, the phase field model requires that the Gibbs energy and chemical potentials also capture the effect of redox reactions and hence the Gibbs energy in a phase field module takes the following form:

$$g_{\mathsf{PF}} = \sum x_i g_i^{\mathsf{ec}} + RT\left(\sum x_i \ln x_i\right) + g^{\mathsf{ex}}, \tag{7.1}$$

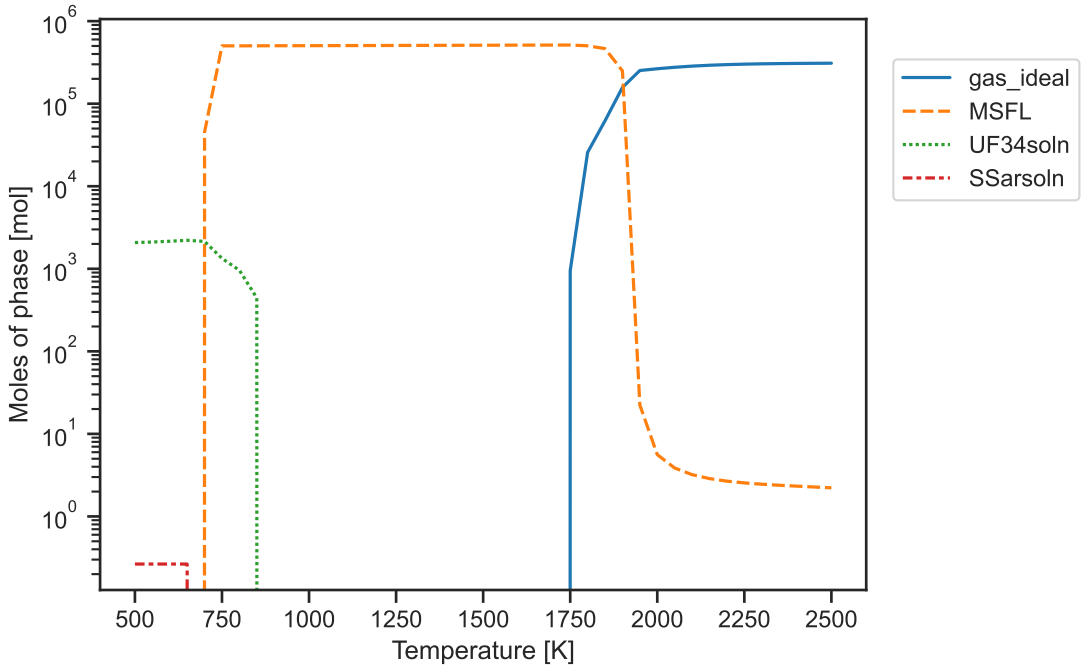


Figure 7.6: Phase evolution in molten salt system.

where $g_i^{\text{ec}}$ denotes the Gibbs energy with the reduction component accounted for.

For the initial demonstration of the methodology, a LiF–$NiF_2$ salt interacting with Ni metal at $1150\,\text{K}$ was selected. The Gibbs energy from the thermodynamic equilibrium code then takes the following form:

$$g_{\text{GEM}} = x_{\text{NiF}_2} g^{\circ}_{\text{NiF}_2} + x_{\text{LiF}} g^{\circ}_{\text{LiF}} + RT\left(x_{\text{NiF}_2} \ln x_{\text{NiF}_2} + x_{\text{LiF}} \ln x_{\text{LiF}}\right) + g^{\text{ex}}.$$

To reduce the number of variables in the phase field model, the reference Gibbs energy of $LiF_2$ is set to zero. Physically, since LiF is not modelled, the energy should be based on the metallic form of Ni which is done by changing the reference energy. $NiF_2$ is assumed to be formed from Ni metal by reducing HF into $H_2$ and the Gibbs energy of formation of $NiF_2$ is then equal to $g^{\circ}_{\text{NiF}_2} - 2g^{\circ}_{\text{HF}} + g^{\circ}_{\text{H}_2} + \nu F \Delta E_{\text{F}}$. This gives the following Gibbs energy expression for the phase field model

$$g_{\text{PF}} = x_{\text{NiF}_2}\left(g^{\circ}_{\text{NiF}_2} - 2g^{\circ}_{\text{HF}} + g^{\circ}_{\text{H}_2} + \upsilon F \Delta E_{\text{F}}\right) + RT\left(x_{\text{NiF}_2} \ln x_{\text{NiF}_2} + x_{\text{LiF}} \ln x_{\text{LiF}}\right) + g^{\text{ex}},$$

where $\upsilon$ represents the valency (2 for $Ni^{2+}$), $F$ is Faraday's constant and $\Delta E_{\text{F}}$ denotes the fluoride potential of the salt which is the energy required for the $HF \longrightarrow H_2 + F^-$ redox reaction. The fluoride potential is empirically derived based on experimental data and represents

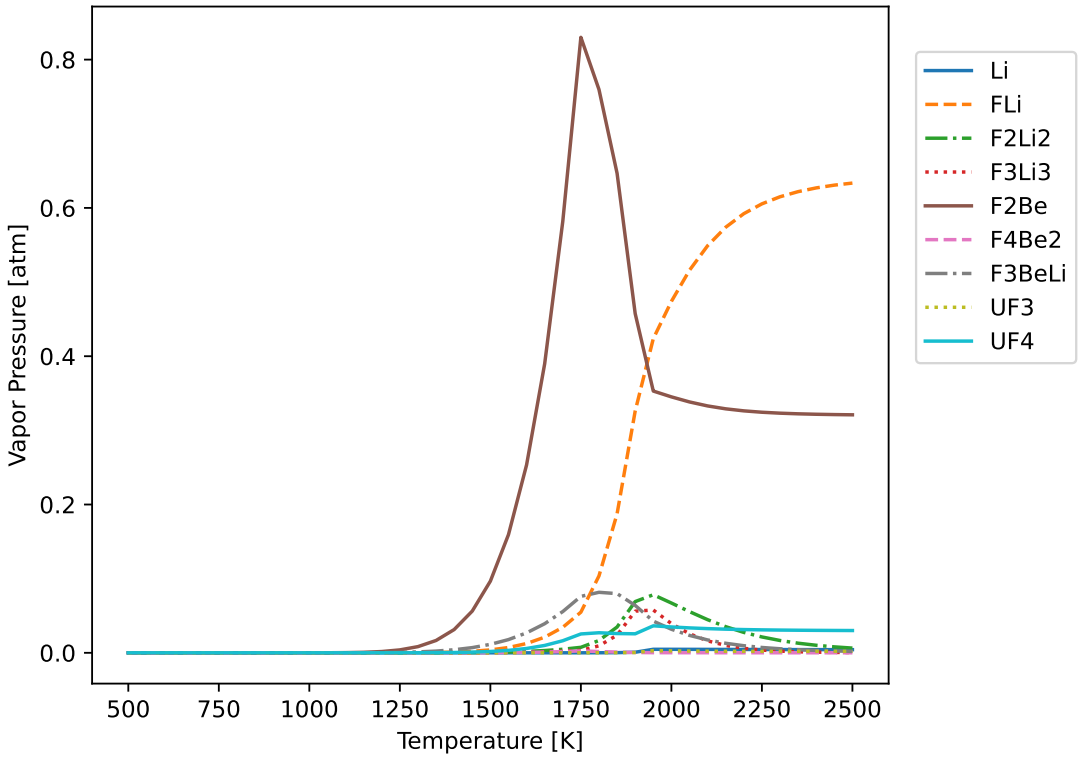


Figure 7.7: Vapour pressure prediction in a molten salt system.

how oxidising the environment is (higher $\Delta E_{\mathrm{F}}$ is less oxidising). To use Yellowjacket–GEM calculations in the phase field model, the Gibbs energy can then be reconciled as follows:

$$g_{\mathrm{PF}} = g_{\mathrm{GEM}} - x_{\mathrm{NiF_2}} \left( 2g^{\circ}_{\mathrm{HF}} - g^{\circ}_{\mathrm{H_2}} - g^{\circ}_{\mathrm{LiF}} - \nu F \Delta E_{\mathrm{F}} \right).$$

A phase field simulation was performed by collaborators at the University of Florida[2] to demonstrate the potential of coupling the Gibbs energy minimiser with the phase field model. The reference phase field model used the Nernst equation for the Gibbs energy equation, which does not capture the excess mixing contribution. As shown in Figure 7.9, the use of GEM allowed capturing the excess mixing effects which were not captured previously. While the difference for the binary system considered was relatively small, the excess mixing contributions for larger systems such as ones with impurities can be significant and being able to capture the additional contributions can significantly improve the fidelity of phase field models.

Ni leaching with molten LiF–$NiF_2$ was simulated under two conditions: $\Delta E_{\mathrm{F}} = 2.871$ V, which represents oxidising conditions and $\Delta E_{\mathrm{F}} = 3.0$ V which represents reducing conditions. The mole fraction of Ni in the molten salt phase was fixed as $x_{\mathrm{Ni}} = 0.001$. This essentially

[2]The phase field calculations were performed by Chaitanya Bhave, PhD candidate at the University of Florida.

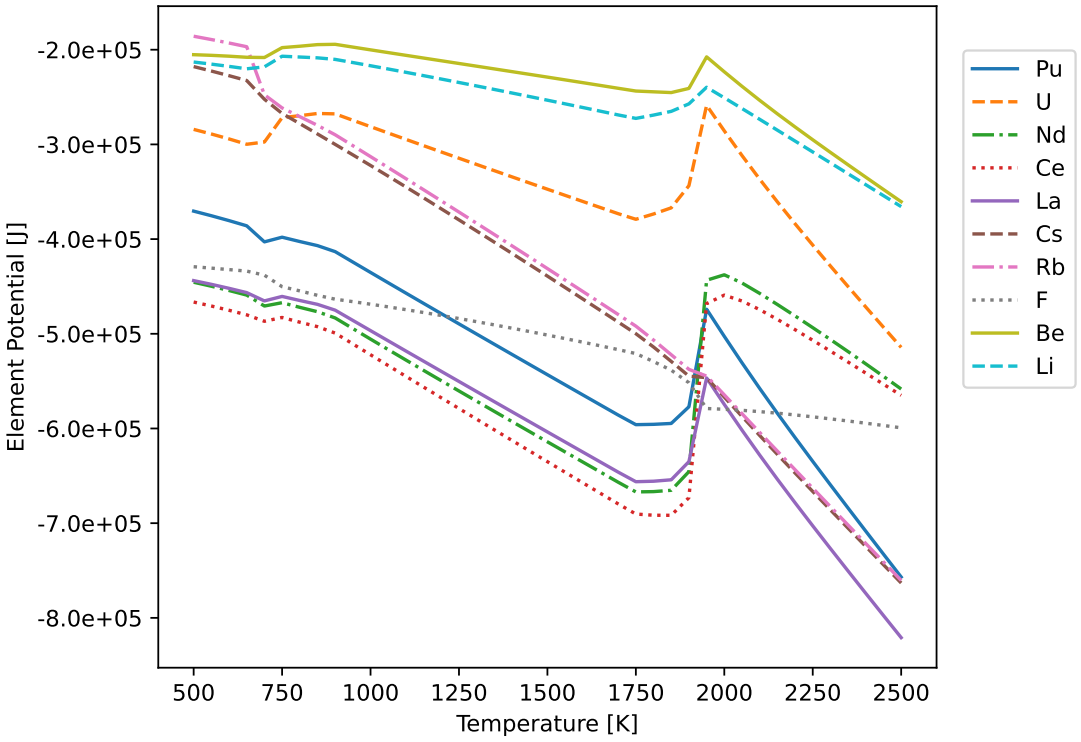


Figure 7.8: Element potential evolution in an MSR.

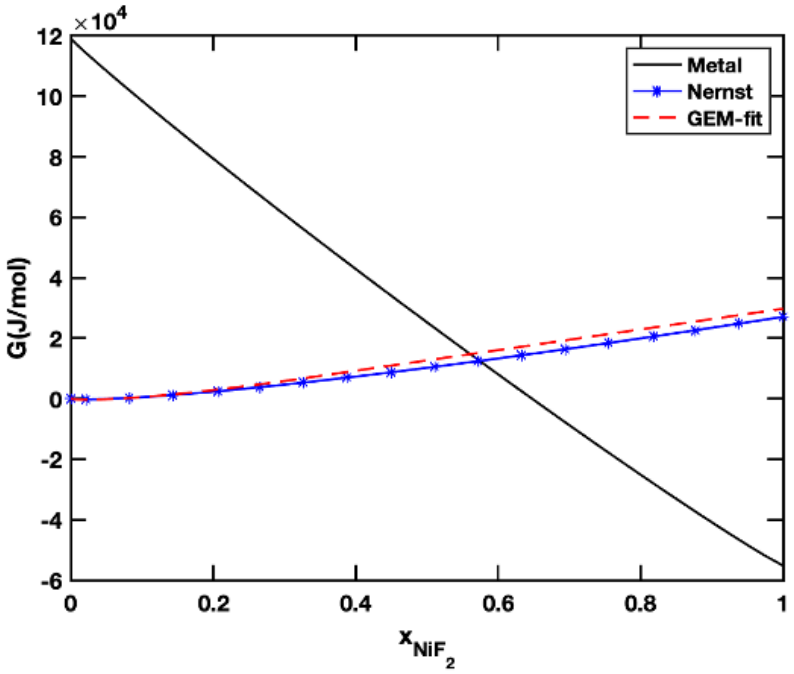


Figure 7.9: Comparison of Gibbs energy predicted by Yellowjacket–GEM vs. the dilute Nernst energy model used previously.

makes the molten salt a large reservoir of Ni and allows the corrosion of the structural material to be simulated without having to account for the mass inventory in the salt. The results of Ni leaching have been shown in figures 7.10 and 7.11. Under oxidising conditions, Ni metal gets leached into the molten salt and the interface moves to the left as shown in Figure 7.10 while the opposite happens under reducing conditions, as shown in Figure 7.11.

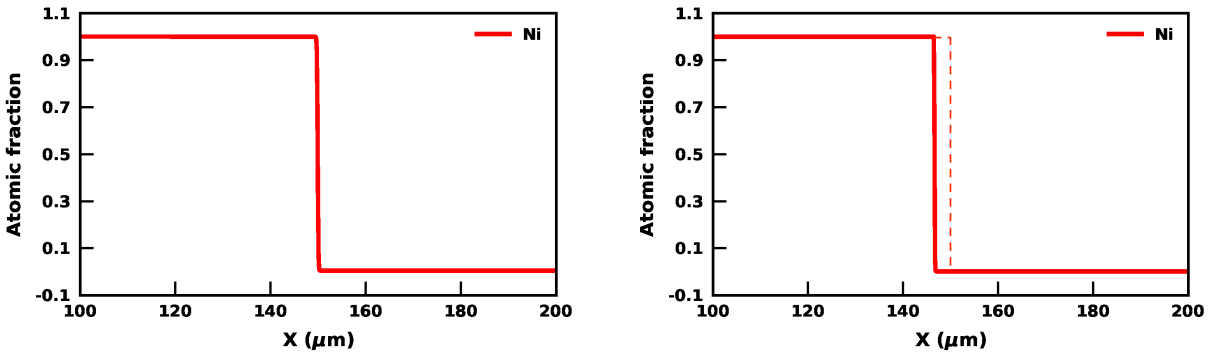


(a) Start of simulation

(b) End of simulation

Figure 7.10: Simulation of Ni corrosion by LiF−$NiF_2$ salt under oxidising condition ($\Delta E_F = 2.871$). Initially, the domain contained Ni in the left half of the domain and molten salt in the right half as in subfigure (a). At the end of the simulation shown in subfigure (b), the oxidation of Ni metal leads to the leaching of Ni into the molten salt as exhibited by the interface shifting to the left (the dashed line denotes the initial position of interface).

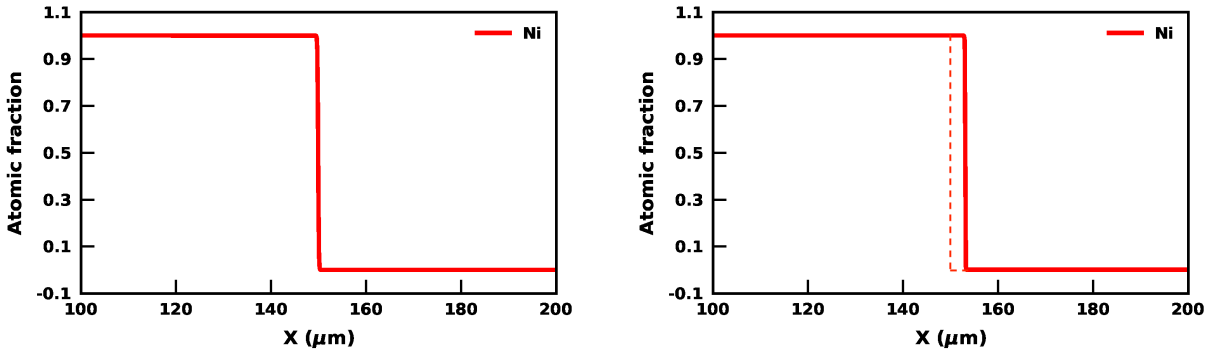


(a) Start of simulation

(b) End of simulation

Figure 7.11: Simulation of Ni corrosion by LiF−$NiF_2$ salt under reducing condition ($\Delta E_F = 3.0$). The initial interface is shown in subfigure (a) while at the end of the simulation shown in subfigure (b), the reduction of Ni metal leads to gain of Ni metal from the molten salt as exhibited by the interface shifting to the right (the dashed line denotes the initial position of interface).

For the direct coupling of Yellowjacket–GEM with the phase field module, the UserObject

described in Chapter 6 was developed. The UserObject allows a two way communication between the two parts of Yellowjacket wherein the phase field code provides the state-space to the thermodynamic equilibrium solver which returns the Gibbs energy and chemical potentials of the species to the phase field code. The UserObject system is now being deployed to perform fully-coupled simulations.

# 8

# Conclusions

Equilibrium thermodynamics provides the thermodynamic properties and driving forces for a wide variety of phenomena in nuclear reactors and a new equilibirium solver called Yellowjacket–GEM has been developed. Yellowjacket–GEM has been developed with the goal of enabling direct coupling of thermodynamic equilibrium calculations in multiphysics simulations performed using the Multiphysics Object Oriented Simulation Environment (MOOSE). Incorporating equilibrium calculations in multiphysics simulations comes with several challenges many of which are related to the existing software infrastructure. Though the most substantial contribution of this work is the creation of the software from ground up, several additional contributions were made to the field. First, while several algorithms from the literature are used, their implementation has a significant impact on the computational performance and this work had to be cognisant of this fact. The algorithms in the literature were modified to reflect the evolution in computing architectures. Second, despite model and database development being relatively mature, it was realised that knowledge gaps exist in the understanding of many models, such as the Modified Quasichemcial Model in Quadruplet Approximation (MQMQA) and this work helped in improving the understanding of such models. Third, there is often a lack of understanding about the algorithms, their capabilities and limitations, and the interpretation of the results from equilibrium thermodynamics softwares and, through this work, an effort was made to clarify some these choices. Lastly, despite years of research into global optimisation algorithms, a majority of current equilibrium codes use a rather simplistic sampling approach that often leads to failure to converge or inaccurate results. This work used an approach based on numerical experiments to quantitatively compare some promising global optimisation approaches in terms of their applicability to the phase equilibria problem.

The development of the code was motivated by the need for a modelling tool for molten salt corrosion. Modelling corrosion requires understanding of the microstructure for which the phase field model is often used. The phase field model, in turn, requires several thermodynamic quantities which must be computed through an optimisation algorithm. Coupling with the phase field module of MOOSE was the primary goal for developing this code and the code must be able to handle several thermodynamic models used to describe such systems. The model most widely used for the molten salts is the MQMQA which wasn't very well understood previously. As part of this work, the MQMQA was analysed to get a better understanding and the chemical potential expressions were derived and published. Derivation of chemical potentials for non-ideal models is not trivial and most papers in open literature don't describe the models in sufficient details let alone giving the expressions of chemical potentials which can be implemented into code by software developers. The chemical potentials for some commonly used excess mixing models were shown in Chapter 4.

Calculation of thermodynamic equilibrium is based on the fundamental laws of thermodynamics and several algorithms already reported in the literature were used to satisfy the necessary and sufficient conditions described in Chapter 5. The levelling method was used for initialisation followed by the full non-linear solution through the method of Lagrange multipliers. There are several factors that can impact the performance of the solver and the implementation of the code had to account for these factors. In doing so, the implementations were optimised to offer flexibility in terms of the system size, models that can be used, convergence criteria and others. Though the code cannot be presented herein due to export control restrictions, the algorithms used in the development were described in Chapter 6 through flowcharts and the reasoning behind main design decisions were also justified. A major challenge in satisfying the sufficient condition of thermodynamic equilibrium is the need for global optimisation algorithms. This condition requires that the driving force of all metastable phases be positive but the driving force function is often non-convex for non-ideal models and ensuring that the driving force is indeed positive is not a straightforward task. Despite major advances in global optimisation methods, the applications to thermodynamic equilibrium have been few and are mostly limited to very simple problems such as vapour-liquid equilibrium. As part of this dissertation, significant effort was spent on performance considerations of global optimisation algorithms. The Spatial Branch & Bound (sBB) algorithm was experimentally compared with an Adaptive Particle Swarm Optimisation (APSO) to prove their applicability to the equilibrium problems. It was shown that compared to the often used grid sampling, both the selected algorithms show a higher reliability to cost ratio. While sBB had the highest reliability, it came at a computational cost. On the other hand, APSO showed a great compromise between cost and reliability and

though it failed to converge a few times, it was usually noticeably faster than sBB. Since both algorithms have their pros and cons, justifying the choice of implementation depends on the application and therefore both the algorithms were implemented with the choice left to the end-user. Valuable insights into the performance of global optimisation algorithms was thus obtained and can help inform the decision of not only end-users but also of other developers.

Though the work was aimed at developing capabilities rather than performing predictive calculations, several examples of potential applications were shown through demonstrations in Chapter 7. A simple coupling between the phase field and Yellowjacket–GEM code shows how the fidelity of corrosion models may improve by adding equilibrium calculations. Moreover, the code will be a valuable tool in modelling other physical processes and in particular will be useful in source-term analyses and material modelling under non-normal operating conditions of nuclear reactors. To instil confidence in the accuracy of results predicted by the code, the results of Yellowjacket–GEM were compared to the commercial code FactSage and excellent agreement was observed.

In summary, the software developed as part of this work adds native thermodynamic equilibrium capability to the multiphysics simulation framework MOOSE. It would enable direct coupling of phase equilibrium calculations with other multiphysics codes in the MOOSE environment and allow modelling and simulation of complex physical phenomena helping in design and discovery of nuclear materials and help expedite the deployment of advanced reactors, in particular the molten salt reactors. This dissertation also addresses several knowledge gaps and concerns in the field of thermodynamic equilibrium modelling with the most significant being a better understanding of the MQMQA and a rigorous experimental comparison of methods for global optimisation applied to phase equilibrium calculations.

# 9

# Recommendations

Several improvements can be made to the software to extend the range of applications and to enhance the computational performance. Currently, explicit expressions of Gibbs energy and chemical potential are required for each model. Implementing the pre-derived expressions allows reductions in computational expenses but has a number of limitations. First, not-only is significant effort required to implement new models but doing so can inevitably introduce typographical errors creating bugs which might be tedious to debug. Second, every time a new derivative is required, such as with respect to temperature to calculate heat capacity, the user or developer must invest significant time. With automatic differentiation methods maturing, their impact on performance has significantly reduced and their implementation is not as big an impediment as it was until a few years ago. Using MetaPhysicL [240], the disadvantages of hard-coded expressions can be overcome and by strategically invoking this capability, negligible performance impact can be achieved. Another recommendation is efforts to reduce the computational cost of equilibrium calculations. There is a foreseeable advantage in improving the initialisation strategy and one such effort has been partly tried in this work. This idea is based on caching the previous calculations and using the nearest previous calculation to initialise a new calculation. Each calculation can be indexed as nodes of a $k$-dimensional tree ($k$-d tree) and the strategy has already been implemented in MOOSE albeit not tested for Yellowjacket–GEM despite the data-structures being designed for such application. Though one must consider the impact on memory requirements and search time, this strategy is promising and should be tested and fully implemented in Yellowjacket–GEM. There is also potential for further improving global optimisation algorithms. The convergence of sBB may be significantly improved by implementing heuristics and improved bound tightening strategies specific to the

nature of the problem explored here. Similarly, further optimising the hyper-parameters used in APSO may allow improvements to both its performance and reliability, helping improve the performance of Yellowjacket–GEM as well.

In terms of real applications, the code may benefit from the addition of several other models which are often used in modelling nuclear materials. The magnetic contribution to Gibbs energies was neglected in this work. Also, less-frequently used models such as the sub-ionic liquid model (SUBI) were not implemented. Implementing these models will allow much broader applications of code. In the same light, implementation of parsing capability for ThermoCalc format (`*.tdb`) data files might be of interest since many databases, like TAF-ID, are often only available in this format and the tools for converting one format to another are still nascent and bug-riddled. Despite the best attempts at reducing the computational cost of equilibrium calculations, and gains made in that direction in this work, they are inherently expensive and can often impede and even prohibit any real-world simulation. Several strategies can be considered with the goal of accelerating equilibrium calculations in multiphysics simulations. The most promising and simplest to implement would be using the previously mentioned $k$-d tree to interpolate the results in regions with high confidence without running full equilibrium calculations. As an example, if a new composition lies in a solution phase region, its properties can be estimated reasonably well with the lever rule, saving computational cost. In doing so, one may even look at more advanced strategies such as use of surrogate models.

Though the code developed as part of this work is a significant contribution as it is, the potential for growth is significant and some of the most promising applications might only be explored in future. Implementing some of the recommendations will vastly improve the performance and capability of the equilibrium code and allow it to achieve a lot more than it already can.

# References


[1] Generation IV International Forum (GIF), "Gen IV International Forum Annual Report 2021." Report, 09 2022.

[2] S. Zinkle and G. Was, "Materials challenges in nuclear energy," *Acta Materialia*, vol. 61, no. 3, pp. 735–758, 2013.

[3] T. Allen, J. Busby, M. Meyer, and D. Petti, "Materials challenges for nuclear systems," *Materials Today*, vol. 13, no. 12, pp. 14–23, 2010.

[4] M. Stan, "Discovery and design of nuclear fuels," *Materials Today*, vol. 12, no. 11, pp. 20 – 28, 2009.

[5] R. Williamson, J. Hales, S. Novascone, M. Tonks, D. Gaston, C. Permann, D. Andrs, and R. Martineau, "Multidimensional multiphysics simulation of nuclear fuel behavior," *Journal of Nuclear Materials*, vol. 423, no. 1, pp. 149 – 163, 2012.

[6] J. W. McMurray, K. Johnson, B. Collins, A. Graham, K. Lee, B. Betzler, Z. Taylor, R. Salko Jr, S. Henderson, M. H. A. Piro, R. Hu, and D. E. Holcomb, "Integration roadmap for multi-scale, multi-physics mass accountancy in Molten Salt Reactors," Tech. Rep. ORNL/TM-2021/1866, Oak Ridge National Laboratory, Oak Ridge, TN, United States, 09 2021.

[7] H. Lukas, S. Fries, and B. Sundman, *Computational Thermodynamics: The CALPHAD Method*. Cambridge University Press, 2007.

[8] M. Zinkevich, "Computational thermodynamics: Learning, doing and using." Presentation at the International Max Planck Research School for Advanced Materials, 06 2003.

[9] C. J. Permann, D. R. Gaston, D. Andrš, R. W. Carlsen, F. Kong, A. D. Lindsay, J. M. Miller, J. W. Peterson, A. E. Slaughter, R. H. Stogner, and R. C. Martineau, "MOOSE: Enabling massively parallel multiphysics simulation," *SoftwareX*, vol. 11, 2022/10/05 2020.

[10] B. Kirk, J. Peterson, R. Stogner, and G. Carey, "libMesh: A C++ library for parallel adaptive mesh refinement/coarsening simulations," *Engineering with Computers*, vol. 22, no. 3–4, pp. 237–254, 2006.

[11] S. Balay, S. Abhyankar, M. F. Adams, S. Benson, J. Brown, P. Brune, K. Buschelman, E. M. Constantinescu, L. Dalcin, A. Dener, V. Eijkhout, J. Faibussowitsch, W. D. Gropp, V. Hapla, T. Isaac, P. Jolivet, D. Karpeev, D. Kaushik, M. G. Knepley, F. Kong, S. Kruger, D. A. May, L. C. McInnes, R. T. Mills, L. Mitchell, T. Munson, J. E. Roman, K. Rupp, P. Sanan, J. Sarich, B. F. Smith, S. Zampini, H. Zhang, H. Zhang, and J. Zhang, "PETSc Web page." https://petsc.org/, 2022.

[12] S. Balay, S. Abhyankar, M. F. Adams, S. Benson, J. Brown, P. Brune, K. Buschelman, E. Constantinescu, L. Dalcin, A. Dener, V. Eijkhout, J. Faibussowitsch, W. D. Gropp, V. Hapla, T. Isaac, P. Jolivet, D. Karpeev, D. Kaushik, M. G. Knepley, F. Kong, S. Kruger, D. A. May, L. C. McInnes, R. T. Mills, L. Mitchell, T. Munson, J. E. Roman, K. Rupp, P. Sanan, J. Sarich, B. F. Smith, S. Zampini, H. Zhang, H. Zhang, and J. Zhang, "PETSc/TAO Users Manual," Tech. Rep. ANL-21/39 - Revision 3.18, Argonne National Laboratory, Lemont, IL, United States, 2022.

[13] G. Giudicelli, A. Lindsay, P. Balestra, R. Carlsen, J. Ortensi, D. Gaston, M. DeHart, A. Abou-Jaoude, and A. J. Novak, "Coupled Multiphysics Transient Simulations of the MK1-FHR reactor Using the Finite Volume Capabilities of the MOOSE Framework," in *Mathematics and Computation for Nuclear Science and Engineering*, American Nuclear Society, 2021.

[14] G. L. Giudicelli, A. D. Lindsay, R. Freile, and J. Lee, "NEAMS-TH-CRAB," Tech. Rep. INL/EXT-21-62895, Idaho National Laboratory, Idaho Falls, ID, United States, 2021.

[15] D. P. Adhikary, C. Jayasundara, R. K. Podgorney, and A. H. Wilkins, "A robust return-map algorithm for general multisurface plasticity," *International Journal for Numerical Methods in Engineering*, vol. 109, pp. 218–234, 01 2016.

[16] A. Wilkins, B. W. Spencer, A. Jain, and B. Gencturk, "A method for smoothing multiple yield functions," *International Journal for Numerical Methods in Engineering*, vol. 121, no. 3, pp. 434–449, 2020.

[17] E. Shemon, Y. S. Jung, S. Kumar, Y. Miao, K. Mo, A. Oaks, and S. Richards, "MOOSE Framework Meshing Enhancements to Support Reactor Analysis," Tech. Rep. ANL/NSE-21/43, Argonne National Laboratory, Lemont, IL, United States, 09 2021.

[18] H. Zhang, D. Andrš, J. Hansel, L. Zou, R. Berry, and R. Martineau, "RELAP-7 Web page." https://moose.inl.gov/relap7/, 2019.

[19] Y. Wang, S. Schunert, J. Ortensi, V. Laboure, M. DeHart, Z. Prince, F. Kong, J. Harter, P. Balestra, and F. Gleicher, "Rattlesnake: A MOOSE-Based Multiphysics Multischeme Radiation Transport Application," *Nuclear Technology*, vol. 207, no. 7, pp. 1047–1072, 2021.

[20] M. Tonks, D. Gaston, P. Millett, D. Andrs, and P. Talbot, "An object-oriented finite element framework for multiphysics phase field simulations," *Journal of Nuclear Materials*, vol. 51, pp. 20–29, 2012.

[21] J. W. Mcmurray, T. M. Besmann, J. Ard, B. Fitzpatrick, M. Piro, J. Jerden, M. Williamson, B. S. Collins, B. R. Betzler, and A. L. Qualls, "Multi-physics simulations for molten salt reactor evaluation: Chemistry modeling and database development," Tech. Rep. ORNL/SPR-2018/864, Oak Ridge National Laboratory, Oak Ridge, TN, United States, 2018.

[22] J. W. McMurray, N. D. B. Ezell, D. Andersson, C. Jiang, and T. Besmann, "Molten Salt Reactor Chemistry: Properties, database development, and Modeling." Presentation at Molten Salt Reactor Workshop at Oak Ridge National Laboratory, 10 2020.

[23] K. Sridharan and T. Allen, "Corrosion in Molten Salts," in *Molten Salts Chemistry* (F. Lantelme and H. Groult, eds.), pp. 241–267, Oxford: Elsevier, 2013.

[24] G. Zheng and K. Sridharan, "Corrosion of structural alloys in high-temperature molten fluoride salts for applications in molten salt reactors," *JOM*, vol. 70, no. 8, pp. 1535–1541, 2018.

[25] W. Zhou, Y. Yang, G. Zheng, K. B. Woller, P. W. Stahle, A. M. Minor, and M. P. Short, "Proton irradiation-decelerated intergranular corrosion of Ni−Cr alloys in molten salt," *Nature Communications*, vol. 11, no. 1, p. 3430, 2020.

[26] Z. Zhu, H. Huang, G. Lei, Y. Wu, C. Ren, A. Liu, and Z. Zhu, "Synergistic effect of irradiation and molten salt corrosion: Acceleration or deceleration?," *Corrosion Science*, vol. 185, p. 109434, 2021.

[27] S. S. Raiman and S. Lee, "Aggregation and data analysis of corrosion studies in molten chloride and fluoride salts," *Journal of Nuclear Materials*, vol. 511, pp. 523–535, 2018. Special Section on "18th International Conference on Fusion Reactor Materials".

[28] R. Pillai, S. Raiman, and B. Pint, "First steps toward predicting corrosion behavior of structural materials in molten salts," *Journal of Nuclear Materials*, vol. 546, p. 152755, 2021.

[29] S. Guo, J. Zhang, W. Wu, and W. Zhou, "Corrosion in the molten fluoride and chloride salts and materials development for nuclear applications," *Progress in Materials Science*, vol. 97, pp. 448–487, 2018.

[30] C. V. Bhave, M. Tonks, K. Sridharan, and G. Zheng, "Development of an Electrochemical Model for Corrosion of 316H Stainless Steel by Molten FLiNaK Using Meso-scale YellowJacket," in *Materials and Chemistry for Molten Salt Systems*, (Anaheim, CA, USA), TMS 2022 Annual Meeting & Exhibition, 2022.

[31] F. van Zeggeren and S. Storey, *The Computation of Chemical Equilibria*. Cambridge University Press, 2011.

[32] W. B. White, S. M. Johnson, and G. B. Dantzig, "Chemical equilibrium in complex mixtures," *The Journal of Chemical Physics*, vol. 28, no. 5, pp. 751–755, 1958.

[33] S. R. Brinkley, "Calculation of the Equilibrium Composition of Systems of Many Constituents," *The Journal of Chemical Physics*, vol. 15, no. 2, pp. 107–110, 1947.

[34] F. J. Krieger and W. B. White, "A simplified method for computing the equilibrium composition of gaseous systems," *The Journal of Chemical Physics*, vol. 16, no. 4, pp. 358–360, 1948.

[35] F. J. Zeleznik and S. Gordon, "Calculation of complex chemical equilibria," *Industrial & Engineering Chemistry*, vol. 60, no. 6, pp. 27–57, 1968.

[36] F. P. Boynton, "Chemical Equilibrium in Multicomponent Polyphase Systems," *The Journal of Chemical Physics*, vol. 32, no. 6, pp. 1880–1881, 1960.

[37] G. Eriksson, "Thermodynamic studies of high temperature equilibria. XII. SOLGASMIX, a computer program for calculation of equilibrium compositions in multiphase systems.," *Chemica Scripta*, vol. 8, no. 3, pp. 100–103, 1975.

[38] G. Eriksson and E. Rosen, "General equations for the calculation of equilibria in multiphase systems," *Chemica Scripta*, vol. 4, pp. 193–194, 1973.

[39] G. Eriksson, "An algorithm for the computation of aqueous multi-component, multiphase equilibria," *Analytica Chimica Acta*, vol. 112, no. 4, pp. 375 – 383, 1979.

[40] P. Koukkari and R. Pajarre, "Calculation of constrained equilibria by Gibbs energy minimization," *CALPHAD*, vol. 30, no. 1, pp. 18 – 26, 2006.

[41] G. Eriksson and K. Hack, "ChemSage – A Computer Program for the Calculation of Complex Chemical Equilibria," *Metallurgical and Materials Transactions B*, vol. 21B, pp. 1013–1023, 1990.

[42] R. Pajarre, P. Koukkari, and E. Räsänen, "Inclusion of the Donnan effect in Gibbs energy minimization," *Journal of Molecular Liquids*, vol. 125, no. 1, pp. 58 – 61, 2006. Selected Papers on Molecular Liquids.

[43] S. H. Storey and F. Van Zeggeren, "Computation of chemical equilibrium compositions," *The Canadian Journal of Chemical Engineering*, vol. 42, no. 2, pp. 54–55, 1964.

[44] G. Lantagne, B. Marcos, and B. Cayrol, "Computation of complex equilibria by nonlinear optimization," *Computers & Chemical Engineering*, vol. 12, no. 6, pp. 589 – 599, 1988.

[45] J. Nocedal and S. Wright, *Numerical Optimization*. Springer Series in Operations Research and Financial Engineering, Springer, 2006.

[46] G. Eriksson and W. Thompson, "A procedure to estimate equilibrium concentrations in multicomponent systems and related applications," *CALPHAD*, vol. 13, no. 4, pp. 389 – 400, 1989.

[47] M. Piro and S. Simunovic, "Performance enhancing algorithms for computing thermodynamic equilibria," *CALPHAD*, vol. 39, pp. 104–110, 2012.

[48] W. White, "Numerical determination of chemical equilibrium and the partitioning of free energy," *Journal of Chemical Physics*, vol. 46, no. 11, pp. 4171–4175, 1967.

[49] M. Piro, *Computation of Thermodynamic Equilibria Pertinent to Nuclear Materials in Multi-Physics Codes*. PhD thesis, Royal Military College of Canada, Kingston, ON, Canada, 2011.

[50] M. Piro, S. Simunovic, T. Besmann, B. Lewis, and W. Thompson, "The Thermochemistry Library THERMOCHIMICA," *Computational Materials Science*, vol. 67, pp. 266–272, 2013.

[51] P. Bajpai and M. H. Piro, "Corrigendum to "The thermochemistry library Thermochimica"," *Computational Materials Science*, vol. 198, p. 110659, 2021.

[52] N. Riel, B. J. P. Kaus, E. C. R. Green, and N. Berlie, "MAGEMin, an Efficient Gibbs Energy Minimizer: Application to Igneous Systems," *Geochemistry, Geophysics, Geosystems*, vol. 23, no. 7, p. e2022GC010427, 2022.

[53] A. Kruskopf, *Multiphysical Modeling Approach for Basic Oxygen Steelmaking Process*. PhD thesis, Aalto University, Finland, 2018.

[54] M. Srinivas and G. Rangaiah, "Implementation and evaluation of random tunneling algorithm for chemical engineering applications," *Computers and Chemical Engineering*, vol. 30, pp. 1400–1415, 2006.

[55] G. B. Dantzig, S. Johnson, and W. B. White, "A Linear Programming Approach to the Chemical Equilibrium Problem," Tech. Rep. Paper P-1060, The RAND Corporation, United States, 1957.

[56] G. Dantzig, S. Johnson, and W. White, "A Linear Programming Approach to the Chemical Equilibrium Problem," *Management Science*, vol. 5, no. 1, pp. 38–43, 1958.

[57] G. Dantzig, *Linear Programming and Extensions*. Princeton University Press, 2016.

[58] G. Eriksson, "Thermodynamic Studies of High Temperature Equilibria: III. SOLGAS, A Computer Program for Calculating the Composition and Heat Condition of an Equilibrium Mixture," *Acta Chemica Scandinavica*, vol. 25, pp. 2651– 2658, 1971.

[59] Chemistry Software, "HSC Chemistry 9 Web page." http://hsc-chemistry.net/index.html.

[60] W. Thompson, A. Pelton, and C. Bale, "Extension to solgasmix for interactive calculations with the F*A*C*T thermodynamic database," *CALPHAD*, vol. 7, no. 2, 1983.

[61] C. Bale, P. Chartrand, S. Degterov, G. Eriksson, K. Hack, R. Mahfoud, J. Melançon, A. Pelton, and S. Peterson, "FactSage Thermochemical Software and Databases," *CALPHAD*, vol. 26, no. 2, 2002.

[62] G. Eriksson and E. Koenigsberger, "FactSage and ChemApp: Two tools for the prediction of multiphase chemical equilibria in solutions," *Pure and Applied Chemistry*, vol. 80, pp. 1293–1302, 2008.

[63] S. Petersen and K. Hack, "The thermochemistry library ChemApp and its applications," *International Journal of Materials Research*, vol. 98, pp. 935–945, 2007.

[64] J.-O. Andersson, T. Helander, L. Höglund, P. Shi, and B. Sundman, "ThermoCalc & DICTRA, computational tools for materials science," *CALPHAD*, vol. 26, no. 2, pp. 273 – 312, 2002.

[65] B. Sundman, U. R. Kattner, M. Palumbo, and S. G. Fries, "OpenCalphad - a free thermodynamic software," *Integrating Materials and Manufacturing Innovation*, vol. 4, no. 1, 2015.

[66] R. Otis and Z.-K. Liu, "pycalphad: CALPHAD-based Computational Thermodynamics in Python," *Journal of Open Research Software*, vol. 5, no. 1, 2017.

[67] B. Cheynet, C. Bonnet, and M. Stankov, "GEMINI - DiagPlot: 2D & 3D Ternary Phase Diagrams," *CALPHAD*, vol. 33, no. 312-316, 2009.

[68] M. Poschmann, P. Bajpai, B. W. Fitzpatrick, and M. H. Piro, "Recent developments for molten salt systems in Thermochimica," *Calphad*, vol. 75, p. 102341, 2021.

[69] J. P. S. Palma, R. Gong, B. J. Bocklund, R. Otis, M. Poschmann, M. Piro, Y. Wang, T. G. Levitskaia, S. Hu, H. Kim, Z.-K. Liu, and S.-L. Shang, "Thermodynamic modeling with uncertainty quantification using the modified quasichemical model in quadruplet approximation: Implementation into PyCalphad and ESPEI." arXiv preprint, 2022.

[70] B. Baurens, J. Sercombe, C. Riglet-Martial, L. Desgranges, L. Trotignon, and P. Maugis, "3D thermo-chemical–mechanical simulation of power ramps with ALCYONE fuel code," *Journal of Nuclear Materials*, vol. 452, no. 1, pp. 578 – 594, 2014.

[71] H. Greiner, "Computing complex chemical equilibria by generalized linear programming," *Mathematical and Computer Modelling*, vol. 10, no. 7, pp. 529 – 550, 1988.

[72] D. G. Goodwin, H. K. Moffat, and R. L. Speth, "Cantera: An Object-oriented Software Toolkit for Chemical Kinetics, Thermodynamics, and Transport Processes." http://www.cantera.org, 2017.

[73] M. Castier, P. Rasmussen, and A. Fredenslund, "Calculation of simultaneous chemical and phase equilibria in nonideal systems," *Chemical Engineering Science*, vol. 44, no. 2, pp. 237 – 248, 1989.

[74] K. Shobu, "CatCalc: New thermodynamic equilibrium calculation software," *CALPHAD*, vol. 33, pp. 279–287, 2009.

[75] S. Gordon and B. McBride, "Computer Program for Calculation of Complex Chemical Equilibrium Compositions and Applications," Tech. Rep. 1311, NASA, Cleveland, OH, United States, 1994.

[76] P. Koukkari, K. Penttila, K. Hack, and S. Petersen, *CHEMSHEET – An Efficient Worksheet Tool for Thermodynamic Process Simulation*, pp. 323–330. John Wiley & Sons, Ltd, 2005.

[77] M. Ahafat, *Computation of Stoichiometric Phase Coexistence in Multicomponent Systems*. PhD thesis, Queen's University, Kingston, ON, Canada, 1992.

[78] D. S. Ebel, M. S. Ghiorso, R. O. Sack, and L. Grossman, "Gibbs energy minimization in gas + liquid + solid systems," *Journal of Computational Chemistry*, vol. 21, no. 4, pp. 247–256, 2000.

[79] M. Rafal, J. Berthold, and D. Linz, "Introduction to electrolytes," technical white paper, OLI Systems Inc., 2003.

[80] C. Bale and A. Pelton, "Optimization of Binary Thermodynamic and Phase Diagram Data," *Metallurgical Transactions B*, vol. 14B, pp. 77–83, 1983.

[81] I. K. Karpov, K. V. Chudnenko, D. A. Kulik, and V. A. Bychinskii, "The convex programming minimization of five thermodynamic potentials other than Gibbs energy in geochemical modeling," *American Journal of Science*, vol. 302, no. 4, pp. 281–311, 2002.

[82] T. Cool, A. Bartol, M. Kasenga, K. Modi, and R. E. García, "Gibbs: Phase equilibria and symbolic computation of thermodynamic properties," *CALPHAD*, vol. 34, no. 4, pp. 393 – 404, 2010.

[83] C. M. McDonald and C. A. Floudas, "GLOPEQ: A new computational tool for the phase and chemical equilibrium problem," *Computers & Chemical Engineering*, vol. 21, no. 1, pp. 1 – 23, 1997.

[84] L. G. Sillén, "High-speed Computers as a Supplement to Graphical Methods," *Acta Chemica Scandinavica*, vol. 16, pp. 159–172, 1962.

[85] N. Ingri, W. Kakolowicz, L. G. Sillén, and B. Warnqvist, "High-speed computers as a supplement to graphical methods – V: Haltafall, a general program for calculating the composition of equilibrium mixtures," *Talanta*, vol. 14, no. 11, pp. 1261 – 1286, 1967.

[86] G. Han and G. P. Rangaiah, "A method for multiphase equilibrium calculations," *Computers & Chemical Engineering*, vol. 22, no. 7, pp. 897 – 911, 1998.

[87] Y. P. Lee, G. P. Rangaiah, and R. Luus, "Phase and chemical equilibrium calculations by direct search optimization," *Computers & Chemical Engineering*, vol. 23, no. 9, pp. 1183 – 1191, 1999.

[88] H. Lukas, E. Henig, and B. Zimmermann, "Optimization of phase diagrams by a least squares method using simultaneously different types of data," *CALPHAD*, vol. 1, no. 3, pp. 225–236, 1977.

[89] E. Kozeschnik and B. Buchmayr, "MatCalc - a simulation tool for multicomponent thermodynamics, diffusion and phase transformation kinetics," in *Mathematical Modeling of Weld Phenomena*, pp. 349–361, 2001.

[90] R. Davies, A. Dinsdale, and J. Gisby, "MTDATA - Thermodynamic and Phase Equilibrium Software from the National Physical Laboratory," *CALPHAD*, vol. 26, no. 2, pp. 229–271, 2002.

[91] H. Loukusa, "Computational module for the calculation of thermochemical equilibria in nuclear fuel," Master's thesis, Aalto University, Finland, 2014.

[92] W. Cao, S.-L. Chen, F. Zhang, K. Wu, Y. Yang, Y. Chang, R. Schmid-Fetzer, and W. Oates, "PANDAT Software with PanEngine, PanOptimizer and PanPrecipitation for multi-component phase diagram calculation and materials property simulation," *CALPHAD*, vol. 33, no. 328-342, 2009.

[93] F. E. Pereira, G. Jackson, A. Galindo, and C. S. Adjiman, "A duality-based optimisation approach for the reliable solution of (P, T) phase equilibrium in volume-composition space," *Fluid Phase Equilibria*, vol. 299, no. 1, pp. 1 – 23, 2010.

[94] C. Rossi, M. Berezuk, L. Cardozo-Filho, and R. Guirardello, "Simultaneous calculation of chemical and phase equilibria using convexity analysis," *Computers & Chemical Engineering*, vol. 35, no. 7, pp. 1226 – 1237, 2011.

[95] E. Schnedler, "The calculation of complex chemical equilibria," *CALPHAD*, vol. 8, no. 3, pp. 265 – 279, 1984.

[96] W. R. Smith and R. W. Missen, "Strategies for solving the chemical equilibrium problem and an efficient microcomputer-based algorithm," *The Canadian Journal of Chemical Engineering*, vol. 66, no. 4, pp. 591–598, 1988.

[97] T. M. Besmann, "SOLGASMIX-PV, a computer program to calculate equilibrium relationships in complex chemical systems," Tech. Rep. ORNL/TM-5775, Oak Ridge National Laboratory, Oak Ridge, TN, United States, 1977.

[98] W. Song and M. A. Larson, "Phase equilibrium calculation by using large-scale optimization technique," *Chemical Engineering Science*, vol. 46, no. 10, pp. 2513 – 2523, 1991.

[99] W. Reynolds, "The element potential method for chemical equilibrium analysis: Stanjan," tech. rep., Stanford University, United States, 1986.

[100] C. de Capitani and T. H. Brown, "The computation of chemical equilibrium in complex systems containing non-ideal solutions," *Geochimica et Cosmochimica Acta*, vol. 51, no. 10, pp. 2639 – 2652, 1987.

[101] T. J. Heams, D. A. Williams, N. A. Johns, A. Mason, N. E. Bixler, A. J. Grimley, C. J. Wheatley, L. W. Dickson, I. Osborn-Lee, P. Domagala, S. Zawadzki, J. Rest, C. A. Alexander, and R. Y. Lee, "VICTORIA: A mechanistic model of radionuclide behavior in the reactor coolant system under severe accident conditions.," Tech. Rep. NUREG/CR-5545-Rev.1, Nuclear Regulatory Commission, United States, 1992.

[102] W. A. Wakeham and R. P. Stateva, "Numerical solution of isothermal, isobaric, phase equilibrium problem," *Reviews in Chemical Engineering*, vol. 20, no. 1-2, pp. 1–56, 2004.

[103] Y. Teh and G. Rangaiah, "A Study of Equation-Solving and Gibbs Free Energy Minimization Methods for Phase Equilibrium Calculations," *Chemical Engineering Research and Design*, vol. 80, no. 7, pp. 745 – 759, 2002.

[104] P. M. Pardalos, H. Romeijn, and H. Tuy, "Recent developments and trends in global optimization," *Journal of Computational and Applied Mathematics*, vol. 124, no. 1, pp. 209 – 228, 2000. Numerical Analysis 2000. Vol. IV: Optimization and Nonlinear Equations.

[105] C. Floudas, *Deterministic Global Optimization: Theory, Methods and Applications*. Springer, 1999.

[106] D. Nichita, S. Gomez, and E. Luna, "Multiphase equilibria calculations by direct minimization of Gibbs free energy with a global optimization," *Comptuers and Chemical Engineering*, vol. 26, pp. 1703–1724, 2002.

[107] J. B. Riggs, *An Introduction to Numerical Methods for Chemical Engineers*. Texas Tech University Press, 2nd ed., 1994.

[108] F. Jalali, J. Seader, and S. Khaleghi, "Global solution approaches in equilibrium and stability analysis using homotopy continuation in the complex domain," *Computers & Chemical Engineering*, vol. 32, no. 10, pp. 2333 – 2345, 2008.

[109] H. Zhang, A. Bonilla-Petriciolet, and G. Rangaiah, "A review on global optimization methods for phase equilibrium modeling and calculations," *The Open Thermodynamics Journal*, vol. 5, pp. 71–92, 2011.

[110] M. Piro and S. Simunovic, "Global optimization algorithms to compute thermodynamic equilibria in large complex systems with performance considerations," *Computational Materials Science*, vol. 118, pp. 87–96, 2016.

[111] G. P. Rangaiah, *Stochastic Global Optimization: Techniques And Applications In Chemical Engineering*. World Scientific, 2010.

[112] C. Blum and A. Roli, "Metaheuristics in Combinatorial Optimization: Overview and Conceptual Comparison," *ACM Computing Surveys*, vol. 35, no. 3, pp. 268–308, 2003.

[113] S. H. Brooks, "A Discussion of Random Methods for Seeking Maxima," *Operations Research*, vol. 6, no. 2, pp. 244–251, 1958.

[114] R. Luus and T. H. I. Jaakola, "Optimization by direct search and systematic reduction of the size of search region," *AIChE Journal*, vol. 19, no. 4, pp. 760–766, 1973.

[115] F. Glover and M. Laguna, "Tabu search," in *Modern Heuristic Techniques for Combinatorial Problems* (C. R. Reeves, ed.), Blackwell Scientific Publications, 1993.

[116] M. Srinivas and G. Rangaiah, "A study of differential evolution and tabu search for benchmark, phase equilibrium and phase stability problems," *Computers & Chemical Engineering*, vol. 31, no. 7, pp. 760 – 772, 2007.

[117] Y. Teh and G. Rangaiah, "Tabu search for global optimization of continuous functions with application to phase equilibrium calculations," *Computers and Chemical Engineering*, vol. 27, pp. 1665–1679, 2003.

[118] J. Barhen, V. Protopopescu, and D. Reister, "TRUST: A Deterministic Algorithm for Global Optimization," *Science*, vol. 276, pp. 1094–1097, 1997.

[119] S. Chaikunchuensakun, L. I. Stiel, and E. L. Baker, "A Combined Algorithm for Stability and Phase Equilibrium by Gibbs Free Energy Minimization," *Industrial & Engineering Chemistry Research*, vol. 41, no. 16, pp. 4132–4140, 2002.

[120] B. Sundman, X.-G. Lu, and H. Ohtani, "The implementation of an algorithm to calculate thermodynamic equilibria for multi-component systems with non-ideal phases in a free software," *Computational Materials Science*, vol. 101, pp. 127–137, 2015.

[121] R. Otis, M. Emelianenko, and Z.-K. Liu, "An improved sampling strategy for global energy minimization of multi-component systems," *Computational Materials Science*, vol. 130, pp. 282–291, 2017.

[122] A. Cheung, C. S. Adjiman, P. Kolar, and T. Ishikawa, "Global optimization for clusters of flexible molecules – solvent-solute interaction energy calculations," *Fluid Phase Equilibria*, vol. 194-197, pp. 169 – 183, 2002. Proceedings of the Ninth International Conference on Properties and Phase Equilibria for Product and Process Design.

[123] M. Srinivas and G. P. Rangaiah, "Differential Evolution with Tabu List for Global Optimization and Its Application to Phase Equilibrium and Parameter Estimation Problems," *Industrial & Engineering Chemistry Research*, vol. 46, no. 10, pp. 3410–3421, 2007.

[124] Y. Zhu, H. Wen, and Z. Xu, "Global stability analysis and phase equilibrium calculations at high pressures using the enhanced simulated annealing algorithm," *Chemical Engineering Science*, vol. 55, no. 17, pp. 3451 – 3459, 2000.

[125] G. P. Rangaiah, "Evaluation of Genetic Algorithms and Simulated Annealing for Phase Equilibrium and Stability Problems," *Fluid Phase Equilibria*, vol. 187, pp. 83–109, 2001.

[126] A. Bonilla-Petriciolet, G. P. Rangaiah, and J. G. Segovia-Hernández, "Constrained and unconstrained Gibbs free energy minimization in reactive systems using genetic algorithm and differential evolution with tabu list," *Fluid Phase Equilibria*, vol. 300, no. 1, pp. 120 – 134, 2011.

[127] K. Lin and D. Chen, "Hybrid artificial immune system and its application to calculation of chemical reaction and phase equilibrium," *Journal of Chemical Industry & Engineering*, vol. 58, pp. 1348–1352, 2007.

[128] P. B. Staudt and R. de P. Soares, "Reliability vs. efficiency when solving multiphase equilibrium problems with hybrid optimization codes," in *10th International Symposium*

*on Process Systems Engineering: Part A* (R. M. de Brito Alves, C. A. O. do Nascimento, and E. C. Biscaia, eds.), vol. 27 of *Computer Aided Chemical Engineering*, pp. 585 – 590, Elsevier, 2009.

[129] A. M. Scurto, G. Xu, J. F. Brennecke, and M. A. Stadtherr, "Phase behaviour and reliable computation of high pressure solid fluid equilibrium with cosolvents," *Industrial and Engineering Chemistry Research*, vol. 42, pp. 6464–6475, 2003.

[130] A. Bonilla-Petriciolet and J. G. Segovia-Hernández, "Particle Swarm Optimization for Phase Stability and Equilibrium Calculations in Reactive Systems," in *19th European Symposium on Computer Aided Process Engineering* (J. Jeżowski and J. Thullie, eds.), vol. 26 of *Computer Aided Chemical Engineering*, pp. 635–640, Elsevier, 2009.

[131] P. C. Myint, L. X. Benedict, C. J. Wu, and J. L. Belof, "Minimization of Gibbs Energy in High-Pressure Multiphase, Multicomponent Mixtures through Particle Swarm Optimization," *ACS Omega*, vol. 6, no. 20, pp. 13341–13364, 2021. PMID: 34056482.

[132] A. Bonilla-Petriciolet, G. A. Iglesias-Silva, and K. R. Hall, "Calculation of homogeneous azeotropes in reactive and non-reactive mixtures using a stochastic optimization approach," *Fluid Phase Equilibria*, vol. 281, no. 1, pp. 22 – 31, 2009.

[133] A. Lucia, L. Padmanabhan, and S. Venkataraman, "Multiphase equilibrium flash calculations," *Computers & Chemical Engineering*, vol. 24, no. 12, pp. 2557 – 2569, 2000.

[134] D. Nichita, S. Gomez, and E. Luna-Ortiz, "Multiphase Equilibria Calculation by Direct Minimization of Gibbs Free Energy Using the Tunnelling Global Optimization Method," *Journal of Canadian Petroleum Technology*, vol. 43, no. 05, pp. 13–16, 2004.

[135] J. Higgs, B. Lewis, W. Thompson, and Z. He, "A conceptual model for the fuel oxidation of defective fuel," *Journal of Nuclear Materials*, vol. 366, pp. 99–128, 2007.

[136] M. Welland, W. Thompson, B. Lewis, and D. Manara, "Computer simulations of non-congruent melting of hyperstoichiometric uranium dioxide," *Journal of Nuclear Materials*, vol. 385, no. 2, pp. 358–363, 2009.

[137] S. Simunovic, T. M. Besmann, E. Moore, M. Poschmann, M. H. Piro, K. T. Clarno, J. W. McMurray, and W. A. Wieselquist, "Modeling and simulation of oxygen transport in high burnup LWR fuel," *Journal of Nuclear Materials*, vol. 538, p. 152194, 2020.

[138] SCALE, "SCALE: A Modular Code System for Performing Standardized Computer Analyses for Licensing Evaluation," Tech. Rep. ORNL/TM-2005/39, Version 6, Vols. I – III, Oak Ridge National Laboratory, Oak Ridge, TN, United States, 2005.

[139] M. Poschmann, S. Simunovic, and M. Piro, "Acceleration of Thermochimica calculations in Bison," Tech. Rep. ORNL/TM-2020/1473, Oak Ridge National Laboratory, Oak Ridge, TN, United States, 2019.

[140] M. Poschmann, M. H. Piro, T. M. Besmann, K. T. Clarno, and S. Simunovic, "Thermochemically-informed mass transport model for interdiffusion of U and Zr in irradiated U−Pu−Zr fuel with fission products," *Journal of Nuclear Materials*, vol. 554, p. 153089, 2021.

[141] J. Hirschhorn, M. Tonks, and C. Matthews, "A CALPHAD-informed approach to modeling constituent redistribution in Zr-based metallic fuels using BISON," *Journal of Nuclear Materials*, vol. 544, p. 152657, 2021.

[142] P. Konarski, J. Sercombe, C. Riglet-Martial, L. Noirot, I. Zacharie-Aubrun, K. Hanifi, M. Frégonèse, and P. Chantrenne, "3D simulation of a power ramp including fuel thermochemistry and oxygen thermodiffusion," *Journal of Nuclear Materials*, vol. 519, pp. 104 – 120, 2019.

[143] M. H. Piro, D. Sunderland, S. Livingstone, J. Sercombe, R. W. Revie, A. Quastel, K. A. Terrani, and C. Judge, "Pellet-clad interaction behavior in zirconium alloy fuel cladding," in *Comprehensive Nuclear Materials (Second Edition)* (R. J. Konings and R. E. Stoller, eds.), pp. 248–306, Oxford: Elsevier, second edition ed., 2020.

[144] B. Michel, C. Nonon, J. Sercombe, F. Michel, and V. Marelle, "Simulation of Pellet-Cladding Interaction with the PLEIADES Fuel Performance Software Environment," *Nuclear Technology*, vol. 182, no. 2, pp. 124–137, 2013.

[145] Samuelsson, Karl, Dumas, Jean-Christophe, Sundman, Bo, and Lainet, Marc, "An improved method to evaluate the "Joint Oxyde-Gaine" formation in $(U,Pu)O_2$ irradiated fuels using the GERMINAL V2 code coupled to Calphad thermodynamic computations," *EPJ Nuclear Science and Technology*, vol. 6, p. 47, 2020.

[146] C. Guéneau, J.-C. Dumas, and M. H. Piro, "In-reactor behavior," in *Advances in Nuclear Fuel Chemistry* (M. H. Piro, ed.), Woodhead Publishing Series in Energy, pp. 419–467, Woodhead Publishing, 2020.

[147] U. Grafe, B. Böttger, J. Tiaden, and S. Fries, "Coupling of multicomponent thermodynamic databases to a phase field model: application to solidification and solid state transformations of superalloys," *Scripta Materialia*, vol. 42, no. 12, pp. 1179–1186, 2000.

[148] Q. Chen, A. Engström, L. Höglund, H. Strandlund, and B. Sundman, "Thermo-Calc Program Interface and Their Applications - Direct Insertion of Thermodynamic and Kinetic Data into Modelling of Materials Processing, Structure and Property," in *PRICM-5*, vol. 475 of *Materials Science Forum*, pp. 3145–3148, Trans Tech Publications Ltd, 1 2005.

[149] L. Zhang, M. Stratmann, Y. Du, B. Sundman, and I. Steinbach, "Incorporating the CALPHAD sublattice approach of ordering into the phase-field model with finite interface dissipation," *Acta Materialia*, vol. 88, pp. 156–169, 2015.

[150] D. Schwen, L. Aagesen, J. Peterson, and M. Tonks, "Rapid multiphase-field model development using a modular free energy based approach with automatic differentiation in MOOSE/MARMOT," *Computational Materials Science*, vol. 132, pp. 36–45, 2017.

[151] D. Schwen, C. Jiang, and L. Aagesen, "A sublattice phase-field model for direct CALPHAD database coupling," *Computational Materials Science*, vol. 195, p. 110466, 2021.

[152] B. Böttger, M. Apel, M. Budnitzki, J. Eiken, G. Laschet, and B. Zhou, "Calphad coupled phase-field model with mechano-chemical contributions and its application to rafting of $\gamma'$ in CMSX-4," *Computational Materials Science*, vol. 184, p. 109909, 2020.

[153] S. Chatterjee and N. Moelans, "A grand-potential based phase-field approach for simulating growth of intermetallic phases in multicomponent alloy systems," *Acta Materialia*, vol. 206, p. 116630, 2021.

[154] X. Zuo, A. Miotti Bettanini, A. Hilhorst, P. J. Jacques, and N. Moelans, "Influence of 5 at.%Al-Additions on the FCC to BCC Phase Transformation in CrFeNi Concentrated Alloys," *Journal of Phase Equilibria and Diffusion*, vol. 42, no. 5, pp. 794–813, 2021.

[155] Y. A. Coutinho, A. Kunwar, and N. Moelans, "Phase-field approach to simulate BCC-B2 phase separation in the $Al_nCrFe_2Ni_2$ medium-entropy alloy," *Journal of Materials Science*, vol. 57, no. 23, pp. 10600–10612, 2022.

[156] M. Poschmann, M. H. Piro, and M. S. Greenwood, "Dynamic mass accountancy modeling of a molten salt reactor using equilibrium thermodynamics," *Nuclear Engineering and Design*, vol. 390, p. 111695, 2022.

[157] B. Fitzpatrick, M. Piro, and B. Collins, "Progress in coupling of thermodynamics, fluid dynamics and isotopics in molten salt reactor multi-physics simulations," *Proceedings of American Nuclear Society*, Philadelphia, PA 2018.

[158] B. A. T. Breeden, "Using MELCOR with enhanced predictive capabilities via Thermochimica to model two severe accident cases of a generic BWR with Zry-2 and FeCrAl," Master's thesis, University of Ontario Institute of Technology, Oshawa, Canada, 2022.

[159] J. W. Gibbs, "On the equilibrium of heterogeneous substances," *American Journal of Science*, vol. 16, no. 96, pp. 441–458, 1878.

[160] M. Zemansky and R. Dittman, *Heat and Thermodynamics*. McGraw-Hill, 6th ed., 1981.

[161] A. Pelton, S. Degterov, G. Eriksson, C. Robelin, and Y. Dessureault, "The Modified Quasichemical Model I – Binary Solutions," *Metallurgical and Materials Transactions B*, vol. 31B, pp. 651–659, 2000.

[162] A. Pelton and P. Chartrand, "The Modified Quasichemical Model II – Multicomponent Solutions," *Metallurgical and Materials Transactions A*, vol. 32A, pp. 1355–1360, 2001.

[163] P. Chartrand and A. Pelton, "The Modified Quasichemical Model III – Two Sublattices," *Metallurgical and Materials Transactions A*, vol. 32, pp. 1397–1407, 2001.

[164] A. Pelton, P. Chartrand, and G. Eriksson, "The Modified Quasichemical Model IV – Two-Sublattice Quadruplet Approximation," *Metallurgical and Materials Transactions A*, vol. 32, pp. 1409–1416, 2001.

[165] G. Lambotte and P. Chartrand, "Thermodynamic optimization of the ($Na_2O + SiO_2 + NaF + SiF_4$) reciprocal system using the modified quasichemical model in the quadruplet approximation," *Journal of Chemical Thermodynamics*, vol. 43, pp. 1678–1699, 2011.

[166] M. Hillert, "The compound energy formalism," *Journal of Alloys and Compounds*, vol. 320, no. 2, pp. 161 – 176, 2001.

[167] M. Piro, M. Poschmann, and P. Bajpai, "On the interpretation of chemical potentials computed from equilibrium thermodynamic codes: Applications to molten salts," *Journal of Nuclear Materials*, vol. 526, p. 151756, December 2019.

[168] P. Bajpai, M. Poschmann, and M. H. A. Piro, "Derivations of Partial Molar Excess Gibbs Energy of Mixing Expressions for Common Thermodynamic Models," *Journal of Phase Equilibria and Diffusion*, vol. 42, no. 3, pp. 333–347, 2021.

[169] Z.-K. Liu and Y. Wang, *Computational Thermodynamics of Materials*. Cambridge University Press, 2016.

[170] D. Olander, *General Thermodynamics*. CRC Press, 2008.

[171] J. E. Dennis, Jr. and R. B. Schnabel, *Numerical Methods for Unconstrained Optimization and Nonlinear Equations*. Classics in Applied Mathematics, SIAM, 1996.

[172] M. Piro, T. Besmann, S. Simunovic, B. Lewis, and W. Thompson, "Numerical verification of equilibrium thermodynamic computations in nuclear fuel performance codes," *Journal of Nuclear Materials*, vol. 414, no. 3, pp. 399 – 407, 2011.

[173] L. Kaufman and H. Bernstein, *Computer calculation of phase diagrams: With special reference to refractory metals*. United States: Academic Press Inc, 1970.

[174] J. Ocadiz-Flores, E. Capelli, P. Raison, R. Konings, and A. Smith, "Thermodynamic assessment of the $LiF-NiF_2$, $NaF-NiF_2$ and $KF-NiF_2$ systems," *Journal of Chemical Thermodynamics*, vol. 121, pp. 17–26, 2018.

[175] T. M. Besmann and J. Schorne-Pinto, "Developing Practical Models of Complex Salts for Molten Salt Reactors," *Thermo*, vol. 1, no. 2, pp. 168–178, 2021.

[176] J. C. Ard, J. A. Yingling, K. E. Johnson, J. Schorne-Pinto, M. Aziziha, C. M. Dixon, M. S. Christian, J. W. McMurray, and T. M. Besmann, "Development of the Molten Salt Thermal Properties Database – Thermochemical (MSTDB–TC), example applications, and LiCl–RbCl and $UF_3-UF_4$ system assessments," *Journal of Nuclear Materials*, vol. 563, p. 153631, 2022.

[177] M. Piro, "Updating the estimated assemblage of stable phases in a Gibbs energy minimizer," *CALPHAD*, vol. 58, pp. 115–121, 2017.

[178] M. Hillert, "Some viewpoints on the use of a computer for calculating phase diagrams," *Physica B+C*, vol. 103, no. 1, pp. 31–40, 1981.

[179] H. Lukas, J. Weiss, and E.-T. Henig, "Strategies for the calculation of phase diagrams," *Calphad*, vol. 6, no. 3, pp. 229–251, 1982.

[180] M. Kaye, B. Lewis, and W. Thompson, "Thermodynamic treatment of noble metal fission products in nuclear fuel," *Journal of Nuclear Materials*, vol. 366, pp. 8–27, 2007.

[181] C. Guéneau, N. Dupin, B. Sundman, C. Martial, J.-C. Dumas, S. Gossé, S. Chatain, F. D. Bruycker, D. Manara, and R. J. Konings, "Thermodynamic modelling of advanced oxide and carbide nuclear fuels: Description of the U−Pu−O−C systems," *Journal of Nuclear Materials*, vol. 419, no. 1-3, pp. 145–167, 2011.

[182] C. Guéneau, N. Dupin, L. Kjellqvist, E. Geiger, M. Kurata, S. Gossé, E. Corcoran, A. Quaini, R. Hania, A. Smith, M. Piro, T. Besmann, P. Turchi, J. Dumas, M. Welland, T. Ogata, B. Lee, J. Kennedy, C. Adkins, M. Bankhead, and D. Costa, "TAF-ID: An international thermodynamic database for nuclear fuels applications," *Calphad*, vol. 72, p. 102212, 2021.

[183] X. L. Liu, T. Gheno, B. B. Lindahl, G. Lindwall, B. Gleeson, and Z.-K. Liu, "First-Principles Calculations, Experimental Study, and Thermodynamic Modeling of the Al−Co−Cr System," *PLOS ONE*, vol. 10, pp. 1–24, 04 2015.

[184] B. Sundman, B. Jansson, and J.-O. Andersson, "The Thermo-Calc databank system," *CALPHAD*, vol. 9, no. 2, pp. 153–190, 1985.

[185] S. Chen, K. Chou, and Y. Chang, "On a New Strategy for Phase Diagram Calculation: 1. Basic Principles," *CALPHAD*, vol. 17, no. 3, pp. 237–250, 1993.

[186] S. Chen, K. Chou, and Y. Chang, "On a New Strategy for Phase Diagram Calculation: 2. Binary Systems," *CALPHAD*, vol. 17, no. 3, pp. 287–302, 1993.

[187] A. H. Land and A. G. Doig, "An automatic method of solving discrete programming problems," *Econometrica*, vol. 28, no. 3, pp. 497–520, 1960.

[188] J. Falk and R. Soland, "An Algorithm for Separable Nonconvex Programming Problems," *Management Science*, vol. 15, no. 9, pp. 550–569, 1969.

[189] C. McDonald and C. Floudas, "Global optimization and analysis for the Gibbs free energy function using the UNIFAC, Wilson, and ASOG equations," *Industrial and Engineering Chemistry Research*, vol. 34, pp. 1674–1687, 1995.

[190] E. M. d. B. Smith, *On the optimal design of continuous processes*. PhD thesis, University of London, London, United Kingdom, 1996.

[191] M. Tawarmalani and N. V. Sahinidis, *Convexification and Global Optimization in Continuous and Mixed-Integer Nonlinear Programming: Theory, Algorithms, Software, and Applications*, vol. 65. Springer Science & Business Media, 2013.

[192] G. P. McCormick, "Computability of global solutions to factorable nonconvex programs: Part I – Convex underestimating problems," *Mathematical Programming*, vol. 10, no. 1, pp. 147–175, 1976.

[193] E. M. Smith and C. C. Pantelides, "Global optimisation of nonconvex MINLPs," *Computers & Chemical Engineering*, vol. 21, pp. S791–S796, 1997.

[194] E. Smith and C. Pantelides, "A symbolic reformulation/spatial branch-and-bound algorithm for the global optimisation of nonconvex MINLPs," *Computers & Chemical Engineering*, vol. 23, no. 4, pp. 457–478, 1999.

[195] P. Belotti, J. Lee, L. Liberti, F. Margot, and A. Wächter, "Branching and bounds tightening techniques for non-convex MINLP," *Optimization Methods and Software*, vol. 24, no. 4-5, pp. 597–634, 2009.

[196] P. Belotti, "Couenne GitHub Repository." https://github.com/coin-or/Couenne, 10 2022.

[197] L. Liberti, "Writing global optimization software," in *Global Optimization: From Theory to Implementation*, pp. 211–262, Boston, MA: Springer US, 2006.

[198] I. P. Androulakis, C. D. Maranas, and C. A. Floudas, "$\alpha$bb: A global optimization method for general constrained nonconvex problems," *Journal of Global Optimization*, vol. 7, no. 4, pp. 337–363, 1995.

[199] C. S. Adjiman and C. A. Floudas, "Rigorous convex underestimators for general twice-differentiable problems," *Journal of Global Optimization*, vol. 9, no. 1, pp. 23–40, 1996.

[200] C. Adjiman, I. Androulakis, and C. Floudas, "Global optimization of MINLP problems in process synthesis and design," *Computers & Chemical Engineering*, vol. 21, pp. S445–S450, 1997.

[201] I. Quesada and I. Grossmann, "Global optimization of bilinear process networks with multicomponent flows," *Computers & Chemical Engineering*, vol. 19, no. 12, pp. 1219–1242, 1995. An International Journal of Computer Application in Chemical Engineering.

[202] J. P. Shectman and N. V. Sahinidis, "A finite algorithm for global minimization of separable concave programs," *Journal of Global Optimization*, vol. 12, no. 1, pp. 1–36, 1998.

[203] N. V. Sahinidis, "Global Optimization and Constraint Satisfaction: The Branch-and-Reduce Approach," in *Global Optimization and Constraint Satisfaction* (C. Bliek, C. Jermann, and A. Neumaier, eds.), (Berlin, Heidelberg), pp. 1–16, Springer Berlin Heidelberg, 2003.

[204] M. Tawarmalani and N. V. Sahinidis, "Global optimization of mixed-integer nonlinear programs: A theoretical and computational study," *Mathematical Programming*, vol. 99, no. 3, pp. 563–591, 2004.

[205] T. Achterberg, T. Koch, and A. Martin, "Branching rules revisited," *Operations Research Letters*, vol. 33, no. 1, pp. 42–54, 2005.

[206] B. Kalantari and J. B. Rosen, "An algorithm for global minimization of linearly constrained concave quadratic functions," *Mathematics of Operations Research*, vol. 12, no. 3, pp. 544–561, 1987.

[207] M.-L. Liu, N. V. Sahinidis, and J. P. Shectman, "Planning of chemical process networks via global concave minimization," in *Global Optimization in Engineering Design*, pp. 195–230, Boston, MA: Springer US, 1996.

[208] R. Eberhart and J. Kennedy, "A new optimizer using particle swarm theory," in *MHS'95. Proceedings of the Sixth International Symposium on Micro Machine and Human Science*, (Nagoya, Japan), pp. 39–43, IEEE, 1995.

[209] J. Kennedy and R. Eberhart, "Particle Swarm Optimization," in *Proceedings of International Conference on Neural Networks*, vol. 4, pp. 1942–1948, IEEE, 1995.

[210] D. Freitas, L. G. Lopes, and F. Morgado-Dias, "Particle Swarm Optimisation: A Historical Review Up to the Current Developments," *Entropy*, vol. 22, no. 3, 2020.

[211] M. R. Bonyadi and Z. Michalewicz, "Particle Swarm Optimization for Single Objective Continuous Space Problems: A Review," *Evolutionary Computation*, vol. 25, pp. 1–54, 03 2017.

[212] A. Carlisle and G. Dozier, "An off-the-shelf PSO," in *Proceeding of Workshop on Particle Swarm Optimization*, (Indianapolis, IN), 2001.

[213] I. C. Trelea, "The particle swarm optimization algorithm: convergence analysis and parameter selection," *Information Processing Letters*, vol. 85, no. 6, pp. 317–325, 2003.

[214] F. van den Bergh and A. Engelbrecht, "A study of particle swarm optimization particle trajectories," *Information Sciences*, vol. 176, no. 8, pp. 937–971, 2006.

[215] G. Xu, "An adaptive parameter tuning of particle swarm optimization algorithm," *Applied Mathematics and Computation*, vol. 219, no. 9, pp. 4560–4569, 2013.

[216] K. R. Harrison, A. P. Engelbrecht, and B. M. Ombuki-Berman, "Self-adaptive particle swarm optimization: a review and analysis of convergence," *Swarm Intelligence*, vol. 12, no. 3, pp. 187–226, 2018.

[217] B. J. Leonard and A. P. Engelbrecht, "On the optimality of particle swarm parameters in dynamic environments," in *2013 IEEE Congress on Evolutionary Computation*, pp. 1564–1569, 2013.

[218] Y. Shi and R. C. Eberhart, "Parameter selection in particle swarm optimization," in *Evolutionary Programming VII* (V. W. Porto, N. Saravanan, D. Waagen, and A. E. Eiben, eds.), (Berlin, Heidelberg), pp. 591–600, Springer Berlin Heidelberg, 1998.

[219] A. Ratnaweera, S. Halgamuge, and H. Watson, "Self-organizing hierarchical particle swarm optimizer with time-varying acceleration coefficients," *IEEE Transactions on Evolutionary Computation*, vol. 8, no. 3, pp. 240–255, 2004.

[220] A. Chatterjee and P. Siarry, "Nonlinear inertia weight variation for dynamic adaptation in particle swarm optimization," *Computers & Operations Research*, vol. 33, no. 3, pp. 859–871, 2006.

[221] S.-K. S. Fan and Y.-Y. Chiu, "A decreasing inertia weight particle swarm optimizer," *Engineering Optimization*, vol. 39, no. 2, pp. 203–228, 2007.

[222] F. van den Bergh and A. Engelbrecht, "Effects of swarm size on cooperative particle swarm optimisers," in *Proceedings of the 3rd annual conference on genetic and evolutionary computation*, pp. 892–899, 2001.

[223] C. L. Sun, J. C. Zeng, and J. S. Pan, "An improved vector particle swarm optimization for constrained optimization problems," *Information Sciences*, vol. 181, no. 6, pp. 1153–1163, 2011.

[224] A. R. Jordehi, "A review on constraint handling strategies in particle swarm optimisation," *Neural Computing and Applications*, vol. 26, no. 6, pp. 1265–1275, 2015.

[225] X. Hu and R. Eberhart, "Solving constrained nonlinear optimization problems with particle swarm optimization," in *Proceedings of the sixth world multiconference on systemics, cybernetics and informatics*, vol. 5, pp. 203–206, 2002.

[226] C.-x. Guo, J.-s. Hu, B. Ye, and Y.-j. Cao, "Swarm intelligence for mixed-variable design optimization," *Journal of Zhejiang University-SCIENCE A*, vol. 5, no. 7, pp. 851–860, 2004.

[227] C. L. Sun, J. C. Zeng, and J. S. Pan, "A New Vector Particle Swarm Optimization for Constrained Optimization Problems," in *2009 International Joint Conference on Computational Sciences and Optimization*, vol. 1, pp. 485–488, 2009.

[228] K. E. Parsopoulos and M. N. Vrahatis, "Unified Particle Swarm Optimization for Solving Constrained Engineering Optimization Problems," in *Advances in Natural Computation* (L. Wang, K. Chen, and Y. S. Ong, eds.), pp. 582–591, Springer Berlin Heidelberg, 2005.

[229] G. Pulido and C. Coello, "A constraint-handling mechanism for particle swarm optimization," in *Proceedings of the 2004 Congress on Evolutionary Computation*, vol. 2, pp. 1396–1403 Vol.2, 2004.

[230] K. Deb, "An efficient constraint handling method for genetic algorithms," *Computer Methods in Applied Mechanics and Engineering*, vol. 186, no. 2, pp. 311–338, 2000.

[231] A. Woronow, "Generating random numbers on a simplex," *Computers & Geosciences*, vol. 19, no. 1, pp. 81–88, 1993.

[232] K. Yasuda, N. Iwasaki, G. Ueno, and E. Aiyoshi, "Particle swarm optimization: a numerical stability analysis and parameter adjustment based on swarm activity," *IEEJ Transactions on Electrical and Electronic Engineering*, vol. 3, no. 6, pp. 642–659, 2008.

[233] K. R. Harrison, A. P. Engelbrecht, and B. M. Ombuki-Berman, "Inertia weight control strategies for particle swarm optimization," *Swarm Intelligence*, vol. 10, no. 4, pp. 267–305, 2016.

[234] A. E. Slaughter, C. J. Permann, J. M. Miller, B. K. Alger, and S. R. Novascone, "Continuous Integration, In-Code Documentation, and Automation for Nuclear Quality Assurance Conformance," *Nuclear Technology*, vol. 207, no. 7, pp. 923–930, 2021.

[235] K. Lipkina, K. Palinka, E. Geiger, B. Fitzpatrick, O. Vălu, O. Beneš, and M. Piro, "Thermodynamic investigations of the LiF − CsF and NaF − CsF pseudo-binary systems," *Journal of Nuclear Materials*, vol. 568, p. 153901, 2022.

[236] M. H. A. Piro, "Thermodynamically Informed Nuclear Fuel Codes – A Review and Perspectives," *Thermo*, vol. 1, no. 2, pp. 262–285, 2021.

[237] M. H. Piro, "Thermodynamic predictions of CANDU fuel volatilization and fission product behaviour under severe accident conditions," *Journal of Nuclear Materials*, vol. 558, p. 153371, 2022.

[238] C. Guéneau, S. Gossé, A. Quaini, N. Dupin, B. Sundman, M. Kurata, T. Besmann, P. Turchi, J. Dumas, E. Corcoran, M. Piro, T. Ogata, R. Hania, B. Lee, R. Kennedy, and S. Massara, "FUELBASE, TAF-ID Databases and OC Software: Advanced Computational Tools to Perform Thermodynamic Calculations on Nuclear Fuel Materials," in *The 7th European Review Meeting on Severe Accident Research*, 2015.

[239] D. E. Holcomb, A. Huning, M. Muhlheim, R. S. Denning, and G. Flanagan, "Molten Salt Reactor Fundamental Safety Function PIRT," Tech. Rep. ORNL/TM-2021/2176, Oak Ridge National Laboratory, Oak Ridge, TN, United States, 09 2021.

[240] A. Lindsay, R. Stogner, D. Gaston, D. Schwen, C. Matthews, W. Jiang, L. K. Aagesen, R. Carlsen, F. Kong, A. Slaughter, C. J. Permann, and R. C. Martineau, "Automatic Differentiation in MetaPhysicL and Its Applications in MOOSE," *Nuclear Technology*, vol. 207, no. 7, pp. 905–922, 2021.

# List of Publications

## Peer Reviewed Journal Articles

1. **P. Bajpai**, M. Poschmann, M.H.A. Piro, *Derivations of useful partial molar excess Gibbs energy of mixing expressions of common thermodynamic models*, Journal of Phase Equilibria and Diffusion, 42 (2021) 333-347.
2. M. Poschmann, **P. Bajpai**, B.W.N. Fitzpatrick, M.H.A. Piro, *Recent developments for molten salt systems in Thermochimica*, Calphad, 75 (2021) 102341.
3. **P. Bajpai**, M.H.A. Piro, *Corrigendum to 'The thermochemistry library Thermochimica'*, Computational Materials Science, 198 (2021) 110659.
4. M.H.A. Piro, M. Poschmann, **P. Bajpai**, *On the interpretation of chemical potentials computed from equilibrium thermodynamic codes: Applications to molten salts*, Journal of Nuclear Materials, 526 (2019) 151756.
5. **P. Bajpai**, D. Schwen, M.H.A. Piro, *Performance Considerations of Global Optimisation Algorithms for Computing Chemical Equilibrium in Multicomponent Systems*, In preparation, to be submitted to Journal of Global Optimization.
6. **P. Bajpai**, M. Poschmann, D. Schwen, M.H.A. Piro, *Yellowjacket–GEM: A thermodynamic equilibrium solver for multiphysics simulations in MOOSE*, In preparation, to be submitted to Calphad.

## Peer Reviewed Conference Proceedings

1. **P. Bajpai**, M. Poschmann, D. Andrš, C. Bhave, M. Tonks and M. Piro, *Development of a new thermochemistry solver for multiphysics simulations of nuclear materials*, TMS 2020 Supplemental Proceedings, TMS 2020 - 149$^{th}$ Annual Meeting & Exhibition, San Diego, February 23-27, 2020.
2. **P. Bajpai**, M. Poschmann, D. Andrš and M. Piro, *Progress in developing a new thermochemistry code for corrosion modelling and multiphysics simulation of nuclear fuels*, 39$^{th}$ Annual Conference of the Canadian Nuclear Society and 43$^{rd}$ Annual CNS/CNA Student Conference, Ottawa, June 23-26, 2019.

## Conference / Workshop Talks & Posters

1. **P. Bajpai**, C. Bhave, M. Poschmann, D. Schwen, M. Tonks and M. Piro, *Yellowjacket Gibbs Energy Minimiser: Computing Thermochemical Equilibrium for Multiphysics Simulations of Molten Salt Reactors*, 15th International Conference on CANDU Fuel, Ajax, Canada, August 21-24, 2022..
2. **P. Bajpai**, C. Bhave, M. Poschmann, D. Schwen, M. Tonks and M. Piro, *Yellowjacket: Coupling Gibbs Energy Minimisation with Phase Field Method for Corrosion Modelling in Molten Salt Reactors*, Workshop for the Molten Salt Thermal Properties Working Group, Virtual, November 15-17, 2021.
3. **P. Bajpai**, C. Bhave, M. Poschmann, D. Schwen, M. Tonks and M. Piro, *Yellowjacket: Coupling Gibbs Energy Minimisation with Phase Field Method for Corrosion Modelling in Molten Salt Reactors*, NuFuel 2021, Bangor, United Kingdom, March 15-18, 2021.
4. **P. Bajpai**, C. Bhave, M. Poschmann, D. Andrš, M. Tonks and M. Piro, *Yellowjacket: A New MOOSE-based Corrosion Modelling Application for Molten Salt Reactors*, TMS 2021 - 150th Annual Meeting & Exhibition, Virtual, March 15-18, 2021.
5. **P. Bajpai**, M. Poschmann, D. Andrš, C. Bhave, M. Tonks and M. Piro, *Development of a new thermochemistry solver for multiphysics simulations of nuclear materials*, TMS 2020 - 149th Annual Meeting & Exhibition, San Diego, United States, February 23-27, 2020.
6. **P. Bajpai**, M. Poschmann, D. Andrš and M. Piro, *Progress in developing a new thermochemistry code for corrosion modelling and multiphysics simulation of nuclear fuels*, 39th Annual Conference of the Canadian Nuclear Society and 43rd Annual CNS/CNA Student Conference, Ottawa, Canada, June 23-26, 2019.